

University of Alberta

Dissolved Oxygen Model and Passive Samplers for the Athabasca River

by

Nancy Martin

A thesis submitted to the Faculty of Graduate Studies and Research
in partial fulfillment of the requirements for the degree of

Doctor of Philosophy

in

Environmental Engineering

Department of Civil and Environmental Engineering

©Nancy Martin

Spring 2014

Edmonton, Alberta

Permission is hereby granted to the University of Alberta Libraries to reproduce single copies of this thesis and to lend or sell such copies for private, scholarly or scientific research purposes only.

Where the thesis is converted to, or otherwise made available in digital form, the University of Alberta will advise potential users of the thesis of these terms.

The author reserves all other publication and other rights in association with the copyright in the thesis and, except as herein before provided, neither the thesis nor any substantial portion thereof may be printed or otherwise reproduced in any material form whatsoever without the author's prior written permission.

Dedication

I want to dedicate this thesis to my family. Their words of support keep me going when I needed more encouragement. I want to especially thank my husband. This adventure was in part possible due to the vision and leadership of my life companion. Thank you for being there in my nights of desperation and through my successes. Thank you for your love and patience.

I want to thank my parents who always gave me their trust and the freedom to dream. Thank you for showing me the importance of hardwork and dedication, and for being close even though the distance. I also want to thank my grandparents and parents-in-law who are a great inspiration for me. I am so blessed to have you in my life.

I also want to show my appreciation to the people who made this experience unforgettable with their friendship: Hamed, Azadeh, Mario, Deisy, Ruzma, Waqar, Helen, Alan, Po Yee and Gavin. I want to especially thank Evelyn for her kindness and invaluable help to gain confidence in my English pronunciation and writing.

Above all, thank you to Him who gives us the denarius and place angels in our way.

~ . ~

Quiero dedicar esta tesis a mi familia. Sus palabras de apoyo me motivaron cuando más lo necesitaba. En especial quiero dar gracias a mi esposo. Gracias por escucharme en mis noches de desesperación y por celebrar mis éxitos. Esta aventura fue en parte resultado de tu visión y liderazgo... siempre hemos hecho un gran equipo. Gracias por tu amor y paciencia.

También estoy profundamente agradecida a mis papás, Judith y Agustín. Ustedes me dieron las herramientas, confianza y libertad para perseguir mis sueños. Gracias por enseñarme la importancia de poner dedicación en lo que haces y por siempre estar a mi lado a pesar de la distancia.

Asimismo quiero agradecer a mis abuelitos y a mis suegros quienes son una gran fuente de inspiración y un ejemplo a seguir. Estoy muy bendecida por tenerlos en mi vida... ustedes siempre me echaron porras y quiero que sepan que los quiero mucho.

Esta experiencia fue inolvidable gracias a Hamed, Azadeh, Mario, Deisy, Ruzma, Waqar, Helen, Alan, Po Yee y Gavin. Quiero agradecer especialmente a Evelyn por su bondad e invaluable ayuda para ganar confianza con mi pronunciación y escritura de Ingles.

Gracias ante todo a Él que nos da los denarios y que nos pone ángeles en el camino.

Abstract

This thesis documents the research undertaken to develop and assess modeling and monitoring tools to improve the water quality management in the Athabasca River, Alberta. The Upper Athabasca River (UAR) has experienced dissolved oxygen (DO) sags, which may affect the aquatic ecosystem. A water quality model for an 800 km reach of this river was customized, calibrated, and validated for DO and the factors that determine its concentration. The model showed that the sediment oxygen demand (SOD) represents about 50% of the DO sink in winter. The DO calibration was improved by implementing an annual SOD based on the biochemical oxygen demand (BOD) load. The model was used to estimate the assimilative capacity of the river based on a trigger DO concentration of 7 mg/L. The results revealed a maximum assimilative BOD load of 8.9 ton/d at average flow conditions, which is lower than the maximum permitted load. In addition, the model predicted a minimum assimilative flow at average BOD load of 52 m³/s. A three-level warning-system is proposed to manage the BOD load proactively at different river discharges. Other mitigation options were explored such as upgrading the wastewater treatment from the major BOD point source, and oxygen injection into the effluents. The model can be used as a management tool to forecast the DO in low flow years and evaluate mitigation measures.

After improving the modeling tools for the UAR, monitoring tools for the Lower Athabasca River (LAR) were assessed. Naphthenic acids (NAs) have been identified as a main toxic component in the oil sands process affected water. However, it is desired to improve the current monitoring methods for NAs. Having a state-of-the-art monitoring system to quantify NAs in the LAR and its tributaries will allow calibrating robust models for this reach of the Athabasca River in the future. Passive samplers and the application of fluorescence spectroscopy using organic solvents were explored as a cost-effective alternative to quantify mass loading of NAs.

Nine organic solvents, polar protic (methanol, ethanol, and propanol), polar aprotic (dichloromethane, acetone, and acetonitrile) and non-polar (hexane, toluene, and diethyl ether) were evaluated for quantification of NAs using fluorescence. The calibration curves of the polar protic solvents performed the best with lower light scattering and higher method sensitivity. Methanol was selected for further experiments having a strong linearity for concentrations lower than 250 mg/L ($R^2 > 0.99$), and a low relative standard deviation ($< 10\%$). The synchronous fluorescence mode with a reduced offset value of $\Delta\lambda = 10$ nm demonstrated potential for fingerprinting.

Two passive samplers, the polar organic chemical integrative sampler (POCIS) and the Chemcatcher, were assessed for naphthenic acid monitoring. POCIS presented high partitioning of NAs to the polyether-sulphone (PES) membrane in combination with low diffusion to the resin. The Chemcatcher sampler with PTFE (Teflon®) membrane and C18 disk presented a high mass transfer, and it was further evaluated using commercial NAs. The sampler was integrative for a 30-day experiment having a reduced lag time, allowing the sampler to satisfactorily account for changes of NAs concentration in water. The temperature and turbulence had a high effect on the uptake rate with a 4-fold increase from 4 to 20 °C, and a 2-fold increase from 60 to 300 rpm. Furthermore, the uptake rate of commercial NAs was lower using river water, likely due to partitioning to colloids. The uptake rate of NAs from the oil sands process water was one order of magnitude lower than that obtained for commercial NAs, which may be due to the selective adsorption of acyclic ($Z = 0$) compounds with high number of carbons (n). These compounds were more abundant in the commercial NAs. Uptake rates may be required for each compound or group of compounds in the NA mixture depending on the n and Z distribution. Due to the complexity of the NAs mixture (> 3000 different compounds at isomer level), it is recommended to target the compounds with greater toxicity and abundance for further uptake rate evaluation and sampler optimization.

Acknowledgement

I would like to thank Dr. Yuefeng Xie, Dr. Selma Guigard, Dr. Scott Chang, Dr. Tong Yu, Dr. Preston McEachern and Dr. David Zhu for being part of my PhD Thesis defense committee. I thank my supervisor Dr. Yu for giving me very interesting projects and providing me with the resources to perform my work. Thank you for the opportunities that you gave me to upgrade my degree, and to start an early career in my field. Thank you to Dr. McEachern for always finding a time to meet with me, and for pointing out new vertices to my work. I highly appreciate that you introduced me to great people in Alberta Environment who were very helpful to my research. I especially want to thank Zvonko Burkus who constantly challenged me in my experimental work. Thank you for your thorough review of my papers and for the advice that you always provided.

I would like to thank Jela Burkus and Maria Demeter for providing technical support in the laboratory experiments. I also want to acknowledge the financial support from the Mexican National Council of Science and Technology (CONACYT), Natural Sciences and Engineering Research Council of Canada (NSERC). Many people in Alberta Environment and Sustainable Resource Development helped me with advice and data for this project.

Table of Contents

Chapter 1. General introduction	1
1.1. Background	1
1.2. Thesis objectives	2
1.3. Thesis outline	3
1.4. References	3
Chapter 2. Literature review: dissolved oxygen model for the Upper Athabasca River	5
2.1. The Athabasca River	5
2.2. Dissolved oxygen in aquatic ecosystems	6
2.3. Dissolved oxygen sags in the Upper Athabasca River	7
2.4. Water quality models	8
2.4.1. Water quality models as management tools	8
2.4.2. Hydrodynamic water quality models	9
2.5. Dissolved oxygen modeling	11
2.5.1. Transport	12
2.5.2. Dissolved oxygen balance	12
2.6. Previous dissolved oxygen modeling in the Upper Athabasca River	17
2.7. References	19
Chapter 3. Data analysis for dissolved oxygen sources and sinks	23
3.1. Air temperature	23
3.2. Photosynthesis	24
3.3. In-stream and tributary discharge	25
3.4. Pulp mill loading	26
3.5. References	27
Chapter 4. Model development for prediction and mitigation of dissolved oxygen sags in the Athabasca River	28
4.1. Introduction	28

4.2.	Methods.....	28
4.2.1.	Model customization.....	29
4.2.2.	Calibration and validation.....	36
4.2.3.	Model application.....	38
4.3.	Results and discussion.....	39
4.3.1.	Calibration and validation.....	39
4.3.2.	Model application.....	48
4.4.	Conclusions.....	52
4.5.	References.....	53
Chapter 5. Literature review: passive samplers for naphthenic acids.....		56
5.1.	Oil sands in the Lower Athabasca Basin.....	56
5.2.	Naphthenic acids chemistry and toxicity.....	57
5.3.	Analysis of NAs using fluorescence spectroscopy.....	59
5.4.	Passive samplers for naphthenic acids monitoring.....	65
5.4.1.	Uptake model.....	68
5.4.2.	Passive samplers widely used.....	72
5.4.3.	Factors affecting the uptake rate in passive samplers.....	75
5.4.4.	Use of passive samples for regulatory monitoring.....	76
5.5.	References.....	76
Chapter 6. Naphthenic acids quantification in organic solvents using fluorescence spectroscopy.....		83
6.1.	Introduction.....	83
6.2.	Materials and methods.....	85
6.3.	Results.....	88
6.3.1.	Spectral behavior of commercial NAs in different organic solvents.....	88
6.3.2.	Naphthenic acids quantification using fluorescence in methanol.....	92
6.4.	Discussion.....	97
6.4.1.	Advantages of using methanol over water for NAs determination using fluorescence spectroscopy.....	97

6.4.2.	Use of fluorescence spectroscopy after sample extraction using organic solvents	99
6.4.3.	Improved selectivity using synchronous fluorescence mode	100
6.5.	Conclusions	102
6.6.	References	103
Chapter 7. Feasibility of using POCIS and Chemcatcher passive samplers for naphthenic acids		
		106
7.1.	Introduction	106
7.2.	Materials and methods	106
7.2.1.	Naphthenic acid recovery from HLB resin and Empore disks	108
7.2.2.	C18 and HLB adsorption capacity for NAs sampling	109
7.2.3.	Membrane and sorbent diffusion and partitioning	109
7.2.4.	Naphthenic acid mass balance for POCIS and Chemcatcher uptake experiments	110
7.3.	Results and discussion	111
7.3.1.	Recovery of NAs from sorbents	111
7.3.2.	Determination of disk and resin capacity	112
7.3.3.	Diffusion of NAs through membranes	112
7.3.4.	Partitioning of NAs to membranes and resins	113
7.3.5.	Mass balance in uptake experiments	114
7.4.	Conclusions	118
7.5.	References	118
Chapter 8. Evaluation of uptake rates for commercial naphthenic acids using chemcatcher passive sampler		
		121
8.1.	Introduction	121
8.2.	Materials and methods	121
8.2.1.	Environmental factors influencing adsorption of NAs	122
8.2.2.	Integrative experiment and lag time	123
8.2.3.	Changes of NAs concentration in solution	124
8.2.4.	Storage conditions	125

8.2.5.	Matrix effects on the uptake rate using river water	125
8.3.	Results and discussion	126
8.3.1.	Environmental effects on commercial NAs passive sampling	126
8.3.2.	Integrative sampling time	127
8.3.3.	Chemcatcher response to fluctuations in concentration of NAs	128
8.3.4.	Storage conditions.....	130
8.3.5.	Matrix effect of river water	131
8.4.	Conclusions.....	132
8.5.	References.....	132
Chapter 9.	Evaluation of uptake rates for OSPW-NAs using Chemcatcher passive sampler.....	134
9.1.	Introduction.....	134
9.2.	Materials and methods.....	134
9.3.	Results and discussion	135
9.3.1.	Chemcatcher uptake rates using OSPW extract	135
9.3.2.	Selective adsorption of OSPW-NAs compounds	135
9.3.3.	Different uptake rates obtained analyzing the extracts by fluorescence or LC-MS/MS.....	137
9.3.4.	Uptake rate of individual compounds using LC-MS/MS.....	137
9.3.5.	Uptake rate for n and Z groups	138
9.4.	Conclusions.....	138
9.5.	References.....	139
Chapter 10.	General Conclusions and Recommendations for Future Research	140
Appendices.....		144
Appendix A.	Difference between previous model set up and this model	144
Appendix B.	Box plots for in-stream, tributaries and pulp mills constituents concentration	145
Appendix C.	Water quality available for tributaries.....	150
Appendix D.	Dissolved oxygen at Grand Rapids, air temperature at Athabasca and pulp mills load 2000-2006.....	156

Appendix E. Normality check for LHS analysis	159
Appendix F. Preliminary run from Town of Athabasca to Grand Rapids	168
Appendix G. Error measures used	169
Appendix H. Extended results for calibration and validation	170
Appendix I. Extended results for model application	175
Appendix J. Alberta Environment NAs synoptic survey using POCIS	178
Appendix K. Lab Pictures	180
Appendix L. Lower Athabasca River and tributaries pH and hardness.....	183
Appendix M. Preliminary experiments: degradation, evaporation and partitioning of NAs	185
Appendix N. Calibration curves for low concentration of NAs in water	188
Appendix O. Example of uptake rate calculation.....	189
Appendix P. Raw data for NAs analysis using LC-MS/MS from Axys Analytical.....	190
Appendix R. Mass balance for POCIS experiment using different exposure periods .	193

List of Tables

Table 2-1. Impact of varying levels of dissolved oxygen for salmonidae class that represents a cold-water fish environment (US EPA 1986)	6
Table 2- 2. Municipalities in the UAR with population > 1000 people (Alberta Municipal Affairs 2008)	7
Table 2- 3. Pulp mills discharging into the UAR.....	7
Table 2- 4. Modeling goals (Khandan and Nirmalakhandan 2002)	8
Table 2- 5. Characteristics of the last two DO models developed for the UAR	18
Table 3-1. Correlation between February's DO at Grand Rapids and flow in January at different stations	25
Table 3-2. 7Q10 flow (1952-2007) and monthly average flow for Athabasca River at Town of Athabasca (m ³ /s).....	26
Table 3-3. Correlation between February's DO at Grand Rapids and winter pulp mills' load.....	27
Table 4-1. Names and codes of stations used in the model customization, calibration and validation ¹	30
Table 4-2. Weather statements used for determining cloud cover	31
Table 4-3. Parameter transformation to CE-QUAL-W2 state variables	35
Table 5- 1. Analytical techniques used for NAs determination	60
Table 5-2. Naphthenic acids concentration in the Lower Athabasca River	66
Table 6-1. Fluorescence spectrophotometer settings.....	86
Table 6-2. Physical properties and IDHL concentration of selected solvents.....	88
Table 6-3. Results of calibration curves using different solvents and commercial NAs ...	91
Table 6-4. Calibration curves using different% DI water in methanol solution without inner filtering correction	94
Table 6-5. Concentration of OSPW-NAs stock solution estimated by gravimetric, fluorescence (using calibration curve of commercial NAs), and LC-MS/MS method. Slope of the OSPW-NAs calibration curve is based on the stock solution concentration.....	96
Table 8- 1. Factorial design for assessing the effect of temperature, pH, hardness and turbulence in the uptake rate.....	123

List of Figures

Figure 2-1. Model classification according to techniques used to represent the real system	9
Figure 2-2. Instream models widely used for TMDL studies.....	10
Figure 2- 3. Timeline of water quality modeling (adapted from Chapra (2008))	11
Figure 2- 4. Sciences involved in water quality modeling	12
Figure 2-5. Dissolved oxygen sources and sinks in rivers.....	13
Figure 2- 6. Photosynthetic algae in rivers (pictures from Flickr).....	15
Figure 2- 7. Previous dissolved oxygen models developed for the UAR.....	17
Figure 3-1. The lowest 1-day minimum and 7-day mean DO concentration in for each winter from 1989 to 2010 at Grand Rapids	23
Figure 3-2. Accumulated temperature from a) October to December, b) January to February, c) March to May, winter was defined using the consecutive months (e.g. Nov. 2002 –April 2003 is winter 2003).....	24
Figure 3- 3. Delta in hourly DO from the daily average in February	25
Figure 3- 4. Average pulp mills loads in winter (January -March), pie chart shows the overall average a) BOD, b) NH4. Hinton Pulp Mill (HPM), Alberta News Print (ANP), Millar Western Pulp (MWP), Slave Lake Pulp (SLP), Alberta Pacific (ALPAC).....	26
Figure 4-1. General approach for model development	28
Figure 4-2. Map of study area with pulp mills and stations used in the model	29
Figure 4-3. Watershed area used to estimate the tributary flow	33
Figure 4-4. Box plots showing DOC and DO concentration in the tributaries, from left to right increases distance downstream Hinton	33
Figure 4-5. Flow-DO power relationship used for input file creation a) McLeod River, b) Pembina River.....	34
Figure 4-6. Schematics showing a) relevant segments with tributaries, point sources and in-stream stations, b) elevation profile, c) side view, d) end view, e) top view	37
Figure 4-7. Hydrodynamic and water temperature calibration and validation at Athabasca station a) flow, b) elevation, and c) water temperature showing ice simulated	40
Figure 4-8. Water quality calibration and validation at Athabasca station a) ammonia, b) phosphate, c) nitrates-nitrite, d) phytoplankton algae	43
Figure 4-9. LHS analysis for SOD showing correlations with a) MAE and b) DO at 1150 Julian Day (winter 2003)	43

Figure 4-10. DO calibration and validation at different stations a) Windfall, b) Smith, c) Athabasca, d) Grand Rapids.....	44
Figure 4-11. Average DO sources and sinks in January. Algal production (AP), algal respiration (AR), epiphyton production (EP), epiphyton respiration (ER), particulate organic matter (POM), dissolved organic matter (DOM), nitrification (NITR), reaeration (REAR).....	46
Figure 4-12. Model validation using synoptic survey performed in Fall 2006 by Sharma et al. a) observed vs. predicted, b) comparison for different sampling points along the Athabasca River.....	47
Figure 4-13. DO concentration and BOD mass flux longitudinal profile through the river reach (day with the lowest DO in 2003).....	47
Figure 4-14. Average BOD load and standard deviation (bars) for simulation period (2000- 2006) and government permit level (West Fraser, 2011; Alberta-Pacific Forest Industries, 2006; Millar Western, 2007).....	48
Figure 4-15. Model results using different engineering controls: wastewater treatment upgrading (HPM), DO injection (15,000 lb/d O ₂) and pulp mills shut down (0BOD). The scenarios were applied under a “worst-case scenario” AV with high BOD, SOD and low background DO (1BOD&SOD&DO).....	50
Figure 4-16. Flow-BOD-DO contour plot using three DO levels: red DO < 5.5 mg/L, orange DO < 7 mg/L, green DO > 7 mg/L.....	51
Figure 4-17. DO winter warning system chart for flow at Athabasca < 75 m ³ /s, 1BOD (increase 1σ), 2BOD (increase 2σ), 3BOD (increase 3σ).....	52
Figure 5- 1. Naphthenic acids concentration in the Lower Athabasca River and tributaries (RAMP, 2011).....	66
Figure 5- 2. Type of compounds sampled by passive samplers	72
Figure 6-1. Intensity at different excitation wavelengths for 50 mg/L standard a) EEM in methanol, b) average relative peak intensity at different λ_{ex} , bars showing standard deviation.	89
Figure 6-2. EEM contour plot without inner filtering correction showing light scattering and area of maximum intensity for standards with 50 mg/L nominal concentration in methanol, a) commercial NAs, b) OSPW extract.....	90
Figure 6-3. Calibration curve of NAs for different solvents using peak intensity at λ_{ex} = 280 nm after inner filtering correction.....	91
Figure 6-4. Calibration curve of NAs in methanol without inner filtering correction using as instrumental response a) peak intensity at λ_{ex} = 280 nm, b) area at λ_{ex} = 280 nm curve, or c) excitation-emission volume λ_{em} = 260-500 nm, λ_{ex} = 250-310 nm.....	92
Figure 6-5. Calibration curve using methanol at low NAs concentration.....	93

Figure 6-6. Calibration curves for commercial NAs at different% deionized water in methanol.....	94
Figure 6-7. Synchronous fluorescence of commercial NAs at $\Delta\lambda= 10$ nm, a) instrument response at different concentration, b) calibration curve NAs-methanol at different peaks or area	95
Figure 6-8. Calibration curves for OSPW-NAs fluorescence in methanol using three different methods for calculating the stock solution concentration: the fluorescence standard curve for commercial NAs, weight of the OSPW extract and LC-MS/MS.....	96
Figure 6-9. OSPW extract and commercial NAs SFS response at $\Delta\lambda= 10$ nm (~250 mg/L)	97
Figure 7-1. Top and side view of sampler a) POCIS, b) Chemcatcher (open)	107
Figure 7-2. NAs percentage recovery from HLB resin using different solvents	112
Figure 7-3. Change in concentration of NAs in the acceptor chamber due to diffusion using different membranes (cellulose, CELL)	113
Figure 7-4. NAs partitioning to different membrane and sorbent materials, bars represent standard deviation	114
Figure 7-5. Concentration of Fluka NAs before water renewal in POCIS and Chemcatcher uptake experiments	115
Figure 7-6. Mass distribution of NAs in different phases in POCIS and Chemcatcher uptake experiments after 4 d.....	117
Figure 8-1. Microcosms experiment.....	122
Figure 8-2. Flow-through set up for integrative time experiment	124
Figure 8-3. Uptake rate of Fluka NAs onto C18 disk at high and low a) temperature, b) hardness, c) pH, and d) turbulence (lines are used to guide the eye,see levels in Table 2.4-1)	126
Figure 8-4. Integrative behavior for commercial NAs uptake in Chemcatcher	128
Figure 8-5. Chemcatcher performance estimating the TWA concentration (a) spike, or (b)decrease in concentration of Fluka NAs; both in the midst of sampling period.....	129
Figure 8-6. Change in the mass of adsorbed NAs after storing Chemcatcher sampler at different temperature	130
Figure 9-1. LC-MS/MS profile of a) OSPW NAs stock solution, and OSPW NAs adsorbed onto b) HLB resin TW, c) C18 disk RW, and d) C18 disk DIW, after uptake experiments	136
Figure 9-2. EEM contour plots for a) OSPW acid extract stock solution diluted to 11 mg/L b) extract from C18 disk after uptake experiment in DIW, 6 mg/L	136

Figure 9- 3. Uptake rate for different n and Z numbers in Chemcatcher experiments, a) HLB resin in tap water, b) C18 disk in river water, and c) C18 disk in deionized water . 137

Figure 9-4. Correlation of average uptake rate of OSPW NAs on different Chemcatcher configurations vs. NAs structure a) carbon, and b) Z numbers 138

List of Abbreviations

7Q10	Lowest 7-Day average flow that occurs on average once every 10 years
AG	Maximum Algal Growth Rate
ALG	Phytoplankton Algae
ALPAC	Alberta Pacific
ANP	Alberta Newsprint
CBOD	Carbonaceous Biochemical Oxygen Demand
CBODS	CBOD Settling Rate
CF	Critical Flow
CMC	Critical Micelle Concentration
DCM	Dichloromethane
DIW	Deionized Water
DO	Dissolved Oxygen
DOC	Dissolved Organic Carbon
DOM	Dissolved Organic Matter
EEM	Excitation-Emission Matrix
EFDC	Environmental Fluid Dynamics Code
EG	Maximum Epiphyton/Periphyton Growth Rate
FTIR	Fourier Transform Infrared Spectroscopy
GMC	General Circulation Models
HPM	Hinton Pulp Mill
IR	Integrative Ratio
ISS	Inorganic Suspended Solids
KBOD	5-Day BOD Decay Rate
LAR	Lower Athabasca River
LC ₅₀	Lethal Concentration 50%
LD ₅₀	Lethal Dose 50%
LDOM	Labile Dissolved Organic Matter
LDOMDK	Labile Dissolved Organic Matter Decay Rate
LDPE	Low-Density Polyethylene
LHS	Latin Hypercube Sampling
LLE	Liquid-Liquid Extraction
LPOM	Labile Particulate Organic Matter
LPOMDK	Labile Particulate Organic Matter Decay Rate
MAE	Mean Absolute Error

MWP	Millar Western Pulp
NAs	Naphthenic Acids
NBOD	Nitrogenous Biochemical Oxygen Demand
NH ₄	Ammonia
NH ₄ DK	Ammonium Decay Rate
NO ₃	Nitrates
NO ₃ DK	Nitrate Decay Rate
OSPW	Oil Sands Process-affected Water
PAD	Passive Accumulating Device
PAH	Polycyclic Aromatic Hydrocarbon
PES	Polyethersulfone
PO ₄	Phosphate
POCIS	Polar Organic Chemical Integrative Sampler
POMS	Particulate Organic Matter Settling Rate
PRC	Performance Reference Compound
PTFE	Polytetrafluoroethylene
RBOD	Ratio of CBOD ₅ to Ultimate CBOD
RDOM	Refractory Dissolved Organic Matter
RMAE	Relative Mean Absolute Error
RPOM	Refractory Particulate Organic Matter
RW	River Water
SFS	Synchronous Fluorescence Spectroscopy
SLP	Slave Lake Pulp
SOD	Sediment Oxygen Demand
SOP	Standard Operating Procedure
SPE	Solid Phase Extraction
SPMD	Semipermeable Membrane Device
SWE	Snow-Water-Equivalent
TDS	Total Dissolved Solids
TIE	Toxicity Identification Evaluation
TMDL	Total Maximum Daily Load
TOC	Total Organic Carbon
TW	Tap Water
TWA	Time-Weighted Average
UAR	Upper Athabasca River

Chapter 1. General introduction

1.1. Background

The Athabasca River is the longest river in Alberta winding 1,538 km northeast of the province (Noel & Wilson, 1995). This river has been crucial for the development of two industries that are pillars of the Albertan economy: the pulp mills and the oil sands industry. At the same time, it is the habitat of a great variety of organisms, and it is fundamental to the sustainability of a complex ecosystem. For example, it is estimated that up to one million lake-whitefish (*Coregonus clupeaformis*) migrate each year from Lake Athabasca to spawn in the river due to the specific conditions that they can find there (Alberta Environment, 1996).

The Athabasca River has two sections easily distinguished by their physical characteristics, land uses, water quality challenges, and current basin management regimes: the Upper Athabasca River (UAR) and the Lower Athabasca River (LAR). The pulp mills are located on the UAR, where periods of low dissolved oxygen (DO) concentration in winter have been observed. On the other hand, the oil sands developments are located on the LAR where the high concentration of naphthenic acids (NAs) contained in the vast area of tailings ponds has the potential of seeping into the river. Naphthenic acids have been found to represent the main toxic component of those ponds (Frank et al., 2008).

In order to make decisions that balance the industrial development and the preservation of the aquatic environment, it is necessary to apply a holistic approach through state-of-the-art monitoring systems, data analysis and modeling. The science behind the DO balance in rivers is thoroughly researched. There are well developed monitoring techniques for most of the parameters that affect it, and several models are available. In order to apply any of these models as a managerial tool, they need to have a proper customization, calibration and validation. Although there have been different attempts to model the DO in the UAR, there is not a robust model able to predict the DO sags in winter. The sediment oxygen demand (SOD) has been identified as a main DO sink in winter (Stantec 2001; Tian 2005). The SOD sampling methods have been recently improved and updated SOD rates are now available (Sharma 2012). This thesis developed a DO model using for first time a hydrodynamic two-dimensional model (CE-QUAL-W2) for the complete UAR and including improved SOD rates. The model can be

used as a managerial tool to predict the DO, assess the river's assimilative capacity and evaluate engineering controls.

Having developed a model for the UAR, this thesis focused on the water quality issues in the LAR. In order to develop a model that can be used to evaluate the NAs fate in this reach of the river, a more robust set of data is required. The NAs concentration in the LAR has been traditionally monitored by collecting grab samples and analyzing the extract by Fourier transform infrared spectroscopy (FTIR). However, the low FTIR sensitivity has resulted in a great number of samples below the detection limit (RAMP 2011; Kannel and Gan 2012). More recently, mass spectroscopy techniques have replaced FTIR; however, their cost can be prohibitive for a widespread network in the LAR and tributaries. Passive samplers were evaluated in this thesis as a novel and cost-effective way of monitoring NAs. These samplers accumulate the target compound for periods of up to one month improving the sensitivity and giving a time-weighted average concentration. Once the sampling methodologies are developed, and a more complete record of NAs concentration in the river is available, further research will be required to develop and calibrate a model for this compound. Therefore, the first step towards a robust water quality management in this part of the river is developing the techniques to get representative measurements of these compounds.

Although this thesis is divided in two sections, the findings from each section are applicable to the whole river. The pulp mill effluents have resin acids, which are very similar to the NAs, and their salts are responsible for much of the toxicity associated with untreated pulp mill effluents (CCREM, 1987). Likewise, under the stress of low oxygen conditions, aquatic organisms may become more susceptible to NAs toxicity (Lloyd, 1961). Therefore, there is potential for the evaluated samplers to be used upstream, and the developed model to be extended to the lower portion to assess these synergistic effects.

1.2. Thesis objectives

The specific objectives of this thesis are:

1. Develop and calibrate a DO model for the UAR using CE-QUAL-W2 and the most updated SOD rates.
2. Determine which parameters the model is more sensitive to; hence future efforts can be focused on getting better predictors of those parameters.
3. Use the model to determine the main DO balance contributors in winter. Management actions would be more effective if they involve changes to those contributors.

4. Apply the model to predict the DO under different management actions and climate change.
5. Use the model to determine the river's assimilative capacity.
6. Determine if POCIS or Chemcatcher is a feasible technology for NA sampling.
7. Evaluate the effect of environmental factors such as pH, turbulence, temperature and hardness on the uptake rate.
8. Determine for how long the sampler can be used in monitoring campaigns, and how well it can integrate changes in concentration.
9. Further explore fluorescence spectroscopy as an analytic method to quantify NAs.

1.3. Thesis outline

This thesis consists of two sections. The development of a dissolved oxygen model for the UAR and its application as a management tool is documented in the first section. This part of the thesis has three chapters: the literature review (Chapter 2) is followed by data analysis of the DO sources and sinks (Chapter 3), and the model development and application (Chapter 4). Chapter 4 has been published in a peer-reviewed journal (Martin et al. 2013). The second section of this thesis documents the results of evaluating passive accumulating devices for measuring NAs in the LAR. This section consists of five chapters. The literature review outlines the current knowledge and gaps regarding NAs quantification (Chapter 5). The results of evaluating the fluorescence technique to quantify NAs using organic solvents are presented Chapter 6; this chapter has been published in a peer-reviewed journal (Martin et al. 2014). POCIS and Chemcatcher are evaluated in Chapter 7. Chemcatcher is selected for further evaluation of its performance in Chapter 8, and Chapter 9 presents the results of evaluating the uptake rate using OSPW-NAs. The general conclusions and recommendations for further research are presented in Chapter 10.

1.4. References

Alberta Environment. (1996). "1996 Alberta State of the Environment Report - Aquatic Ecosystems." *Rep. No. 1*, Alberta Environment, Alberta, Canada.

Alberta Environment. (2012). "River Network Station Water Quality Data." <http://envext02.env.gov.ab.ca/crystal/aenv/viewreport.csp?RName=River%20Network%20Station%20Water%20Quality%20Data> (accessed June 2011).

Canadian Council of Resource and Environment Ministers (CCREM). (1987). "Canadian Water Quality Guidelines.", Winnipeg, Manitoba, Canada

Frank, R. A., Kavanagh, R., Kent Burnison, B., Arsenault, G., Headley, J. V., Peru, K. M., Van Der Kraak, G., and Solomon, K. R. (2008). "Toxicity assessment of collected fractions from an extracted naphthenic acid mixture." *Chemosphere*, 72(9), 1309-1314.

Kannel, P. R., and Gan, T. Y. (2012). "Naphthenic acids degradation and toxicity mitigation in tailings wastewater systems and aquatic environments: A review." *Journal of Environmental Science & Health, Part A: Toxic/Hazardous Substances & Environmental Engineering*, 47(1), 1-21.

Lloyd, R. (1961) "Effect of Dissolved Oxygen Concentrations on the Toxicity of Several Poisons to Rainbow Trout (*Salmo Gairdnerii* Richardson)" *Journal of Experimental Biology*, 38, 447-455.

Martin, N., Burkus, Z., McEachern, P., and Yu, T. (2014). "Naphthenic acids quantification in organic solvents using fluorescence spectroscopy." *Journal of Environmental Science & Health, Part A: Toxic/Hazardous Substances & Environmental Engineering*, 49:3, 294-306.

Martin, N., McEachern, P., Yu, T., and Zhu, D. Z. (2013). "Model development for prediction and mitigation of dissolved oxygen sags in the Athabasca River, Canada." *Science of the Total Environment*, 443(0), 403-412.

Noel, L. E., and Wilson, H. (1995). *Voyages: Canada's heritage rivers*. Breakwater Books, Breakwater Press, Saint John's.

RAMP. (2011). "Query water quality data [online]." <http://www.ramp-alberta.org/data/Water/water.aspx> (accessed October 2011).

Sharma, K. (2012). "The Athabasca River sediment under ice cover". Doctor of Philosophy. University of Alberta, Edmonton, AB.

Stantec, C. L. (2001). "Sensitivity analysis of a dissolved oxygen model for the Athabasca River from Hinton to Grand Rapids." *Rep. No. 108-59295*, Edmonton, AB.

Tian, Y. (2005). "A dissolved oxygen model and sediment oxygen demand study in the Athabasca River". MSc. University of Alberta, Edmonton, AB.

Dissolved Oxygen Model for the Upper Athabasca River

Chapter 2. Literature review: dissolved oxygen model for the Upper Athabasca River

2.1. The Athabasca River

The Athabasca River forms part of the Mackenzie River system in Western Canada and is the second largest river in Alberta. It begins in Jasper National Park high in the Rocky Mountains (Columbia Ice-field) and empties through a shallow delta into Lake Athabasca (Alberta Environment 1996). The Athabasca River watershed has a surface area of 160,000 km², which represents about one-fourth of Alberta's surface area. The Athabasca River minimum, mean and maximum flows (1913-2007) at the Town of Athabasca are 37 m³/s, 442 m³/s and 5,440 m³/s, respectively (Environment Canada 2010).

The Athabasca River basin contains an estimated 5,800 km of streams. The main sub-basins are the Pembina, McLeod, Berland, Lesser Slave, La Biche and Clearwater River systems. Tributary streams add high levels of sulfate from mountain springs. On the forested plains, the gradient flattens and the river slows. Tributaries swell the Athabasca River's volume, adding sediment, nutrients, and dissolved minerals such as sodium and chloride, while at the same time diluting the sulfate content of the water. The basin is highly covered in peat lands being higher in the riparian area close to the mainstream (Alberta Environment 1996). Between Fort McMurray and the delta, streams draining vast areas of peat lands add dissolved organic matter to the river, turning it reddish-brown. The bedrock geology is divided into two main sections of upper cretaceous (sandstone, shale, coal, bentonite), and lower Cretaceous (shale, oil sands). It has been classified as the Boreal Forest Natural Region (Alberta Environment 1996). Typical vegetation is aspen forest (*Populus*), and typical soil is Gray Luvisol (AESRD, 2012).

The highest fish populations occur near the junction with large tributaries. About 40% of the basin can be classed as cold-water fish habitat; in particular bull trout needing high oxygen and cold temperatures for their eggs to develop spawn in the headwaters. The Athabasca River is noted for the large whitefish such as mountain (*Prosopium williamsoni*) and lake-whitefish (*Coregonus clupeaformis*) and the rare pygmy whitefish (*Prosopium coulterii*). Other species such as grayling (*Thymallus thymallus*) are also present in the mountain and foothill reaches. Below the McLeod River junction, the

Athabasca River is considered cool-water habitat with the main species being pike (*Esox*), walleye (*Sander vitreus*), goldeye (*Hiodontidae*), and lake whitefish (Nelson and Paetz 1992).

Major land uses are forestry, agriculture, mining, exploration and development of petroleum reserves. Rivers supply 84% of the basin water demand, with about three quarters supplied by the Athabasca River. Most of the water allocated in the basin is for industry, 63% is used for pulp mills, the rest going mainly to oilfield injection and cooling water for thermal power plants. About 80% of the water used by the pulp mills is returned to the river (Alberta Environment 1996). None of the water used for oilfield injection is currently returned to the river.

2.2. Dissolved oxygen in aquatic ecosystems

The dissolved oxygen (DO) concentration in a river is an indicator of the overall health of the aquatic ecosystem. A low concentration may affect spawning success (Corsi et al. 2011). Incubation of burbot eggs at 6 mg/L delayed spawning up to 5 weeks. Mountain whitefish eggs incubated at 6.5 mg/L took much longer to hatch than eggs at higher DO concentration, while for bull trout eggs incubated at 5 mg/L, post-hatch alevins were smaller (Giles et al. 1996). A low DO level increases susceptibility to disease, and alter survival behavior such as predator avoidance, feeding, migration and reproduction. In extreme cases, low DO could even lead to cellular breakdown death in fish (Giles et al. 1996).

Table 2-1. Impact of varying levels of dissolved oxygen for salmonidae class that represents a cold-water fish environment (US EPA 1986)

Effect	DO (mg/L)	
	Embryo and larvae stages	Other life stages
No production impairment	11	8
Slight production impairment	9	6
Moderate production impairment	8	5
Severe	7	4
Acute mortality limit	6	3

The minimum concentration of DO differs from specie to specie, and also varies by life stage. Young trouts require higher DO concentrations than adults. Trout, long nose suckers (*Lepisosteus osseus*), and burbot (*Lota lota*) require relatively high concentrations of DO, whereas species such as northern pike can survive under lower concentrations (EPA 1986). Based on a review of laboratory and field data on the impact

of varying levels of DO in freshwater ecosystems, US EPA (1986) set a DO guideline of 6.5 mg/L for the 30-day mean (Table 2-1). The minimum DO concentration requirement established under the *Surface Water Quality Guidelines for use in Alberta* is 5 mg/L for acute and 6.5 mg/L for chronic exposure (Alberta Environment 1999).

2.3. Dissolved oxygen sags in the Upper Athabasca River

The Upper Athabasca River (UAR) receives contaminants from municipalities, pulp mills and other non-point sources such as run-off from agriculture and forestry. The dissolved oxygen concentration is affected by biochemical oxygen demand (BOD) loadings with the most important sources being the municipalities and pulp mill effluents. Five municipalities and five pulp mills discharge effluents into the UAR (Table 2- 2 and Table 2- 3).

Table 2- 2. Municipalities in the UAR with population > 1000 people (Alberta Municipal Affairs 2008)

Municipality	Population	WWTP
Jasper	4,745	
Hinton	9,769	✓ ¹
Whitecourt	9,202	✓
Slave Lake	7,031	
Athabasca	7,592	✓

¹Sewer from Hinton goes to Hinton Pulp mill wastewater treatment plant

Table 2- 3. Pulp mills discharging into the UAR

Pulp Mill	Actual BOD ₅ loading (kg/d) ¹	Licensed BOD ₅ loading (kg/d) ²	Startup	Location
Hinton Pulp Mill	2296	3100	1957	Hinton
Alberta Newsprint Co.	109	2000	1990	Whitecourt
Millar Western Pulp	450	2250	1988	Whitecourt
Slave Lake Pulp	517	1750	1991	Slave Lake
Alberta Pacific Forest Industries	280	2500	1993	Athabasca

¹Actual loading is 2000 – 2006 average

²Licensed loading obtained from pulp mill's sustainability reports (West Fraser, 2011; Alberta-Pacific Forest Industries, 2006; Millar Western, 2007)

The dissolved oxygen in the Athabasca River has a strong seasonal and spatial change being at its minimum values in late winter and upstream Grand Rapids. Passing over the falls and down the steep mountain gradient, the river picks up high levels of DO downstream of Grand Rapids. Although the DO saturation in the Athabasca River in winter at 0 °C reaches 13.5 mg/L, dissolved oxygen concentrations were below recommended values for aquatic life protection in the 2002-2003 winter upstream the

Grand Rapids (Alberta Environment 1996). The ice-cover in winter limits the re-aeration to the open leads mainly downstream the point sources. Although the BOD and sediment oxygen demand (SOD) rates diminish in low temperatures, the flow is minimum in winter and as a result the BOD dilution. Moreover, photosynthesis decreases in winter because of the shorter hours of daylight and because the ice-cover attenuates the solar radiation.

2.4. Water quality models

2.4.1. Water quality models as management tools

Modeling has long been an integral component in organizing, synthesizing and rationalizing observations and measurements from real systems and in understanding their causes and effects in a cost-effective way (Khandan and Nirmalakhandan 2002).

Table 2- 4. Modeling goals (Khandan and Nirmalakhandan 2002)

Research-oriented	Management-oriented
Interpret the system	Operate the system
Analyze its behaviour	Control it to achieve desired outcomes
Forecast its response under varying conditions	Design methods to improve or modify it

Environmental models are needed to relate the engineering activities of control, treatment, or remediation to environmental concentrations (Table 2-4). Water quality models are excellent tools to be used in the implementation of policy, regulatory development, remediation, and enforcement. They help to assess processes modified by natural and human-induced changes in the river system in a cost-effective manner (Lung 2001). Even though model development seldom exceeds 1% of the capital cost of new water resources projects and less than 0.1% of facility costs, in nearly all cases they can bring savings on the capital works (Palmer 2001). Models are even more attractive when there is good data available, because the cost of collecting the site-specific data generally accounts for 50% to 70% of the modeling costs (Palmer 2001).

Effluents discharged into water bodies must be approved and meet specific limits at their point of discharge. Limits are based on best available technology or determined to protect the water quality in a receiving water body. Models have been widely used as a requirement for environmental assessment in order to specify effluent limitations (Palmer 2001). The EPA's Total Maximum Daily Load (TMDL) rule, promulgated in 2000, calls for a monitoring and modeling plan to be an integral part of the TMDL's implementation plan.

Models will estimate the maximum pollutant loading from point and non-point sources that receiving waters can accept without violating water quality standards (Lung 2001).

Different legislation and initiatives have taken place in Alberta to manage the surface water quality. The "Water for Life" strategy led by Alberta Environment as the basis of managing Alberta's water resources includes keeping healthy aquatic ecosystems as one of its four main work areas. Under the Fisheries Act (Province of Alberta 2013) pulp mills are required to monitor, on a three-year cycle the environmental effects of their effluents on the rivers they discharge to. Additionally, the *Water Quality Based Effluent Limits Procedure Manual* (Alberta Environment 1995) requires using a computerized modeling tool to calculate the potential for any effluent to meet guidelines. Due to the important expansion of the pulp mill industry in the UAR, the Northern River Basins Study took place in the 90s with one of its objectives being to develop appropriate water quality models.

2.4.2. Hydrodynamic water quality models

The overall modeling capacity has been highly influenced from the development of high-speed computers and programming languages in the last decades. However, the complexity of a model should be kept to a minimum, as required to achieve the objectives. Different modeling techniques are presented in Figure 2-1. The characteristics of the desirable water quality model for the UAR are highlighted:

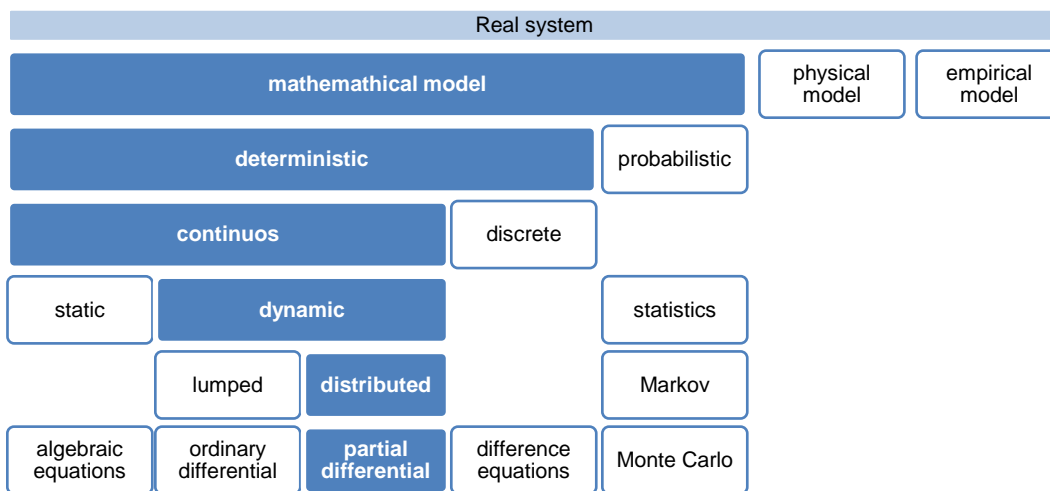


Figure 2-1. Model classification according to techniques used to represent the real system

There are different widely available water quality models. However, few of them are able to simulate the river's hydrodynamics (Figure 2-2). The Environmental Fluid Dynamics

Code (EFDC) is a state-of-the-art hydrodynamic model that can be used as vertically averaged or 3-D model. However, this model does not simulate the ice formation and break-up. As a result, the ice cover has to be externally provided. Additionally, this software is very complex for non-expert users as it does not have a model interface.

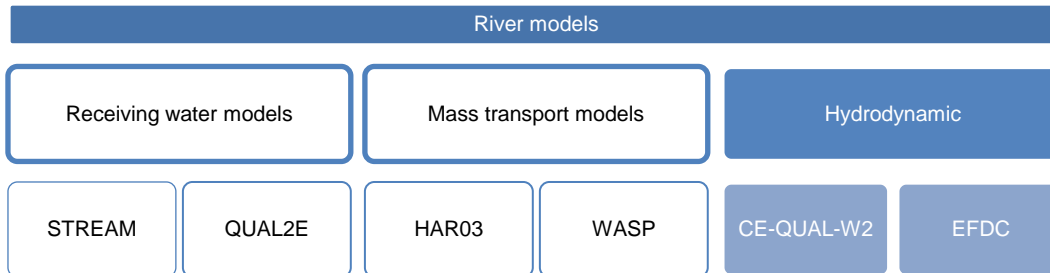


Figure 2-2. Instream models widely used for TMDL studies

CE-QUAL-W2 is a hydrodynamic two-dimensional model (assuming complete mixing in the lateral direction). This model was developed by Portland State University and U.S. Army Corps of Engineers. It has been used since 1986, and it has been updated and improved through seven versions by 2009. This model simulates water surface elevations, velocities, temperature, ice cover, sediment processes, and multiple water quality constituents. The DO is calculated through a deterministic and mechanistic approach by taking into account algae respiration and photosynthesis, organic matter decay, BOD, SOD and nitrification in modular algorithms (Cole and Wells 2008). Implicit finite difference solution methods are used, and an automated time-step selection algorithm allows for efficient simulation while ensuring that numerical stability requirements are not violated.

The theory behind the DO modeling using CE-QUAL-W2 is very well documented in its manual (Cole and Wells 2008). The mass transport and hydrodynamic governing equations are obtained by performing a mass and a momentum balance of the fluid phase in a control volume. The resulting three laterally averaged equations are continuity and momentum in the longitudinal and vertical direction. The instantaneous velocity and concentration are decomposed into a mean and an unsteady component, which uses dispersion coefficients. The sources and sinks for constituents either come from outside boundaries or internal processes resulting from reactions.

For high-latitude rivers, it is very relevant that this software is capable of calculating onset and breakup of ice cover. On the other hand, it is important to take into account the model limitations, one of the most important in this research is that it does not model the SOD diagenesis; it only models labile sediment decay (Cole and Wells 2008).

Additionally, it is laterally averaged, making it more adequate for lakes and reservoirs for which the change in concentration through the depth is more significant. In rivers, the vertical mixing is assumed to occur instantaneously (Fischer et al. 1979), while the transversal mixing is an important process in the dilution of the contaminants. For this reason, a 2-D model (vertically averaged) would be more appropriate.

It is also important to take into account that there are inherent limitations in any model, as it is a simplification of the real system. The main assumptions of this model are:

- Complete mixing in each cell (average length > 4 km)
- One species is enough to model the biotic components (epiphyte/periphyton phytoplankton, macrophyte and zooplankton)
- The stoichiometric ratios do not change with time, and one value is representative of all the organic matter.
- The bathymetry used is representative (no major flood event after the survey and cross-sections evenly distributed)

2.5. Dissolved oxygen modeling

Dissolved oxygen is a very important water quality parameter for aquatic life and a key water quality indicator since it is affected by various processes such as water temperature, re-aeration, organic carbon decay, nitrification, and algae growth and decay (Tetra Tech 2009). For this reason, the problem of dissolved oxygen was a pioneer in water quality modeling (Figure 2- 3). The stabilization of the organic and inorganic oxidizable material discharged into a body of water (in the water or sediments), and through interaction of aquatic plant life, results in the decrease of DO to concentrations that may interfere with desirable water uses.

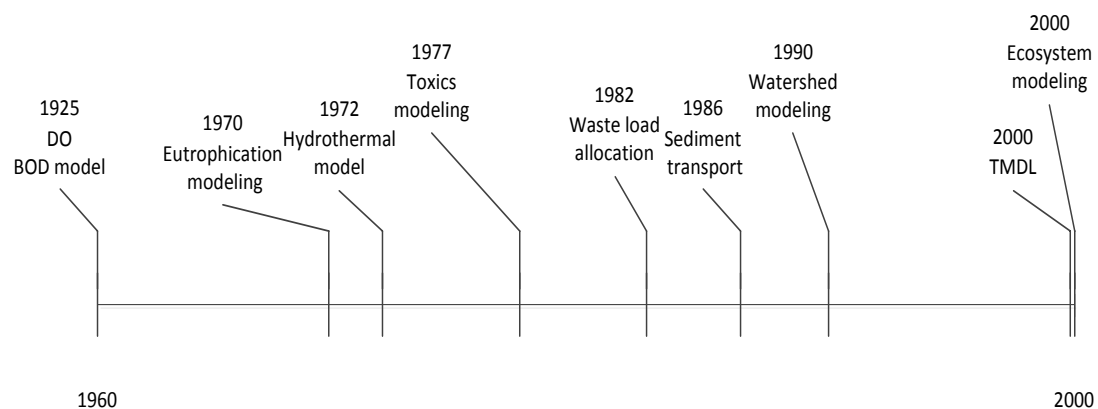


Figure 2- 3. Timeline of water quality modeling (adapted from Chapra (2008))

The fate of a pollutant in a water body is a complex process that involves its advective and dispersive transport, the chemical-biological decay, and the equilibrium between different compartments. As a result, several sciences interact in water quality modeling (Figure 2- 4).

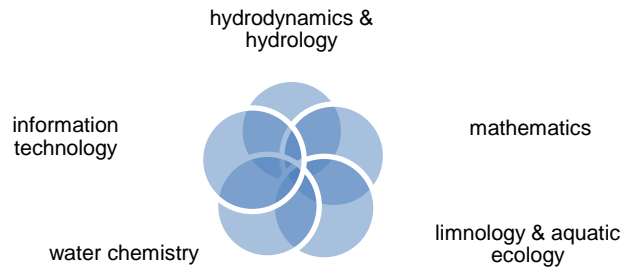


Figure 2- 4. Sciences involved in water quality modeling

2.5.1. Transport

The screening of pollutants in a river is performed assuming a steady-state plug flow system, which represents the case of purely advective transport. If the water quality is to be modeled over a long distance and a short time interval of discharge, then the longitudinal dispersion must be considered. One-dimensional transport systems that include both advection and dispersion are often represented by a plug flow with dispersion model.

Models that have analytical solutions generally require significant simplifying assumptions (e.g., steady-state conditions and spatial homogeneity or complete mixing). However, heterogeneous systems with temporal variability, multi-component chemistry, or nonlinear transformation processes require more sophisticated numerical models, though these are often constructed by piecewise aggregation of multiple idealized reactor units for local areas or zones. These techniques solve differential equations describing the pollutant mass balance over discrete cells in space and/or discrete steps in time. Most of the available models for hydrodynamic simulation apply finite difference solution methods to some form of the Navier-Stokes and continuity equations, though models are also available using finite element methods.

2.5.2. Dissolved oxygen balance

Mechanistic water-quality models are based on the conservation of mass within a finite volume of water. The DO sources and sinks are illustrated in Figure 2-5. Three factors have been recognized as fundamental in the DO balance of the Athabasca River in

winter: BOD, SOD and re-aeration due to the ice-cover ratio. Special attention has to be taken in the selection and use of these parameters in the model. A short explanation of each source and sink follows in this section.

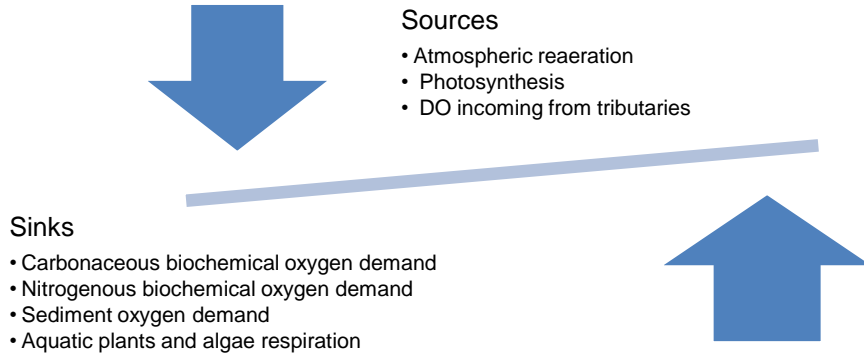


Figure 2-5. Dissolved oxygen sources and sinks in rivers

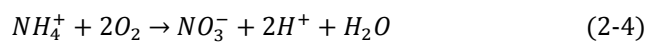
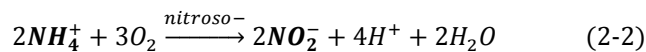
CBOD & NBOD

The carbonaceous biochemical oxygen demand (CBOD) is exerted by the presence of heterotrophic organisms, while the nitrogenous biochemical oxygen demand (NBOD) is exerted by nitrifying bacteria. A simplification of the CBOD and NBOD kinetics assumes first-order kinetics (Thomann and Mueller 1987).

$$CBOD_t = CBOD_u[1 - e^{-Kt}] \quad (2-1)$$

Where K is the first-order rate coefficient and t is time with a 5-day standard measurement period. The ratio between $CBOD_u/CBOD_5$ will depend on the degree of wastewater treatment. The ratio will increase as the material is more refractory and less susceptible to biochemical oxidation. Increased temperature increases the rate of oxidation.

The NBOD comes from the nitrification process (Tchobanoglous 2003).



Paper mill wastes, are deficient in any nitrogen forms and therefore do not have significant nitrification (Thomann and Mueller 1987).

SOD

The stabilization of settleable waste material and aquatic plants or other organic material brought through natural runoff will use oxygen at the bottom of the river. The SOD will depend on the benthic community and the rate of deposition of this material, which in turn depends on the river flow. Since this is a biological mediated process, it also depends on temperature. The SOD can be as low as 0.05 g/m²/d in mineral soils to 4 g/m²/d downstream sewage outfall at 20 °C (Thomann and Mueller 1987). Other factors influencing SOD are nutrients, chemical reducing agents, algae and invertebrates (Tian 2005). Benthic sediments become more prevalent as rivers become bigger, deeper, and slower, though the increased depth of these systems implies less net benthic influence on the quality of the overlying water column. It has been suggested that particulate organic carbon load increases substantially the SOD rates in the UAR (Yu 2006).

There is not a standard method to measure the SOD in the river bed as compared with the BOD in the water column. Measuring the SOD in a river is challenging because the system should not be perturbed, while it needs to be isolated to measure the change in DO with time. This is even more complicated for deep rivers or ice-covered rivers. Three methods have been used to measure the SOD in the Athabasca River: core incubation, in situ closed chambers and microsensors (Yu 2006; Tian 2005; Sharma 2012). The closed chamber method needs to be carried out in the field, and can be very labor intensive. Additionally, the mixing system may not represent the actual river mixing, and SOD may be underestimated as a result (Yu 2006). On the other hand, core incubation can disturb the sediment and because of the smaller diameter of the vessel in comparison to the closed chamber, it can only take gravel and sediments and not rocks that can exert a significant SOD. In this method, care must be taken reproducing the adequate mixing and river temperature. Microsensors are useful analyzing the factors that affect the SOD, such as nutrients and organic matter; however, they do not account for the total SOD. For this reason, the SOD methods are still in development and the estimated rates are part of the uncertainty in the river DO modeling. The model developed used the SOD values obtained in a survey performed in 2006 with an improved core incubation method (Sharma 2012).

Photosynthesis and respiration

Phytoplankton, macrophyte and periphyton (Figure 2- 6) are photosynthetic algae and plants that affect the DO balance. The water interaction with pure oxygen generated by photosynthesis can lead to supersaturated values. However, the production of oxygen proceeds only during daylight hours and the respiration occurs continuously. Minimum

DO values usually occur in the early morning, and maximums in the early afternoon. The diurnal range may be large and minimum values may create a potential for a fishkill. The oxygen production can be estimated from the chlorophyll- α mass and adjusted for the light attenuation factor over depth (Thomann and Mueller 1987).

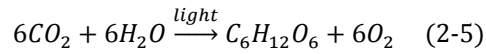


Figure 2- 6. Photosynthetic algae and aquatic plants (macrophytes) in rivers (pictures from Flickr)

Re-aeration

The oxygen saturation level is given by the Henry's law, and it is proportional to the atmospheric pressure. The oxygen saturation level decreases as the water temperature and salinity increase (Chapra 2008). The oxygen exchange makes use of the two-film theory where the liquid film is the controlling phase. According to Fick's Law, the rate of transfer of oxygen from the atmosphere to the water body will depend on the difference between the current DO concentration, C , and the oxygen saturation, C_s , level.

$$\frac{dC}{dt} = K_a(C_s - C) \quad (2-6)$$

The re-aeration coefficient, K_a , depends on the turbulence of the system (Thomann and Mueller 1987). There are different empirical equations that relate the river's velocity and depth to the re-aeration coefficient.

Dissolved oxygen balance in ice covered rivers

The dissolved oxygen sags in rivers have been traditionally related to the warm days of summer when eutrophic water bodies have high algal productivity and big diurnal DO changes. Different case studies have documented DO modeling in open water conditions (Droic and Koncan 1999; Gautam and Sharma 2011; Turner et al. 2009; Williams and Boorman 2012); however, DO depressions have also been observed under winter ice-covered conditions (Whitfield and McNaughton 1986; Schallock and Lotspeich 1974; Schreier et al. 1980; Mossewitsch 1961). The DO balance under these circumstances is

affected by limited re-aeration and photosynthesis. Additionally, the low volumetric flow generates minimum pollutant dilution and longer travel-time allowing greater BOD consumption. Few model applications have investigated the DO balance under these conditions (Pietroniro et al. 1998).

The ice cover depends on many factors as meteorological (air temperature, wind velocity, solar radiation), hydraulic, and effluent temperature. In river freezing, the flow velocities and turbulence as well as meteorological factors are important (Hicks 2009). The ice-cover ratio in the Athabasca River has been related to air temperature, finding that it varies logarithmically. However, there were not enough data points to obtain a more accurate regression model from the statistical point of view (Tian 2005). Moreover, a better prediction would be found using all the significant factors that affect ice-cover ratio.

In one study of the pulp mill effluent effect on the open leads, the ALPAC effluent temperature was reported about 10 °C to 22 °C when the air temperature was below - 30 °C. This heat exchange generated open leads that could range from a few hundred meters to several kilometers. The impact of these open leads was also studied, and a DO increase of 0.26 mg/L was found with an open lead of 6.07 km (Lima Neto et al. 2007). The open lead was modeled using CORMIX® for the warm plume hydrodynamics, and the effluent temperature was found a dominant parameter. The ice break-up in late winter can occur in the form of gradual melting or sudden ice-cover ruptures that start with the water rising. When the width of the river has increased and the size of the layers of ice has decreased, they start to move with the flow clearing the upstream (Hicks 2009).

During periods of ice cover, oxygen replacement through re-aeration and photosynthesis slows or ceases. As winter progresses, oxygen is used up for bacterial decomposition of organic matter and in sediments. For some rivers, DO concentration increases before ice break-up due to increased photosynthetic activity caused by increasing light levels and after it for the turbulence caused, while for other rivers with high organic material, the annual minimum can occur under these circumstances due to the particulate re-suspension and the accelerating metabolism for the increase in temperature (Prowse 2001). In a study of two Yukon Rivers, Nordenskiöld and Takhini, it was found that the depression of DO occurred in two stages: a rapid decline during the formation of the ice cover and a gradual declining afterwards (Whitfield and McNaughton 1986). The absolute depression and its rate were higher in the river with the highest organic content. It was also found that the DO increased to near saturation prior to the breakup of the ice cover.

Based on the data of nine rivers without point sources, Chambers *et al.* (1997) demonstrate the impact of these on the spatial DO profile. In these rivers, the DO was

constant over their length contrasting with other studies where it decreases downstream the point sources (Prowse 2001).

2.6. Previous dissolved oxygen modeling in the Upper Athabasca River

The point source pollutants' travel time from the release location to upstream Grand Rapids, where the minimum DO concentration has been observed, is from 15 to 30 days. Without a model that can predict whether the DO would decline below the guideline, there is a risk of a substantial lag time between management action and mitigation of low DO levels monitored at Grand Rapids. For this reason, there has been great interest since the early 1990s in developing a robust model for the UAR (Figure 2- 7) (Chambers 1996; Golder Associates 1995; Stantec 2001; Tian 2005; Yu 2006). However, an accurate oxygen model is a scientific challenge because it requires a thorough understanding of the complex natural processes that control oxygen levels in a system that is large, and experiences dramatic seasonal temperature fluctuations (Alberta Environment 1996).

Although previous models have successfully predicted large-scale trends in average oxygen concentrations, they have not been able to predict low DO concentrations downstream of the pulp mills and upstream of the Grand Rapids at different periods. The sensitivity analyses of previous modeling efforts have shown a strong relation between SOD and the DO in winter (Stantec 2001; Tian 2005). Important advancements in SOD techniques during the last few years (Sharma et al. 2009; Sharma 2012; Tian 2005; Yu 2006) have improved the available data for model calibration and thus have enhanced the representation of in-river processes and model reliability. Additionally, the complexity of the models available has also increased with more powerful processors.



Figure 2- 7. Previous dissolved oxygen models developed for the UAR

The first attempt to model the DO in the Athabasca River was done with DOSTOC a stochastic one-dimensional model. This model did not take into account the NBOD and did not represent adequately the photosynthesis and respiration. As a result, the model was not capable of reproducing the DO dynamic in the river. Chambers *et al.* (1996)

showed that the DO decreases linearly from Hinton to Grand Rapids using DOSTOC with a deterministic and a stochastic solution at 50% and 95% probability; however, they recommended to use a dynamic model.

An attempt to improve the DO predictions was done using a dynamic model, the Water Quality Analysis Simulation Program (WASP) from US EPA in one dimension (Golder Associate Ltd. 1995). The model divided the stream from Hinton to Grand Rapids into 39 segments and took into account 15 major tributaries. The calibration was done in two stages: one for the BOD and SOD and the second for the re-aeration. The velocity, width and depth in the different segments of the river were calculated with the Leopold-Maddox equations that relate these parameters to the flow. Although this technique improved the DO simulation, it did not accurately predict the 1993 observations. The segmentation used in this previous study was used in a new version of WASP by Stantec in 2001. The importance of SOD was confirmed with sensitivity analysis, and it was included in the DO model making a more realistic approach of the impact of the pulp mill effluents; however, it did not predict the low DO in 2002 (Tian 2005).

The work of Golder and Stantec was revisited with a new WASP version integrating updated SOD values (Tian 2005). The SOD rate was measured by core incubation, microsensors and with in-situ closed chambers in 2004. The results of the last method were used in the model. The model was calibrated with the winter data of 1999-2000 and the 2002-2003 winter data was used to validate the model. This model was not able to predict the ice-cover, and it was calibrated. Additionally, the ice cover ratio was assumed to be homogenous over all the segments when open leads are predominantly present downstream the pulp mills. The sensitivity analysis of this study demonstrated a strong relation between SOD, pulp mill effluents and DO in the river.

Table 2- 5. Characteristics of the last two DO models developed for the UAR

Characteristic	Tian, 2005	Yu, 2006
Model	WASP6	CE-QUAL-W2
SOD (g O ₂ /m ² /d)	0.12 (closed chamber)	0.21 (core incubation)
Tributaries	15	4
Point sources	2	2
Dimensions	1	2
Ice-cover	Calibration of one ratio for all the stream	Prediction of thickness for each segment
Segments	39	102
Water quality parameters	5	15

Yu (2006) used CE-QUAL-W2 to examine a short reach of the UAR; however, this study only included the direct discharge of one of the five pulp mills. Furthermore, the DO was simulated only for winter. The DO was modeled by a two-dimensional model, using 15 water quality parameters instead of five in the previous work (Table 2- 5). The hydrodynamics of the river were improved even in low flow periods, and ice-cover was predicted by the model. It also incorporated an SOD rate measured with an improved core incubation method. The river reach was chosen the same as in the previous work and the DO was simulated only for winter. This time the calibration was done for four winters (1999-2000 to 2002-2003) instead of only one. The model changed from just 39 segments to 102 taking into account four representative slopes in the river.

In the model customization developed as part of this thesis, the modeling approach complexity increased significantly from the previous study performed by Yu in 2006. In the computational grid setup, closer values to the bathymetry were used (longitudinal change in the depth). More constituents were input in the tributaries' files, and a better approach was used to estimate the tributaries flow for Calling and Pelican River. Additionally, the phosphates were included in this calibration, and a space variable SOD was included. The temporal and spatial extents were increased, which has several advantages. Having a model for the whole year allows studying trends in summer that could impact the winter DO levels. Increasing the model reach improves its functionality as a management tool and allows a better calibration. In the previous model domain, there was not any gauge available to perform the hydrodynamic calibration. In this study, the elevation was calibrated at two stations and a new station was included in the water quality calibration (Town of Athabasca). It is very important the use of this station because there is not a long-term station at Grand Rapids and as a result the estimated "observed" values for nutrients and algae calibration are uncertain. The drawback of increasing the model complexity was the increase in the run time over 12-fold (see Appendix A).

2.7. References

Alberta Environment. (1995). "Water Quality Based Effluent Limits Procedure Manual." Government of Alberta, Edmonton, AB.

Alberta Environment. (1996). "1996 Alberta State of the Environment Report - Aquatic Ecosystems." *Rep. No. 1*, Alberta Environment, Edmonton, AB.

Alberta Environment. (1999). "Surface Water Quality Guidelines for Use in Alberta." Government of Alberta, Edmonton, AB.

Alberta Environment and Sustainable Resource Development (AESRD). (2012). *Regional Forest Landscape Assessment Upper Athabasca Region*, Forest Management Branch, Edmonton, AB.

Alberta-Pacific Forest Industries. (2006). "Sustainability Report 2005-2006." Edmonton, AB.

Chambers, P. (1996). "Assessment and validation of modelling under-ice dissolved oxygen using DOSTOC, Athabasca River, 1988 to 1994." *Northern River Basins Study*, Edmonton, AB.

Chambers, P. A., Scrimgeour, G. J., and Pietroniro, A. (1997). "Winter oxygen conditions in ice-covered rivers: the impact of pulp mill and municipal effluents." *Canadian Journal of Fisheries and Aquatic Sciences*, 54(12), 2796-2806.

Chapra, S. C. (2008). *Surface Water-Quality Modeling*. Waveland Press Inc, Long Grove, IL.

Cole, T. M., and Wells, S. A. (2008). *CE-QUAL-W2: A Two-Dimensional Laterally Averaged, Hydrodynamic and Water Quality Model, Version 3.6*. U.S. Army Corps of Engineers, Washington, DC.

Corsi, S. R., Klaper, R. D., Weber, D. N., and Bannerman, R. T. (2011). "Water- and sediment-quality effects on Pimephales promelas spawning vary along an agriculture-to-urban land-use gradient." *Science of the Total Environment*, 409(22), 4847-4857.

Drolc, A., and Koncan, J. Z. (1999). "Calibration of QUAL2E Model for the Sava River (Slovenia)." *Water Science & Technology*, 40(10), 111.

Environment Canada. (2010). "Hydrometric data." <http://www.wsc.ec.gc.ca/applications/H2O/index-eng.cfm> (accessed April 2010).

Fischer, H., List, J., Koh, R., Imberger, J., and Brooks, N. (1979). *Mixing in Inland and Coastal Waters*. Academic Press, New York.

Gautam, D. K., and Sharma, M. R. (2011). "Water quality modelling and management of Seer stream in lower Himalayas." *Nature Environment and Pollution Technology*, 10(4), 535-542.

Giles, M. A., Brown, S. B., Van der Zweep, M., Vandenbyllaardt, L., Van der Kraak, G., and Rowes, K. (1996). "Dissolved oxygen requirements of burbot (*Lota lota*) of the Peace, Athabasca and Slave river basins: a laboratory study." *Rep. No. 91*, Northern River Basin Study, Edmonton, AB.

Golder Associates, L. (1995). "Continuous Dissolved Oxygen Modeling: Athabasca River, Hinton to Upstream Grand Rapids." Report prepared for Alberta Forest Products Association and Alberta Environmental Protection, Edmonton, AB.

Hicks, F. (2009). "An overview of river ice problems: CRIPE07 guest editorial." *Cold Regions Science and Technology*, 55(2), 175-185.

Khandan, N. N., and Nirmalakhandan, N. (2002). *Modeling tools for environmental engineers and scientists*. CRC Press, Boca Raton, FL.

Lima Neto, I. E., Zhu, D. Z., Rajaratnam, N., Yu, T., Spafford, M., and McEachern, P. (2007). "Dissolved Oxygen Downstream of an Effluent Outfall in an Ice-Covered River: Natural and Artificial Aeration." *Journal of Environmental Engineering*, 133(11), 1051-1060.

Lung, W. (2001). *Water Quality Modeling for Waste Allocations and TMDLs*. John Wiley and Sons, New York, NY.

Millar Western. (2007). "Sustainability Report." Edmonton, AB.

Mossewitsch, N. A. (1961). "Sauerstoffdefizit in den Flüssen des Westsibirischen Tieflandes, Seine Ursachen und Einflüsse auf die aquatische Fauna." *Verh. Int. Ver. Angew. Limnol.*, 14 447-450.

Nelson, J. S., and Paetz, M. J. (1992). *The Fishes of Alberta*. University of Alberta Press, Edmonton, Alta.

Palmer, M. D. (2001). "Water Quality Modeling : A Guide to Effective Practice." *Rep. No. ISBN 0-8213-4863-9*, World Bank, Washington, DC.

Pietroniro, A., Chambers, P. A., and Ferguson, M. E. (1998). "Application of a Dissolved Oxygen Model to an Ice-Covered River." *Canadian Water Resources Journal*, 23(4), 351-368.

Province of Alberta. (2013). "Fisheries (Alberta) Act." Alberta Queen's Printer, Edmonton, AB.

Schallock, E. W., and Lotspeich, F. B. (1974). "Low winter dissolved oxygen in some Alaskan rivers." *Rep. No. U.S. EPA-660/3-74-008*, U.S. Environmental Protection Agency, Washington, D.C.

Schreier, H., Erlebach, W., and Albright, L. (1980). "Variations in water quality during winter in two Yukon rivers with emphasis on dissolved oxygen concentration." *Water Research*, 14 1345-1351.

Sharma, K. (2012). "The Athabasca River sediment under ice cover". Doctor of Philosophy. University of Alberta, Edmonton, AB.

Sharma, K., Mceachern, P., Spafford, M., Zhu, D., and Yu, T. (2009). "Spatial Variation of Sediment Oxygen Demand in Athabasca River: Influence of Water Column Pollutants." *ASCE Conference Proceedings*, 342(41036), 647.

Stantec, C. L. (2001). "Sensitivity analysis of a dissolved oxygen model for the Athabasca River from Hinton to Grand Rapids." *Rep. No. 108-59295*, Edmonton, AB.

Stantec, C. L. (2001). "Upgrading of a dissolved oxygen model for the Athabasca River from Hinton to Grand Rapids." *Rep. No. 108-59295*, Alberta Forest Products Association, Edmonton, AB.

Tetra Tech Inc. (2007). "The Environmental Fluid Dynamics Code User Manual Version 1.01." US EPA, Fairfax, VA.

Tetra Tech. (2009). "Hydrodynamic and water quality model of the North Saskatchewan River." North Saskatchewan Watershed Alliance, Edmonton, AB.

Thomann, R. V., and Mueller, J. A. (1987). *Principles of surface water quality modeling and control*. Harper & Row, New York, NY.

Tian, Y. (2005). "A dissolved oxygen model and sediment oxygen demand study in the Athabasca River". MSc. University of Alberta, Edmonton, AB.

Turner, D. F., Pelletier, G. J., and Kasper, B. (2009). "Dissolved oxygen and pH modeling of a periphyton dominated, nutrient enriched river." *Journal of Environmental Engineering*, 135(8), 645-652.

US EPA. (1986). "Quality Criteria for Water." *Rep. No. EPA 440/5-86-001*, Office of Regulations and Standards, Washington DC.

West Fraser. (2011). "Sustainability Report." Vancouver, BC, Canada.

Whitfield, P. H., and McNaughton. (1986). "Dissolved-oxygen depressions under ice cover in two Yukon Rivers." *Water Resources Research*, 22(12), 1675-1679.

Williams, R. J., and Boorman, D. B. (2012). "Modelling in-stream temperature and dissolved oxygen at sub-daily time steps: an application to the River Kennet, UK." *Science of the Total Environment*, 423(0), 104-110.

Yu, M. (2006). "Sediment oxygen demand investigation and CE-QUAL-W2 model calibration in the Athabasca River". MSc. University of Alberta, Edmonton, AB.

Chapter 3. Data analysis for dissolved oxygen sources and sinks

sinks

The dissolved oxygen is measured using datasondes by Alberta Environment during the ice cover period (November to March). The data collected for each winter comprises two calendar years, for simplicity, the years referred in this section are related to late winter. For example, November 2002 to March 2003 is the winter of 2003 –as the DO sags usually happen in late winter.

In the last 20 years, the winters of 1993, 1994, 2002 and 2003 had dissolved oxygen (DO) concentration very close or below the provincial chronic guideline of 6.5 mg/L (Alberta Environment, 1999) at Grand Rapids (Figure 3-1). Most notably, a historic low was reached in 2003 with a 7-day average of 5.5 mg/L, and 1-day minimum of 5.4 mg/L reaching values close to the acute guideline of 5 mg/L. The critical DO usually occurs in February having a valley through January-March. February's average for the period 2000-2006 was 7.66 ± 1.45 mg/L. In order to understand the high variability observed in the DO during this period, the main sources and sinks were analyzed with a special focus on data from 2003.

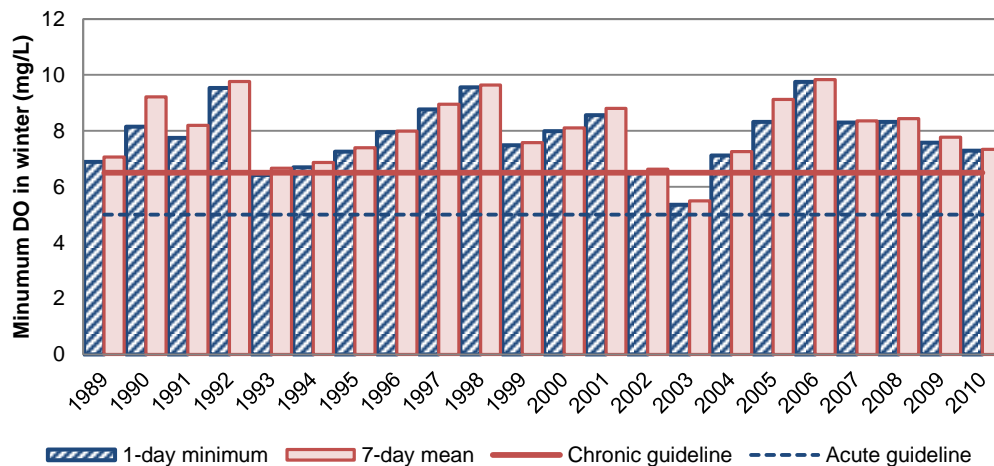


Figure 3-1. The lowest 1-day minimum and 7-day mean DO concentration in for each winter from 1989 to 2010 at Grand Rapids

3.1. Air temperature

Air temperature plays an important role in the duration of the ice cover in winter, and, as a result, in the river's re-aeration. The accumulated air temperature during three periods in winter (October-December, January-March and March-May) are plotted in Figure 3-2. A negative trend is observed starting in late October with most of the winters crossing the zero line in late November. It can be observed in Figure 3-2a that the 2003 winter had a

colder November, which may have caused ice to form early. Additionally, Figure 3-2c shows that while for most years the accumulated temperature became positive in late April, in 2002 and 2003 it was after May. This could have delayed ice break up in these years.

During the ice cover period (January-March) in 2002 and 2003, only one day had an average temperature above 0 °C, while in 2005, there were 20 days above 0 °C. In each of the remaining years, there were at least 7 warm days. Warmer days create much larger open leads in the river, for instance, decreasing the average air temperature from 0 to -20 °C decreased the final open lead length by 0.7 km downstream of ALPAC's effluent (Lima Neto, et al. 2007). The colder winter in 2003 may have been a factor that contributed to the low DO observed in that year (see *Appendix D.*)

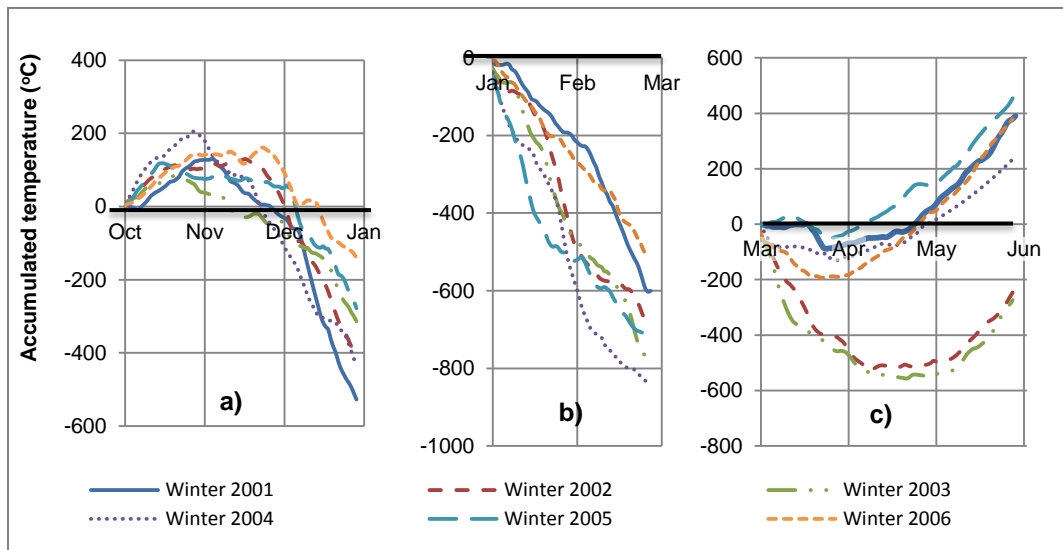


Figure 3-2. Accumulated temperature from a) October to December, b) January to February, c) March to May, winter was defined using the consecutive months (e.g. Nov. 2002 –April 2003 is winter 2003).

3.2. Photosynthesis

Photosynthesis is significantly diminished in winter due to shorter days and cold temperatures that limit algal growth. This can be confirmed by analyzing the change in DO throughout the day. According to the February's daily DO profile at the Smith station the difference between the DO at noon and midnight (Δ DO) was around 0.10 mg/L most years.

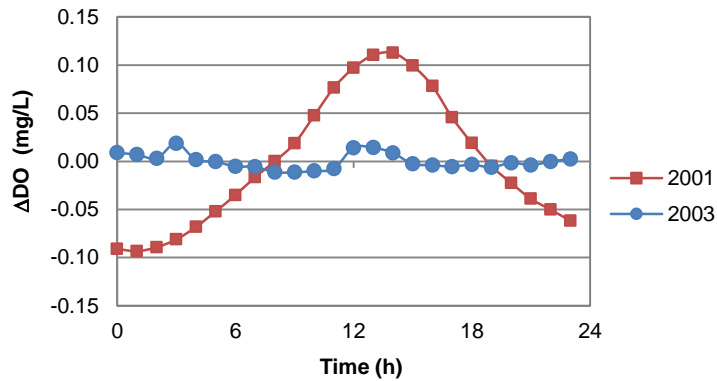


Figure 3- 3. Delta in hourly DO from the daily average in February

In 2001, a higher algal activity ($\Delta\text{DO} = 0.20 \text{ mg/L}$) was observed, while in 2003, this activity was insubstantial ($\Delta\text{DO} = 0.03 \text{ mg/L}$) (Figure 3- 3). These differences reflect the importance of appropriate calibration for the incident light regime and accounting for snow depth and albedo.

3.3. In-stream and tributary discharge

DO is expected to be positively correlated to the average flow in winter. This flow will be the main reservoir of oxygen available when the river is covered by ice. The average DO at Grand Rapids in February correlated with the inflow at Hinton, as well as the total flow (inflow + tributaries + point sources), and the flow of the four largest tributaries, which account for about 90% of the total tributaries' flow (Table 3-1). The DO in February did not correlate strongly with the flow in February; however, February's DO correlated with January's flow. This can be explained by the water retention time through the 800 km river section estimated to be 25 days (Van Der Vinne, 1992).

Table 3-1. Correlation between February's DO at Grand Rapids and flow in January at different stations

at Hinton	at Athabasca	Pembina	Berland	McLeod	Lesser	Total
0.81	0.91	0.85	0.60	0.85	0.71	0.91

The lowest flow for seven consecutive days that would be expected to occur once in ten years (7Q10), and the average flows at the Athabasca station for the months of January through March are presented in Table 3-2. The flow in January 2003 was very close to the critical 7Q10 flow, and was the lowest in the simulated period.

Table 3-2. 7Q10 flow (1952-2007) and monthly average flow for Athabasca River at Town of Athabasca (m³/s)

Year	January	February	March	Average
7Q10	53.16	58.25	59.74	57.1
2000	77.7	70.8	69.4	72.6
2001	71.4	56.3	62.6	63.4
2002	61.0	58.9	56.6	58.8
2003	54.4	63.8	70.6	62.9
2004	68.2	66.7	82.4	72.4
2005	117.8	119.9	178.3	138.7
2006	103.6	84.2	86.6	91.5

3.4. Pulp mill loading

The pulp mills are an important source of biochemical oxygen demand (BOD) in winter. The dilution factor based on the inflow is about 10 times lower in winter than in summer. The degree of wastewater treatment is reflected in the BOD load of the different pulp mills. Hinton Pulp Mill (HPM) uses aerated lagoons and clarifiers, while the rest of the pulp mills have installed more complete activated sludge treatments. The BOD concentration of HPM effluent is about 10 times higher than ALPAC's. For this reason, it is the main source of BOD load in winter, as observed in Figure 3-4.

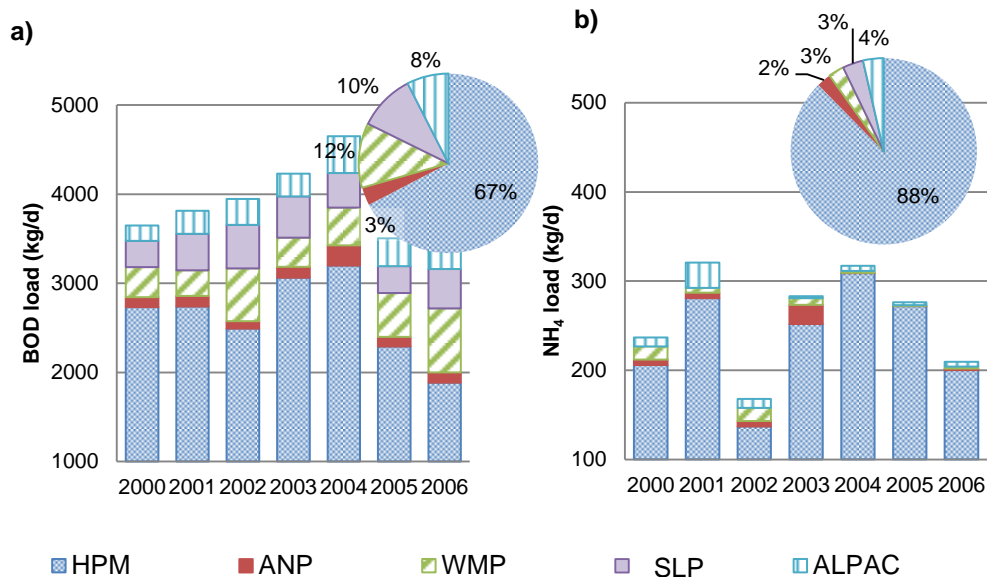


Figure 3- 4. Average pulp mills loads in winter (January -March), pie chart shows the overall average a) BOD, b) NH₄. Hinton Pulp Mill (HPM), Alberta News Print (ANP), Millar Western Pulp (MWP), Slave Lake Pulp (SLP), Alberta Pacific (ALPAC)

Based on the BOD loading from each pulp mill it is not surprising that HPM correlates significantly with the average DO at Grand Rapids in February (Table 3-3). The ammonia load of the Millar Western Pulp (MWP) and Alberta Newsprint (ANP) also correlated with the DO. However, the parameter in general for all the pulp mills did not have a high correlation.

Table 3-3. Correlation between February's DO at Grand Rapids and winter pulp mills' load

Constituent	HPM	ANP	MWP	SLP	ALPAC	Total
BOD	-0.74	-0.19	0.37	-0.46	0.15	-0.74
NH4	0.16	-0.64	-0.57	NA	0.15	0.05

In late December 2002, HPM had a peak release with a BOD load about three times the long-term average. Even though this effluent could have been flushed by February when the lowest DO was observed, it may have impacted the sediment oxygen demand (SOD). In December, the velocity of the river is low enough to let some large colloids settle and remain in the system for a long period of time, until its stabilization is complete or the spring runoff comes. To test this theory, the HPM's December BOD load over the winter average was computed, and it correlated highly (-0.80) with February's average DO.

Even though 2002 was a cold winter, with low flow and DO coming from Hinton, the BOD from HPM was significantly higher in 2003 (paired T-tests 95% confidence interval). This higher BOD likely worked synergistically with the unfavorable natural conditions to create a worst-case year and deeper DO sag in 2003.

3.5. References

Alberta Environment. (1999). "Surface Water Quality Guidelines for Use in Alberta." Government of Alberta, Edmonton, AB.

Lima Neto, I. E., Zhu, D. Z., Rajaratnam, N., Yu, T., Spafford, M., and McEachern, P. (2007). "Dissolved oxygen downstream of an effluent outfall in an ice-covered river: natural and artificial aeration." *Journal of Environmental Engineering*, 133(11), 1051-1060.

Van Der Vinne, G., and Andres, D. (1992). "Winter low flow tracer dye studies, Athabasca River, Hinton, Athabasca." *Rep. No. SWE-92/03*, Environmental Research and Engineering Department, Alberta Research Council, Alberta, Canada.

Chapter 4. Model development for prediction and mitigation of dissolved oxygen sags in the Athabasca River

4.1. Introduction

Northern rivers exposed to high biochemical oxygen demand (BOD) loads are prone to dissolved oxygen (DO) sags in winter due to limited re-aeration to few open leads, reduced photosynthesis, and minimum pollutant dilution. The Upper Athabasca River (UAR) has experienced these sags which may affect the aquatic ecosystem. A water quality model for an 800 km reach of this river was customized, calibrated, and validated specifically for DO and the factors that determine its concentration. This model improved previous model's customization (Yu 2006) by including summer and winter data, and increasing the spatial scope to the representative river reach. After validation, the model was used to assess the assimilative capacity of the river and mitigation measures that could be deployed. The calibrated and validated model is a management tool that can be used to predict low DO events and guide the mitigation measures. It can also help to understand what the main sources and sinks are, the extent of the DO sag, and the parameters the model is more sensitive to.

4.2. Methods

The general methodology for the model development followed five well defined stages: data collection, model set up, calibration, validation and application (Figure 4- 1).

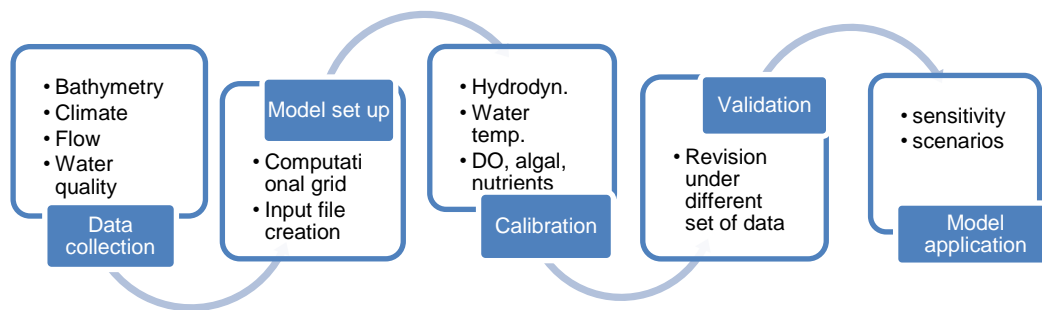


Figure 4-1. General approach for model development

In the model set up, CE-QUAL-W2 was customized, and the input files were generated. The default parameters and kinetic coefficients were refined through calibration for the years 2000 to 2003. These years represent extreme DO conditions reaching minimum values in winter > 8 mg/L and < 5.5 mg/L in 2001 and 2003, respectively. After the predicted concentration agreed with the observed values, the model was run with a second set of data from 2004 to 2006 for validation. Finally, the model was used to

evaluate different scenarios and guide in mitigation. These stages are explained in detail in the following subsections.

4.2.1. Model customization

Model domain

The model domain (Figure 4-2) was from Hinton to Grand Rapids (800 km), which drains about half of the total watershed area. This river reach was selected because it includes the point sources, and the DO sags are observed within the selected model domain.

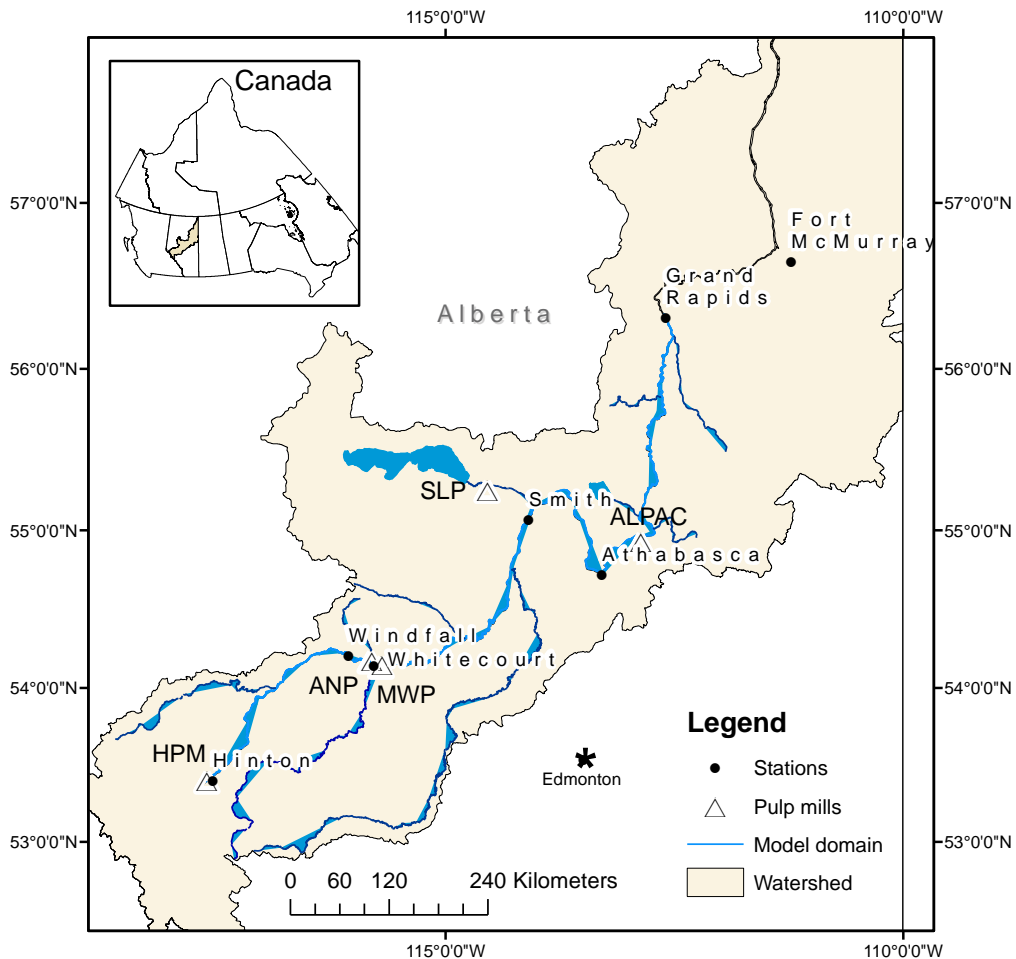


Figure 4-2. Map of study area with pulp mills and stations used in the model

The population density in this area is considerably lower than the rest of the province as only four towns have more than 2,000 people (Government of Alberta 2011). This part of the river, however, receives the effluents of five pulp mills: Hinton Pulp Mill (HPM), Alberta Newsprint (ANP), Millar Western Pulp (MWP), Slave Lake Pulp (SLP) and Alberta Pacific (ALPAC). Additionally, the three towns of Hinton, Whitecourt and Athabasca

release municipal effluents into the river. Hinton’s sewage water is treated in combination with HPM wastewater; when combined with municipal effluent will be referred as HPM&S. This reach of the river also receives the discharge of ten major tributaries, listed with their distance from Hinton, Berland River (105 km), Sakwatamau River (201 km), McLeod River (202 km), Freeman River (289 km), Pembina River (376 km), Lesser Slave River (430 km), La Biche River (596 km), Calling River (610 km), Pelican River (720 km) and House River (770 km).

Data compilation

Different federal and provincial sources provided data, flow (Environment Canada 2010), water surface elevation Environment Canada, (Lazowski, Personal communication), and meteorological (Environment Canada 2012). Alberta Environment provided the water quality and temperature data for tributaries (McEachern, Personal communication); for the Athabasca River at the Hinton, Athabasca and Fort McMurray stations (Alberta Environment 2012); and at Windfall, Smith and Grand Rapids stations (Jackson, Personal communication). Table 4-1 shows the stations used for input file creation and calibration.

Table 4-1. Stations used in the model customization, calibration and validation¹

Type	Flow	Water quality & temperature	Meteorological	Elevation
<i>Tributaries</i>				
Berland River	07AC007	AB07AC0010		
Sakwatamau River	07AH003	AB07AH0010		
McLeod River	07AG007	AB07AG039/ AB07AG0390		
Freeman River	07AH001	AB07AH0420/ AB07AH0430		
Pembina River	07BC002	AB07BC0070		
Lesser Slave River	07BK001	AB07BK0125/ AB07BK0130		
La Biche River	07CA011	AB07CA0040		
Calling River		AB07CB0640/ AB07CB0630		
Pelican River		AB07CB0720		
House River	07CB002	AB07CB0770		
<i>In-stream</i>				
Hinton	07AD002	AB07AD0110/ AB07AD0100	306A009	
Windfall	07AE001	AB07AE0210		07AE001
Whitecourt			3067371	
Smith		AB07BD0066		
Athabasca	07BE001	AB07BE0010	3060L20	07BE001
Grand Rapids		AB07CC0140		
Fort McMurray	07DA001	AB07CC0030	3062693	

¹Gray cells represent not available or required data

Most of the data were obtained for the 2000 to 2006 period, except the flow at La Biche River (1982 to 1995), and the tributary water quality and temperature (see Appendix C). The tributary water quality information was very scarce, as only Pembina River, McLeod River and Lesser Slave River had recent records (See *Appendix C. Water quality available for tributaries*). For the remaining tributaries, the available data came from sporadic sampling campaigns from 1984 to 1996. The flow and elevation data were available with a daily interval. For the Berland, Sakwatamau River, Freeman River, House River and Windfall stations, the flow was available only in the open-water period. The Hinton, Athabasca and Fort McMurray water quality in-stream stations form part of the provincial Long Term River Network with a monthly sampling frequency throughout the year. In contrast, Windfall, Smith and Grand Rapids Data Sonde stations only work through the ice-cover period measuring water temperature, pH, conductivity and DO every 15 min. The daily average air temperature was obtained for the Hinton and Athabasca stations, whereas the dew point temperature, wind speed and wind direction was available for the Whitecourt and Fort McMurray stations hourly. The Fort McMurray station also included weather statements such as *clear* and *cloudy* these descriptors were transformed to cloud cover rating (0-10) as presented in Table 4-2.

Table 4-2. Weather statements used for determining cloud cover

Weather	Cloud Cover
Clear	0
Cloudy	8.5
Mainly Clear	1
Mostly Cloudy	7.5
Other	5

The point source flow, temperature and constituents were obtained from pulp mills' personnel for HPM&S (Start, Personal communication), MWP (Shipton, Personal communication), and ANP (Moore, Personal communication). The effluent information for ALPAC was obtained from Alberta Environment (McEachern, Personal communication), and for SLP from the Lesser Slave River model developed by Alberta Environment (Hazewinkel, Personal communication). Pulp mills' sustainability reports provided their maximum permitted BOD load (Alberta-Pacific Forest Industries 2006; Millar Western 2007; West Fraser 2011). Alberta Environment provided the effluent quality for the two municipalities (Shaw, Personal communication). This information was obtained from the 2000 to 2006 period, except for Whitecourt for which the 2001 year was not available. The flow and temperature were reported on a daily basis for the point sources, except for Athabasca, which was monthly. The CBOD was reported three times per week for most

of the pulp mills except for MWP, which was recorded daily. The nutrients were measured on a daily (MWP, Whitecourt effluent), weekly (ANP, SLP) and monthly basis (ALPAC, HPM&S, Athabasca effluent). The effluent DO was only measured by MWP and Whitecourt on a daily basis.

The sediment oxygen demand (SOD) values used in the model were obtained from the last survey performed by Sharma *et al.* (2009). The values of these samples ranged from 0.22 g/m²/d to 1.82 g/m²/d at 20 °C. These SOD measurements were spatially interpolated to use a specific value per segment, and adjusted using temperature coefficients (99% at 20 °C and 10% at 0 °C).

Data estimation and preparation

As previously mentioned, the winter flow information was not available for all the tributaries. Less than 20% of all hydrometric data published in Canada represents stream flow under ice-covered conditions (Hamilton and Moore 2012). This is in part due to instrument malfunction and inadequacy of stage discharge rating techniques (Guay et al. 2012). The winter flow was estimated using annual hydrographs from the flow stations presenting similar flow regime, which had a complete record. Rivers in this geographic region are characterized by flows that decline rapidly to a low level during late autumn, winter and early spring due to a sub-zero cold (Haines et al. 1988). The hydrographs were obtained using daily flows expressed as a percentage of the average open-water flow (April to October). The flow in the ice-covered period represented about 10% to 20% of the average flow in the open-water season for most of the rivers with complete record. The Lesser Slave River sub-basin is different from the rest of the tributaries since it represents the outlet of a big lake. The daily flow as a percentage of the open-water flow was averaged for the rest of the tributaries, and it was used to calculate the winter flow for the tributaries without record. For La Biche River, whose flow data was only available from 1982 to 1995, a runoff coefficient (flow/precipitation) was used to calculate the flow. For Calling River and Pelican River the flow was calculated using the watershed ratio of the closest tributary with records (Figure 4- 3). The watershed areas were calculated using Arc-View GIS ® (House /Pelican = 0.94, Calling /La Biche = 0.32).

Slave Lake Pulp discharges into the Lesser Slave River about 50 km upstream where the river intersects with the Athabasca River. The BOD entering the Athabasca River was calculated using the first-order kinetic equation $C = C_o \exp(-kt)$, which considered the Lesser Slave River's flow, temperature and velocity.

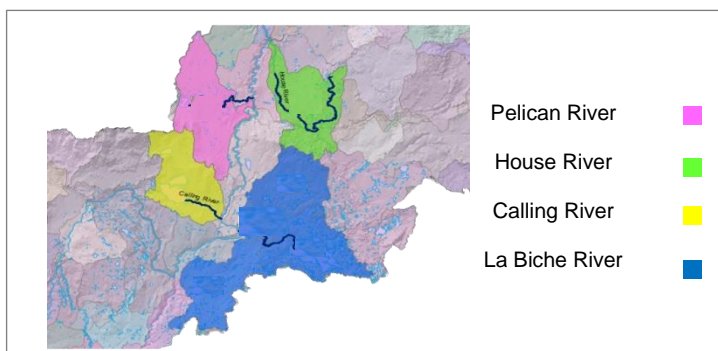


Figure 4-3. Watershed area used to estimate the tributary flow

Since the water quality information was very limited for most of the tributaries, the monthly average values were calculated for each parameter using the available information for each tributary. This approach may be improved in the future by using a watershed model such as HSPF or SWAT. Figure 4-4 shows how the dissolved organic carbon (DOC) is usually higher for the rivers most downstream in the studied reach (See *Appendix B*. Box plots for in-stream, tributaries and pulp mills constituent concentration for other constituents).

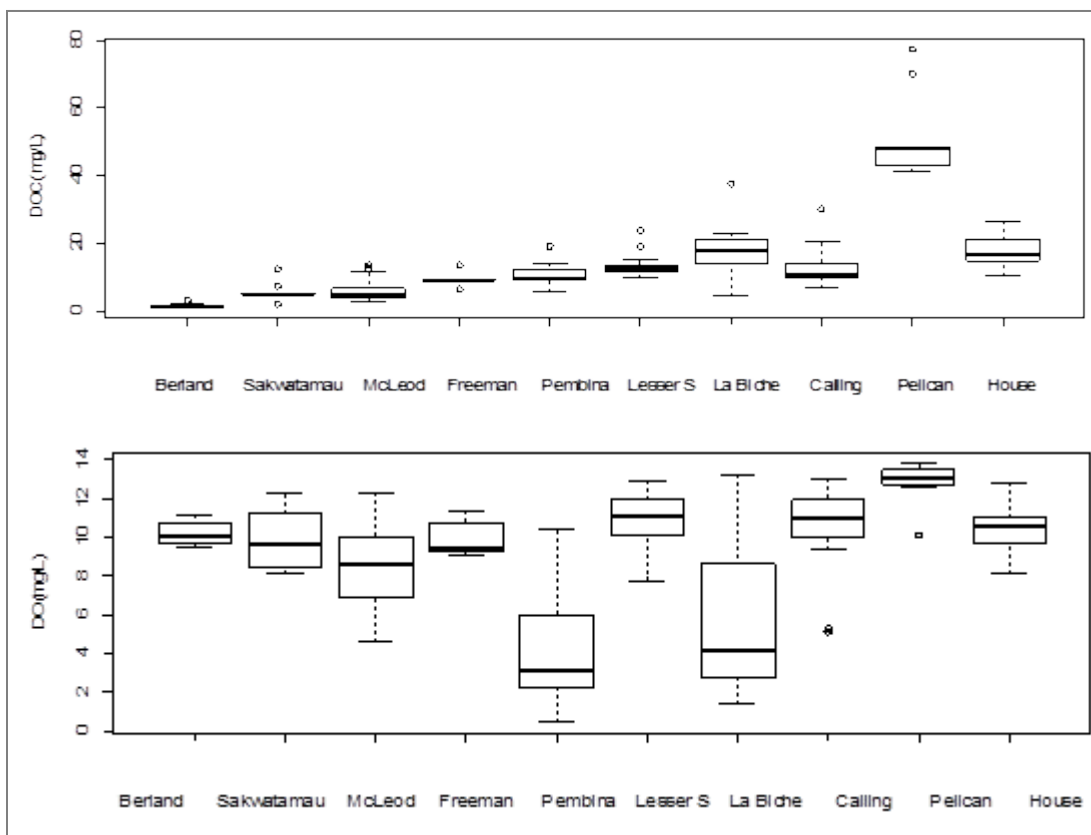


Figure 4-4. Box plots showing DOC and DO concentration in the tributaries, from left to right increases distance downstream Hinton

The DO reaches very low values for some tributaries such as Pembina and La Biche, which may lower the Athabasca's River DO concentration after mixing. This can be even more pronounced for Pembina River, whose flow is about 10% of the total flow at the Town of Athabasca. A power function that relates the flow to the concentration has been used to estimate tributary mass loadings (Littlewood 1992; Thomann and Mueller 1987). Noton (1996) used linear regression to correlate the DO to the Pembina River discharge using six measurements from 1989 to 1993, with a correlation $R^2 = 0.42$. However, the DO correlation to the daily discharge increased when using a power function (Figure 4-5), $DO = 1.059Q^{0.735}$, $R^2 = 0.88$ ($n=6$ from 1990 to 1996 and $n=4$ in 2003). Even though this approach may need further improvement, implementing this equation produced better results than using a monthly average that is constant for the simulated years.

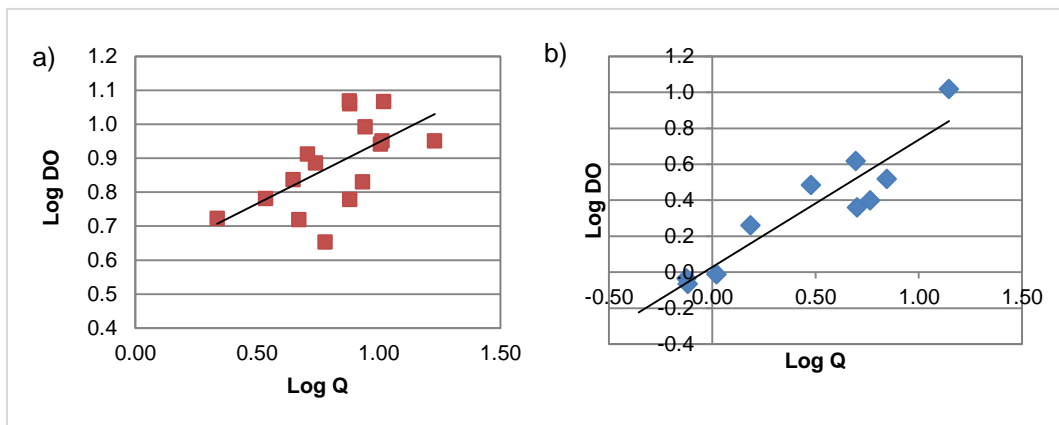


Figure 4-5. Flow-DO power relationship used for input file creation a) McLeod River, b) Pembina River

The distributed tributaries were estimated by flow calibration. The flow that is not accounted with the major tributaries in January in the water balance is very likely to come from groundwater infiltration, which has a low DO concentration. When the flow is low, the groundwater infiltration increases. For this reason, it is suspected that 2003 may be a year with important ground water contribution. Chambers *et al.* (1997) attributed part of DO depletion under ice cover to oxygen-depleted groundwater. Groundwater discharges to a surface water body when the phreatic surface or water table is above the water body level (lowu, 2007). These conditions are likely to happen in winter when the mainstream flow and elevation reach minimum annual values. Additionally, the distributed tributaries required for flow balance in the open-water season usually come from non-perennial creeks. The distributed tributaries used for flow balance in January and February were therefore assumed to come from groundwater, with a DO concentration of 0 mg/L. A field

dye study performed below ALPAC suggested the existence of important groundwater contribution close to La Biche River (Zhang and Zhu 2011).

All the information was organized, analyzed and cleaned previously to be used as input data. The steps that were applied in for the creation of the time series were:

1. The concentration values below the detection limit were used as the 50% of the threshold.
2. In order to fill gaps of less than three days linear interpolation was used.
3. Outliers were analyzed and if the values were > three standard deviations the data was not included to evaluate the error in the calibration.

Some water quality variables monitored by Alberta Environment are different from the state-variables used by the model. They were transformed using the relationships and parameters presented in Table 4-3, relying initially on average literature-derived values, which were then adjusted as necessary within reported ranges during the calibration process.

Table 4-3. Parameter transformation to CE-QUAL-W2 state variables

Parameter	Abbreviation	Equation used for variable transformation
Inorganic Suspended Solids	ISS	=NFR-(TOC-DOC) *K ₁
Dissolved Reactive Phosphorous	PO4	= K ₂ * TDP
Particulate silica	PSI	=NFR/FR* DSI
Labile dissolved organic matter	LDOM	= ((DOC)* K ₁)* K ₃
Refractory dissolved organic matter	RDOM	= ((DOC)* K ₁)*(1- K ₃)
Labile particulate organic matter	LPOM	= [(TOC - DOC)* K ₁]* K ₄
Refractory particulate organic matter	RPOM	= [(TOC - DOC)* K ₁]* (1-K ₄)
Algae	ALG	= CHL / K ₅
Total inorganic carbon	TIC	= (HCO ₃ ⁻ + CO ₃ ²⁻ + H ₂ CO ₃)* (1-NFR/FR)

K₁ Factor to convert from organic carbon to organic matter, K₂ Fraction from total dissolved phosphorus that is phosphate, K₃ Fraction from dissolved organic matter that is labile, K₄ Fraction from particulate organic matter that is labile, NFR, non filterable residue or TSS; FR, filterable residue or TDS

Model setup

The computational grid (Figure 4-6) consisted of five branches, each one representing a river slope (1.3, 0.9, 0.6, 0.4, 0.6) m/km. The model used 219 active segments with an average length of 3.5 km. Each segment had six active layers for a total of 1314 cells. The layers were 1 m deep, except for the first one, which was 0.5 m deep. The last layer

improved numerical stability under low flow, since those conditions can dry up segments in the middle of a branch causing the model to stop running (Cole and Wells 2008). The surface layer width was obtained by using the simplified method for generating cross-sections for long river reaches from (Hicks 1996), which was adapted using Google Earth's ruler tool instead of topographic maps. The remaining layers' widths were calculated as a percentage of this surface layer using the proportions of the bathymetric survey performed by Alberta Environment in the '70s. The layer's widths were slightly adjusted during calibration when changing the Manning's friction coefficient did not bring water levels close to observed values.

4.2.2. Calibration and validation

The calibration (2000-2003) was completed in four different stages: hydrodynamics, temperature, water quality and DO. The calibrated water quality parameters were ammonia (NH_4), nitrates-nitrites (NO_3), phosphates (PO_4) and phytoplankton-algae (ALG), each of which are important in controlling oxygen demand. The validation was performed from 2004 to 2006 after the model reproduced concentrations at the Athabasca station. The model was further validated using the results of a synoptic survey performed by Sharma *et al.* (2009) in the fall of 2006. The statistics used for the calibration and validation were mean absolute error (MAE) and relative mean absolute error (RMAE) (See *Appendix G* for a description of these and other statistics used).

The hydrodynamic calibration consisted of checking that the flow and water surface elevation predicted were close to the observed at the Athabasca and Windfall stations. The flow calibration was achieved by generating the distributed tributary input files for each branch. Afterwards, the elevation was calibrated by adjusting the Manning's coefficient, by refining the channel slope, and tuning the segment's width, following the recommendation in the model's manual (Cole and Wells 2008). The water temperature was calibrated at the Athabasca station using the three coefficients in the wind speed formulation and the wind sheltering coefficient (Cole and Wells 2008). The ice cover was calibrated by changing the albedo coefficient, the coefficient of water-ice heat exchange, and the fraction of solar radiation absorbed in the ice surface.

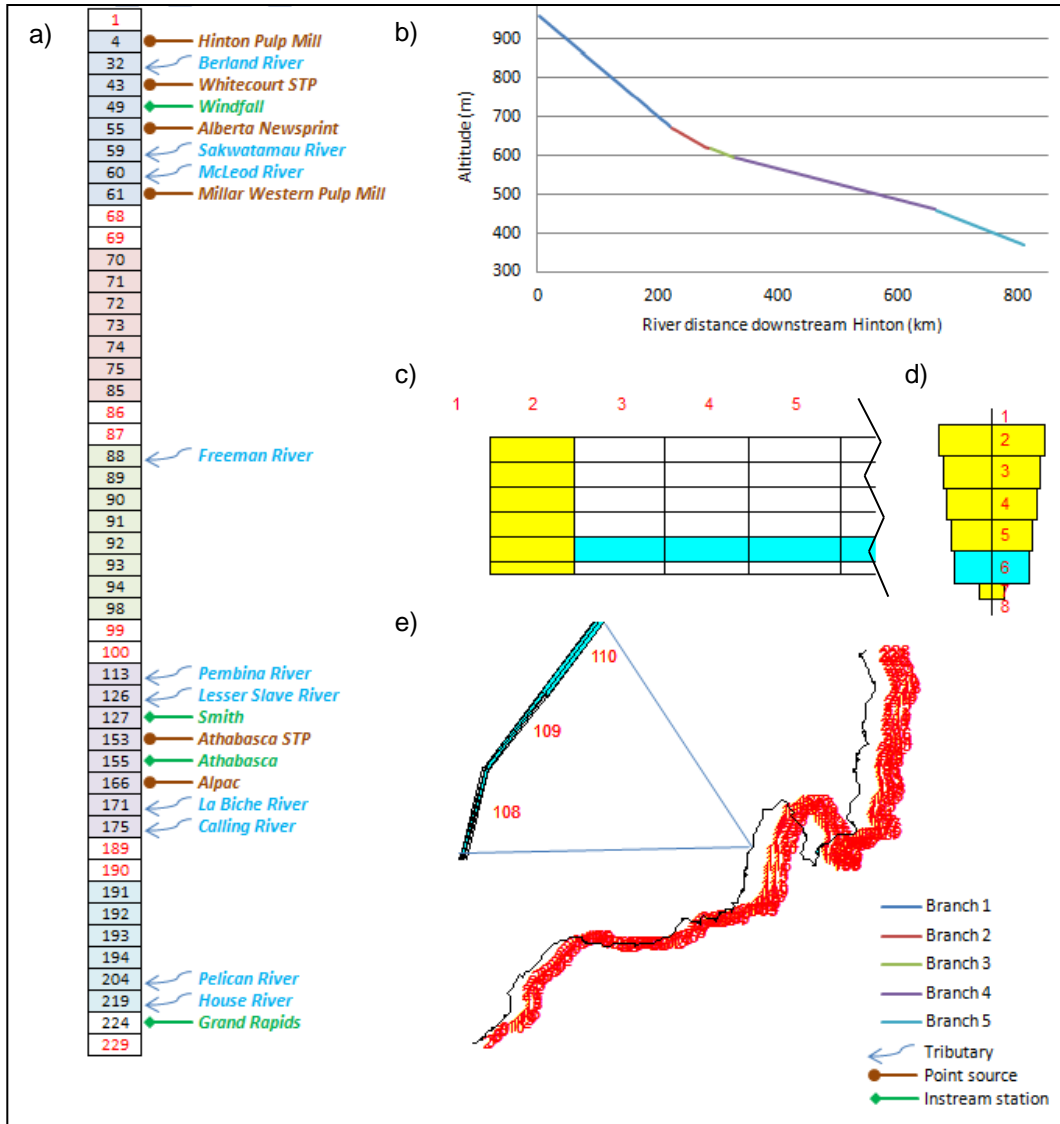


Figure 4-6. Schematics showing a) relevant segments with tributaries, point sources and in-stream stations, b) elevation profile, c) side view, d) end view, e) top view

The water quality was calibrated at the Windfall, Smith and Grand Rapids datasonde stations for DO in winter, and at the Athabasca station for all the year round calibrated constituents. A preliminary sensitivity analysis determined which kinetic coefficients and parameters [AG (maximum algal growth rate), EG (maximum epiphyton/periphyton growth rate), LDOMDK (labile dissolved organic matter decay rate), LPOMDK (labile particulate organic matter decay rate), POMS (particulate organic matter settling rate), KBOD (5-day BOD decay rate), RBOD (ratio of CBOD5 to ultimate CBOD), NH4DK (ammonium decay rate), NO3DK (nitrate decay rate), CBODS (CBOD settling rate), SOD (zero-order sediment oxygen demand)] have a stronger impact in the DO. The analysis followed the Latin Hypercube Sampling (LHS) Technique (Jaffe and Ferrara 1984)

performing 48 simulations by randomly changing the kinetic coefficients according to their values in the literature and their normal or log-normal distribution (See Appendix E). The DO calibration was performed in two stages, first by using a constant SOD value over time, and by varying the SOD with respect to the BOD in early winter.

4.2.3. Model application

Once the model was validated, different scenarios were evaluated under winter conditions. The base scenario was defined using average values (2000–2006), and a critical flow (CF) calculated as the 30% of the upstream boundary condition (Hinton) and main tributary flow. This resulted in a flow at the Athabasca station very close to the 7Q10 or seven-day consecutive low flow with a ten-year return frequency. The assimilative capacity was defined using a DO threshold of 7 mg/L, which provided a safety factor of 0.5 mg/L higher than the provincial chronic guideline to account for changes in the SOD and background DO.

Effect of different parameters

The effect of different parameters on the DO level was assessed by changing the pulp mills BOD, background DO, SOD and tributary load (organic matter and nutrients) to determine for which parameter the model is more sensitive. The BOD of all the pulp mills was increased by one standard deviation (σ) or 43%, and the results were compared to a proportional increase of the tributary load; to increasing the SOD by the same percentage, and to a decrease in the background DO by 1σ . Afterwards, the effect of coupling either high SOD or low background DO with a 1σ increase in BOD was also assessed. The combination of these three scenarios was deemed as the “worst-case scenario” and it was used to evaluate mitigation options.

Climate change

Kerkhoven and Gan (2011) evaluated the potential hydrologic impact of climate change to the Athabasca River Basin. They used the general circulation models (GCM) and CO₂ emission combinations, projecting an average temperature increase of 5 °C in the basin, which will shorten the snowfall season and increase sublimation in the Athabasca River Basin. The mean annual snowpack in the basin is strongly correlated to the mean annual flow, which is predicted to decline significantly by the end of the twenty-first century. The average change in the mean minimum flow is estimated to be -41%. The base case scenario, AV, was modified by taking into account this flow reduction and an air temperature increase of 5 °C.

Variable flow and BOD load

Different scenarios were run by increasing the pulp mills' average load by 1σ , 2σ , 3σ and the maximum permitted load at different flow conditions. The results were evaluated in a contour graph with three DO levels (> 7 mg/L optimum level, 7 mg/L to 5.5 mg/L critical DO range, < 5.5 mg/L acute critical range). This contour graph was then used to determine the maximum assimilative BOD at average flow conditions and the minimum assimilative flow at average BOD loads. Since the water elevation at the Athabasca station is available on near-real-time, a warning system can be developed with respect to the pulp mills' BOD released to the river at certain flow-elevation value. A three-level warning system was suggested from these results based on variable BOD load objectives at different flow thresholds.

Engineering controls

Engineering controls were evaluated under the worst-case scenario, which simulated values similar to the 2003 winter. HPM&S is the main contributor of BOD in the river, due in part to its high flow and level of wastewater treatment. ALPAC, on the other hand, has better technology in place for treatment. The effect of upgrading HPM&S wastewater treatment to achieve BOD levels comparable to ALPAC's effluent was evaluated. Another alternative assessed was injecting oxygen into the effluent. The standard oxygen transfer efficiency for ALPAC's effluent was estimated as 53% (Lima Neto et al. 2007). The minimum oxygen that needs to be injected to bring the DO concentration at the guideline level under the worst-case scenario was found using the model and taking into account this efficiency.

4.3. Results and discussion

4.3.1. Calibration and validation

The calibration and validation performed comparably with similar absolute error values. For brevity, the MAE or RMAE was calculated by joining both datasets and they are presented in the following sections (See complete set of graphs and error values in *Appendix H*. Extended results for calibration and validation).

Hydrodynamics

The initial simulation without distributed tributaries could predict the rising and falling limb timing, but not the magnitude of the peak flows with an RMAE of 22% at the Athabasca station. Most of this error came from the hydrograph peaks in summer, due to runoff of

small tributaries and creeks not taken into account in the model. After including the distributed tributaries, the model was effective in decreasing the RMAE (2.57% at Windfall and 5.99% at Athabasca station). The results for the Athabasca station are presented in Figure 4-7a. While the use of synthetic hydrographs was not optimal, the results demonstrated that the methods adequately derived these flows.

Figure 4-7b shows the simulated and observed water surface elevation for the Athabasca station. The MAE in the open-water period was 9 cm for the Windfall station and 7 cm for the Athabasca station, while the year round MAE at the Athabasca station was 15 cm. Even though the model produced a reliable elevation in the open-water period, it underestimated the elevation and the travel time in winter. This is because the model does not have the capability to include ice friction in winter, and therefore, it over-predicts the water velocity and under-predicts the water depth.

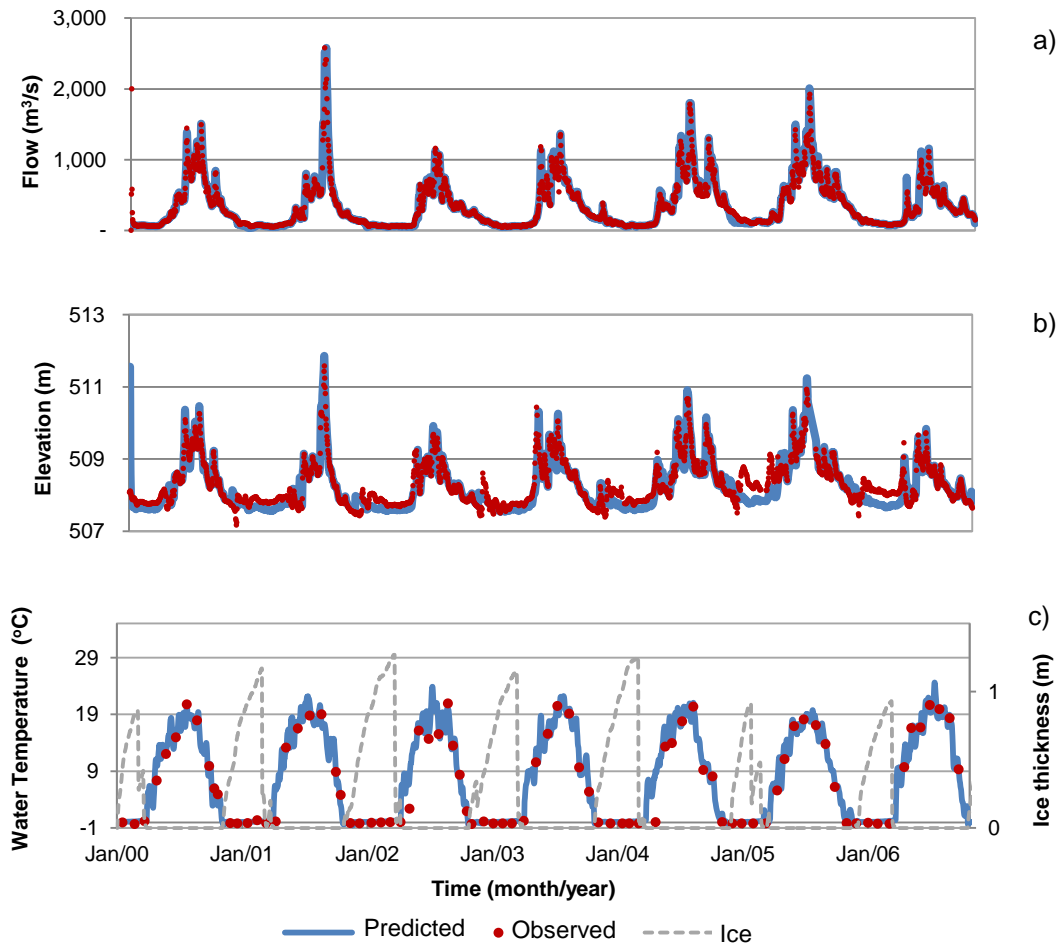


Figure 4-7. Hydrodynamic and water temperature calibration and validation at Athabasca station a) flow, b) elevation, and c) water temperature showing ice simulated

The travel time in winter was estimated as 21.3 ± 4.4 d using the conductivity in the Windfall and Grand Rapid stations for the 2000 - 2006 period. This agrees with the value reported from a field study of 25 d (Van Der Vinne and Andres 1992). However, the model predicted a lower travel time of 14 d as the hydrodynamic solution does not take into account ice roughness (Cole and Wells 2008). While it is possible to artificially increase the bottom roughness to account for the ice friction, it will require separate bottom roughness for open water and ice cover conditions. In addition, the velocity field modeled under such an assumption will not be accurate as the actual ice-covered flow is different. For these reasons, the model was calibrated using a unique bottom roughness coefficient, and the difference in the travel time was counterbalanced by increasing the oxygen related kinetic coefficients. Even with this adjustment, the calibrated coefficients were still within the range reported in the literature as presented in the water quality section. However, it is worth mentioning that observed water elevation in winter is deemed to have higher uncertainty than in open water conditions (Hamilton and Moore 2012). There is an inadequacy of the open-flow stage discharge rating technique for under-ice flow, caused primarily by backwater effects. Additionally, the area calculated from the open flow stage-area rating in winter could be erroneous depending on the shape of the ice cover, resulting in a positively biased stage reading (Guay et al. 2012).

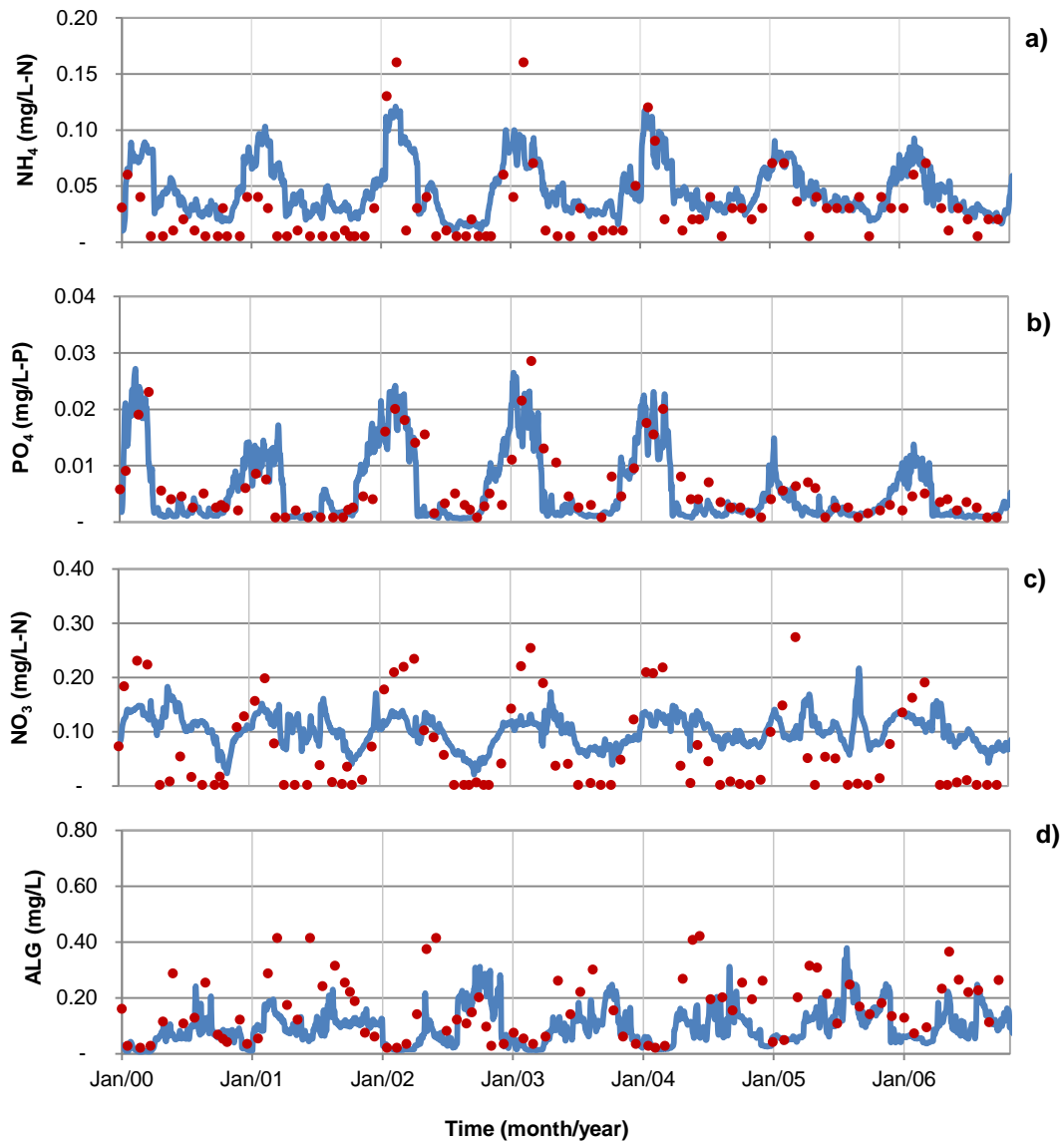
Water temperature

The water temperature affects the rate of the biological and chemical reactions in the river, and also determines the ice formation and break-up timing. As observed in Figure 4-7c, the annual trend was properly simulated with an MAE of 0.88 °C at the Athabasca station. The majority of this error came from the break-up period, when the model usually predicted an early melt. However, the model was able to effectively predict the ice cover for all winters, as well as forecast the earlier break up for the warmer years of 2005 and 2006. The albedo is set up in the model as a constant value even though the snow-water-equivalent (SWE) changes every year (35.55 mm, 42.45 mm and 42.20 mm for 2000, 2001 and 2002 respectively (Mahabir 2007)). The ice-break up is very sensitive to this value, for some years the correct ice break-up timing was predicted with a value of 0.6 while others it was 0.8. Further research is required to determine the feasibility of adding the SWE as a parameter in the meteorological input file to get more accurate temperature and ice cover predictions.

Water quality

The overall annual water quality patterns were satisfactorily simulated; predicting higher concentrations in winter due to low dilution, except for phytoplankton algae whose growth

is more favorable in summer (Figure 4-8). Even though benthic algae is more likely to survive winter conditions, the Long-Term River Network only reports phytoplankton biomass (as chlorophyll-*a* in $\mu\text{g/L}$), there is not available information for epilithic or benthic algae that could be used for calibration. The algal values were under predicted for some years, which may be attributed to the lack of input concentration for the tributaries (few samples and most of them > 10 years old).



○ Observed — Predicted

Figure 4-8. Water quality calibration and validation at Athabasca station a) ammonia, b) phosphate, c) nitrates-nitrite, d) phytoplankton algae

The LHS sensitivity analysis showed a very weak relationship with most of the kinetic coefficients with R^2 coefficients of 0.03 ± 0.04 except for SOD, which had a high correlation (Figure 4-9). The SOD was identified as a very important parameter for the DO calibration, which coincides with previous studies (Stantec 2001; Tian 2005). The SOD values used in this model were based on the most recent measurements with an improved sediment core sampling method (Sharma et al. 2009). These values were in general higher than previous rates reported (Tian 2005; Yu 2006). Since the SOD was input variable through the river length, a more accurate DO longitudinal profile is expected to be modeled. By using the SOD values obtained in the 2006 survey, the model was able to simulate both the DO trend and magnitude, predicting the higher values in 2005 and 2006 (Figure 4-10).

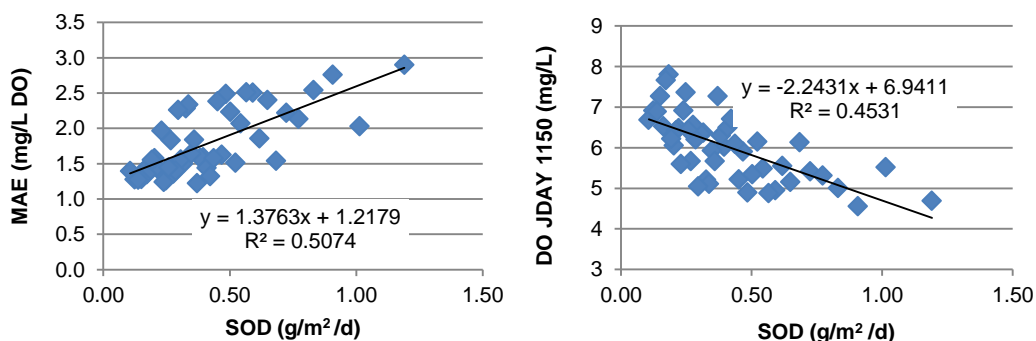


Figure 4-9. LHS analysis for SOD showing correlations with a) MAE and b) DO at 1150 Julian Day (winter 2003)

A preliminary model setup from the Town of Athabasca to Grand Rapids presented better results for the DO calibration (see Appendix F. Preliminary run from Town of Athabasca). It was observed that most of the time the errors and DO values did not change a lot from Athabasca to Grand Rapids. This may be because of the shorter reach and lower inflow received from tributaries. Therefore, it is recommended to focus the calibration effort from Hinton to Athabasca, which will reduce the run time, and then polish the calibration for the complete reach.

Although the model with the complete model domain predicted that the lowest DO would occur in 2003, it overestimated the actual amount. The model accurately reproduced the DO levels at the Windfall station for each year; however, at the Smith station, it started to

depart from the observed values in 2001 and 2003. These two years represent two extremes in DO concentration. Even though 2001 had low flow and an average BOD load, the DO was higher than normal. In an average year, the DO drops by about 4 mg/L from Windfall to Grand Rapids, but in 2001, it only dropped about half this value. This made it very difficult to bring the DO in 2003 close to the observed values using constant SOD values without compromising the fit in 2001. The MAEs were 0.54, 0.95, 1.07, and 1.32 mg/L for the Windfall, Smith, Athabasca and Grand Rapids stations, respectively.

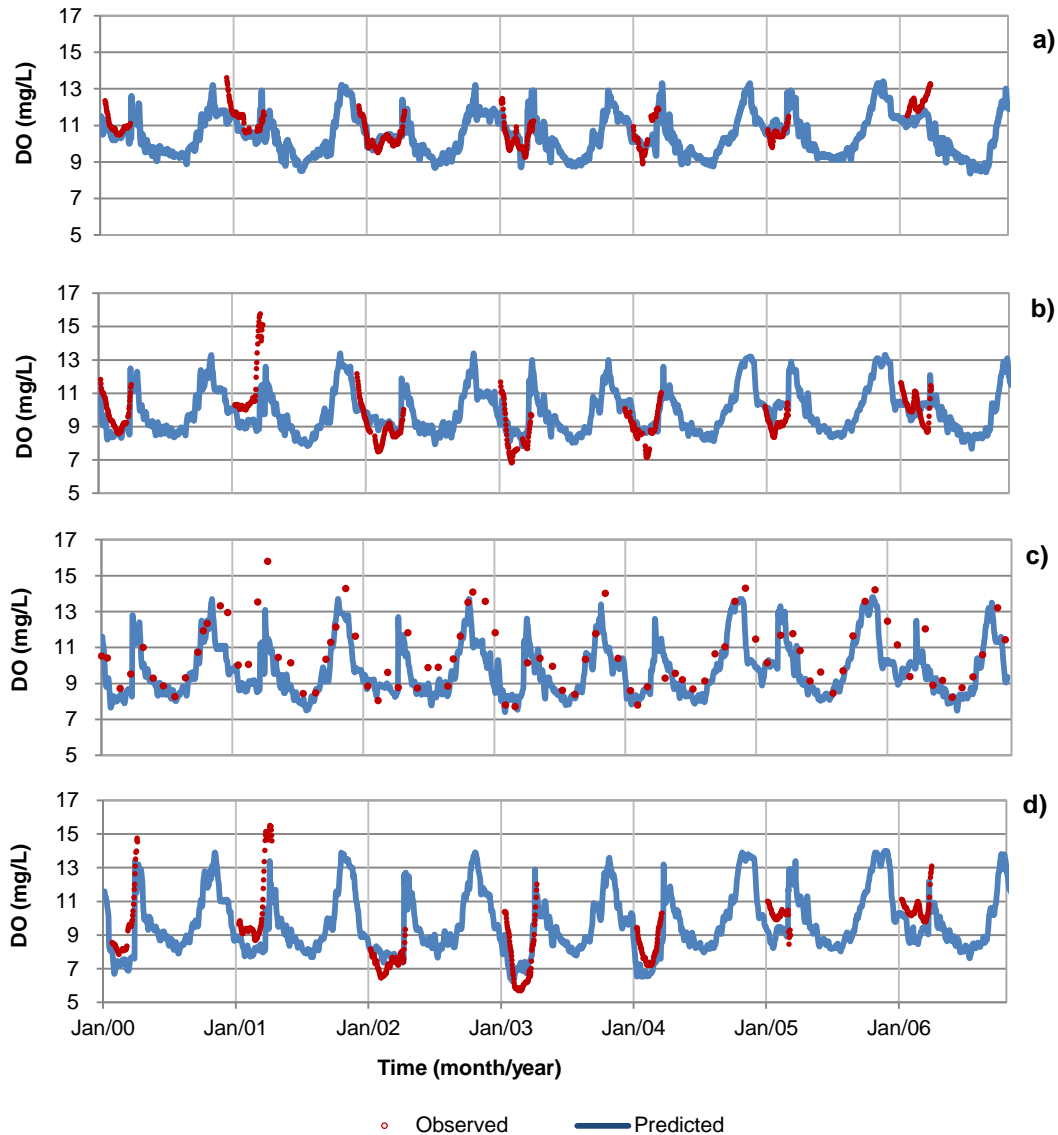


Figure 4-10. DO calibration and validation at different stations a) Windfall, b) Smith, c) Athabasca, d) Grand Rapids

The difficulties in predicting the high DO concentration in 2001 could be related to the model's inability to properly take into account all the important processes in the DO

balance such as the ice cover. Another cause could be due to external forcing factors (boundary conditions, point sources, and meteorological data) not well represented. Temperature plays an important role in the extent of the open leads downstream of the pulp mills. The open lead downstream ALPAC can range from a few hundred meters to several kilometers. However, the model does not consider the effect of the open leads because this would require a finer grid with segments through the cross-section. Although CE-QUAL-W2 cannot model differences in transversal direction, the main advantage of this model over other widely used 3D models is that CE-QUAL-W2 consistently predicts ice formation and breakup, while for other models such as EFDC and WASP, the ice cover is externally provided. These models were developed where the winters are not so long and cold. The DO depletion in these regions regularly occurs in summer when the algal growth reaches its maximum. Therefore, the accurate simulation of the ice breakup is not as important as it is to simulate the DO dynamics in the high-latitude rivers.

The contribution from Berland, McLeod, Pembina and Lesser Slave River to the Athabasca River's flow and water chemistry is very important in winter. This was confirmed with the longitudinal profile of DO in the river (Figure 4-13) in which there is a DO drop at Pembina River. Therefore, more complete water quality information from those tributaries will improve the model's reliability. Li *et al.* (2008) presented the genetic adaptive general regression neural networks as a method to predict the nitrogen composition in streams. This method could be a feasible and cost-effective way that can be explored. On the other hand, there are available watershed models that can be used to calculate these sources. The Hydrological Simulation Program-FORTRAN (HSPF) has been widely reviewed and applied since 1980, and from 11 models reviewed it has the most complex mechanisms for the simulation of subsurface water quality processes (Yang and Wang 2010).

Another challenge for the model calibration was the SOD data availability. Even though the SOD is a major factor consuming DO in aquatic environments (Thomann and Mueller 1987; Truax et al. 1995), there was a lack of annual representative SOD values for the model customization. When examining the DO sinks for February's inter-annual average (Figure 4-11 **Error! Reference source not found.**), the SOD is the highest DO sink in the river (46%), followed by the carbonaceous BOD (31%), with the rest coming from autochthonous organic matter decay, nitrification, and algae and epiphyte respiration. The SOD contribution agreed with other authors who found it to be responsible for about 50% of the oxygen depletion (Hanes and Irvine 1968; Matlock et al. 2003).

The SOD results from organic matter deposited on the channel bed from external sources (leaf litter or humic substances) or internal (settling of BOD) (Cox 2003). The oxygen demand on the river bed is expected to change from year to year depending on the depositional processes in the river. Peak BOD loads from pulp mills in periods with low river velocity may enhance the SOD. The effect of December's BOD load on DO was evaluated by increasing or decreasing the SOD proportionally. The results were favorable as the model decreased the MAE to 1.26 mg/L, reducing the overestimation in 2003 and underestimation in 2005 and 2006. A significant part of the remaining error came from the high DO values observed in late winter in 2000 and 2001 (Figure 4-10). These predicted values correspond to DO saturations close to 99%, and for this reason the water in those years was supersaturated of DO before the ice break-up. This may be due to higher solar radiation and algal activity that the model was not able to reproduce. The MAE at Grand Rapids decreased to 1.09 mg/L only by considering the DO observed with values lower than 11 mg/L, which avoided the late winter data points.

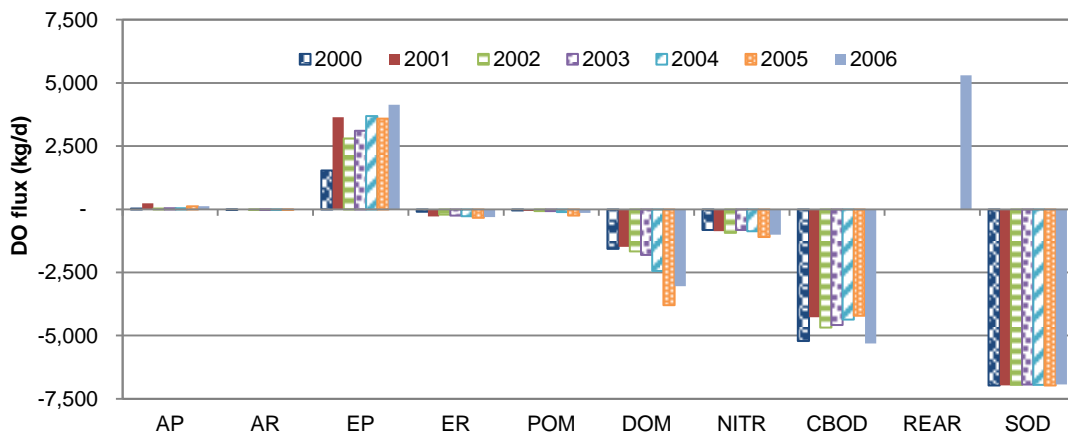


Figure 4-11. Average DO sources and sinks in January. Algal production (AP), algal respiration (AR), epiphyton production (EP), epiphyton respiration (ER), particulate organic matter (POM), dissolved organic matter (DOM), nitrification (NITR), reaeration (REAR)

The final kinetic coefficients were within the range previously documented (Cole and Wells 2008; Bowie et al. 1985) maximum algal rate 2 d^{-1} , labile dissolved organic matter decay 0.1 d^{-1} , CBOD 5-day decay rate 0.2 d^{-1} , ammonium decay rate 1.2 d^{-1} . The model gave better results by setting the minimum reaction rate multiplier to $2 \text{ }^{\circ}\text{C}$ instead of the model's default of $5 \text{ }^{\circ}\text{C}$. The ultimate-to-BOD₅ ratio (RBOD) used was from 1.8 for ALPAC to 2.8 for HPM&S. A higher ratio indicates the presence of refractory material that will take longer to decompose and will have an effect on the DO further downstream. The use of these coefficients in the model was further validated by using the synoptic survey

performed by Sharma *et al.* in 2006. As shown in Figure 4-12, the model's prediction was close to the observed values.

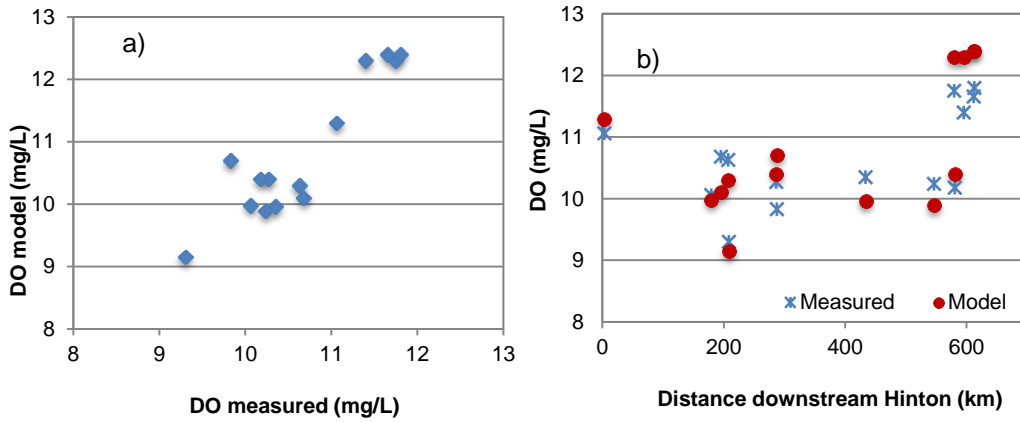


Figure 4-12. Model validation using synoptic survey performed in Fall 2006 by Sharma *et al.* a) observed vs. predicted, b) comparison for different sampling points along the Athabasca River

The winter DO longitudinal profile of the lowest concentration day in the winter 2003 (Figure 4-13) indicated that the concentration had a linear drop of about 0.7 mg/L every 100 km. The DO reached a concentration below the chronic guideline downstream Pelicana River (720 km from Hinton). As a result, about 80 km were compromised by low DO levels. This is consistent with previous estimates of up to 100 km in length (Chambers *et al.* 1997).

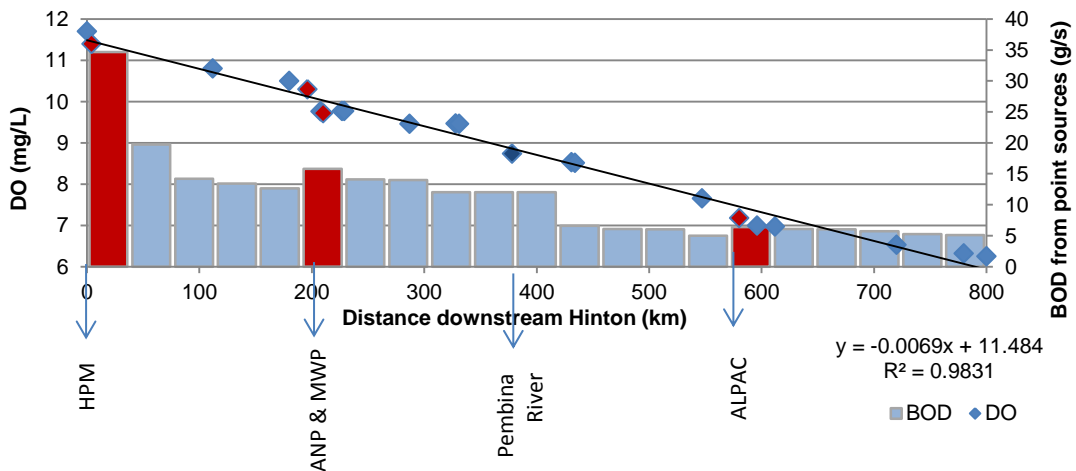


Figure 4-13. DO concentration and BOD mass flux longitudinal profile through the river reach (day with the lowest DO in 2003)

4.3.2. Model application

Pulp mills' maximum government permitted BOD load

The AV scenario produced a minimum DO concentration in winter of approximately 8 mg/L, which is consistent with the long-term average. The CF scenario revealed the significance of the flow on the DO by decreasing its concentration by 0.6 mg/L. By using the pulp mills maximum permitted BOD load (Figure 4-14) the DO decreased below the guideline level to values close to 5.5 mg/L. Although most of the pulp mills have loads much lower than their permit level, HPM's load is very close to this level. Even effluent fluctuations of one standard deviation result in a BOD load higher than the permitted. For this reason, it is highly recommended that HPM&S's wastewater treatment processes are upgraded.

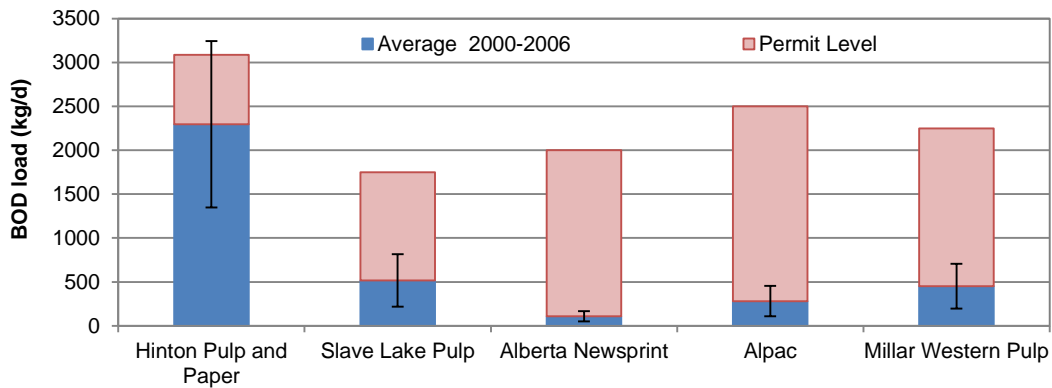


Figure 4-14. Average BOD load and standard deviation (bars) for simulation period (2000- 2006) and government permit level (West Fraser, 2011; Alberta-Pacific Forest Industries, 2006; Millar Western, 2007)

Comparison of different parameters at a low flow

The DO was more sensitive to a 43% SOD increase than to a proportional increase in the BOD load, tributary load, or to a decrease in the background DO. The model revealed a DO reduction of 0.53 mg/L because of the SOD increase. The SOD effect on the DO concentration depends on the river's wetted area. As a result, the model's representation of the bathymetry is very important. The same bottom area in high and low flow periods is calculated by using rectangular channels. However, the river usually has a trapezoidal cross-section whose wetted area decreases at a higher rate than a rectangular with flow changes. For this reason, CE-QUAL-W2 improves the SOD representation by using layers with variable width. The SOD effect was lower than estimated in a previous

sensitivity analysis performed with WASP, where a 1.5 increase lowered the DO by 1.5 mg/L (Tian, 2005). The previous model used a 1D model, which considered the same bottom area in high and low flow periods.

Coupling effects of SOD, BOD and low DO

It is very likely that a year of low flow will promote a lower DO concentration in the upstream boundary condition and tributaries. It is also probable that the higher BOD in the water column will enhance the SOD. By coupling any of these scenarios with a 1σ increase in BOD, the DO concentration reached the guideline value with minimum concentration below 6.5 mg/L. The combination of these three scenarios will create DO conditions similar to those observed in 2003, reaching minimum values in the order of 5.8 mg/L.

Climate change

The climate change scenario predicted shorter ice cover duration with 13 d later formation and 17 d earlier breakup. The maximum ice thickness predicted was 0.80 m instead of 1.31 m. However, under this climate change scenario the average DO in January and February dropped to 5.90 mg/L. It would be recommended to incorporate the prediction of the open leads for further refinement of this scenario. The increase in the extent of these open leads could counterbalance the effect of a lower flow.

Engineering controls

Different engineering controls for dissolved oxygen are: (i) reduction of CBOD and NBOD by decreasing the effluent concentration and/or flow, (ii) aeration of a point source effluent, (iii) increase in river flow to improve dilution, (iv) in-stream re-aeration by turbines and aerators, (v) control of SOD through dredging or inactivation, and (vi) control of nutrients to reduce aquatic plants (Thomann and Mueller 1987).

The model revealed that neither the NBOD nor the algal respiration was one of the main DO sinks in winter. The Athabasca River is a non-regulated river and for this reason the increase in river flow is not a feasible solution. SOD is related to the CBOD from the pulp mills; however, CBOD reduction may be preferred because it is more localized and does not disturb the river benthic community. Effluent aeration was selected for scenario evaluation over having turbines and diffusers since it may require less infrastructure.

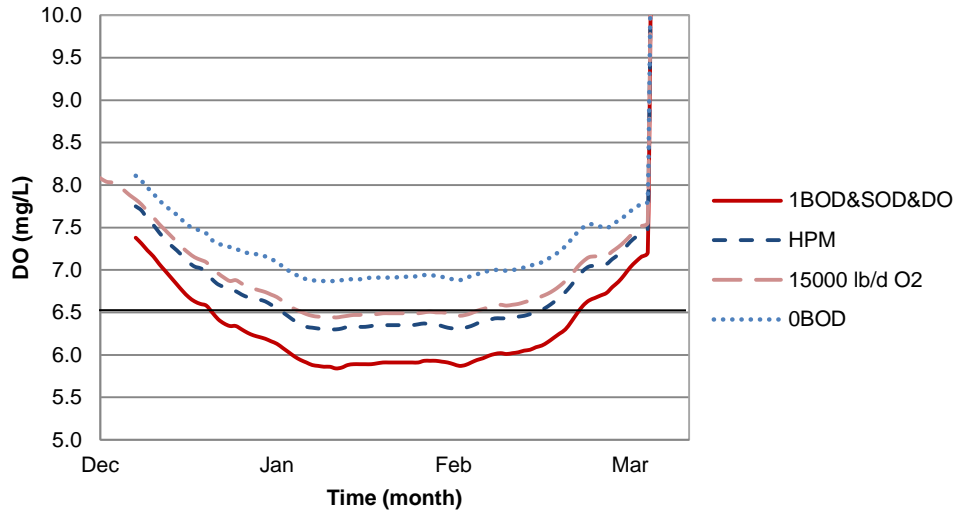


Figure 4-15. Model results using different engineering controls: wastewater treatment upgrading (HPM), DO injection (15,000 lb/d O₂) and pulp mills shut down (0BOD). The scenarios were applied under a “worst-case scenario” AV with high BOD, SOD and low background DO (1BOD&SOD&DO)

The engineering controls evaluated under the worst-case scenario that simulated values similar to the 2003 winter showed that upgrading HPM’s wastewater treatment to achieve BOD levels comparable to ALPAC’s effluent improved the DO by 0.42 mg/L (Figure 4-15). By injecting oxygen directly into the pulp mills’ effluent to supersaturate it, the minimum oxygen that needs to be injected to bring the DO concentration at the guideline level is 15,000 lb/d or 5.60 ton/d. The DO concentration in the river increased to similar levels either improving HPM’s wastewater treatment or injecting oxygen in the river. However, upgrading HPM’s WWTP could have additional benefits, such as reducing nutrients that can be a concern in the future during the open-water season.

Pulp mills operators’ guidelines

Figure 4-16 presents the results of increasing the pulp mills’ average load by 1 σ , 2 σ , 3 σ and the maximum permitted load at different flow conditions to establish a flow-based management approach. This contour graph indicates that the maximum assimilative BOD at average flow conditions is 8.9 ton/d. This load is lower than the maximum permitted load and represents the BOD released if all the pulp mills were to increase their load by 3 σ . For this reason, the model recommends planning production to avoid these BOD peaks in winter, especially in late January. Building equalization tanks for the pulp mill effluents to avoid releasing these high BOD values is an alternative that could also be explored.

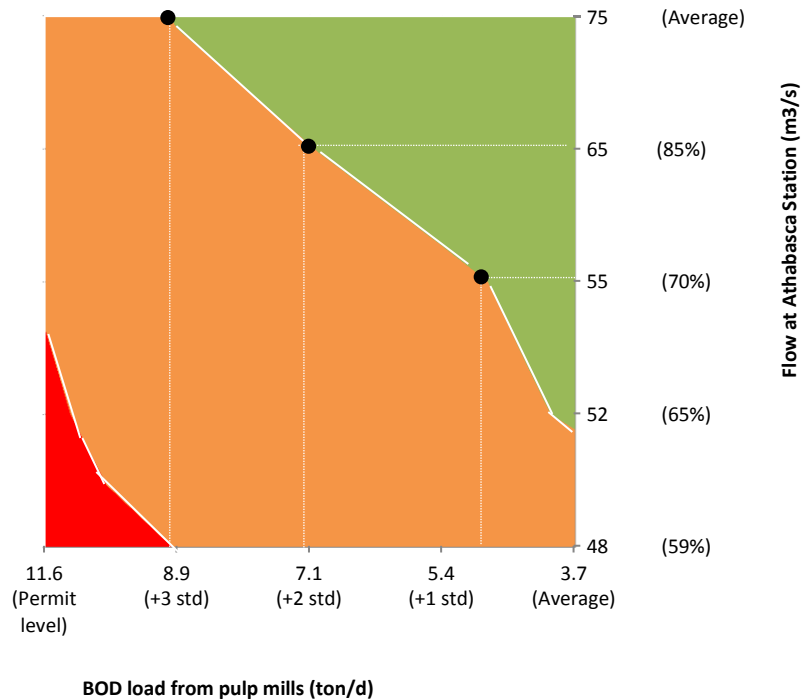


Figure 4-16. Flow-BOD-DO contour plot using three DO levels: red DO < 5.5 mg/L, orange DO < 7 mg/L, green DO > 7 mg/L

The first warning level would be implemented when the Athabasca station's flow is lower than the 2000-2006's average (Figure 4-17). When this flow is in the 75-65 m³/s range, BOD loads should be lower than 7.1 ton/d ($\mu + 2\sigma$). The second warning level would be for flows of 64-55 m³/s where the BOD load should be lower than 4.8 ton/d ($\mu + \sim 1\sigma$). The third level is recommended for a flow of 55-50 m³/s. When the river has a discharge this low, the total BOD load should be lower than 3.7 ton/d (2000-2006's average). Additionally, at flow < 52 m³/s, which represents the minimum assimilative flow, the DO at Grand Rapids may be forecasted using the developed model with updated SOD values. If the predicted DO is below the threshold of 7.0 mg/L, it would be recommended that the pulp mill operators have oxygen ready to be injected into the effluent as a mitigation measure. The accumulated temperature as discussed in section 3.1, can also be used as an early indicator of the likelihood of a year with a DO sag. An unusually cold and long winter will generate smaller open leads downstream the pulp mills.

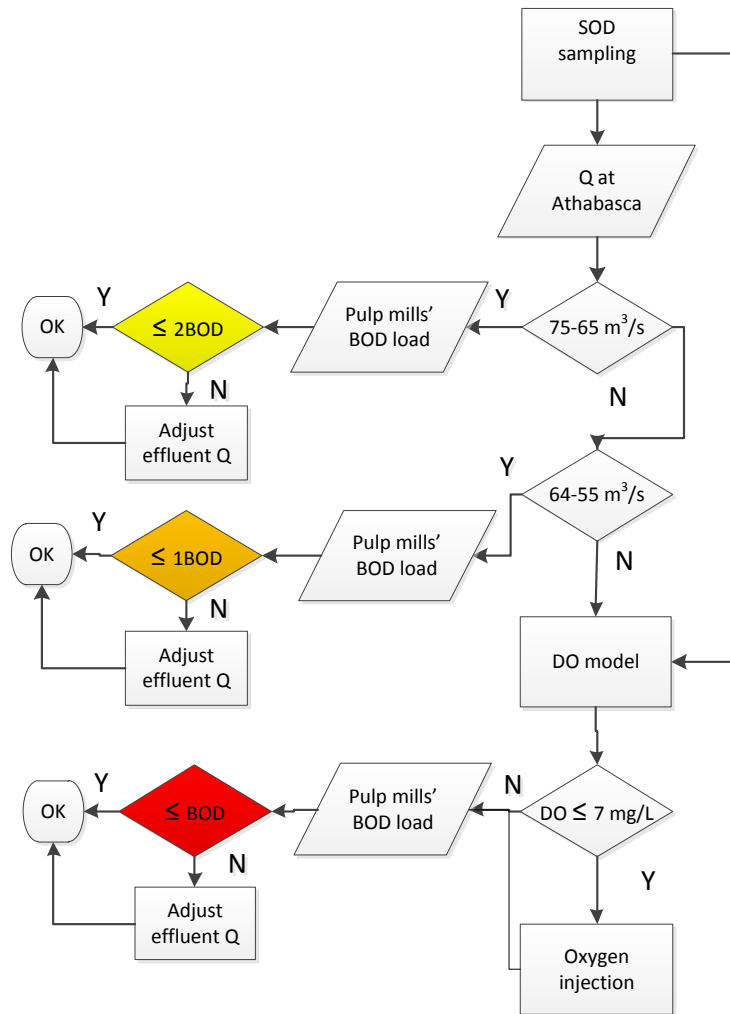


Figure 4-17. DO winter warning system chart for flow at Athabasca <math>< 75 \text{ m}^3/\text{s}</math>, 1BOD (increase 1σ), 2BOD (increase 2σ), 3BOD (increase 3σ)

4.4. Conclusions

The customized model successfully reproduced the hydrodynamics, water temperature, and dissolved oxygen of the river. The results confirmed that the predicted DO was very sensitive to the SOD value used. Consequently, updating the SOD value downstream of the pulp mills on an annual basis is highly recommended. The climate change scenario is not promising for the DO in the river, as it predicts a concentration which is lower than the guideline at average BOD loads. In order to alleviate potential damage, a DO warning system should be implemented by the pulp mills' wastewater treatment operators, applying standards for the BOD load released under critical flow. This could avoid DO sags that may impact aquatic life. Additionally, upgrading HPM&S's wastewater treatment is recommended as it is a significant BOD contributor. Finally, the developed model can

be used as a management tool to evaluate different mitigation options and understand the different processes involved in the DO balance in winter.

A version of this chapter has been published. Martin, N., McEachern, P., Yu, T., and Zhu, D. Z. (2013). "Model development for prediction and mitigation of dissolved oxygen sags in the Athabasca River, Canada." Science of the Total Environment, 443(0), 403-412

4.5. References

Alberta Environment. (2012). "River Network Station Water Quality Data." <http://envext02.env.gov.ab.ca/crystal/aenv/viewreport.csp?RName=River%20Network%20Station%20Water%20Quality%20Data> (accessed May 2011).

Alberta-Pacific Forest Industries. (2006). "Sustainability Report 2005-2006." Edmonton, AB.

Bowie, G. I., Mills, W. B., Pocella, D. B., Campbell C.L., Pagenkopf, J.R., Rupp, G.L., Johnson, K.M., Chan .W., Gherini, S.A. (1985). *Rates, constants, and kinetics formulations in surface water quality modeling*. U.S. Environmental Research Laboratory, Athens, Georgia.

Chambers, P. A., Scrimgeour, G. J., and Pietroniro, A. (1997). "Winter oxygen conditions in ice-covered rivers: the impact of pulp mill and municipal effluents." *Canadian Journal of Fisheries and Aquatic Sciences*, 54(12), 2796-2806.

Cole, T. M., and Wells, S. A. (2008). *CE-QUAL-W2: A Two-Dimensional Laterally Averaged, Hydrodynamic and Water Quality Model, Version 3.6*. U.S. Army Corps of Engineers, Washington, DC.

Cox, B. A. (2003). "A review of currently available in-stream water-quality models and their applicability for simulating dissolved oxygen in lowland rivers." Elsevier, 335-377.

Environment Canada. (2010). "Hydrometric data." <http://www.wsc.ec.gc.ca/applications/H2O/index-eng.cfm> (accessed May 2012).

Environment Canada. (2012). "Canadian Climate Data On-line Customized Search." http://www.climate.weatheroffice.gc.ca/advanceSearch/searchHistoricData_e.html (accessed May 2011).

Government of Alberta. (2011). "2011 Official Population List." *Rep. No. ISBN 978-0-7785-7978-6*, Edmonton, AB.

Guay, C., Choquette, Y., and Durand, G. (2012). "Hydroacoustic doppler technology: a key element in the improvement of winter hydrometric data quality." *Canadian Water Resources Journal*, 37(1), 37-46.

Haines, A. T., Finlay, B. L., and McMahon, T. A. (1988). "A global classification of river regimes." *Applied Geography*, 8 255-272.

Hamilton, A. S., and Moore, R. D. (2012). "Quantifying uncertainty in streamflow records." *Canadian Water Resources Journal*, 37(1), 3-21.

Hanes, N. B., and Irvine, R. L. (1968). "New technique for measuring oxygen uptake rates of benthic systems." *Journal (Water Pollution Control Federation)*, 40(2, Part I), pp. 223-232.

Hicks, F. E. (1996). "Hydraulic flood routing with minimal channel data: Peace River, Canada." *Canadian Journal of Civil Engineering*, 23 524-535.

Jaffe, P. R., and Ferrara, R. A. (1984). "Modeling sediment and water column interactions for hydrophobic pollutants." *Water Research*, 18(9), 1169-1174.

Kerkhoven, E., and Gan, Y. (2011). "Differences and sensitivities in potential hydrologic impact of climate change to regional-scale Athabasca and Fraser River basins of the leeward and windward sides of the Canadian Rocky Mountains respectively." *Climatic Change*, 106 583-607.

Li, X., Nour, M. H., Smith, D. W., and Prepas, E. E. (2008). "Modelling nitrogen composition in streams on the Boreal Plain using genetic adaptive general regression neural networks." *Journal of Environmental Engineering and Science*, (7),.

Lima Neto, I. E., Zhu, D. Z., Rajaratnam, N., Yu, T., Spafford, M., and McEachern, P. (2007). "Dissolved Oxygen Downstream of an Effluent Outfall in an Ice-Covered River: Natural and Artificial Aeration." *Journal of Environmental Engineering*, 133(11), 1051-1060.

Littlewood, I. G. (1992). "Estimating Contaminant Loads in Rivers: A Review." *Hydrological Sciences Journal*, 37 644.

Mahabir, C. L. (2007). "River ice breakup forecasting with fuzzy and neuro-fuzzy models". Doctoral Dissertation, University of Alberta, Edmonton, AB.

Matlock, M. D., Kasprzac, K. R., and Osborn, G. S. (2003). "Sediment oxygen demand in the Arroyo Colorado River." *Journal of the American Water Resources Association*, 39 267-275.

Millar Western. (2007). "Sustainability Report." Edmonton, AB.

Noton, L. R. (1996). "Lower Pembina River system Fall-Winter 1993-1994 water quality survey." *Rep. No. W9605*, Edmonton, AB.

Sharma, K., McEachern, P., Spafford, M., Zhu, D., and Yu, T. (2009). "Spatial variation of sediment oxygen demand in Athabasca River: influence of water column pollutants." *ASCE Conference Proceedings*, 342(41036), 647.

Stantec, C. L. (2001). "Sensitivity analysis of a dissolved oxygen model for the Athabasca River from Hinton to Grand Rapids." *Rep. No. 108-59295*, Edmonton, AB.

Thomann, R. V., and Mueller, J. A. (1987). *Principles of surface water quality modeling and control*. Harper & Row, New York, NY.

Tian, Y. (2005). "A dissolved oxygen model and sediment oxygen demand study in the Athabasca River". MSc. University of Alberta, Edmonton, AB.

Truax, D. D., Shindala, A., and Sartain, H. (1995). "Comparison of Two Sediment Oxygen Demand Measurement Techniques." *Journal of Environmental Engineering*, 121(9), 619.

Van Der Vinne, G., and Andres, D. (1992). "Winter low flow tracer dye studies, Athabasca River, Hinton to Athabasca." *Rep. No. SWE-92/03*, Environmental Research and Engineering Department, Alberta Research Council, Alberta, Canada.

West Fraser. (2011). "Sustainability Report." Vancouver, BC, Canada.

Yang, Y. S., and Wang, L. (2010). "A review of modelling tools for implementation of the EU water framework directive in handling diffuse water pollution." *Water Resource Management*, 24(9), 1819-1843.

Yu, M. (2006). "Sediment oxygen demand investigation and CE-QUAL-W2 model calibration in the Athabasca River". MSc. University of Alberta, Edmonton, AB.

Zhang, W., and Zhu, D. (2011). "Transverse mixing in an unregulated northern river." *Journal of Hydraulic Engineering*, 137(11), 1426-1440.

Passive Samplers for Naphthenic Acids

Chapter 5. Literature review: passive samplers for naphthenic acids

The term naphthenic acid (NA), as commonly used in the petroleum industry, refers collectively to all the carboxylic acids present in crude oil (Wiley 2007), and heavy oil (e.g. bitumen) has the highest content (American Petroleum Institute, 2003). These compounds [CAS: 1338-24-5] consist predominantly of alkyl-substituted cycloaliphatic carboxylic acids, with smaller amounts of acyclic aliphatic (paraffinic or fatty) acids. Aromatic, olefinic, hydroxy, and dibasic acids are considered to be minor components. In Alberta's heavy oil, NAs have been estimated to comprise 0.1-0.2 wt% of the bitumen and 10% of the organic acid content (Schramm 2000). Commercial naphthenic acids are derived from straight-run distillates of petroleum, mostly from kerosene and diesel fractions (Wiley 2007) by extraction with caustic soda solution and subsequent acidification (Lewis 2002). The chief use of naphthenic acids is in the production of metallic naphthenates for paint driers and cellulose preservatives. Other uses are as solvents, detergents and rubber reclaiming agents (Lewis 2002).

5.1. Oil sands in the Lower Athabasca Basin

Alberta's oil sands areas, Athabasca, Peace River, and Cold Lake, together represent two-thirds of the bitumen in the world (World Energy Council 2010). The total crude bitumen reserves are 170 billion barrels (ERCB 2013) forming one of the very largest known petroleum accumulations in the world ranking with the Middle East, Venezuela, Russia and United States. Bitumen is recovered by open-pit mining, or in-situ methods at greater depths. Crude bitumen production in Alberta's oil sands areas totaled 112 million m³ in 2012 split almost equally between in-situ and mining. The bitumen production is forecasted to double by 2022 (ERCB 2013). The Athabasca oil sands have the largest cumulative and annual production with an initial volume in place of crude bitumen representing 83% of the total in Alberta (ERCB 2013).

Commercial plants extract bitumen from mined oil sands using a hot-water conditioning and flotation process. In this process, steam and NaOH are added to increase the temperature between 40 °C and 80 °C, and raise the pH. In the conditioning process, disengagement of bitumen from solids will be favored if their respective surfaces can be made more hydrophilic. The conditioning agent used, NaOH, saponifies natural surfactants from the bitumen, which are primarily carboxylic salts of NAs (Schramm

2000). The interfacial tension decreases at high pH, enhancing oil recovery due to the increase of ionized naphthenic acid at the interface (Brandal 2005).

The bitumen is separated from the solids and water after conditioning through solids sedimentation and froth flotation. The tailings from the primary, secondary and tertiary flotation processes are combined and hydraulically transported to a settling basin. The coarse sand fraction settles out, while the fine sand, silt, clays and unrecovered hydrocarbons run off to a containment pond (Schramm 2000). The hot-water conditioning process uses a great amount of water (approx. 0.8 ton/ton sand). Most of this water is recycled to represent over 70% of the water demand (Schramm 2000), and the rest extracted from the Athabasca River. Mining extraction generates larger quantities of oilsands process-affected water (OSPW) than in-situ processes where the majority of the water is recycled (Scott et al. 2008).

5.2. Naphthenic acids chemistry and toxicity

Although NAs are beneficial to bitumen recovery, they represent both operational and environmental concerns due to corrosion and toxicity. Most of the short term detrimental biological effects of the OSPW to aquatic organisms have been associated with the organic acids in the dissolved organic fraction (Schramm 2000). The surface active properties result in toxic responses to an array of biota that may affect the water management and reclamation options available to the oil sands industry. A “zero discharge” policy has resulted in the creation of big reservoirs of process affected water or tailings.

The studies reviewed by Clemente and Fedorak (2005) have shown toxic effects of NAs on plants, fish, zooplankton, bacteria and rats. Toxicity tests have shown values of LC₅₀ (96 h) of 5 mg/L and 0.0026 mg/L for three-spine stickleback (*Gasterosteus aculeatus*) and bluegill (*Lepomis macrochirus*) respectively, while LD₅₀ values for rats have been between 3 g/kg and 5.88 g/kg bw (American Petroleum Institute 2003). Copper and zinc naphthenate salt-containing products are regulated in the United States due to their toxicity for freshwater fish and invertebrates (US EPA 2007). Dokholyan and Magomedov (1984) found that zooplankton tolerated NAs concentrations up to only 0.15 mg/L, and suggested using this concentration as the maximum allowable concentration in fresh water.

The application of specific concentration limits for environmental criteria of water quality may be required due to the differences in relative toxicity of the various compounds in the OSPW acid extract (Schramm 2000). In a toxicity identification evaluation (TIE) study

performed on oil sands tailings water, it was found that most of the acute toxicity was isolated to the fraction removed by a C18 (octadecyl) adsorbent at all pHs using solid phase extraction (Schramm 2000).

Naphthenic acids are slow to biodegrade (Mohamed et al. 2008); however, natural bioremediation processes are proceeding in the OSPW. A decrease of OSPW toxicity was observed in aged samples with a higher proportion of compounds with > 22 carbons. This indicates that natural processes, including microbial activity, likely affected the toxic components in the waters through the selective removal of smaller compounds (Holowenko et al. 2002).

Naphthenic acids have relatively low molecular weight components (typically < 500 Daltons) (Clemente et al. 2003). They are amphiphilic molecules, where the carboxylic acid group represents the hydrophilic part and the carbon moiety represents the hydrophobic part (Brandal 2005). As an anionic surfactant the molecules form an oriented monolayer at water interfaces (Schramm 2000), making them surface-interfacial active (Havre et al. 2002). As a result, they can form oil-water emulsions causing environmental problems (Havre et al. 2002). They are generally weak acids with pKa values of ~ 4.9 (Havre et al. 2003). At low pH, oil sands NAs are un-dissociated and partition to solids, while at high pH they partition to liquids. As mentioned previously, the use of hydroxide salts in oil sands extraction promotes this behavior and the separation of the oil from the solids.

The chemical equilibrium of NAs is complex at high pH because of micelle and reverse micelle formation in water and oil respectively (Havre et al. 2002). Micelle formation occurs in water when amphiphilic compounds like NAs form organized aggregates of molecules. In these aggregates, the hydrophobic tails align to the interior, leaving the hydrophilic part in contact with the aqueous medium. Micelles are formed at the critical micelle concentration (CMC). The logarithm of the CMC varies linearly with the size of the hydrophobic part of the surfactant. Havre *et al.* (2002) determined the CMC for Fluka NAs at pH 11.3 as 8E-4 M (192 mg/L using an average Fluka MW of 240 g/mol (Havre et al. 2003)). The physicochemical properties of the surfactants vary markedly at the CMC, for example, the adsorption of surfactant onto rock surfaces increases very little (Schramm 2000).

Solubility in water is typically enhanced at lower molecular weight. The log K_{ow} values for carboxylic acids with more than ten carbons are usually > 4 (Yaws 1999). For NAs with 10 to 16 carbons and with one, two or three saturated rings the partitioning coefficients log K_{ow} are between 2.05 (C10) and 4.72 (C16) increasing linearly with the number of

carbons (Havre et al. 2003). Schramm (2000) has reported lower partition coefficients for NAs with values close to 1 at pH 7 and 0 above pH 9.

Naphthenic acids may undergo dimerization, forming metallic soaps (mainly calcium naphthenates) not soluble in water or oil. When the pH of the solution increases, the concentration of dissociated acid also increases, which in turn favors the formation of calcium naphthenate (Magnusson et al. 2008). The calcium naphthenate amorphous film has a lower density than water, thus it may remain at the surface.

Concentrations of naphthenic acids within the tailings ponds have been found in the range of 20-120 mg/L (Holowenko et al. 2002; Holowenko et al. 2001). The average molecular weight of the NAs in tailings water has been found in the range of 220-360 g/mol, with aged tailings increasing the proportion of high molecular weight compounds (Yen et al. 2004). The NAs found in natural surface waters in the oil sands region have been mainly acyclic, with palmitic and stearic acids being the major components (Grewer et al. 2010). It has been reported that even the contact between natural waters and exposed oil sands in eroded banks (in the McMurray Formation) will result in the release of low background levels of NAs into the waters of the area (Schramm 2000).

5.3. Analysis of NAs using fluorescence spectroscopy

Current methods to identify and calculate naphthenic acid concentrations in a complex mixture are in a state of development. Total NAs concentration can be obtained using spectroscopy or mass spectroscopy methods. However, to obtain qualitative information of the sample fingerprint, an improved resolution of the mass spectroscopy technique is required (Table 5- 1). An ultrahigh resolution is necessary to characterize the different isomers in the sample. The widely accepted method in the past for NAs quantification was Fourier transform infrared spectroscopy (FTIR) (Jivraj et al. 1995). However, this method determines total organic carboxylates, and is sensitive to a broader range of structures such as phthalate (Schramm 2000). FTIR has been found to overestimate the NAs concentration in comparison to other techniques such as HPLC-MS, TOC, fluorescence spectroscopy (Ewanchuk 2011), and GC-MS (Scott et al. 2008). Currently, mass spectrometry is the method of choice to study the environmental distribution or fate of NAs in OSPW. However, there is a trade-off, for accurate mass analysis tends to be a longer time required for data acquisition and data analysis (Headley et al. 2009). Mass spectrometry requires specialized and expensive instrumentation, along with advanced expertise in their operation and data analysis (Holowenko et al. 2002).

Table 5- 1. Analytical techniques used for NAs determination

Resolution		Technique	Reference
Low	Spectroscopy	FTIR	Fourier transform infrared spectroscopy (Jivraj et al. 1995; Scott et al. 2008; Yen et al. 2004)
		Fluorescence	Fluorescence spectroscopy (Kavanagh et al. 2009; Mohamed et al. 2008; Ewanchuk 2011)
		UV/VIS	Ultraviolet-visible spectrophotometry (Yen et al. 2004; Mohamed et al. 2008)
Medium-Low < 1x10 ⁴	Mass spectroscopy	FICI-MS	Fluoride Ion Chemical Ionization Mass Spectrometry (Dzidic et al. 1988)
		FAB-MS	Negative Ion Fast Atom Bombardment Mass Spectrometry (Fan 1991)
		GC-MS	Gas Chromatography Mass Spectrometry (Holowenko et al. 2002; Merlin et al. 2007; Scott et al. 2008)
		ESI-MS	Negative-Ion Electrospray Ionization Mass Spectrometry (Rudzinski et al. 2002; Lo et al. 2006; Rogers et al. 2002)
		APCI-MS	Atmospheric Pressure Chemical Ionization (Rudzinski et al. 2002; Lo et al. 2006)
		LC-MS	Liquid Chromatography Tandem Mass Spectrometry (Shang et al. 2013)
		HPLC-MS/MS	Liquid Chromatography Tandem Mass Spectrometry (Woudneh et al. 2013)
High 1x10 ⁴ - 1x10 ⁵		GCxGC-TOF-MS	Two-Dimensional Gas Chromatography/Time-Of-Flight Mass Spectrometry (Hao et al. 2005; Jones et al. 2012)
		HPLC-TOF-MS	Liquid Chromatography Accurate Mass Time-Of-Flight Mass Spectrometry (Hindle et al. 2013)
Ultra-high > 1x10 ⁵		FTICR-MS	Fourier Transform Ion Cyclotron Resonance Mass Spectrometry (Qian et al. 2001; Barrow et al. 2004; Headley et al. 2007; Grewer et al. 2010)

Although GC-MS instrumentation is accessible in most environmental labs, it requires derivatization steps, which may bring uncertainty to the results. First, the analyst has to ensure that there is an excess of derivatizing agent in the reaction mixture (Holowenko et al. 2002). The quantification of the derivatized esters brings challenges as the extracts exposed to moisture will transform to the parent acid, and esters originally present in the sample may be misrepresented as NAs (Headley et al. 2009). Additionally, it is assumed that the efficiency of the derivatization is the same for all compounds in the commercial mixture used to calibrate the method, and for all the compounds in the sample being analyzed (Scott et al. 2008; Holowenko et al. 2002).

Qian *et al.* (2001) analyzed the acid extract of a South American heavy crude oil using ultra-high resolution mass spectroscopy identifying more than 3000 chemically different elemental compositions with structures ranging from C15 to C55 with cyclic (1 - 6 rings) and aromatic (1 - 3 ring), which may contain two to four oxygen molecules and sulfur. However, the majority of the NAs analyses have used a resolution that does not allow the determination of isomers in the mixture. The results of these lower resolution mass spectroscopy analyses are usually fitted to the classical NAs formulae. This sub-group of naphthenic acids has been recurrently described as saturated aliphatic and alicyclic carboxylic acids where this functional group is usually attached to a side chain using the formula $C_nH_{2n+Z}O_2$, where n indicates the carbon number, and Z indicates the number of hydrogen lost for each saturated ring structure in the molecule (Schramm 2000). The NAs are grouped by their number of carbons (n) and number of rings (-Z/2) based on their molecular weight. The molecular weights differ by 14 units (CH_2) between n series and by two mass units (H_2) between Z-series. However, more than 37 carboxylic acid isomers fit to the single formula $C_{10}H_{18}O_2$ (Z=-2) (Clemente and Fedorak 2005). A few studies have considered oxy-NAs ($C_nH_{2n+Z}O_x$) in their data analysis (Hindle *et al.* 2013; Headley *et al.* 2007; Grewer *et al.* 2010; Qian *et al.* 2001). However, even considering oxy-NAs, this only gives a partial picture of the compounds in the acid extract. Grewer *et al.* (2010) found that when the peak abundances were considered, < 50% of the total abundance could be assigned to the classical and oxy-NAs.

Regardless of the method selected, for any of them, it is a challenge to get an accurate standard calibration curve for quantitation purpose (Jivraj *et al.* 1995). The response factors of the various components in the NAs mixtures may change depending on the molecular weight, structure, or the origin of the sample. Hindle *et al.* (2013) compared 39 model naphthenic acids using HPLC-TOF-MS and the results revealed significant variability in response factors. For this reason, most of the time, commercial naphthenic acid mixtures have been used for quantitation, rather than model compounds. The commercial mixture selected has to be representative of the naphthenic acids in the mixture being analyzed (Scott *et al.* 2008). Commercial NAs are nearly devoid of compounds with > 22 carbons and have a few abundant ions. However, there is a high heterogeneity in the composition of environmental NAs. For example, nearly 23% of the ions detected in the Suncor ore had > 22 carbons and only 6% in Syncrude's (Clemente *et al.* 2003). Furthermore, there is not a reagent grade standard available for the complex mixture of naphthenic acids. Using a calibration curve obtained from naphthenic acids extract from a given oil sands source would not be effective for environmental samples that may receive NAs from different sources. Due to the challenge to obtain reliable calibration curves, the current methods tend to be semi-quantitative (Headley *et al.* 2009).

Alternatives may be explored in the future, such as the utility of using representative model NAs surrogates, and development of congener-specific analysis of the principal toxic components (Headley et al. 2009).

Fluorescence spectroscopy has been used in the quantification of NAs (Ewanchuk 2011; Kavanagh et al. 2009; Mohamed et al. 2008), but requires further development. Some benefits of fluorescence methods are:

- Non destructive
- No hazardous by-products
- Small sample
- Fast
- Simple
- Cost-effective
- Amenable to field applications
- High sensitivity compared to other spectroscopic techniques (infrared < UV-VIS (10 to 100 times) < fluorescence (1,000 to 10,000 times) (Pharr et al. 1992))

Fluorescence spectroscopy is an optical phenomenon in which the molecular absorption of a photon moves electrons to a higher energy level. These electrons return from their excited state to their ground energy level through various irradiative and non-irradiative mechanisms. Fluorescence is an irradiative mechanism, in which they emit another photon usually with longer wavelength. This phenomenon is related to the atomic structure of the molecules. Unlike saturated compounds, aromatic constituents have weaker π bonds, which are experimentally feasible to promote to higher levels of energy (Alostaz 2008). Typically, compounds of less than eight conjugated double bonds absorb light only in the ultraviolet region and are colorless to the human eye. However, it can be quantified using UV/VIS spectroscopy. With every double bond added, the system absorbs photons of longer wavelength and the compound ranges from yellow to red.

There are three important quantitative aspects of fluorescence: excited-state lifetime, quantum yield, and Stokes shift. The fluorescence lifetime is the time a molecule stays in its excited state undergoing irradiative and non-irradiative de-excitation processes. This lifetime follows first-order kinetics, and is an important parameter for time resolved spectroscopy. The quantum yield is a measure of emission efficiency expressed as the dimensionless ratio of photons emitted to the number of photons absorbed. It varies with environmental factors such as pH, concentration and solvent polarity. The Stokes shift is the energy difference between absorption and emission maxima (emission peaks occur

at a longer wavelength due to loss of energy in non-irradiative mechanisms) (Lakowicz 2006).

The fluorescence spectra can be scanned from the radiation emitted or as a function of the excitation wavelength. The first represents the transition from the vibrational levels, while the second represents the intensity that the fluorophore is able to absorb to promote electrons to various excited states. Fluorescence intensity can be derived using Beer's law and the fluorescence quantum yield Φ_F (Sauer et al. 2011)

$$\frac{I_F}{I_0} = K \Phi_F \epsilon b c \quad (5-1)$$

Where I_0 is the incident radiation, and I_F is the remaining intensity exiting the sample, K is an instrument constant, ϵ the molar absorptivity (extinction coefficient) of the absorber, b the path length, and c the molar concentration of the absorbing species in the material. This expression shows that there is a linear relationship between the signal and the concentration of the fluorescing compound. The intensity is affected by both the concentration and fluorescence efficiency. Inner filtering correction ($A > 0.01 \text{ cm}^{-1}$) accounts for the attenuation of the excitation beam before reaching the center of the cuvette where the signal is detected.

Alternative fluorescence measurement techniques are Synchronous Fluorescence Spectroscopy (SFS), excitation-emission matrix (EEM) and time-resolved fluorescence spectroscopy. EEM combines excitation and emission spectra into a single display forming a three dimensional matrix. It is usually displayed as a top-view fluorescence contour map. In time-resolved fluorescence spectroscopy, the lifetime dimension is included in the analysis. This additional factor helps to distinguish between two compounds with overlapping spectra but different lifetimes. SFS involves the simultaneous scanning of emission and excitation monochromators with a fixed wavelength difference $\Delta\lambda = \lambda_{exc} - \lambda_{em}$. SFS offers some advantages over EEM as the spectral profile is simpler, there is less background from scattered light, and there are sharper peaks (Pharr et al. 1992). A narrower wavelength difference, $\Delta\lambda$, reduces fluorophore overlap. Conversely, EEM fluorescence emission spectra result in a broad indistinct peak that reduces the technique suitability for fingerprinting.

The excitation wavelength depends on the size, rigidity, and number of conjugated double bonds in the compound. Monocyclic aromatics such as benzene, toluene, xylenes, phenols, and their substituted analogs exhibit a peak between 270-310 nm when $\Delta\lambda = 3$. Aromatic compounds with two rings like naphthalene have a peak between 310-

350 nm, phenanthrenes (three-ring systems) > 350 nm with more condensed ring systems exhibiting peaks at higher wavelengths (Han et al. 2006).

Petroleum hydrocarbons, polycyclic aromatic hydrocarbons (PAHs), proteins, steroids, phenols, oil surfactants, humic and fulvic acids, have the property of fluorescing when illuminated with UV light (Kavanagh et al. 2009; Alostaz 2008). Baker (2003) used fluorescence spectrophotometry to monitor dissolved organic matter with tryptophan (aromatic protein) as an indicator of sewage contamination. Synchronous fluorescence spectroscopy has been shown to be a powerful tool for fingerprinting petroleum contaminants such as gasoline, kerosene, diesel oil, various grades of fuel oil and asphalt (Pharr et al. 1992).

Although classical NAs should not fluoresce because they lack unsaturation, recent developments in mass spectrometry have confirmed a number of other components that do not fit the fully saturated structure (Grewer et al. 2010). Qian *et al.* (2001) determined by ultrahigh mass spectroscopy that most of the acids in a crude oil extract contained at least one aromatic ring. Up to 3-ring aromatics were observed with monoaromatics close to 34%, diaromatics 17% and triaromatics 2.5% of the compounds. Elemental research on the chemistry of naphthenic acids has included model carboxylic acids compounds with aromatic rings (Sjöblom et al. 2003), and research about their toxicity has included these aromatic compounds as representative structures (Rudzinski et al. 2002).

Mohamed *et al.* (2008) presented fluorescence as a screening technique for estimation of levels of NAs in water samples. The method detection limit was 1 mg/L, with a linearity range 1-100 mg/L and precision 10% r.s.d. (triplicates). The intensity of the maxima for the emission spectra was observed to be variable with different excitation wavelengths, which indicated that there were multiple fluorophores in the naphthenic acid mixture. Quantitative calibration curves were obtained for fluorescence emission using the excitation wavelength of 290 nm and maximum intensity at 346 nm to monitor chromophoric surrogates at variable concentrations and pH conditions.

Kavanagh *et al.* (2009) used SFS ($\Delta\lambda=18$ nm) to analyze OSPW, commercial NAs and surface water samples. The OSPW and commercial NAs displayed similar spectra with a minor peak at 282.5 nm, and a greater fluorescence between 320 nm and 340 nm. Surface water close to the oil sands presented only a small fluorescence at 282.5 nm, while the reference natural water away from oil sands operations had a broad peak beyond 345 nm attributed to humic and fulvic acids. The naphthenic acid concentration measured using SFS had a positive correlation with the concentration determined by FTIR.

Ewanchuk (2011) analyzed the EEM fluorescence signals of three OSPWs and found that after inner filtering correction the maximum signal was observed at an excitation wavelength of 280 nm and emission at 343 nm. She also found that the fluorescence components of the samples were found in the acid extract. She used the volume intensity, the area under the 280 nm excitation, and the peak value of this curve to generate the calibration curves having $R^2 > 0.96$. When comparing the signals of OSPW and Sigma Aldrich NAs' this later showed peaks at lower wavelengths (270 and 310 nm). The concentration of naphthenic acid in the OSPW samples obtained with FTIR correlated well with the fluorescence peak intensity. She analyzed the EEM using the PARAFAC technique observing five fluorescent species in those samples and three in the commercial NAs (Fluka).

The signature of the NA extract is likely not due to PAH because the extraction method used removes base-neutral organics (PAH < 1 ng/L and at this concentration it is non-detectable). Additionally, the fluorescent signature of model PAHs (toluene, naphthalene, quinoline, fluorine, phenanthrene, anthracene) is different to the signal of OSPW and NA extract (Kavanagh et al. 2009). Phenols can be present in the acid extract fraction (US EPA 1996); however, the total concentration of phenols is usually very low in OSPW. For example, in the upper zone of the Syncrude's Mildred Lake Settling Basin (MLSB) the phenol concentration is ~ 8 µg/L (Rogers et al. 2002). Humic and fulvic acids are ubiquitous in water from northern Alberta; however, the signal of these acids is at higher wavelengths than NAs in OSPW (peaks at 390 and 484 respectively) (Kavanagh et al. 2009). Additionally, they can also be removed by ultrafiltration since these molecules are usually > 1000 MW (Rogers et al. 2002).

5.4. Passive samplers for naphthenic acids monitoring

Because of the acute toxicity of NAs to many aquatic organisms at concentrations found in OSPW, the oil sands companies are required to monitor and report concentrations from various waters on, and near their leases (Yen et al. 2004). The Environmental Protection and Enhancement Act (Province of Alberta 2013) require the submission of environmental impact assessment reports before the development of any oil sands project. In these assessments, the background concentrations of NAs in surface and ground waters must be addressed (Grewer et al. 2010). A rapid, sufficiently specific and low cost analytical method is needed to conduct large scale screening, surveillance and monitoring in the oil sands region's waters (Shang et al. 2013).

Historically, most of the water samples from the oil sands region have used the FTIR method (1997-2008) to quantify NAs (Table 5-2). More recently, GC-HRMS and GC-MS-

ion trap (RAMP 2011) have been favored. The average concentration varies for the different tributaries as observed in Figure 5- 1. The NAs concentration in the Athabasca River and tributaries is about 0.25 mg/L upstream of the oil sands developments.

Table 5-2. Naphthenic acids concentration in the Lower Athabasca River (RAMP, 2011)

Method	FTIR	GC-HRMS	GC-MS-ion trap
Sampling years	1997-2008	2010	2009-2010
Count	668	36	133
Average	0.77	0.01	0.18
Max	20	0.09	2.76
DL	1	0.005	

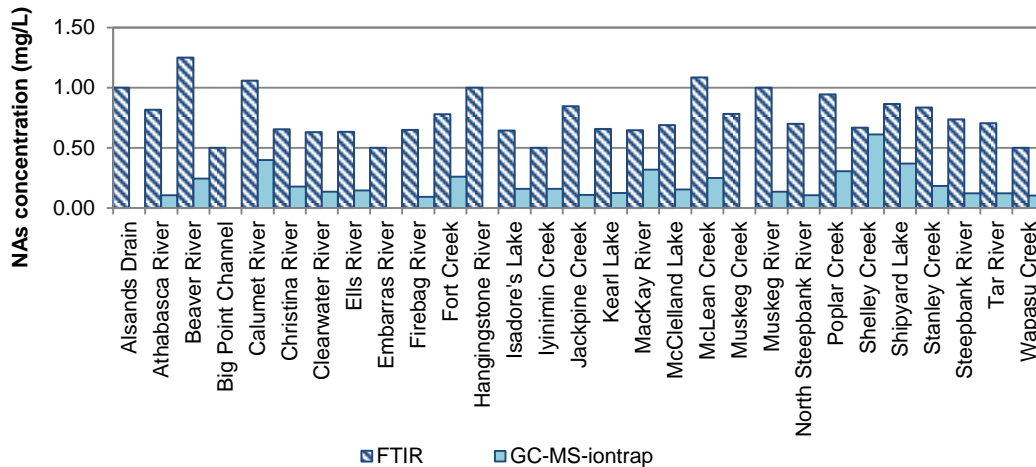


Figure 5- 1. Naphthenic acids concentration in the Lower Athabasca River and tributaries (RAMP, 2011)

Passive samplers, polyethylene devices, have been deployed to monitor polycyclic aromatic hydrocarbons (PAHs) in the surface water close to the oil sands operations (Kelly et al. 2010). In an effort to understand the sources of PAHs to surface waters in the region, Headley *et al.* (2001) analyzed sediment samples from local rivers over three years. The analysis confirmed that the tributaries contain significant levels of naturally derived PAHs predominantly from petrogenic sources (Headley et al. 2001).

Grab sampling has been traditionally used in water monitoring through discrete or composite samples. However, grab samples may not be representative of the water quality when pollutant concentrations fluctuate widely. It is usually difficult to perform event-triggered sampling, due to the inconvenience of collecting samples at certain hours or at unpredictable times. Additionally, there is low reproducibility when the contaminant is at trace concentrations (Harman et al. 2012). The use of automatic samplers is

restricted in widespread monitoring networks due to cost and a secure site required. Additionally, the tubing that feeds the autosampler may freeze in winter (Vermeirssen et al. 2005).

Samples of sediment or biota can represent time-integrated waterborne contamination (Stuer-Lauridsen 2005). In the analysis of sediment samples, it can be difficult to assess the influence of sediment bioturbation and resuspension effects, sediment sorbent quality, degradation and elimination rates. In biomonitoring, organisms (fish, bivalves, macro algae) are deployed for extended periods of time during which they accumulate pollutants from the surrounding water. Analysis of tissue extracts can give an indication of the level of time-integrated waterborne contamination (Stuer-Lauridsen 2005). A number of factors can increase the uncertainty of the results obtained, including metabolism, depuration rates, excretion, stress, and the condition of test organisms. Additionally, the extraction procedure required is complex and time-consuming (Vrana et al. 2005). For this reason, they are not usually aimed at providing quantitative information, but rather indicate the level of contamination in the aquatic media.

Passive samplers have the benefit of expanding the sampling window as in biomonitoring, but with an improved reproducibility (El-Shenawy et al. 2009). They allow determining the time-weighted average (TWA) concentration, which is a fundamental part of an ecological risk assessment for chemical stressors (Kot-Wasik et al. 2007). Passive samplers also improve the sensitivity, allowing very low concentrations to be determined. In these devices, a barrier is applied, which allows a selective transfer of target analytes from the aqueous matrix to the accumulating medium. They usually combine sampling, selective analyte isolation, pre-concentration and in some cases preservation in a single step (Vrana et al. 2005).

Due to the similarities of passive samplers to biological systems (hydrophobic depots covered with a semi-permeable membrane) their potential as surrogates for assessing exposure of aquatic organisms has attracted interest among scientists (Kot-Wasik et al. 2007). Vermeirssen *et al.* (2005) found that the polar organic chemical integrative sampler (POCIS) appears to accumulate estrogens in a way very similar to the brown trout. Because passive samplers adsorb only the truly dissolved phase, which is considered to be the primary concentration available for toxicity and bioaccumulation, they present potential to be coupled with toxicity tests and reduce the need to process large volume of water (Rogers et al. 2002). Toxicity assays that have been used to assess semipermeable devices (SPMD) extracts include (Kot-Wasik et al. 2007):

Microtox®, Mutatox®, mixed-function oxygenase induction EROD activity, Ames mutagenicity test, and YES assay.

Passive samplers, either diffusive or permeative, are formed as tubes or boxes (badges). In general, tube samplers are characterized by a long axial diffusion path and a low cross-sectional area resulting in relatively low sampling rates. Badge-type samplers that have a shorter diffusion path and a greater cross-sectional area typically exhibit higher uptake rates (Kot-Wasik et al. 2007). Analytes may accumulate either by adsorption onto the surface of a solid sorbent material or by absorption in liquids, resin or a polymer coating. The advantage of solid adsorbents is the potential to select materials with a high affinity and selectivity for target compound. However, the sorption capacity of adsorbents is usually limited.

A barrier separates the analyte and the sorbent, and it can be either a static layer of the surrounding medium or a polymer membrane (Seethapathy et al. 2008). However, the sorption phase is usually protected by a membrane. Within the barrier, convective transport of target compound is avoided and the net transport across it occurs mainly due to molecular diffusion following Fick's law. This barrier is intended to control the rate of mass transfer of analyte molecules to the sorption phase. It is also used to define selectivity of the sampler and prevent certain classes (polar or non-polar) of analyte, molecular sizes or species from being sequestered. Several types of polymeric membrane have been used for the construction of passive samplers and some devices are used without a diffusion limiting membrane. Nonporous membranes include low-density polyethylene (LDPE), polypropylene, polyvinyl-chloride, polydimethylsiloxane (PDMS), polyacrylate, and other non-polar polymers. Micro-porous membranes include glass fiber, regenerated cellulose, nylon, polysulfone, polyethersulfone (PES), and polyacrylamide hydro gel.

5.4.1. Uptake model

Passive samplers are based on diffusion of the analyte molecules from the sampled medium to a receiving phase (Namiesnik and Szefer 2010). This mass transfer is driven by a difference in chemical potentials of the analyte in the two media by free flow according to Fick's first law of diffusion. This process continues until equilibrium is reached in the system, or until the sampling process is stopped. The uptake of a compound by a passive sampling device is a multistage mass transfer process. First, water containing the target molecules enter the space that protects the sampler from mechanical damage (usually a cage or cavity in the sampler housing) by convective processes. Molecules then diffuse through the aqueous boundary layer and biofilm layer

(if present). Finally, compound diffuses through the membrane and accumulate in the sorption phase, which has a high affinity for the compounds of interest. This general scheme can vary according to the specific construction of the sampling device.

The exchange kinetics between a passive sampler and the water phase can be described by a first-order, one-compartment mathematical model (Vrana et al. 2005):

$$C_s(t) = C_w \frac{k_1}{k_2} (1 - e^{-k_2 t}) \quad (5-2)$$

$$K_{sw} = \frac{k_1}{k_2} \quad (5-3)$$

$$k_1 = \frac{R_s}{M_{POCIS}} \quad (5-4)$$

Where $C_s(t)$ is the concentration of the analyte in the sampler at exposure time t , C_w is the concentration of the analyte in the bulk water phase, and k_1 and k_2 are the uptake and offload rate constants, respectively.

Whether a passive sampler behaves as an equilibrium or non-equilibrium sampler depends on the partitioning properties of the chemicals. Samplers may be in equilibrium for some environmental pollutants during field sampling, while still being in the non-equilibrium phase for other compounds. For equilibrium sampling, the exposure time is sufficiently long to permit the establishment of thermodynamic equilibrium between the water and sorption phases.

$$K_{sw} = \frac{C_s}{C_w} \quad (5-5)$$

The sorption phase-water partition coefficient, K_{sw} is the driving force for the uptake of compounds by passive sampling devices. For a passive accumulating device based on hydrophobic interaction, it should be possible to estimate the uptake rate from inherent properties of the substance as expressed in values for fugacity of K_{ow} (Stuer-Lauridsen 2005).

The equilibrium concentrations are reached after a known response time, and the device response time needs to be shorter than any fluctuations in concentration in the environmental medium. The amount of analyte accumulated by a passive sampling device is independent of the sample volume as long as analyte depletion does not occur. The analyte concentration measured does not necessarily reflect all the contamination

events during the whole sampling period, but provides a snapshot of the concentration representative for the equilibrium period.

It is usually desired to use the samplers during the initial integrative sampling stage retrieving them before they reach equilibrium. During this stage, desorption is assumed negligible and the device acts as an infinite sink of contaminants. The amount of analyte accumulated is, therefore, linearly proportional to the deployment time and the TWA concentration in water, even for situations where aqueous concentrations fluctuate over time. Most in situ samplers have a slow uptake, and are exposed and collected during the linear phase regime (Stuer-Lauridsen 2005).

$$C_s(t) = C_w k_1 t \quad (5-6)$$

$$m_s(t) = C_w R_s t \quad (5-7)$$

Where m_s is the mass of analyte accumulated in the sorption phase after an exposure time t and R_s is the sampling rate, which may be interpreted as the volume of water cleared of analyte per unit of exposure time by the device. The uptake of a compound into the passive sampler is linear and integrative approximately until the concentration in the sampler reaches half-life.

The sampling rate is characteristic for the individual compound of interest

$$R_s = k_o A = k_e k_{sw} V_s \quad (5-8)$$

Where k_o is the overall mass transfer coefficient (molecular diffusivity in each layer divided by the respective thickness of layers), A is the surface area of a membrane, k_e the overall exchange rate constant and V_s is the volume of the receiving phase. R_s changes depending on whether uptake is under boundary layer control or membrane control (Alvarez et al. 2004):

Under boundary layer control

$$R_s = \left(D_w / \ell_w \right) A \quad (5-9)$$

Where D_w is the diffusion coefficient in water, ℓ_w is the effective thickness of the aqueous boundary layer, and A is the surface area of the sampling device.

Under membrane control

$$R_s = \left(D_M / \ell_M \right) K_{MW} A \quad (5-10)$$

Where D_M is the diffusion coefficient of the membrane, K_{MW} is the equilibrium membrane-water partition coefficient, and ℓ_M is the thickness of the membrane.

Based on relationships such as the Hayduk and Laudie equation, analyte diffusion coefficients across the boundary layer are expected to be directly proportional to temperature (Alvarez et al. 2004).

$$D_w = 1.326 \times 10^{-4} / (\eta_w^{1.14} V_B^{0.589}) \quad (5-11)$$

Where η_w is the viscosity of water for a specific temperature, and V_B is the molal volume of the analyte using LeBas method. A theoretical maximum two-fold increase in the D_w that correlates to a 50% change in the R_s over a 20 °C temperature range would be expected (Alvarez et al. 2004).

In theory, kinetic parameters characterizing the uptake rate can be estimated using semi-empirical correlations employing mass transfer coefficients, physicochemical properties (mainly diffusivities and permeability in various media), and hydrodynamic parameters. However, because of the complexity of the flow of water around passive sampling devices (usually non-streamlined objects) during field exposures, it is difficult to estimate uptake parameters from first principles (Vrana et al. 2005). In most cases, laboratory experiments are needed for the calibration of both equilibrium and kinetic samplers. Uptake rates typically fall in the range of 0.5 to 5 L/d with the most hydrophobic compounds having higher values (Stuer-Lauridsen 2005). The maximum uptake rate can be obtained for samplers in which the limiting barrier is the aqueous boundary layer (Kot-Wasik et al. 2007).

The uptake rate calibrations performed in the lab use either a microcosm with water renewal, continuous flow, or microcosms without renewal method. In this last method, the water concentration is recorded through time, and the results are fitted to a first-order kinetic equation (MacLeod et al. 2007).

$$C_w(t) = C_w(0) \exp[-(k_1 + k_2)t] \quad (5-12)$$

$$R_s = k_1 V \quad (5-13)$$

Where k_1 and k_2 are the uptake and desorption coefficients respectively, and V is the volume.

In contrast, in the continuous flow and microcosm with renewal methods, the concentration in the water is kept constant. The uptake rate, R_s , is calculated using the known water concentration, and the mass of the target compound adsorbed after the exposure time (Eq. 5-7).

5.4.2. Passive samplers widely used

Passive samplers were initially designed for gaseous pollutants in the air, followed by their applications in aqueous matrices, and more recently in solid matrices. The first demonstration of a truly quantitative passive sampling was done by Palmes et al. (1975). The first passive sampler for waterborne pollutants was patented in 1980 by Alyott and Byrne to measure inorganic compounds (Seethapathy et al. 2008), and Sodergren (1987) developed the first application for organic compounds.

The main classification of passive samplers uses to the polarity of the compounds that they can sample. Some authors say that polar samplers should be used for analytes with $\log K_{ow} < 3$ (Kuster et al. 2010), while other authors determine the upper range as $\log K_{ow} < 4$ (Kingston et al. 2000). Different commonly sampled compounds are listed in Fig. 5-2.

Non-polar organic compounds	Polar organic compounds	Other
<ul style="list-style-type: none"> • organochlorine pesticides • polychlorinated biphenyls (PCBs) • polycyclic aromatic hydrocarbons (PAHs) 	<ul style="list-style-type: none"> • polar pesticides • many pharmaceuticals • personal care products • endocrine disrupting compounds 	<ul style="list-style-type: none"> • organometallic compounds • metals • algal toxins.

Figure 5- 2. Type of compounds sampled by passive samplers

The selectivity and specificity of a given sampler are both a function of a number of parameters related to the partitioning process (receiving phase, ionization, K_{ow}), the permeability of the membrane, and the analytical procedures applied after retrieving the sampler from the environment.

Semipermeable membrane device (SPMD)

The SPMD was developed by Huckins *et al.* (1993), and more than 100 studies followed to sample compounds with $\log K_{ow} > 3$. This sampler is the most comprehensively studied PAD (Stuer-Lauridsen 2005). It has a hydrophobic membrane (LDPE) tube filled with

triolein. Even though the SPMD sampler is a more mature technology, it requires a laborious and time-consuming separation of lipid matrix components from target analytes using solvent dialysis with hexane.

Polar organic chemical integrative sampler (POCIS)

The POCIS was developed by Alvarez *et al.* (2004) for compounds with $\log K_{ow} < 3$. These samplers are constructed by forming a membrane-sorbent-membrane sandwich. A piece of PES membrane is placed on the bottom and top of a known amount of solid sorbent, and they are held by two metallic rings (Alvarez *et al.*, 2005). Two sorbents are used: a triphasic sorbent admixture (Isolute ENV+ Ambersorb 1500 dispersed on S-X3 Biobeads) and Oasis HLB. The first one is usually aimed for pesticides and the second for pharmaceuticals. Arrays of POCIS are often deployed by mounting several samplers on a support rod to increase the sensitivity by combining the sorbents.

Two exchanging surface areas of membranes are used (18 cm^2 or 41 cm^2) with different size of washers. However, the standard surface area to sorbent mass ratio is always maintained as $180 \text{ cm}^2/\text{g}$. The average thickness of the PES membrane is approximately $130 \text{ }\mu\text{m}$, and the estimated open-pore volume is 76.5%. The membrane pore length follows a torturous path through the thickness of the membrane with an average opening of $0.1 \text{ }\mu\text{m}$ (Alvarez *et al.* 2004). PES exhibits the best combination of high analyte uptake rates, minimal surficial biofouling, and membrane durability necessary for long term integrative sampling of polar organic chemicals. However, they have a high capacity for non-polar pesticides, and high mass of these compounds have been extracted from the membrane (Kingston *et al.* 2000).

ChemcatcherTM

Chemcatcher is a patented passive sampler, which main components are a solid receiving phase, a selective membrane and a supporting case made of PTFE (Kingston *et al.* 2001). The receiving phase is typically a C18 (octadecanyl) EmporeTM disk, which is made of bonded silica stationary phase particles, immobilized by PTFE fibrils. The membrane used for polar organic compounds is PES and LDPE for non-polar (Kingston *et al.* 2000). Alternatives to the C18 disk are the RPS and XC disks. Even though they are similar, RPS samples slightly more of the hydrophilic compounds and XC more of the hydrophobic compounds (Vermeirssen *et al.* 2009).

It has been found that the uptake rate for PAHs increases when the disks are treated with n-octanol before immersion (Vrana *et al.* 2005), and it has become a normal practice for

its application with hydrophobic compounds. Chemcatcher has presented a high percentage recovery and the uptake rates obtained in lab experiments had a good agreement with theoretical values (Vrana et al. 2005). Additionally, the stability of the analytes in the sampler has been investigated, and for most of the compounds tested the concentration in the sampler did not change after two weeks (Kingston et al. 2000).

Use of a membrane in the passive samplers

The use of membrane has a significant effect on the uptake rate. The mass accumulated in samplers with membranes are believed to be in better agreement with the expected mass for longer periods, but for short periods, they may cause a lag time (Shaw and Mueller 2009). Although naked samplers respond quickly to a peak event and achieve a significantly higher uptake rate (Kuster et al. 2010), by using a similar adsorbent area they may reach equilibrium faster and not be integrative for long deployments. Some researchers have stated that the use of a membrane should be mandatory in order to avoid deterioration of the sorbent and limit the confounding influence from biofouling (Kuster et al. 2010). The standard method for passive sampler analysis includes only the extraction of the sorbent and not the membranes. However, it has been suggested that to account for the fluctuations of concentration, and the lag time between adsorption on the membrane and diffusion to the sorbent, the membrane should be co-extracted (Shaw et al. 2009).

It has been observed that more hydrophobic compounds remained adsorbed onto the PES membrane and not diffusing into the sorbent (Kingston et al. 2000; Vermeirssen et al. 2009). To avoid that, the membrane should have a low affinity for the target compound (Kingston et al. 2000). A polytetrafluoroethylene (PTFE) membrane was originally tested for polar and non-polar pesticides, but it has not been reported for field applications yet. Even though it was observed a 10-fold decrease in the uptake using a PTFE membrane in comparison to the naked disk, all the tested compounds passed through the membrane and were accumulated on the disk (Kingston et al. 2000).

Additionally, membranes alone have been used as passive samplers. In a comparison with seven non-polar samplers, the LDPE membrane had the larger number of compounds detected, a higher method quantification limit, and its TWA concentration was very close to the mean concentration measured in grab samples (Allan et al. 2009).

5.4.3. Factors affecting the uptake rate in passive samplers

Fick's law of diffusion is based on the assumption that steady-state conditions apply; in practice, this is not true for passive sampling due to environmental factors. The uptake rate is often affected by water flow, water temperature, and the extent of biofouling of the diffusive surface. Unprotected surfaces submerged in water eventually become colonized by bacteria and various flora and fauna that may ultimately form a biofilm. During passive sampling, build-up of a biofilm layer can increase the resistance to mass transfer of sampled analyte, thus reducing their sampling uptake rates. Moreover, if the microbial communities that develop on the surface of the sampler possess a potential for biodegradation, they can decompose the analyte in the water that is in contact with the biofilm. This would result in an increase in the concentration gradient between the sorption phase and the biofilm layer. Such effects may result in a serious underestimation of analyte concentrations. Colonizing organisms may also physically damage the surface of membranes that are made of a biodegradable material (e.g. cellulose) (Pawliszyn and Lord 2010).

The PES diffusion membranes used in POCIS and the polar version of the Chemcatcher are less prone to fouling than the LDPE membranes used in SPMDs. This may be due to the low surface energy properties discouraging the initial onset of the biofouling process by creating unfavourable conditions for the settlement of colonizing microorganisms. Alternatively, coating the membrane with a low surface energy material, for example Nafion, can be used to inhibit biofouling. Some solvent-filled membrane devices are protected from fouling by the slow diffusion of the solvent from the sampler. Protective screens made of copper or bronze mesh have also shown to inhibit biofouling; however, they cannot be used when monitoring metals. A novel approach used antibiotics added to the diffusive gradients in thin films (DGT) device (Vrana et al. 2005).

In order to compensate for the effect of environmental variables on sampler performance, sampling devices are spiked prior to exposure with a number of performance reference compounds (PRCs) that do not occur in the environment. The PRC approach is applicable in situations only where the exchange kinetics are isotropic (Mazzella et al. 2010). This is the case when the overall uptake of target pollutants and release of PRCs are governed by first-order kinetics, and the sum of the resistances to mass transfer across the sampler is equal in both directions. These characteristics are observed when the sorption phase consists of an immiscible liquid or a non-polar polymeric film. The selection of a PRC with a sufficient fugacity to enable its release is also important (Mazzella et al. 2010). Measurement of PRC dissipation rate constants during sampler

field exposures and laboratory calibration studies permits the calculation of an exposure adjustment factor that can be used to compensate for variations in environmental conditions during field exposures.

Because the sorptive capacity of sorbents in POCIS is high, it has been suggested the use of a mini SPMD mounted in POCIS rings to act as surrogates PRCs for correction of the uptake rate (Alvarez et al. 2004; Kot-Wasik et al. 2007). Mazzella *et al.* (2010) used atrazine/desisopropyl DIA as a PRC for the analysis of herbicides using pharmaceutical POCIS to correct for turbulence and biofouling variables.

5.4.4. Use of passive samples for regulatory monitoring

Passive samplers may monitor > 75% of the organic micro-pollutants of the EU Water Framework Directive, US and EU Water Quality Criteria, and the Danish monitoring aquatic program (Stuer-Lauridsen 2005). Despite all the advantages of these devices, the validity of this approach in compliance monitoring still needs to be demonstrated before it can be accepted by regulators, water quality managers, and other users of the data. Some researchers consider that these devices are in a relatively early stage of development, but as part of an emerging strategy for monitoring a range of priority pollutants (Kot-Wasik et al. 2007). Assessing the accuracy of passive samplers measurements against other techniques may prove difficult, as the results may not be directly comparable.

5.5. References

Allan, I. J., Booij, K., Paschke, A., Vrana, B., Mills, G. A., and Greenwood, R. (2009). "Field performance of seven passive sampling devices for monitoring of hydrophobic substances." *Environmental Science and Technology.*, 43(14), 5383-5390.

Alostaz, M. (2008). "Improved ultraviolet induced fluorescence UVIF-standard cone penetration testing (CPT) system to detect petroleum hydrocarbon contaminants". Doctoral Dissertation, University of Alberta, Canada.

Alvarez, D. A., Petty, J. D., Huckins, J. N., Jones-Lepp, T. L., Getting, D. T., Goddard, J. P., and Manahan, S. E. (2004). "Development of a passive, in situ, integrative sampler for hydrophilic organic contaminants in aquatic environments." *Environmental Toxicology and Chemistry*, 23(7), 1640-1648.

Alvarez, D. A., Stackelberg, P. E., Petty, J. D., Huckins, J. N., Furlong, E. T., Zaugg, S. D., and Meyer, M. T. (2005). "Comparison of a novel passive sampler to standard water-column sampling for organic contaminants associated with wastewater effluents entering a New Jersey stream." *Chemosphere*, 61(5), 610-622.

American Petroleum Institute. (2003). "Reclaimed substances: naphthenic acid." *Rep. No. 201-14906B*, American Petroleum Institute, Washington D.C. <http://www.epa.gov/hpv/pubs/summaries/resbscat/c14906rs.pdf> (accessed January 2013).

Barrow, M. P., Headley, J. V., Peru, K. M., and Derrick, P. J. (2004). "Fourier transform ion cyclotron resonance mass spectrometry of principal components in oilsands naphthenic acids." *Journal of Chromatography A*, 1058(1-2), 51-59.

Brandal, O. (2005). "Interfacial (o/w) properties of naphthenic acids and metal naphthenates, naphthenic acid characterization and metal naphthenate inhibition". Norwegian University of Science and Technology, Norway.

Clemente, J. S., Prasad, N. G. N., MacKinnon, M. D., and Fedorak, P. M. (2003). "A statistical comparison of naphthenic acids characterized by gas chromatography–mass spectrometry." *Chemosphere*, 50(10), 1265-1274.

Clemente, J. S., and Fedorak, P. M. (2005). "A review of the occurrence, analyses, toxicity, and biodegradation of naphthenic acids." *Chemosphere*, 60(5), 585-600.

Dokholyan, B. K., and Magomedov, A. K. (1984). "Effect of sodium naphthenate on survival and some physiological–biochemical parameters of some fishes." *Journal of Ichthyology*, 23(6), 1013-1019.

Dzidic, I., Somerville, A. C., Raia, J. C., and Hart, H. V. (1988). "Determination of naphthenic acids in California crudes and refinery wastewaters by fluoride ion chemical mass spectrometry." *Analytical Chemistry*, 60(13), 1318.

El-Shenawy, N., Greenwood, R., Abdel-Nabi, I., and Nabil, Z. (2009). "Comparing the Passive Sampler and Biomonitoring of Organic Pollutants in Water: A Laboratory Study." *Ocean Science Journal*, 44(2), 69.

Energy Resources Conservation Board (ERCB). (2013). "Alberta's energy reserves 2012 and supply/demand outlook 2013–2022." *Rep. No. ST98-2013*, Edmonton, AB.

Ewanchuk, A. (2011). *Characterization of Oil Sands Process-Affected Water Using Fluorescence*. MSc Dissertation University of Alberta, Edmonton, AB.

Fan, T. (1991). "Characterization of naphthenic acids in petroleum by fast atom bombardment mass spectrometry." *Energy & Fuels*, 5(3), 371.

Gebhardt, A. C., Schoster, F., Gaye-Haake, B., Beeskow, B., Rachold, V., Unger, D., and Ittekkot, V. (2005). "The turbidity maximum zone of the Yenisei River (Siberia) and its impact on organic and inorganic proxies." *Estuarine Coastal and Shelf Science*, 65(1-2), 61-73.

Grewer, D. M., Young, R. F., Whittal, R. M., and Fedorak, P. M. (2010). "Naphthenic acids and other acid-extractables in water samples from Alberta: What is being measured?" *Science of the Total Environment*, 408(23), 5997-6010.

Gunold, R., Schäfer, R. B., Paschke, A., Schüürmann, G., and Liess, M. (2008). "Calibration of the Chemcatcher® passive sampler for monitoring selected polar and semi-polar pesticides in surface water." *Environmental Pollution*, 155(1), 52-60.

Han, S., Cheng, X., Ma, S., and Ren, T. (2006). "Application of synchronous fluorescence spectrometry in separation of aromatics from hydrotreated naphthenic oil." *Petroleum Science & Technology*, 24(7), 851-858.

Hao, C., Headley, J. V., Peru, K. M., Frank, R., Yang, P., and Solomon, K. R. (2005). "Characterization and pattern recognition of oil-sand naphthenic acids using comprehensive two-dimensional gas chromatography/time-of-flight mass spectrometry." *Journal of Chromatography A*, 1067(1-2), 277-284.

Harman, C., Allan, I. J., and Vermeirssen, E. L. M. (2012). "Calibration and use of the polar organic chemical integrative sampler--a critical review." *Environmental Toxicology and Chemistry*, 31(12), 2724-2738.

Havre, T., Ese, M., Sjöblom, J., and Blokhuis, A. (2002). "Langmuir films of naphthenic acids at different pH and electrolyte concentrations." *Colloid and Polymer Science*, 280(7), 647.

Havre, T. E., Sjöblom, J., and Vindstad, J. E. (2003). "Oil/Water-partitioning and interfacial behavior of naphthenic acids." *Journal of Dispersion Science and Technology*, 24(6), 789-801.

Headley, J. V., Akre, C., Conly, F. M., Peru, K. M., and Dickson, L. C. (2001). "Preliminary characterization and source assessment of PAHs in tributary sediments of the Athabasca River, Canada." *Environmental Forensics*, 2(4), 335-345.

Headley, J. V., Peru, K. M., Barrow, M. P., and Derrick, P. J. (2007). "Characterization of naphthenic acids from athabasca oil sands using electrospray ionization: the significant influence of solvents." *Analytic Chemistry*, 79(16), 6222-6229.

Headley, J. V., Peru, K. M., and Barrow, M. P. (2009). "Mass spectrometric characterization of naphthenic acids in environmental samples: A review." *Mass Spectrometry Review*, 28(1), 121-134.

Hindle, R., Noestheden, M., Peru, K., and Headley, J. (2013). "Quantitative analysis of naphthenic acids in water by liquid chromatography-accurate mass time-of-flight mass spectrometry." *Journal of Chromatography A*, 1286(0), 166-174.

Holowenko, F. M., MacKinnon, M. D., and Fedorak, P. M. (2001). "Naphthenic acids and surrogate naphthenic acids in methanogenic microcosms." *Water Research*, 35(11), 2595-2606.

Holowenko, F. M., MacKinnon, M. D., and Fedorak, P. M. (2002). "Characterization of naphthenic acids in oil sands wastewaters by gas chromatography-mass spectrometry." *Water Research*, 36(11), 2843-2855.

Huckins, J. N., Manuweera, G. K., Petty, J. D., Mackay, D., and Lebo, J. A. (1993). "Lipid-containing semipermeable-membrane devices for monitoring organic contaminants in water." *Environmental Science and Technology*, 27(12), 2489-2496.

Jivraj, M. N., MacKinnon, M., and Fung, B. (1995). *Naphthenic acids extraction and quantitative analyses with FT-IR spectroscopy*. Syncrude Canada Ltd, Edmonton, AB.

Jones, D., West, C. E., Scarlett, A. G., Frank, R. A., and Rowland, S. J. (2012). "Isolation and estimation of the 'aromatic' naphthenic acid content of an oil sands process-affected water extract." *Journal of Chromatography A*, 1247(0), 171-175.

Kavanagh, R. J., Burnison, B. K., Frank, R. A., Solomon, K. R., and Van Der Kraak, G. (2009). "Detecting oil sands process-affected waters in the Alberta oil sands region using synchronous fluorescence spectroscopy." *Chemosphere*, 76(1), 120-126.

Kelly, E. N., Schindler, D. W., Hodson, P. V., Short, J. W., Radmanovich, R., and Nielsen, C. C. (2010). "Oil sands development contributes elements toxic at low concentrations to the Athabasca River and its tributaries." *Proceedings of the National Academy of Sciences of the United States of America*, (37), 16178.

Kingston, J. K., Greenwood, R., Mills, G. A., Morrison, G., and Persson, L. (2000). "Development of a novel passive sampling system for the time-averaged measurement of a range of organic pollutants in aquatic environments." *Journal of Environmental Monitoring*, 2 487.

Kingston, J. K., Greenwood, R., Mills, G., Morrison, G., and Persson, L. (2001). "Monitoring pollutants present in aqueous environments." (Patent # 2 353 860), UK.

Kot-Wasik, A., Zabiegała, B., Urbanowicz, M., Dominiak, E., Wasik, A., and Namieśnik, J. (2007). "Advances in passive sampling in environmental studies." *Analytica Chimica Acta*, 602(2), 141-163.

Kuster, M., De, I. C., Eljarrat, E., López, d. A., and Barceló, D. (2010). "Evaluation of two aquatic passive sampling configurations for their suitability in the analysis of estrogens in water." *Talanta*, 83(2), 493-499.

Lakowicz, J. R. (2006). *Principles of Fluorescence Spectroscopy*. Springer, New York, NY.

Lewis, R. J., Sr. (2002). *Hawley's Condensed Chemical Dictionary (14th Edition)*. John Wiley & Sons, Online version available at: http://www.knovel.com/web/portal/browse/display?EXT_KNOVEL_DISPLAY_bookid=704&VerticalID=0.

Lo, C. C., Brownlee, B. G., and Bunce, N. J. (2006). "Mass spectrometric and toxicological assays of Athabasca oil sands naphthenic acids." *Water Research*, 40(4), 655-664.

MacLeod, S. L., McClure, E. L., and Wong, C. S. (2007). "Laboratory calibration and field deployment of the polar organic chemical integrative sampler for pharmaceuticals and personal care products in wastewater and surface water." *Environmental Toxicology & Chemistry*, 26(12), 2517-2529.

Magnusson, H., Dahl Hanneseth, A., and Sjöblom, J. (2008). "Characterization of C80 naphthenic acid and its calcium naphthenate." *Journal of Dispersion Science & Technology*, 29(3), 464-473.

Mazzella, N., Lissalde, S., Moreira, S., Delmas, F., Mazellier, P., and Huckins, J. N. (2010). "Evaluation of the use of performance reference compounds in an oasis-hlb

adsorbent based passive sampler for improving water concentration estimates of polar herbicides in freshwater." *Environmental Science and Technology* 44(5), 1713-1719.

Merlin, M., Guigard, S. E., and Fedorak, P. M. (2007). "Detecting naphthenic acids in waters by gas chromatography–mass spectrometry." *Journal of Chromatography A*, 1140(1-2), 225-229.

Mohamed, M. H., Wilson, L. D., Headley, J. V., and Peru, K. M. (2008). "Screening of oil sands naphthenic acids by UV-Vis absorption and fluorescence emission spectrophotometry." *Journal of Environmental Science & Health, Part A: Toxic/Hazardous Substances & Environmental Engineering*, 43(14), 1700-1705.

Namiesnik, J., and Szefer, P. (2010). *Analytical Measurements in Aquatic Environments*. CRC Press, London.

Palmes, E. D., Gunnison, A. F., DiMattio, J., Gunnison, J., and Tomczyk, C. (1975). "Personal sampler for nitrogen dioxide." *American Industrial Hygiene Association Journal; (United States)*, .

Pawliszyn, J., and Lord, H. L. (2010). *Handbook of sample preparation [electronic resource]*. Wiley, Hoboken, N.J.

Pharr, D., McKenzie, J. K., and Hickman, A. B. (1992). "Fingerprinting petroleum contamination using synchronous scanning fluorescence spectroscopy." *Ground Water*, 30(4), 484-489.

Province of Alberta. (2013). "Environmental Protection and Enhancement Act." *Rep. No. Chapter E-12*, Alberta Queen's Printer, Edmonton, AB.

Qian, K., Robbins, W. K., Hughey, C. A., Cooper, H. J., Rodgers, R. P., and Marshall, A. G. (2001). "Resolution and identification of elemental compositions for more than 3000 crude acids in heavy petroleum by negative-ion microelectrospray high-field fourier transform ion cyclotron resonance mass spectrometry." *Energy Fuels*, 15(6), 1505-1511.

RAMP. (2011). "Query water quality data [online]." <http://www.ramp-alberta.org/data/Water/water.aspx> (accessed October 2011).

Rogers, V. V., Liber, K., and MacKinnon, M. D. (2002). "Isolation and characterization of naphthenic acids from Athabasca oil sands tailings pond water." *Chemosphere*, 48(5), 519-527.

Rudzinski, W. E., Oehlers, L., Zhang, Y., and Najera, B. (2002). "Tandem Mass Spectrometric Characterization of Commercial Naphthenic Acids and a Maya Crude Oil." *Energy Fuels*, 16(5), 1178-1185.

Sauer, M., Hofkens, J., and Enderlein, J. (2011). "Handbook of Fluorescence Spectroscopy and Imaging: From Single Molecules to Ensembles." WILEY-VCH, 1-29.

Schäfer, R. B., Paschke, A., Vrana, B., Mueller, R., and Liess, M. (2008). "Performance of the Chemcatcher® passive sampler when used to monitor 10 polar and semi-polar pesticides in 16 Central European streams, and comparison with two other sampling methods." *Water Research*, 42(10-11), 2707-2717.

Schramm, L. L. (2000). *Surfactants: Fundamentals and Applications in the Petroleum Industry*. Cambridge University Press, Cambridge, UK.

Scott, A. C., Young, R. F., and Fedorak, P. M. (2008). "Comparison of GC–MS and FTIR methods for quantifying naphthenic acids in water samples." *Chemosphere*, 73(8), 1258-1264.

Seethapathy, S., Górecki, T., and Li, X. (2008). "Passive sampling in environmental analysis." *Journal of Chromatography A*, 1184(1-2), 234-253.

Shang, D., Kim, M., Haberl, M., and Legzdins, A. (2013). "Development of a rapid liquid chromatography tandem mass spectrometry method for screening of trace naphthenic acids in aqueous environments." *Journal of Chromatography A*, 1278(0), 98-107.

Shaw, M., Eaglesham, G., and Mueller, J. F. (2009). "Uptake and release of polar compounds in SDB-RPS Empore™ disks; implications for their use as passive samplers." *Chemosphere*, 75(1), 1-7.

Shaw, M., and Mueller, J. F. (2009). "Time integrative passive sampling: how well do Chemcatchers integrate fluctuating pollutant concentrations?" *Environmental Science and Technology*, 43(5), 1443-1448.

Sjöblom, J., Havre, T. E., and Vindstad, J. E. (2003). "Oil/Water-Partitioning and Interfacial Behavior of Naphthenic Acids." *Journal of Dispersion Science & Technology*, 24(6), 789-801.

Sodergren, A. (1987). "Solvent-filled dialysis membranes simulate uptake of pollutants by aquatic organisms." *Environmental Science and Technology*, 21(9), 855.

Stuer-Lauridsen, F. (2005). "Review of passive accumulation devices for monitoring organic micropollutants in the aquatic environment." *Environmental Pollution*, 136(3), 503-524.

US EPA. (2007). "Registration eligibility decision for copper and zinc naphthanate salts." *Rep. No. 739-R-07-003*, United States Environmental Protection Agency, Washington D.C.

US EPA. (1996). "Method 3650B Acid-base partition cleanup." *Rep. No. 3650B - 7*, U.S. Environmental Protection Agency, Washington D.C.

Vermeirssen, E. L. M., Körner, O., Schönenberger, R., and Burkhardt-Holm, P. (2005). "Characterization of environmental estrogens in river water using a three pronged approach: active and passive water sampling and the analysis of accumulated estrogens in the bile of caged fish." *Environmental Science and Technology*, 39(21), 8191-8198.

Vermeirssen, E. L. M., Bramaz, N., Hollender, J., Singer, H., and Escher, B. I. (2009). "Passive sampling combined with ecotoxicological and chemical analysis of pharmaceuticals and biocides – evaluation of three Chemcatcher™ configurations." *Water Res.*, 43(4), 903-914.

Vrana, B., Mills, G., Greenwood, R., Knutsson, J., Svensson, K., and Morrison, G. (2005). "Performance optimisation of a passive sampler for monitoring hydrophobic organic pollutants in water." *Journal of Environmental Monitoring*, 7 612.

Vrana, B., Allan, I. J., Greenwood, R., Mills, G. A., Dominiak, E., Svensson, K., Knutsson, J., and Morrison, G. (2005). "Passive sampling techniques for monitoring pollutants in water." *TrAC Trends in Analytical Chemistry*, 24(10), 845-868.

Wiley. (2007). *Wiley Critical Content - Petroleum Technology*. John Wiley & Sons, Hoboken, New Jersey.

World Energy Council. (2010). "2010 Survey of Energy Resources." http://www.worldenergy.org/documents/ser_2010_report_1.pdf (accessed August 2013).

Woudneh, M. B., Coreen Hamilton, M., Benskin, J. P., Wang, G., McEachern, P., and Cosgrove, J. R. (2013). "A novel derivatization-based liquid chromatography tandem mass spectrometry method for quantitative characterization of naphthenic acid isomer profiles in environmental waters." *Journal of Chromatography A*, 1293(0), 36-43.

Yaws, C. L. (1999). *Chemical Properties Handbook: Physical, Thermodynamics, Environmental Transport, Safety & Health Related Properties for Organic & Inorganic Chemical*. McGraw-Hill, USA.

Yen, T., Marsh, W. P., MacKinnon, M. D., and Fedorak, P. M. (2004). "Measuring naphthenic acids concentrations in aqueous environmental samples by liquid chromatography." *Journal of Chromatography*, 1033(1), 83-90.

Chapter 6. Naphthenic acids quantification in organic solvents using fluorescence spectroscopy

6.1. Introduction

Our ability to understand the environmental fate, toxicity and the effectiveness of treatment of naphthenic acids (NAs) has been seriously constrained by limited data, which is partially a result of the absence of reliable and cost-effective analytical techniques to measure NAs. The widely accepted method in the past was Fourier transform infrared spectroscopy (FTIR); however, the concentration of NAs in aquatic environments is typically below its detection limit of 1 mg/L (RAMP 2011; Kannel and Gan 2012). Currently, mass spectrometry is the method of choice to study the NAs distribution in OSPW (Scott et al. 2008; Shang et al. 2013; Woudneh et al. 2013; Jones et al. 2012; Hindle et al. 2013; Grewer et al. 2010). Although some of the mass spectroscopy methods do not require extraction or derivatization (Hindle et al. 2013), they may require specialized and expensive instrumentation, along with advanced expertise in their operation, maintenance and data analysis. Fluorescence spectroscopy is presented as an effective alternative. However, the high-resolution mass spectroscopy technique may still be required to obtain qualitative information on the sample composition at isomer level.

Classically defined NAs should not fluoresce because they lack aromatic rings. However, recent developments in mass spectrometry have confirmed the existence of unsaturated structures in the oil sands process-affected water (OSPW) acid extract, and classical saturated NAs accounted for less than 50% of the compounds extracted from OSPW (Grewer et al. 2010; Qian et al. 2001). Aromatic compounds with 1 to 3 ring structures were found in a South American heavy crude oil acid extract (Qian et al. 2001). These aromatic compounds represented 7% of commercial Fluka NAs (Rudzinski et al. 2002), while an analysis of OSPW extract revealed that about 30% are mono and diaromatic structures (Jones et al. 2012).

Research on the chemistry of NAs has therefore included model carboxylic acid compounds with aromatic rings (Sjöblom et al. 2003), and toxicity studies have included these aromatic structures. While it remains unclear which compounds in OSPW mixtures are responsible for toxicity, a modeling study predicted the polycyclic monoaromatic acids would be the most toxic structures due to their potential as estrogenic and androgenic disruptors (Scarlett et al. 2012). If so, fluorescence spectroscopy may be particularly suited to quantify these polycyclic monoaromatic acids.

Previous research has reported that quantification of NAs from water samples using fluorescence spectroscopy correlates positively with mass spectroscopy (Ewanchuk 2011; Mohamed et al. 2008). The OSPW fluorescence signal using synchronous fluorescence spectroscopy (SFS) with an offset of 18 nm has been attributed to mono and diaromatic acids with peak intensity observed at shorter wavelengths (282 nm and 330 nm) than fulvic and humic acids (> 390 nm), reducing potential interference (Kavanagh et al. 2009). Although using fluorescence to directly measure NAs in aquatic environments is very appealing, this technique is sensitive to many environmental factors including pH, temperature and ionic strength (Peuravuori et al. 2002). Additionally, this technique is suitable for aquatic monitoring purposes when the detection limit is below 1 mg/L; if it is not, the NAs would need to be concentrated before being measured.

Alternative methods to decrease the matrix effect and pre-concentrate the NAs are solid phase extraction (SPE) or liquid-liquid extraction (LLE) using organic solvents. A SPE application for NAs has been reported using ethyl ether as solvent, improving the recovery with 10% formic acid (de Conto et al. 2012). Jones *et al.* (2012) used SPE to fractionate OSPW by using hexane to extract alicyclic acids, and hexane with 5% diethyl ether to extract the aromatic structures. In addition to sample preparation, organic solvents are used in the extraction of compounds diffused to passive samplers such as the POCIS. The application of these passive samplers for monitoring in the Lower Athabasca River is of great interest (Environment Canada 2011).

Optical properties of organic fluorophores, such as quantum yield and the absorption and emission spectra, have shown to be highly sensitive to the properties of the solvent used (El-Sayed 2013; Huang and Tam-Chang 2011; Seixas et al. 2003). Shifts in spectra with different solvents have been related to changes in dipole momentum upon excitation (El-Sayed 2013), while changes in quantum yield have been explained as the result of quenching by intra-molecular Photoinduced Electron Transfer processes (nonradiative decay for electronically excited molecules) (Huang and Tam-Chang 2011).

This Chapter evaluates the possibility of quantifying NAs in different organic solvents using fluorescence spectroscopy. The most suitable solvent should have a large linear range and high method sensitivity. The methodology presented here may be used as part of cost-effective analytical methods to characterize OSPW samples, natural water samples, or to investigate the NA fate in the environment.

6.2. Materials and methods

Nine solvents were purchased from Fisher Scientific (Edmonton, AB), methanol, 2-propanol, 90%-ethanol, dichloromethane (DCM), acetone, acetonitrile, n-hexane, toluene and diethyl ether. The solvents were of a reagent grade or higher quality. Commercial naphthenic acids (Fluka) were acquired from Sigma-Aldrich (Oakville, ON), and fresh OSPW was obtained from a bitumen producer in Northern Alberta's oil sands mining region.

The commercial naphthenic acid stock solution was prepared in methanol with a nominal concentration of 5000 mg/L (w/v) using an analytical balance accurate to 0.1 mg. The stock solution represented less than 5% by volume of the standards prepared for each calibration curve. This stock solution was kept in glass vials with Teflon® caps at 4 °C when not in use. Using the stock solution, calibration standards were prepared fresh each time in 10 mL volumetric flasks utilizing chromatographic syringes. Each calibration curve consisted of five points, including the blank and four standards, all prepared in duplicate. The standard concentrations for screening the solvents were 50 mg/L, 125 mg/L, 175 mg/L and 250 mg/L.

The fluorescence of commercial NAs in different solvents was evaluated by their maxima at excitation wavelength (λ_{ex}), emission wavelength (λ_{em}), light scattering and blank intensity. The fluorescence intensity was obtained using a Varian fluorescence spectrophotometer model Cary Eclipse from Agilent Technologies (Mississauga, ON) in a quartz cuvette (10 mm x 10 mm) with a PTFE stopper. The instrument settings are presented in Table 6-1. The inner filtering correction was calculated when the sample was optically saturated (absorbance $> 0.01 \text{ cm}^{-1}$) unless otherwise stated. The primary and secondary inner filtering corrections, associated with the attenuation of the excitation beam and absorption of emitted fluorescence respectively, were obtained following Tucker *et al.* (1992). The absorbance measurements required for this correction were performed with an Ultrospec 1100 pro UV/Visible spectrophotometer (Biochrom, Cambridge, UK), using a 10 mm quartz cell. The absorbance was measured for each standard in the wavelength range 260 nm to 360 nm with a 10 nm interval, and was blank corrected.

Table 6-1. Fluorescence spectrophotometer settings

Setting	Excitation-Emission	Synchronous
Emission/Excitation start (nm)	Emission start: 260	Excitation start: 250
Emission/Excitation stop (nm)	Emission stop: 500 ¹	Excitation stop: 400
Emission slit (nm)	5	5
Excitation slit (nm)	10	5
3D Mode	Yes (excitation)	Yes (offset)
3D Mode start (nm)	Excitation start: 260	Delta start: 5
3D Mode stop (nm)	Excitation stop: 310	Delta stop: 30
3D Mode increment (nm)	Excitation increment: 10	Delta increment: 5
Scan control	medium	medium
Smoothing	off	Savitzky-Golay factor 5
Excitation emission filters	auto	auto

¹ Emission stop increased to 600 for OSPW extract

Calibration curves for each of the solvents were generated using commercial NAs, and their linearity and method sensitivity were compared. These calibration curves were derived using the Emission-Excitation Matrix (EEM) mode by obtaining the linear regression of the peak fluorescence intensity at a specific excitation wavelength. The blank was subtracted from the intensity of every standard for easier comparison of the slope. EEM contour graphs were obtained using the fluorescence instrument software, Cary Eclipse Scan.

Based on the previous performance criteria, linearity and sensitivity, methanol was selected as a solvent of choice and further evaluated for method optimization. The linearity range in methanol was increased in the lower and upper ends. The linearity at low concentration, 0.1 mg/L to 2.5 mg/L, was evaluated for the selected solvent by diluting the standard of 50 mg/L concentration. The upper range was tested at 300 mg/L. The instruments' response options were evaluated for the EEM mode (peak intensity at a specific λ_{em} , area under a specific λ_{ex} , and volume obtained adding the area for all the λ_{ex}), and for the Synchronous mode. Additionally, the effect of having deionized water-methanol mixtures in the calibration curve was evaluated. For comparison, a calibration curve was performed using an aqueous phosphate buffer solution at pH 7.

The fluorescence method was validated using NAs extracted from OSPW. The OSPW-NAs stock solution was obtained following the liquid-liquid extraction method (Jivraj et al., 1995). Briefly, 5 L of OSPW were centrifuged at 3750 rpm for 30 min at 20 °C for solids removal. The pH was raised to pH > 10 with 1 M NaOH, and the basic extraction was performed with 3 x 50 mL DCM per litre of sample in consecutive steps using a 2-L glass funnel. The basic extract containing PAHs was discarded. After the basic extraction, the

pH was brought to pH < 2 using 10 M HCl, and the extraction was performed again with 3 x 50 ml DCM per litre of sample, targeting NAs this time. The extracts were mixed in a pre-weighed beaker and left to dry overnight in the fume hood. The final weight of the beaker with extract was obtained, the NAs were reconstituted with methanol in a 50-mL volumetric flask, and they were transferred to a glass vial with Teflon® cap as the OSPW-NAs stock solution.

The concentration of NAs in the OSPW-NAs solution was obtained by three methods:

- (1) Gravimetric: the concentration was obtained using the mass of the extract and the volume of methanol used.
- (2) Fluorescence: The peak intensity of OSPW-NAs stock solution was measured diluting a 0.25 mL aliquot with methanol in a 10-mL volumetric flask. The stock solution concentration was estimated using the calibration curve previously obtained for commercial NAs.
- (3) LC-MS/MS: A 2 mL aliquot of the OSPW-NAs stock solution was diluted in 25 mL methanol and sent for NAs determination to a commercial lab (Axys Analytical Services Ltd., Sydney, BC). The analysis was performed on a high performance liquid chromatograph coupled to a triple quadrupole mass spectrometer (LC-MS/MS). The LC-MS/MS was run in the positive ion electrospray Multiple Reaction Monitoring (MRM) mode at unit resolution, and the instrumentation used for the analysis was a Waters (Milford, MA, USA) 2690 HPLC with a Micromass Quattro Ultima MS/MS. Instrument settings were proprietary. The concentration of the different compounds that fit the formula of classical NAs ($C_nH_{2n+2}O_2$, $12 < n < 21$) were quantified using the internal standard method, comparing the area of the quantification ion to that of the corresponding ^{13}C -labelled standard and correcting for response factors. The sum of the concentration of all the different NAs compounds was used with the dilution factor to calculate the total NAs concentration in the stock solution.

The NAs concentration obtained using fluorescence technique was compared with the concentration obtained gravimetrically, and by LC-MS/MS analyses. Five standards were generated by diluting the OSPW-NAs stock solution in methanol (0.010, 0.025, 0.050, 0.100, 0.200 v/v) in a similar fashion as explained for the commercial NAs. The fluorescence intensity was obtained for each standard using the same settings used for commercial NAs for the EEM mode. The concentration of NAs in these standards was calculated using the appropriate dilution factor and the stock solution concentration as determined for each of the three methods (gravimetric analysis, LC-MS/MS, or

fluorescence using calibration curve from commercial NAs). Calibration curves were generated using the peak intensity and the calculated concentration. Finally, the OSPW acid extract was analyzed with the Synchronous Fluorescence settings used for commercial NAs. The fingerprint of the OSPW-NAs was compared with the one from commercial NAs.

6.3. Results

Table 6-2 shows the physical properties and the Immediately Dangerous to Life or Health (IDLH) concentration of the nine organic solvents used (Smallwood 1996). Of these solvents, alcohols, acetone and acetonitrile are miscible in water limiting their use for liquid-liquid extraction of OSPW; however, they may be used in SPE protocols. A short evaporation time may be an advantage when concentrating the sample after extraction. However, compounds in the acid extract mixture with a low molecular weight may co-evaporate with the solvent. Evaporation can also be an issue if the sample is not analyzed quickly enough as changes in volume can result in inaccuracies. Furthermore, a solvent with high evaporation and low IDHL concentration represents a health risk for the analyst. DCM has these characteristics, and is classified as a Possible Carcinogen for humans.

Table 6-2. Physical properties and IDHL concentration of selected solvents (Smallwood 1996)

Solvent name	Solubility parameter	Dipole	Dielectric Constant	Polarity (water 100)	Evaporation time ² (ether = 1)	Density (mg/mL)	IDLH (ppmx1000)
Methanol	14.5	1.7	32.6	76.2	6.3	0.791	25
90%-Ethanol	13.4	1.7	22.4	65.4	8.3	0.780	3.3 ¹
2-Propanol	11.5	1.66	18.3	54.6	11	0.785	20
n-Hexane	6.9	0	1.9	0.9	1.4	0.678	5
Toluene	8.9	0.4	2.38	9.9	6.1	0.860	2
Diethyl ether	7.4	1.3	4.3	11.7	1.0	0.715	19
DCM	9.7	1.8	9.1	30.9	1.8	1.330	5
Acetonitrile	11.9	3.2	37.5	46	2.04	0.781	4
Acetone	10	2.9	20.6	35.5	1.8	0.791	20

¹ 100% Ethanol based on NIOSH Pocket Guide to Chemical Hazards <http://www.cdc.gov/niosh/npgd/npgd0262.html>

² Evaporation time of water is 0.36 in the butyl acetate scale (Wypych 2008) and 41.7 in the ether scale using the approximate relationship between the two scales $B = 15/E$ (Smallwood 1996)

6.3.1. Spectral behavior of commercial NAs in different organic solvents

The maximum intensity was observed in a specific λ_{ex} and λ_{em} range for all the solvents except for acetone. All acetone standards had a constant signal close to zero at any λ_{ex}

and λ_{em} . To investigate this lack of signal, the acetone standard with a concentration of 50 mg/L was evaporated overnight at room temperature, and the residue was reconstituted to its original volume in methanol. The reconstituted methanol-naphthenic acid solution had a higher intensity than the instrument upper limit (1000 a.u.) up to 3 times dilution. This intensity was much greater than expected, and the shape of the emission curve presented a wider peak with enhanced intensity at longer wavelengths of 350 nm to 370 nm. Acetone has been previously reported as a fluorescence quencher of 3-methyl 7-hydroxyl Coumarin (Sharma et al. 2007). The analysis of this behavior is beyond the scope of this research; however, chemical reactions and quenching mechanisms could be involved when using acetone as solvent.

For the remaining solvents, the maximum intensity was observed at an λ_{em} in the range 310 nm to 350 nm at any λ_{ex} . The intensity was close to zero for $\lambda_{em} > 470$ nm (Figure 6-1a). The light scattering displayed as the first peak of each excitation curve varied among the solvents. Figure 6-1b shows the different λ_{ex} with their normalized peak intensity for all standards with a concentration of 50 mg/L. The maximum intensity was usually found in an λ_{ex} range of 260 nm to 280 nm.

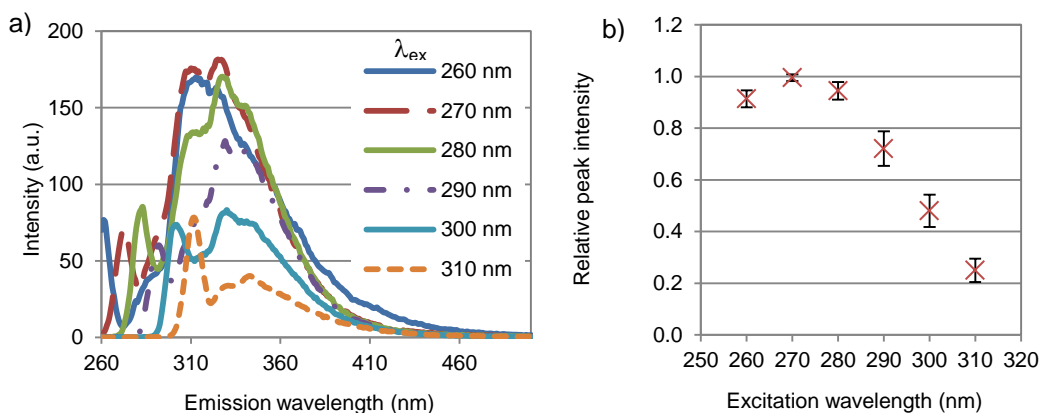


Figure 6-1. Intensity at different excitation wavelengths for 50 mg/L standard a) EEM in methanol, b) average relative peak intensity at different λ_{ex} , bars showing standard deviation.

For toluene, the 260 nm and 270 nm excitation wavelengths produced no signal, and the highest signal was found at longer wavelengths. The 280 nm excitation wavelength was selected to generate the calibration curves for the different solvents because this wavelength produced a high signal for all the solvents including toluene. Previous research, using water as solvent, selected the peak intensity from either the 290 nm

(Mohamed et al. 2008), or 280 nm excitation curve (Ewanchuk 2011), this last wavelength presented higher intensity after inner filtering correction.

In Figure 6-2, the spectral signal of OSPW extract can be compared with the signal of commercial NAs for a 50 mg/L standard in methanol. The maximum intensity for commercial NAs was observed at λ_{ex} of ~265 nm to 275 nm, and λ_{em} of ~305 nm to 330 nm, with values close to zero at $\lambda_{em} > 460$ nm (Figure 6-2a). For the OSPW extract, the maximum λ_{ex} intensity was observed at ~285 nm to 295 nm, and the maximum λ_{em} intensity in the range ~350 nm to 375 nm. This solution fluoresced up to emission wavelengths close to 550 nm (Figure 6-2b).

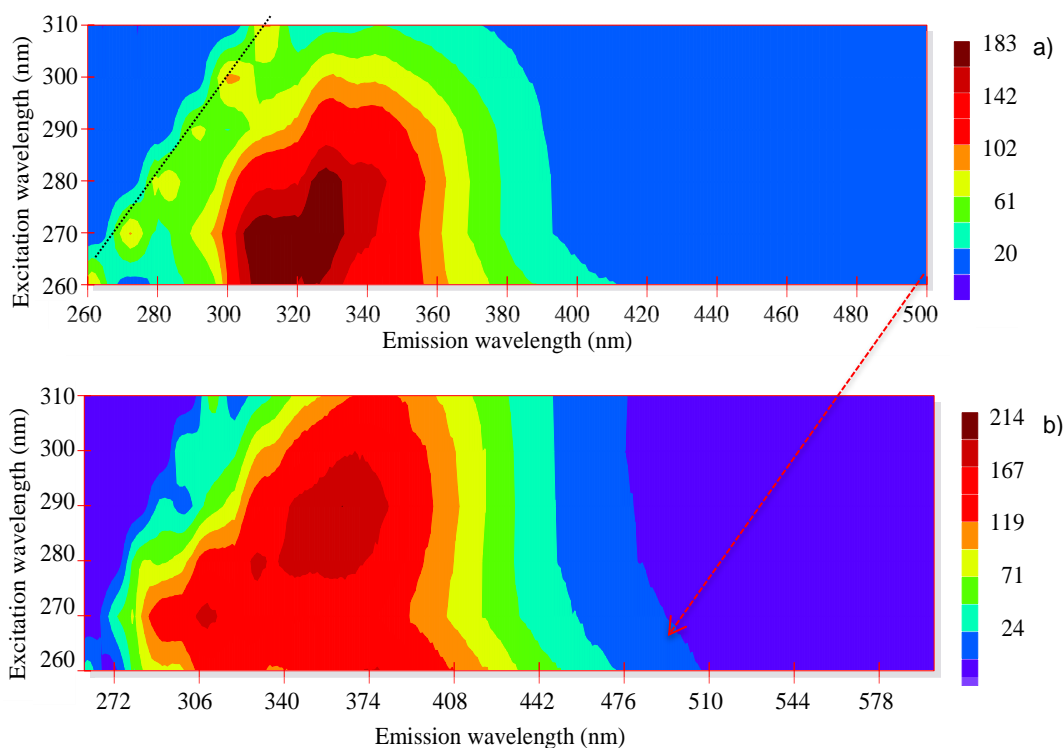


Figure 6-2. EEM contour plot without inner filtering correction showing light scattering and area of maximum intensity for standards with 50 mg/L nominal concentration in methanol, a) commercial NAs, b) OSPW extract.

Calibration curves for commercial NAs in different solvents are presented in Table 6-3 and Figure 6-3. The extent of light scattering was lower for polar protic solvents and higher for toluene. The blank varied among solvents from < 10 a.u. for methanol and 2-propanol to > 70 a.u. for diethyl ether and toluene. Apart from acetone, the response intensity and calibration-curve slope followed a specific order: polar protic > polar aprotic

> non-polar. The reproducibility was good for all solvents with a relative standard deviation < 10%. Additionally, the linear correlations were $R^2 > 0.99$ for all solvents except toluene and acetone. The inner filtering correction was > 10% starting at a concentration of 175 mg/L. This correction generally increased the slope, and improved the correlation coefficient, as the curves were slightly convex at high concentrations. However, for a concentration < 125 mg/L, which is the expected range in tailing ponds, the linearity was excellent even before inner filtering correction.

Table 6-3. Results of calibration curves using different solvents and commercial NAs

Solvent	Type	Light scattering at 50 mg/L (a.u.)	Blank (a.u.)	Before inner filtering correction		After inner filtering correction	
				Slope	R^2	Slope	R^2
Methanol	Polar protic	85.15	6.94	2.9816	0.9978	3.3490	0.9999
Ethanol 90%	Polar protic	71.05	10.49	3.1881	0.9985	3.5179	0.9993
2-Propanol	Polar protic	76.79	6.74	3.3326	0.9966	3.7727	0.9998
n-Hexane	Non polar	96.92	11.18	2.1726	0.9973	2.4370	0.9994
Toluene	Non polar	169.50	74.22	0.3194	0.9384	0.3194	0.9384
Diethyl ether	Non polar	90.78	75.61	2.2373	0.9918	2.4538	0.9900
DCM	Polar aprotic	146.68	33.70	2.4674	0.9910	2.7772	0.9978
Acetonitrile	Polar aprotic	295.46	10.33	2.9788	0.9975	3.3285	0.9973
Acetone	Polar aprotic	-	0.47	-	-	-	-

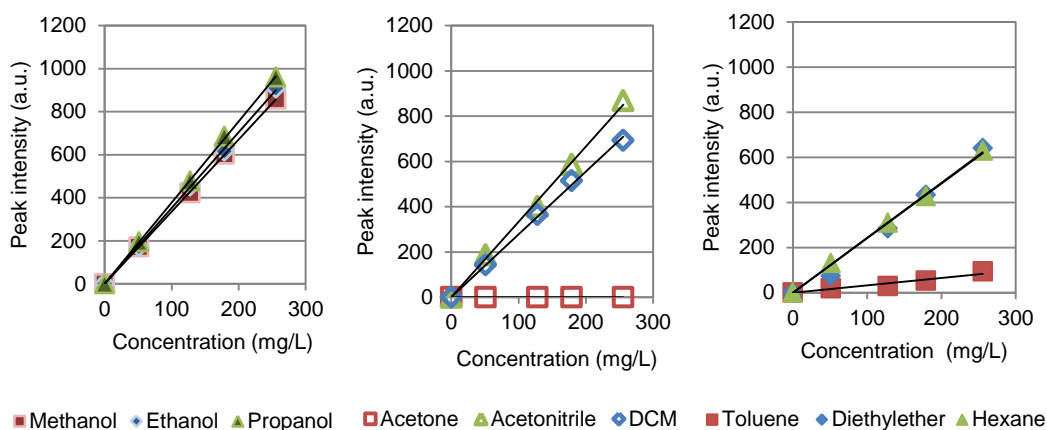


Figure 6-3. Calibration curve of NAs for different solvents using peak intensity at $\lambda_{ex}= 280$ nm after inner filtering correction

These results indicated that the best solvents were the polar-protic solvents and acetonitrile due to a high slope and low blank. Naphthenic acids have been previously quantified using acetonitrile as solvent (Headley et al. 2007). However, methanol was chosen for further analysis because acetonitrile had a higher light scattering and health

risk. Additionally, methanol has been widely cited for SPE of polar compounds (e.g. pesticides).

6.3.2. Naphthenic acids quantification using fluorescence in methanol

Instrument responses in the emission-excitation matrix mode

Because methanol results had low light scattering, the area and volume intensities can be directly used for quantification of NAs with good linearity (Figure 6-4). Using the $\lambda_{ex} = 280$ nm curve, maximum intensity was observed at an emission wavelength close to 329 nm. The blank corrected calibration curve showed similar results by using peak intensity and the intensity at the specific wavelength of 329 nm (Figure 6-4a). However, the peak intensity for the blank was observed at a lower wavelength of 310 nm, and the calibration curve for concentration < 10 mg/L changed depending on the selected method.

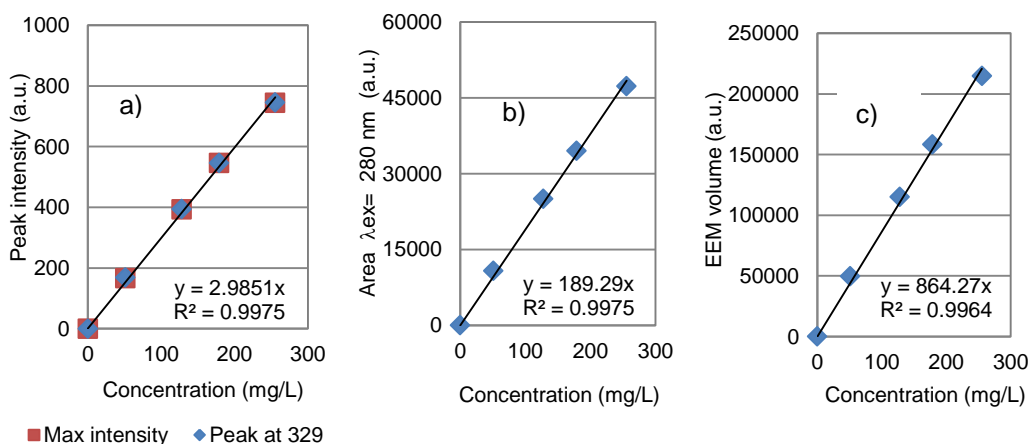


Figure 6-4. Calibration curve of NAs in methanol without inner filtering correction using as instrumental response a) peak intensity at $\lambda_{ex} = 280$ nm, b) area at $\lambda_{ex} = 280$ nm curve, or c) excitation-emission volume $\lambda_{em} = 260$ -500 nm, $\lambda_{ex} = 250$ -310 nm

Calibration curve at high and low concentration

The fluorescence spectrophotometer used in this study had an upper limit of 1000 a.u., and a concentration ≥ 300 mg/L was out of range using the 280 nm peak. The calibration curve using the 290 nm excitation wavelength could be used to increase the maximum concentration that the instrument could measure. However, for lower concentrations of NAs, the 280 nm wavelength produced a higher slope and method sensitivity. Since serial dilutions are always an option to bring the sample in the calibration range, there may be no practical reason to measure concentrations higher than 300 mg/L.

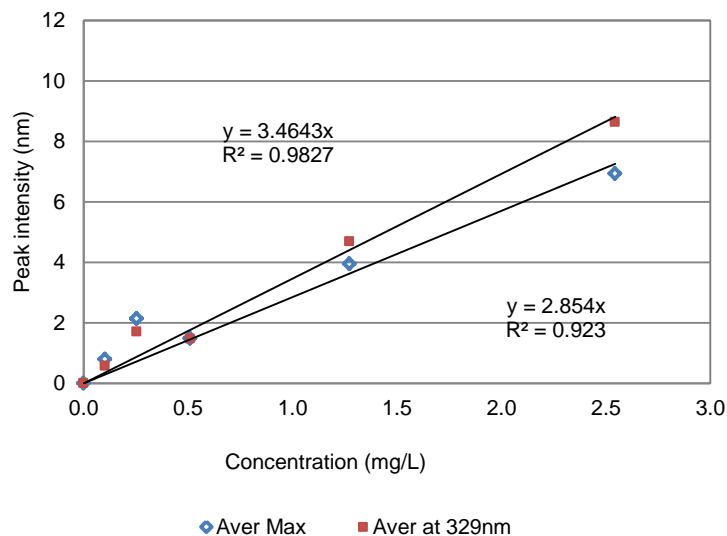


Figure 6-5. Calibration curve using methanol at low NAs concentration

As discussed in the previous section, the method used to obtain the instrument signal (maximum intensity or intensity at a specific λ_{em}) is important at low concentrations. By using the intensity at $\lambda_{em} = 329$ nm, the method sensitivity and the linearity were improved at low concentration (Figure 6-5). The calibration curve gave satisfactory results using standards as low as 0.1 mg/L with a correlation > 0.98 . However, the line presented a consistent hump at a concentration of 0.25 mg/L, which decreased the linearity. This could be due to dimerization of NAs. The fluorescence of face-to-face–stacked H-type dimer aggregates is quenched (Sauer et al. 2011). The slope for low concentration using the intensity at $\lambda_{em} = 329$ nm was only 3% higher than that obtained at a high concentration after inner filtering correction. The method detection limit obtained was 0.40 mg/L for commercial NAs. However, 1 L samples are often collected and concentrated. This may allow measurements of concentrations as low as 0.004 mg/L.

Using methanol-water mixtures as solvent

The fluorescence of NAs in water presented a shift in the emission to longer wavelengths, with maxima at $\lambda = 340$ nm. This red-shift in emission with higher solvent polarity has been previously observed (El-Sayed 2013). As the solvent polarity is increased, the loss of the excess of vibrational energy from the excited fluorophores to the solvent becomes larger (Lakowicz 2006). This results in emission at lower energy or longer wavelengths.

The NAs solubility was higher in organic solvents than in water, creating cloudy solutions in the phosphate buffer solution at concentrations higher than 50 mg/L, which

corresponds to the solubility reported (Kannel and Gan 2012). The lower solubility in water created a significantly higher light scattering and light absorbance. When linearity decreased at high concentration creating a convex curve, the inner filtering correction made the curve concave and also resulted in a poor fit. Mixtures of methanol-water improved the solubility and the method sensitivity (Figure 6-6). The calibration curve slope increased 70% using 50% DI water as compared to pure methanol (0% DI water) (Table 6-4).

Table 6-4. Calibration curves using different% DI water in methanol solution without inner filtering correction

% DI water	Light scattering at 50 mg/L (a.u.)	Blank (a.u.)	Slope	Coefficient of determination, R ²
0	85.15	6.94	2.9957	0.9978
10	76.32	7.20	3.7632	0.9988
30	126.16	8.15	5.2079	0.9998
50	558.73	11.39	4.9104	0.9881
100 ¹	731.26	5.38	2.2324	0.9656

¹Phosphate buffer solution pH 7

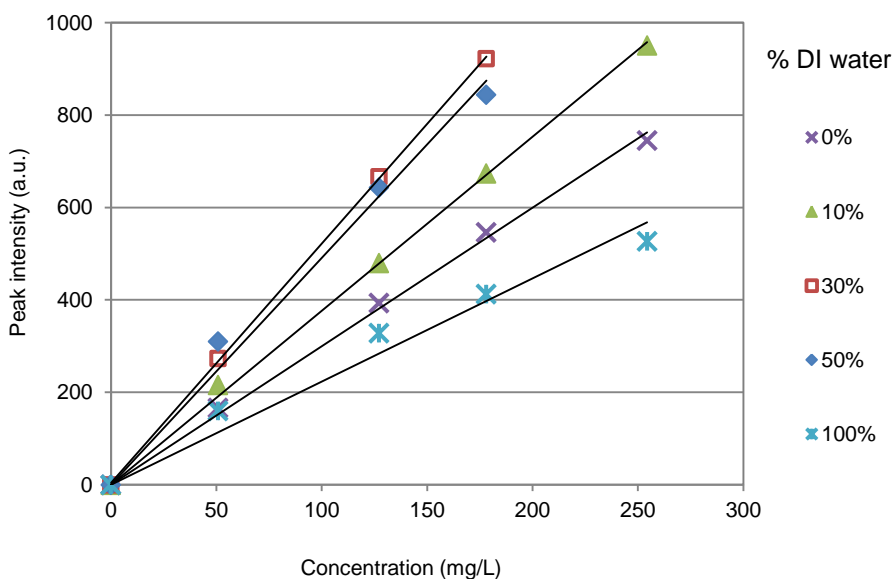


Figure 6-6. Calibration curves for commercial NAs at different% deionized water in methanol

The EEM technique may overlap the signal of different fluorophores, and therefore it is not as powerful for fingerprinting as synchronous fluorescence spectroscopy. The

emission-excitation wavelength offset ($\Delta\lambda$) was tested from 5 nm to 30 nm for commercial NAs. An offset of 5 nm did not produce defined peaks (low peak to valley ratio), while an offset of 15 nm or higher produced either two or one wide peak. The optimum offset was observed by using $\Delta\lambda= 10$ nm, which allowed the identification of three peaks: two main peaks (279 nm and 299 nm), and one minor peak (322 nm). In water, this offset had a low definition with a small peak to noise ratio, potentially requiring a higher offset.

Figure 6-7a shows the three peaks observed in the commercial naphthenic acids. The slope (Figure 6-7b) was lower than the one obtained using EEM with values of 0.2491, 0.3093 and 0.0894 for peak 1, peak 2 and peak 3 respectively, and 11.53 for the area. The linearity was strong in any of the three peaks or the area under the curve with $R^2 > 0.99$. Another advantage of this fluorescence mode is that light scattering is eliminated from the instrument signal.

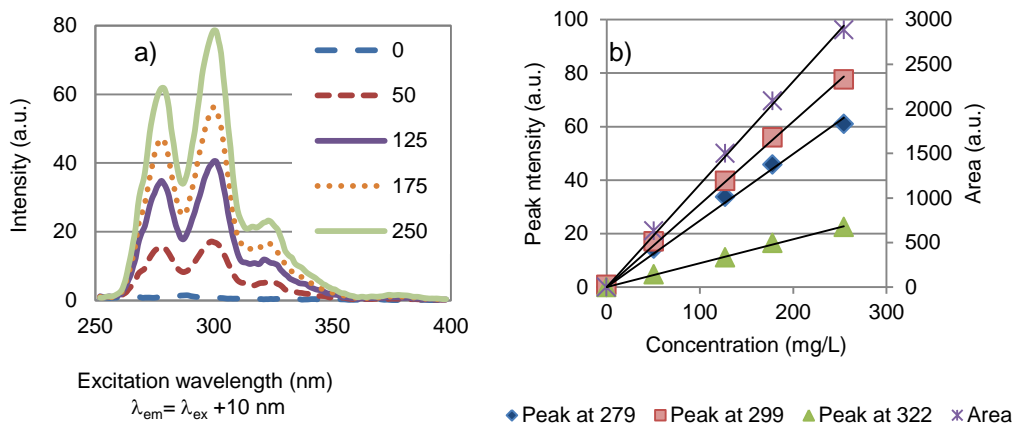


Figure 6-7. Synchronous fluorescence of commercial NAs at $\Delta\lambda= 10$ nm, a) instrument response at different concentration, b) calibration curve NAs-methanol at different peaks or area

Fluorescence of OSPW extract in methanol

The OSPW-NAs stock solution concentration obtained by gravimetric analysis corresponded closely to LC-MS/MS with only 5% difference (**Error! Reference source not found.**). However, the EEM fluorescence method using the calibration curve of commercial NAs overestimated the concentration of NAs in OSPW by 20% when compared with gravimetric determination. Fluorescence calibration curves for OSPW-NAs were obtained based on the stock solution concentration obtained for each of the three different methods. As a result of the difference in NAs concentration calculated, the slope using the fluorescence calibration curve of commercial NAs was lower than the one obtained by weighing the extract or using LC-MS/MS (Table 6-5).

Table 6-5. Concentration of OSPW-NAs stock solution estimated by gravimetric, fluorescence (using calibration curve of commercial NAs), and LC-MS/MS method. Slope of the OSPW-NAs calibration curve is based on the stock solution concentration

Method	OSPW-NAs ¹ (mg/L)	Slope
Gravimetric	1097	4.3198
Fluorescence	1321	3.5896
LC-MS/MS	1045	4.5357

¹ Stock solution concentration

The inner filtering correction for OSPW-NAs standards was significant at concentrations as low as 50 mg/L. The OSPW stock solution was visibly yellow, while the commercial solution at a similar concentration was almost clear. The inner filtering correction improved the linearity producing a good correlation even at a concentration of 200 mg/L. The linearity was $R^2 > 0.999$ for any of the three curves after inner filtering correction (Figure 6-8).

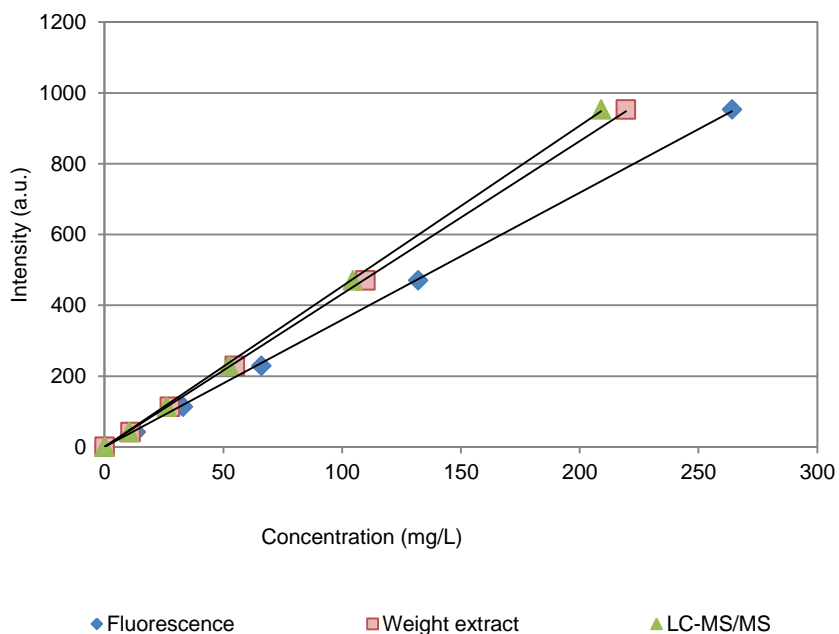


Figure 6-8. Calibration curves for OSPW-NAs fluorescence in methanol using three different methods for calculating the stock solution concentration: the fluorescence standard curve for commercial NAs, weight of the OSPW extract and LC-MS/MS

The synchronous fingerprint at an offset value of 10 nm for commercial NAs and OSPW extract in Figure 6-9 shows that the OSPW presented all the peaks of commercial NAs. However, the OSPW had a fourth peak at an emission wavelength close to 345 nm. The fluorescence intensity of aromatic compounds peak depending on the number of aromatic rings: one ring 250-290 nm, two rings 310-330 nm and three rings 345-355 nm when $\Delta\lambda$

= 3 nm (Pharr et al. 1992). The fourth peak in the OSPW spectra may be related to polyaromatic compounds not found in the commercial NA solution. The magnitude of the first two peaks also changed in these two sources of NAs; the first peak related to monoaromatic compounds was higher for the OSPW-NAs than for the commercial NAs. Kavanagh *et al.* (2009) reported a similar fluorescence spectra between Fluka NAs and NAs isolated from OSPW using an offset value of 18 nm in water. The sample analyzed in that work showed a lower proportion of monoaromatic acids in OSPW than our sample. This could be because we used fresh OSPW, while they used process water from aged tailing ponds. The compounds with larger numbers of aromatic rings are more difficult to degrade than those with smaller numbers (Cerniglia 1992).

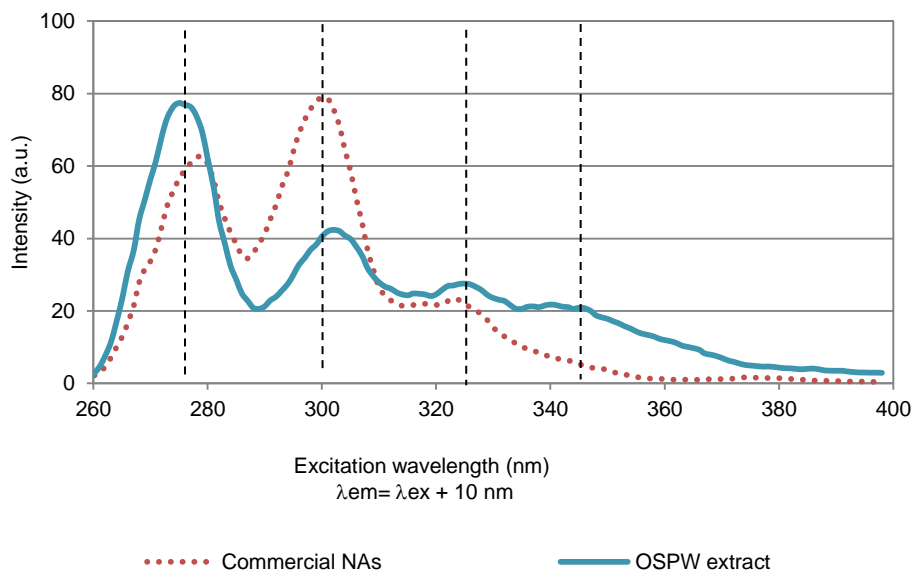


Figure 6-9. OSPW extract and commercial NAs SFS response at $\Delta\lambda= 10$ nm (~250 mg/L)

6.4. Discussion

6.4.1. Advantages of using methanol over water for NAs determination using fluorescence spectroscopy

Even though it is convenient to use inline fluorescence sensors to measure NAs directly in aquatic environments, fluorescence is sensitive to many environmental factors (Peuravuori et al. 2002). First, fluorescence intensity increases with temperature, and the water temperature in the Athabasca River and its tributaries ranges from close to 20 °C in summer to 4 °C or less in winter. Additionally, the fluorescence intensity decreases with pH (Kavanagh et al. 2009), while other dissolved substances may also act as quenchers. Furthermore, NAs have a complex equilibrium in water, including the formation of

micelles at a critical concentration (Sjöblom et al. 2003), which makes the use of organic solvents an attractive alternative to ensure complete solubility.

In addition to decreasing the uncertainty derived from discussed variables, the linear range obtained using methanol increased about two-fold compared to the range obtained in water. This is probably due to higher solubility of NAs in methanol. The upper concentration limit using methanol was 175 mg/L before inner filtering correction and ~300 mg/L after inner filtering correction. This limit is adequate because the concentration of NAs in OSPW is usually lower than 120 mg/L (Holowenko et al. 2002). A higher upper limit may have application for industrial effluents with potential higher concentration of NAs, e.g. refinery effluents. However, the calibration curve using phosphate buffer solution started to bend at a concentration of ~100 mg/L, and the inner filtering correction did not improve the linear fit.

Fluorescence spectroscopy is 1000 to 10000 times more sensitive than UV-Visible spectroscopy, which is 10 to 100 times more sensitive than infrared spectroscopy (Pharr et al. 1992), improving the detection limit. Even though the linearity at low concentration using methanol was satisfactory, a better correlation was obtained at higher concentrations. Environmental samples are expected to be concentrated during the LLE or SPE preparation step. For example, SPE protocols typically use a ratio volume between 0.01 and 0.1 of organic eluent to aqueous sample solution, and therefore concentrate the sample at least 10-fold before analysis (3M Purification Inc., 2013). Although the slope of the lower and higher concentration calibration curves changed when using Fluka NAs in water, the slope did not change significantly when using 50% DI water or only methanol. This could be due to molecule aggregation of NAs as micelles in water. Additionally, methanol presented a lower light scattering when compared with the one obtained using water alone as a solvent. The direct use of peak, area, and volume intensity readings obtained from the 3D instrument set up was possible without further data manipulation due to this low scattering ratio obtained using methanol. The slope increased considerably when using area and volume instead of the peak intensity. However, the area and volume integrate all the fluorophores from the compounds in the NAs sample. Because the NAs composition changes depending on the source, specific calibration curves could be required for each different NAs source.

The solubility of the OSPW extract in methanol was adequate even at high concentrations; however, the light absorbance at 280 nm was significant due to the yellow color of this solution. The observed yellow tone could have resulted from sulfur-containing compounds, as the sulfur content was found to be 1-7% in OSPW extracts

(Grewer et al. 2010), and was negligible in Fluka NAs (Rudzinski et al. 2002). The effect of high absorbance was adjusted by performing inner filtering correction, and then obtaining strong linearity (R^2) for the peak intensity.

The slope of the calibration curve obtained by weighing the OSPW extract was very close to the one obtained by using the concentration from the mass spectroscopy analysis. However, the concentration obtained by the more sophisticated LC-MS/MS technique was 26% higher than the one obtained by fluorescence using the calibration curve derived from commercial NAs. The EEM contour graph for OSPW acid extract in methanol showed a shift in the peak intensity at a higher emission and excitation wavelength in comparison to commercial NAs. Furthermore, the fluorescence intensity was higher than zero at longer wavelengths. This highlights the challenge of quantifying NAs due to the lack of a reliable standard solution for calibration purposes, as NAs are a mixture of different compounds. Calibration curves could be prepared for each NAs source, assuming a constant distribution of NAs. Kavanagh *et al.* (2009) proposed using mass spectroscopy technique to generate a dilution calibration curve for estimating the NAs when using fluorescence. Alternatively, a gravimetric method could be used to correct calibration curves derived from the commercial naphthenic acid standard solution. So far, it appears that the use of calibration curves derived from the commercial NAs standard solution may be problematic for the quantitation of real OSPW NAs in methanol and probably even in water.

6.4.2. Use of fluorescence spectroscopy after sample extraction using organic solvents

In the past few years there has been a general trend to replace LLE with SPE protocols, mainly due to a reduced solvent use (Namiesnik and Szefer 2010). This is especially important for toxicity tests that require the extraction of NAs from hundreds of liters of OSPW (Rogers et al. 2002). Moreover, SPE conveniently concentrates organic analytes in the field, substantially reducing the effort and cost of transporting and preserving large samples. Methanol has been widely used in SPE protocols for pesticide and pharmaceutical extraction. The advantage of using SPE protocol for NAs instead of LLE is that the extract is readily available for analysis using fluorescence spectroscopy without requiring volume reduction. These benefits combined decrease the quantification time considerably.

The LLE method widely used for extraction of NAs from OSPW uses DCM (Zhao et al. 2012). Even though a polar protic solvent may dissolve the NAs more effectively, methanol and 2-propanol are inappropriate for this technique due to their miscibility with

water. However, the extracted NAs could be reconstituted in methanol instead of DCM after recovery and sample reduction, improving the fluorescence method sensitivity. Using methanol and SPE protocol would eliminate this time consuming step. Another advantage of using methanol over DCM is that it lowers the health risk involved for the analyst. Additionally, the evaporation time of DCM is about three times faster than that of methanol (**Error! Reference source not found.**) with a potential error due to concentration changes when the fluorescence readings are not handled carefully and quickly. It is worth mentioning that there was an evaporative loss of commercial NAs in methanol close to 30% by keeping the solution in an open beaker at room temperature overnight, a problem that may be enhanced by DCM. Despite the volatility of OSPW extract is expected to be lower due to its higher average molecular weight, further analysis is required to guarantee that the sample preparation does not cause mass losses of NAs. For this reason, using an SPE method may increase accuracy due to fewer steps that avoid evaporation as a solvent and volatilization of NAs.

Besides NAs determination from water samples, the method presented here may be used for NAs quantification after extraction from crude oil. Naphthenic acids have been used as markers in geochemistry of crude oil. Rudzinski *et al.* (2002) extracted the organic acid fraction in a Maya crude oil using (50:50) acetonitrile: methanol. The NAs fluorescence signal was similar when using any of these two organic solvents with strong linearity in their calibration curves. A calibration curve could be made with this solvent mixture, and it can be used for a rapid NAs determination in the lab or in the field for screening purposes.

6.4.3. Improved selectivity using synchronous fluorescence mode

Synchronous fluorescence spectroscopy reduces the fluorophores overlapping, while increasing the possibility of each one to be identified in a specific spectral range (Peuravuori *et al.* 2002). Kavanagh *et al.* (2009) used an offset value of 18 nm for measuring OSPW in water solutions. However, more defined peaks were observed at a lower offset of 10 nm when using methanol. The three peaks obtained for commercial NAs using synchronous fluorescence at $\Delta\lambda = 10$ nm, correspond with the three fluorescent species found using parallel factor analysis in water (Ewanchuk 2011). As expected, the three peaks increased at different rates. All three peaks found in the commercial NAs were also observed in the OSPW extract. However, the proportions of the first and second peak varied with these two sources. Additionally, the OSPW extract presented a fourth peak at a higher wavelength of 345 nm. Aromatic compounds fluoresce at different wavelengths depending on the number of aromatic rings: more

aromatic rings results in longer wavelengths. The average molecular weight and carbon number of OSPW extract is usually higher than for commercial NAs. This increases the likelihood of having polyaromatic structures in the OSPW extract and may explain the fourth peak at a higher wavelength. Qian *et al.* (2001) identified a dicyclic diaromatic acid and a sulfur-containing triaromatic acid as major components of the acid fraction of heavy crude oil by FT-ICR-MS.

If synchronous mode is used for NAs quantification, the sum of the peaks may be used to generate the calibration curve for a specific source of NAs. Alternatively, the first peak could produce higher method sensitivity, and could measure monoaromatic acids. Scarlett *et al.* (2012) have proposed monoaromatic acids among the most toxic structures in OSPW water. All peaks were observed at lower wavelengths than the expected for fulvic and humic acids. However, the contribution of phenols to the overall fluorescence signal may need further study. The concentration of these compounds can be elevated in tailings pond water, but are usually reported below 1 mg/L (Suncor 2009).

Routine environmental monitoring seeks to determine if the measured NAs originates from oil sands operations or occur naturally in the nearby bodies of water. Previous work has suggested that the source of NAs can be identified based on the relative abundance of acids with hydrogen deficiencies (Greuer *et al.* 2010). Additionally, the relative abundance of the sum of all the NAs with > 22 carbons was used to determine their toxicity and level of biodegradation (Holowenko *et al.* 2002). The relative abundance of peaks found using synchronous fluorescence could be explored as a complementary method to carbon number clusters, or hydrogen deficiencies. This approach has been followed to identify petroleum contaminants (Pharr *et al.* 1992), and characterize natural organic matter in river water (Ahmad *et al.* 2002). The relative abundance of peaks can give insights about the sample biodegradation as compounds with larger numbers of aromatic rings are more difficult to degrade than those with smaller numbers (Cerniglia 1992).

The use of synchronous fluorescence as a fingerprinting technique to distinguish whether the NAs are derived from different natural or industrial processes needs to be further evaluated. However, it can also be used to monitor the separation of aromatics from aliphatic compounds in the OSPW acid extract, and the separation of aromatic fractions by the number of rings. Due to its selectivity, SFS has been successfully used to monitor the separation of the aromatic fractions for hydrotreated naphthenic oil (Han *et al.* 2006).

Although determining speciation of NAs is not feasible using fluorescence spectroscopy, this technique may be used for a quick quantification of the total concentration in the

mixture. The complex mixture of the OSPW acid extract includes isomers that are not resolved by medium to low resolution mass spectrometry alone (Qian et al. 2001; Rudzinski et al. 2002), requiring high to ultrahigh resolution techniques such as FT-ICR-MS. In addition, the cost of using fluorescence spectroscopy is about 10-fold lower than mass spectrometry, it has lower personnel training requirements, and the results for the analysis of one sample can be obtained in ~5 minutes.

6.5. Conclusions

In this study, different organic solvents were tested for quantification of NAs using fluorescence spectroscopy, the tests revealed that polar protic solvents (alcohols) were more promising for total NA quantification due to higher sensitivity, lower light-scattering and lower blank intensity. The linearity expressed as R^2 was excellent, and its precision had a low relative standard deviation. The study also showed that the sensitivity of fluorescence using methanol can be improved by using 50% deionized water as a cosolvent. Using an aqueous buffer or a mild alkali (i.e. 0.1N NaOH) to enhance the signal warrants further method optimization. The calibration curve obtained using commercial NAs may need to be corrected to quantify accurately the OSPW-NAs (i.e. using a gravimetric method). Synchronous fluorescence using $\Delta\lambda = 10$ nm showed three fluorophores for commercial NAs, and four for OSPW acid extract. This fluorescence mode minimized signal overlapping, and identified fluorophores at higher wavelengths for the OSPW-NAs related to compounds with more aromatic rings. The use of fluorescence spectroscopy for NAs determination using polar protic organic solvents shows promising results for cost-effective analysis. Methanol is also an effective preservative for sample storage that would prevent biodegradation, or a potential eluent for qualitative characterization of NAs. The high solubility of NAs in methanol probably prevents partitioning and losses to the walls of storage vessels or handling equipment such as pipettes. The use of SPE for sample preparation utilizing polar solvents combined with fluorescence spectroscopy for quantification is a cost-effective protocol that may be further explored.

A version of this chapter has accepted for publication. Martin, N., Burkus, Z., McEachern, P., and Yu, T. (2014). "Naphthenic acids quantification in organic solvents using fluorescence spectroscopy." Journal of Environmental Science & Health, Part A: Toxic/Hazardous Substances & Environmental Engineering. 49:3, 294-306.

6.6. References

3M Purification Inc. "Empore Extraction Disks: Instructions for Use [online]." http://solutions.3m.com/wps/portal/3M/en_US/Empore/extraction/center/technical-library/disk-instructions/ (accessed January 2013).

Agren, A., Jansson, M., Ivarsson, H., Bishop, K., and Seibert, J. (2008). "Seasonal and runoff-related changes in total organic carbon concentrations in the River Ore, Northern Sweden." *Aquatic Sciences*, 70(1), 21-29.

Ahmad, U. K., Ujang, Z., Yusop, Z., and Fong, T. L. (2002). "Fluorescence technique for the characterization of natural organic matter in river water." *Water Science and Technology*, 46(9), 117-125.

Cerniglia, C. (1992). "Biodegradation of polycyclic aromatic hydrocarbons." *Biodegradation*, 3(2-3), 351-368.

de Conto, J. F., Nascimento, J. d. S., de Souza, Driele Maiara Borges, da Costa, L. P., Egues, Silvia Maria da Silva, Freitas, L. d. S., and Benvenuto, E. V. (2012). "Solid phase extraction of petroleum carboxylic acids using a functionalized alumina as stationary phase." *J. Sep. Science Journal of Separation Science*, 35 1615-9314.

El-Sayed, Y. S. (2013). "Optical properties and inclusion of an organic fluorophore in organized media of micellar solutions and beta-cyclodextrin." *Optics & Laser Technology*, 45(0), 89-95.

Environment Canada. (2011). "Lower Athabasca Water Quality Monitoring Plan Phase 1." *Rep. No. ISBN 978-1-100-18471-5*.

Ewanchuk, A. (2011). *Characterization of Oil Sands Process-Affected Water Using Fluorescence*. University of Alberta, Edmonton, AB.

Grewer, D. M., Young, R. F., Whittal, R. M., and Fedorak, P. M. (2010). "Naphthenic acids and other acid-extractables in water samples from Alberta: What is being measured?" *Science of the Total Environment*, 408(23), 5997-6010.

Han, S., Cheng, X., Ma, S., and Ren, T. (2006). "Application of synchronous fluorescence spectrometry in separation of aromatics from hydrotreated naphthenic oil." *Petroleum Science & Technology*, 24(7), 851-858.

Headley, J. V., Peru, K. M., Barrow, M. P., and Derrick, P. J. (2007). "Characterization of naphthenic acids from athabasca oil sands using electrospray ionization: the significant influence of solvents." *Analytic Chemistry*, 79(16), 6222-6229.

Hindle, R., Noestheden, M., Peru, K., and Headley, J. (2013). "Quantitative analysis of naphthenic acids in water by liquid chromatography-accurate mass time-of-flight mass spectrometry." *Journal of Chromatography A*, 1286(0), 166-174.

Holowenko, F. M., MacKinnon, M. D., and Fedorak, P. M. (2002). "Characterization of naphthenic acids in oil sands wastewaters by gas chromatography-mass spectrometry." *Water Research*, 36 (11), 2843-2855.

Huang, L., and Tam-Chang, S. (2011). "N-(2-(N',N'-Diethylamino)ethyl)perylene-3,4-dicarboximide and its quaternized derivatives as fluorescence probes of acid, temperature, and solvent polarity." *Journal of Fluorescence*, 21(1), 213-222.

Jivraj, M. N., MacKinnon, M., and Fung, B. (1995). *Naphthenic acids extraction and quantitative analyses with FT-IR spectroscopy*. Syncrude Canada Ltd, Edmonton, Canada.

Jones, D., West, C. E., Scarlett, A. G., Frank, R. A., and Rowland, S. J. (2012). "Isolation and estimation of the 'aromatic' naphthenic acid content of an oil sands process-affected water extract." *Journal of Chromatography A*, 1247(0), 171-175.

Kannel, P. R., and Gan, T. Y. (2012). "Naphthenic acids degradation and toxicity mitigation in tailings wastewater systems and aquatic environments: A review." *Journal of Environmental Science & Health, Part A: Toxic/Hazardous Substances & Environmental Engineering*, 47(1), 1-21.

Kavanagh, R. J., Burnison, B. K., Frank, R. A., Solomon, K. R., and Van Der Kraak, G. (2009). "Detecting oil sands process-affected waters in the Alberta oil sands region using synchronous fluorescence spectroscopy." *Chemosphere*, 76(1), 120-126.

Lakowicz, J. R. (2006). *Principles of Fluorescence Spectroscopy*. Springer, New York, NY.

Mohamed, M. H., Wilson, L. D., Headley, J. V., and Peru, K. M. (2008). "Screening of oil sands naphthenic acids by UV-Vis absorption and fluorescence emission spectrophotometry." *Journal of Environmental Science & Health, Part A: Toxic/Hazardous Substances & Environmental Engineering*, 43(14), 1700-1705.

Peuravuori, J., Koivikko, R., and Pihlaja, K. (2002). "Characterization, differentiation and classification of aquatic humic matter separated with different sorbents: synchronous scanning fluorescence spectroscopy." *Water Research*, 36(18), 4552-4562.

Pharr, D., McKenzie, J. K., and Hickman, A. B. (1992). "Fingerprinting petroleum contamination using synchronous scanning fluorescence spectroscopy." *Ground Water*, 30(4), 484-489.

Qian, K., Robbins, W. K., Hughey, C. A., Cooper, H. J., Rodgers, R. P., and Marshall, A. G. (2001). "Resolution and identification of elemental compositions for more than 3000 crude acids in heavy petroleum by negative-ion microelectrospray high-field fourier transform ion cyclotron resonance mass spectrometry." *Energy Fuels*, 15(6), 1505-1511.

RAMP. (2011). "Query water quality data [online]." <http://www.ramp-alberta.org/data/Water/water.aspx> (accessed October 2011).

Rudzinski, W. E., Oehlers, L., Zhang, Y., and Najera, B. (2002). "Tandem mass spectrometric characterization of commercial naphthenic acids and a maya crude oil." *Energy Fuels*, 16(5), 1178-1185.

Sauer, M., Hofkens, J., and Enderlein, J. (2011). "Handbook of Fluorescence Spectroscopy and Imaging: From Single Molecules to Ensembles." Wiley-Vch, 1-29.

- Scarlett, A. G., West, C. E., Jones, D., Galloway, T. S., and Rowland, S. J. (2012). "Predicted toxicity of naphthenic acids present in oil sands process-affected waters to a range of environmental and human endpoints." *Science of the Total Environment*, 425(0), 119-127.
- Scott, A. C., Young, R. F., and Fedorak, P. M. (2008). "Comparison of GC–MS and FTIR methods for quantifying naphthenic acids in water samples." *Chemosphere*, 73(8), 1258-1264.
- Seixas, d. M., Costa, T., Miguel, M. d. G., Lindman, B., and SchillÃn, K. (2003). "Time-resolved and steady-state fluorescence studies of hydrophobically modified water-soluble polymers." *Journal of Physical Chemistry B*, 107(46), 12605-12621.
- Shang, D., Kim, M., Haberl, M., and Legzdins, A. (2013). "Development of a rapid liquid chromatography tandem mass spectrometry method for screening of trace naphthenic acids in aqueous environments." *Journal of Chromatography A*, 1278(0), 98-107.
- Sharma, V. K., Mohan, D., and Sahare, P. D. "Fluorescence quenching of 3-methyl 7-hydroxyl Coumarin in presence of acetone." *Spectrochimica Acta Part A: Molecular and Biomolecular Spectroscopy*, 66 111-113.
- Sjöblom, J., Havre, T. E., and Vindstad, J. E. (2003). "Oil/Water-Partitioning and Interfacial Behavior of Naphthenic Acids." *Journal of Dispersion Science & Technology*, 24(6), 789-801.
- Smallwood, I. M. (1996). *Handbook of Organic Solvent Properties*. Arnold, London.
- Suncor. (2009). *Tailings Reduction Operation*. Suncor Energy Inc., Calgary.
- Tucker, S. A., Amszi, V. L., and Acree, W. E. (1992). "Primary and secondary inner filtering: Effect of $K_2Cr_2O_7$ on fluorescence emission intensities of quinine sulphate." *Journal of Chemical Education*, 69(1), A8-A12.
- Woudneh, M. B., Coreen Hamilton, M., Benskin, J. P., Wang, G., McEachern, P., and Cosgrove, J. R. (2013). "A novel derivatization-based liquid chromatography tandem mass spectrometry method for quantitative characterization of naphthenic acid isomer profiles in environmental waters." *Journal of Chromatography A*, 1293(0), 36-43.
- Wypych, G. (2008). "Knovel Solvents - A Properties Database." *ChemTec Publishing*, .
- Zhao, B., Currie, R., and Mian, H. (2012). "Catalogue of analytical methods for naphthenic acids related to oil sands operations." *Rep. No. TR-21*, Oil Sands Research and Information Network (OSRIN).

Chapter 7. Feasibility of using POCIS and Chemcatcher passive samplers for naphthenic acids

7.1. Introduction

A state-of-the-art monitoring system is desired for the Lower Athabasca River and its tributaries to assess impacts from oil sands developments in this basin. Traditional water monitoring through discrete or composite samples do not give an accurate assessment of mass loading in situations where naphthenic acids (NAs) fluctuate widely. Advanced passive samplers are desired to improve our ability to quantify mass loading of NAs in this difficult and costly northern environment. Passive samplers have the benefit of accumulating target compounds to obtain detectable and time-averaged concentrations much like biomonitoring, but with improved reproducibility (El-Shenawy et al. 2009). Additional benefits of passive sampling are that they are relatively inexpensive, simple to use and do not require any external source of energy for their operation. They usually combine sampling, selective analyte isolation, pre-concentration and in some cases preservation in a single step.

In order to use passive samplers, the compound specific uptake rate has to be determined through field or lab calibrations. The main classification of passive samplers is due to the polarity of the compounds that they can sample. There is some ambiguity in the upper range of polar samplers, since it has been reported as $\log K_{ow} < 3$ (Kuster et al. 2010) and $\log K_{ow} < 4$ (Kingston et al. 2000). Naphthenic acids have been reported both as polar (Schramm 2000) and non-polar organic compounds (American Petroleum Institute 2003; Sjöblom et al. 2003). For this reason, the uptake rate and selectivity of the polar organic chemical integrative sampler (POCIS) originally designed for detection of pharmaceuticals in water, and the Chemcatcher sampler (non-polar) were evaluated in lab experiments.

7.2. Materials and methods

Two badge-type samplers were used in the laboratory uptake rate experiments: the POCIS sampler and the Chemcatcher. The POCIS sampler, including the metal rings, HLB Oasis resin, and polyether sulfone (PES) membrane were obtained from Environmental Sampling Technologies, Inc. (St. Joseph, MO). The membranes and Oasis HLB resin were stored at $-20\text{ }^{\circ}\text{C}$ following the recommendation of the supplier. Chemcatcher PTFE housings and low-density polyethylene (LDPE) membranes were acquired from the School of Biological Sciences, University of Portsmouth. The Empore™ disks 47 mm

(Anion, C18, SDB-XC) were from 3M Purification Inc. (St. Paul, MN). The functional group in the disks (e.g. octadecyl) is entrapped into an inert matrix of PTFE (90% sorbent: 10% PTFE, by weight). The Zefluor™ (PTFE) membrane was from Pall (Port Washington, NY), and the nylon (HNWP, 0.45 µm, Millipore), cellulose (HAWP, 0.45 µm, Millipore) and fiberglass (EPM2000, Whatman) membranes from Fisher Scientific (Edmonton, AB).

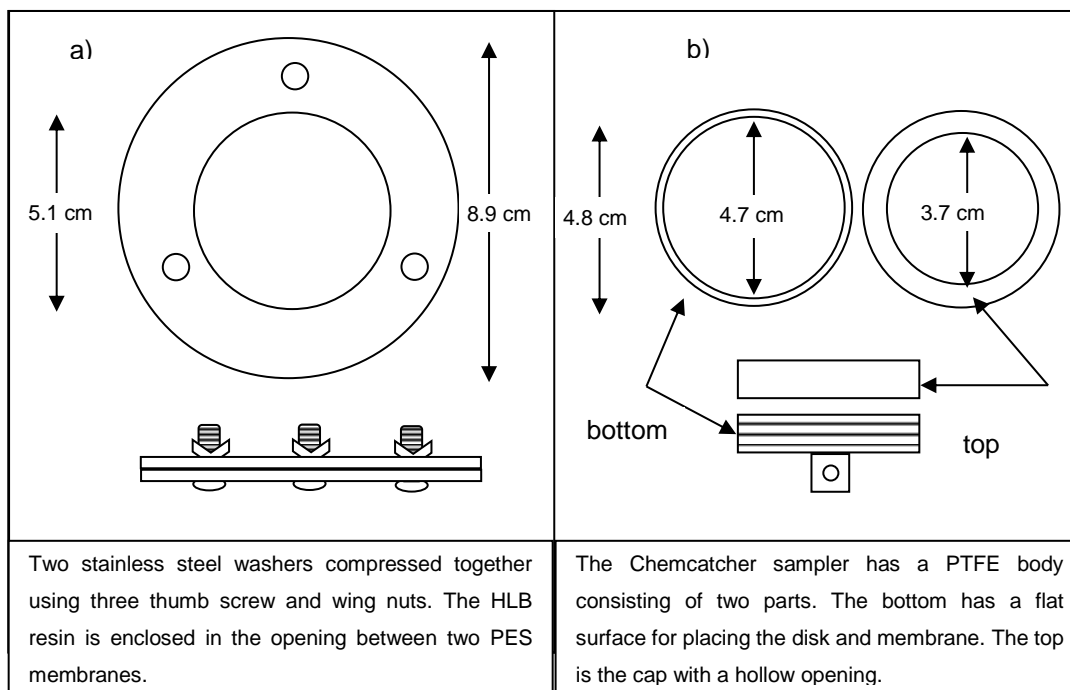


Figure 7-1. Top and side view of sampler a) POCIS, b) Chemcatcher (open)

The solvents methanol, 2-propanol, 95%-ethanol, dichloromethane (DCM), n-hexane and acetone were also purchased from Fisher Scientific. These solvents were reagent grade or higher quality. Commercial naphthenic acids (Fluka) were obtained from Sigma-Aldrich (Oakville, ON), and fresh OSPW was obtained from a bitumen producer in Northern Alberta's oil sands mining region. The extraction procedure and concentration of the NAs stock solution of 1045 mg/L measured by HPLC-MS/MS were reported in Chapter 6. The commercial NAs stock solution was prepared in methanol with a nominal concentration of 1000 mg/L (w/v) using an analytical balance accurate to 0.1 mg. The Fluka and OSPW stock solutions were kept in glass vials with Teflon® caps at 4 °C when not used. Two types of water were used: deionized water (DIW) and Edmonton tap water (TW). The TW had an average pH of 7.7, hardness 163 mg CaCO₃/L, TDS 214 mg/L and TOC 2.2 mg/L (monthly water quality report, EPCOR 2012).

Fluorescence spectroscopy was used for NAs quantification for all the experiments. The fluorescence intensity was obtained using a Varian fluorescence spectrophotometer model Cary Eclipse from Agilent Technologies (Mississauga, ON) in a quartz cuvette (10 mm x 10 mm) with a PTFE stopper. Separate calibration curves were determined for each solvent and NAs source. The instrument settings and the calibration curves for organic solvents and water were reported in Chapter 6. The calibration curve for aqueous solution was obtained from the 280 nm excitation wavelength and the 340 nm emission wavelength (See *Appendix N*).

7.2.1. Naphthenic acid recovery from HLB resin and Empore disks

The recovery of NAs from the HLB resin was assessed using 95%-ethanol, methanol, 2-propanol, DCM and n-hexane. The HLB resin was weighed on a balance to 0.200 g and transferred into a glass gravity/flow chromatography column (1 cm i.d.) fitted with glass wool plugs and stopcocks. The resin was spiked with 20 mL of a 150 mg/L NAs solution in TW. This concentration was selected above the typical sequestered mass to demonstrate that the sorbent had sufficient capacity. The NAs adsorbed onto the resin were extracted using 2 x 20 mL of solvent. The extract was adjusted to 50 mL in a volumetric flask, and analyzed for NAs using fluorescence spectroscopy. The NAs mass retained in the solid phase, and the mass recovered after extraction was determined. A blank was analyzed by extracting the HLB resin without being spiked. The mass retained was the difference of the mass added to the column, and the mass obtained from the water eluted. The mass recovered was obtained from the solvent extract concentration and volume, subtracting the blank.

Three Empore™ disks: C18, Anion and SDB-XC were tested for recovery using a glass vacuum filter holder assembly which consisted of a glass funnel and base, coarse-frit glass filter support, clamp, vacuum flask with rubber stopper and tubing. The disks were cut to a diameter of 8 mm with scissors to fit this system. The receiving phase for the Chemcatcher sampler is typically a C18 disk. Alternatives to the C18 Empore disk are the RPS (not tested) and XC disks. The disks tested were conditioned according to the manufacturer's recommendation (3M Purification Inc, 2013). This procedure generally consisted in soaking the disks in reagents (methanol and reagent water for C18; acetone, methanol, sodium hydroxide 1 M, and reagent water for Anion; acetone and 2-propanol for SDB-XC) and removing the liquid using a vacuum. For each conditioned disk, a 20 mL aliquot of 20 mg/L NAs solution was spiked and a vacuum was applied. The liquid was collected for NAs determination. The NAs adsorbed onto the disk were extracted using 2

x 20 mL of methanol. The extract was brought to 50 ml in a volumetric flask, and analyzed for NAs using fluorescence.

Additionally, the recovery from the C18 disk was also tested using a sonication bath for conditioning and extraction. First, the C18 was conditioned with 20 mL methanol in a 40-mL closed glass vial. The vial with the disk was sonicated for one minute, the methanol was wasted and the process was repeated. A disk was transferred to a 40-mL glass vial with DI water where it was kept until used. Then, the disk was exposed overnight (~12 hr) to 40 mL of a 20 mg/L NAs solution in TW in a 40-mL capped glass vial. The vial was placed on a wrist action shaker, Burrel Scientific model 75 (Pittsburgh, PA), at a medium intensity (5 on a 0 - 10 scale). The disk was transferred with tweezers to an empty glass vial and extracted with 2 x 20 mL methanol using 1 min of sonication. The methanol was adjusted to 50 mL in a volumetric flask. The fluorescence intensity was measured for the final solution and extract for NAs quantification. After recovery testing, Anion and XC disks were eliminated for further analysis as described in more details in the Section 7.3.

7.2.2. C18 and HLB adsorption capacity for NAs sampling

The maximum adsorptive capacity of the C18 disk and HLB resin was assessed to confirm their capacity to adsorb NAs for long sampling periods. A 10 mg/L solution of Fluka NAs in TW was passed through the sorbent in the glass vacuum system and chromatographic glass column used in the recovery experiments for C18 and HLB respectively. The solution was added progressively with volumes ranging from 10 mL to 100 mL and eluted immediately. The peak intensity of the eluted solution was measured. The breakthrough point when the mass retention was < 98% was obtained.

7.2.3. Membrane and sorbent diffusion and partitioning

Diffusion experiments were performed in order to quantify the movement of NAs through the membrane (PES, PTFE, LDPE and cellulose) to the receiving phase (HLB resin or C18 disks). The diffusion assembly was similar to a Franz cell (Shiow-Fern et al. 2010) with modifications to have a continuous flow system according to Fedkin et al. (2002). In this set up, two chambers at different analyte concentration (donor and acceptor) were only separated by a membrane and joined by a clamp (See *Appendix K*). The donor cell (bottom) had a volume of 20 mL, and the acceptor cell (top) of 10 mL, both with an internal diameter of 40 mm. A lateral tube was designed to avoid any hydrostatic pressure from the top chamber. The solution was introduced from the bottom of the first cell and recirculated through the lateral tube using a peristaltic pump at a flow of 1.5 mL/min. The 20 mg/L NAs solution was recirculated from a 1-L Erlenmeyer flask, which

was continuously stirred using a magnetic bar. The change of concentration from the acceptor chamber was monitored every hour. A sample was obtained from the donor chamber at the beginning and the end of the experiment. The experiment was run for four hours, and overnight (~12 h) for the cellulose, PTFE and PES membranes.

The partitioning coefficient was measured for the C18 disk and HLB resin, as well as, for six different membranes: PTFE, nylon, cellulose, LDPE, PES and fiber glass. About 1 cm² of membrane or sorbent material (6 mg for HLB resin) was immersed in 40 mL of 5 mg/L NAs solution in water and shaken in 40-mL glass vials. The exact mass of each material was measured using an analytical balance accurate to 0.1 mg. The blank consisted of a 5 mg/L solution of NAs in a 40-mL glass vial. Two separate vials were prepared for each material and blank for replication. The fluorescence peak intensity was measured for the solution at the beginning of the experiment and after 24 h. The final mass of NAs in the water and solid phase was determined for the two replicates, and the average partitioning coefficient, K_p , was calculated as the mass ratio:

$$K_p = \left(\frac{M_{NAs,sorb} / M_{sorb}}{M_{NAs,water} / M_{water}} \right) \quad (7-1)$$

7.2.4. Naphthenic acid mass balance for POCIS and Chemcatcher uptake experiments

Uptake rate experiments were performed with the POCIS and Chemcatcher samplers following the microcosm with renewal method (Alvarez et al. 2005). In this method, each assembled sampler was suspended using plastic fishing line in a glass beaker containing NAs solution. The beaker was covered with aluminum foil to avoid loss through evaporation. The solution was renewed in the same beaker every 24 h ± 1 h. Before renewal 20 mL of the solution were collected for NAs determination using fluorescence. The experiments were performed at room temperature, and magnetic stirrers were set to a low stirring rate (60 rpm). Additionally, a blank was tested for sampler contamination using DI water instead of NAs solution, and a second set of assembly blanks was used with NAs solution and a POCIS sampler without the HLB resin.

Uptake experiments were performed for POCIS using 1 L of 0.5 mg/L or 1 mg/L NAs solution over an exposure period of 4, 8 and 30 d. The POCIS samplers were assembled according to the method outlined by Alvarez *et al.* (2005) using the large configuration with surface area of ~ 41 cm². Briefly, 0.200 mg HLB Oasis resin was packed inside two PES membranes between two stainless steel washers held together by three thumbscrews and wing nuts (Figure 7-1). At the end of the experiment, the resin was

carefully transferred into the extraction column. The resin stuck onto the membranes was rinsed to the column using DI water. The NAs were extracted from the resin using methanol as explained in the recovery experiment. To measure the mass of NAs adsorbed to the membrane, each side of the two membranes was rinsed with 10 mL of methanol in a 50-ml beaker and the volume adjusted to 50 mL in a volumetric flask. The mass of NAs measured in the solution and extracts, after any blank corrections, was used to calculate a mass balance. The percentage of the mass adsorbed to each surface and the results of the two blanks helped to determine if there was a significant sorption to other surfaces besides the HLB resin.

The Chemcatcher was assembled according to Kingston *et al.* (2000) by placing the adsorbent material and the membrane in the PTFE supporting case. A PTFE membrane was used instead of LDPE due to lower partitioning (Figure 7-4) and two different solid receiving phases were evaluated: C18 disk and HLB resin. For the HLB configuration, 0.100 g HLB Oasis resin was sandwiched between two PTFE membranes. The uptake experiments were performed in a similar way as explained for POCIS. Since this sampler has a smaller diameter than POCIS, two samplers were suspended in a 2-L beaker. The samplers were exposed to commercial NAs for four days at different concentrations (0.5 mg/L, 1 mg/L and 2 mg/L). Two blanks were used to assess the partitioning to surfaces other than the C18 disk using the Chemcatcher housing with and without a PTFE membrane. The extractions of NA from the disk and membrane were performed separately using sonication. In each case, 2 x 20 mL methanol was used in a 40-mL glass vial with Teflon cap, and the extract was adjusted to 50 mL in a volumetric flask. The mass balance and uptake rate was obtained from these experiments. The best membrane and sorbent material were selected for further tests, with details described in Chapter 8.

7.3. Results and discussion

7.3.1. Recovery of NAs from sorbents

The NAs recovery from HLB resin was close to 90% using 95%-ethanol, methanol and 2-propanol, while the recovery with DCM was only 73% (Figure 7-2). The extractions were not feasible using n-hexane because it did not elute from the column. Methanol was previously used for extraction of HLB resin from POCIS (Alvarez *et al.* 2004) and C18 disk in Chemcatcher (Vermeirssen *et al.* 2009). For this reason, it was selected for further experiments. The NAs recovery obtained for the C18 disk using methanol of $96\% \pm 9\%$ (vacuum system) and $92\% \pm 8\%$ (sonication) was comparable with the one obtained

using HLB resin. The recovery for the other two disks was over 100% ($113\% \pm 3\%$ for SDB-XC and $120\% \pm 6\%$ Anion disks). This could be due to the interference of the acetone used in the conditioning steps since this organic solvent seems to affect the fluorescence signal of NAs as reported in Chapter 6. Another reason could be that the disks have some compounds that are co-extracted and interfere with the NAs signal. Further testing may be required to see the feasibility of using those disks. However, the conditioning procedure of C18 is simpler and uses fewer reagents than the Anion and SDB-XC disks. For these reasons, the C18 Empore disk was selected for further experiments.

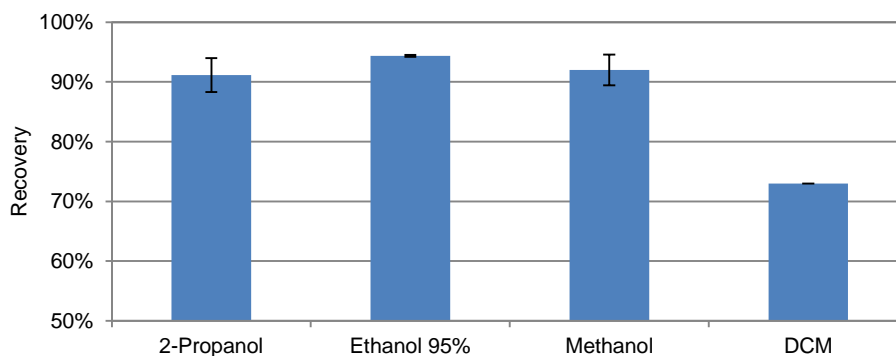


Figure 7-2. NAs percentage recovery from HLB resin using different solvents

7.3.2. Determination of disk and resin capacity

In the maximum capacity experiment, the analysis of the water eluent from the column generally resulted in NAs concentration below the detection limit indicating the commercial NAs had been suitably retained by the HLB resin. The maximum mass adsorbed was 6.28 mg with 98% retention. This represents a capacity of 31.33 mg NAs/g HLB. Assuming an uptake rate of 0.40 L/d, (see Chapter 8), and a TWA concentration of 0.5 mg/L the sampler should be able to retain NAs for > 30-day monitoring campaign. The C18 disk could retain > 98% of the NAs mass up to 1.47 mg or 14.7 mg/g sorbent. The 47 mm disk used in Chemcatcher is about six times bigger than the one used to assess the maximum capacity. For this reason, the disk may hold 8.61 mg of NAs. This should be enough to sample NAs for > 30 days, and very likely behave as an infinite sink.

7.3.3. Diffusion of NAs through membranes

The diffusion of NAs was tested for PES, PTFE, LDPE and cellulose membranes in the continuous system. The concentration of NAs increased very quickly in the acceptor chamber for the cellulose membrane and very slowly for the PES membrane (Figure 7-

3). The diffusion observed followed the order cellulose > PTFE > LDPE >> PES. The increase in concentration in the acceptor chamber using PES membrane was very low even after 24 h.

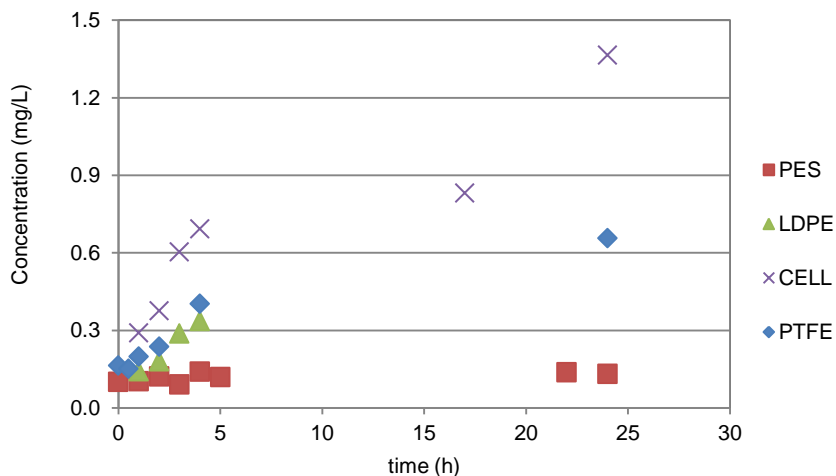


Figure 7-3. Change in concentration of NAs in the acceptor chamber due to diffusion using different membranes (cellulose, CELL)

7.3.4. Partitioning of NAs to membranes and resins

The glass fiber membrane was disintegrated during the experiment due to mechanical forces, and it was not considered in further tests. The results showed that both the receiving phase and the membrane from the POCIS sampler, HLB and PES, had a good affinity for NAs (Figure 7-4). Although the $\log K_p$ was higher for the resin (T-test, $\alpha= 0.05$), a POCIS sampler has 0.200 g of resin and about 0.9 g of PES membrane, thus more NAs could partition onto the membrane.

The cellulose and LDPE membranes had a partition coefficient higher than the C18 disk (T-test, $\alpha= 0.05$). LDPE membrane is used in the non-polar configuration of Chemcatcher; however, NAs had higher affinity for this membrane than for the C18 receiving phase. The PTFE membrane was chosen for further testing because it had low partitioning and high diffusion, making it more suitable as a sampler membrane. A PTFE membrane was originally tested in Chemcatcher laboratory experiments for polar and non-polar pesticides ($\log K_{ow}$ 2.21 to 6.90), but it has not been reported for field applications yet. Even though a 10-fold decrease in the uptake rate was observed in those experiments in comparison to the naked disk, all the tested compounds passed through the membrane and were accumulated in the disk (Kingston et al. 2000).

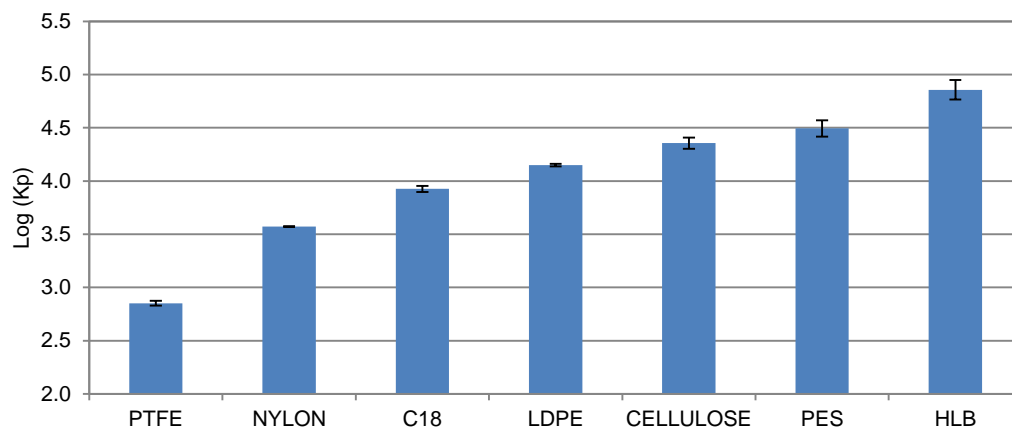


Figure 7-4. NAs partitioning to different membrane and sorbent materials, bars represent standard deviation

7.3.5. Mass balance in uptake experiments

One of the great challenges with NA quantification is awareness of adsorption to surfaces. As an example in this work, preliminary experiments with POCIS and Fluka NAs used plastic foil to cover the beakers in the microcosm with renewal experiments. Surprisingly, the polyethylene foil was responsible for a signal intensity drop > 20%. This was confirmed by rinsing the plastic foil with methanol. The clean plastic foil gave a signal of 16.5 while the foil used in the uptake experiment gave a signal of 50. The signal intensity dropped only 7% using aluminum foil. Thus aluminum foil was used for covering all the microcosms discussed in the following sections, but the results demonstrate the affinity NAs have for virtually any surface typically used in lab extraction procedures.

The method to transfer the HLB resin to the column at the end of the experiment was also improved in the preliminary experiments. Even though most of the resin was easily transferred into the column after letting the sampler drain at the end of the experiment, a thin layer of resin remained adhered to the membrane. This resin was initially transferred into the column by rinsing the membrane with methanol as recommended by Alvarez *et al.* (2004). Due to NAs adsorption onto the membrane, as discussed in Section 7.3.4, rinsing the membrane with methanol generated a high standard deviation in these preliminary tests. The method was modified using DIW for rinsing the membrane, which improved replication significantly. The results in this Section include experiments that took into account the method improvements discussed previously.

Mass balance with POCIS sampler

The concentration of NAs in water showed an unexpected drop in the uptake experiments using POCIS samplers after 24 h exposure. The two different initial concentrations (0.5 mg/L and 1 mg/L) reached a similar minimum concentration close to 0.20 mg/L (Figure 7-5). No clear positive trend was observed for the concentration of NAs in the solution even in the 30-day experiment. The naphthenic acid concentration drop in solution was investigated by running two blanks in parallel. The first blank with metal rings, but without POCIS disk did not result in a substantial decrease in concentration. However, the blank including a POCIS without HLB resin had a similar decrease in NAs concentration to the system with the complete sampler. The NAs depletion by these blanks suggested that the PES membrane was a major sink of NAs, which was supported by the partitioning experiment.

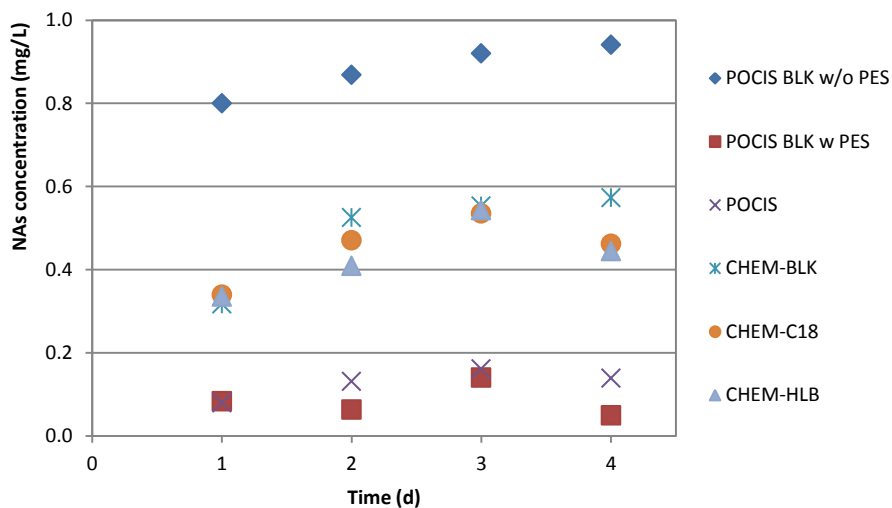


Figure 7-5. Concentration of Fluka NAs before water renewal in POCIS and Chemcatcher uptake experiments

The mass balance including the final NAs concentration in solution, the mass extracted from the HLB resin and membranes accounted for 80% of the mass added to the system. This is reasonable since the NAs recovery from the HLB resin was ~ 90%, and the change of concentration from the blank using only the solution of NAs was 7%. Potential routes for removal of NAs from the water by sorption to the walls of the glass container and metal components of the sampler were examined by rinsing the surfaces with methanol and analyzing the rinsates. In all cases, traces of NAs were negligible. Additionally, the HLB resin was well retained within POCIS assembly (Figure 7- 1) during the experiment with a mass loss < 10% determined gravimetrically.

The mass adsorbed onto the membrane (after subtracting the blank from a clean membrane), as determined by fluorescence was ~4 fold higher than the mass adsorbed onto the resin. This ratio was conserved in the 8 and 30-day experiments, and as a result it was not attributed to an initial stage where the membrane gets saturated with NAs before it starts transferring to the resin. The diffusion experiments showed that once the PES membrane adsorbs the NAs, they were diffused at very low rates. As a result, the mass adsorbed onto the membrane accounted for about 50% of recovered NAs (Figure 7-6) and 40% mass added to the system in the 4-day exposure experiment. The membrane is intended to control the rate of mass transfer of analyte molecules to the sorption phase, and to determine selectivity excluding certain classes (polar or non-polar), molecular sizes or species from being sequestered. However, some studies have observed that more hydrophobic compounds remained adsorbed to the PES membrane (Kingston et al. 2000; Vermeirssen et al. 2009) recommending to use membranes with a low affinity for the analyte (Kingston et al. 2000).

Due to the high adsorption onto the membrane and the corresponding drop in the NAs concentration, the uptake rate for POCIS sampler could not be estimated. However, the uptake rate is proportional to the mass adsorbed, and a low uptake rate is expected using the mass adsorbed onto the receiving phase. The uptake rate of this sampler is based on the adsorption of the analyte in the HLB Oasis resin alone, and the membrane behaves as a selective transfer barrier and protection for the resin. Alternatively, the membrane could be taken into account as an adsorbent. Membranes alone have been used as passive samplers (Allan et al. 2009); however, this brings new challenges for its use in the field that need to be addressed such as biofilm formation. The experiments performed with NAs showed results that were not expected from other POCIS applications for pharmaceuticals, pesticides, and other polar compounds with $\log K_{ow} < 4$ (Alvarez et al. 2004). Although the NAs have a hydrophilic functional group, the log octanol-water partition coefficient for carboxylic acids with > 10 carbons is > 4 (Yaws 1999). For this reason, the non-polar configuration of the Chemcatcher was also assessed.

Mass balance with Chemcatcher sampler

Two configurations with different sorbent (C18 and HLB) were used to evaluate the mass balance in the Chemcatcher uptake experiments (Figure 7-5 and Figure 7-6). For the HLB configuration, two PTFE membranes were used to “sandwich” the resin, while for C18 disk only one membrane was used. In both configurations, the concentration of NAs in solution never dropped as drastically as with the POCIS sampler. Additionally, two

blanks were used, one with the PTFE housing and PTFE membrane, and one only with the housing. The change of peak intensity was negligible in the blank without membrane, and the blank with membrane showed a steady increase of NAs concentration in water reaching values closer to the initial concentration of 1 mg/L at the end of the 4 d experiment (Figure 7-5) meaning that the system underwent equilibrium through the saturation of surfaces with NAs. Similarly, the solution for both configurations of Chemcatcher samplers showed a steady increase in the concentration of NAs in solution with time.

The mass balance for the Chemcatcher with C18 disk performed as described for POCIS evaluation. The total mass was accounted for using the final concentration of NAs in water, the mass extracted from the membrane and sorbent was 79% of the NAs added to the system. The mass balance for the Chemcatcher using HLB resin was lower, likely due to resin loss from the PTFE case. From the mass accounted, the two Chemcatcher configurations retained about 6 and 21 times more NAs in the sorbent (HLB and C18 respectively) than in the membrane, while this ratio for POCIS was 0.2. Even though the total adsorption of the POCIS was higher than any of the two Chemcatcher configurations, the adsorption was mostly on the PES membrane (Figure 7-6).

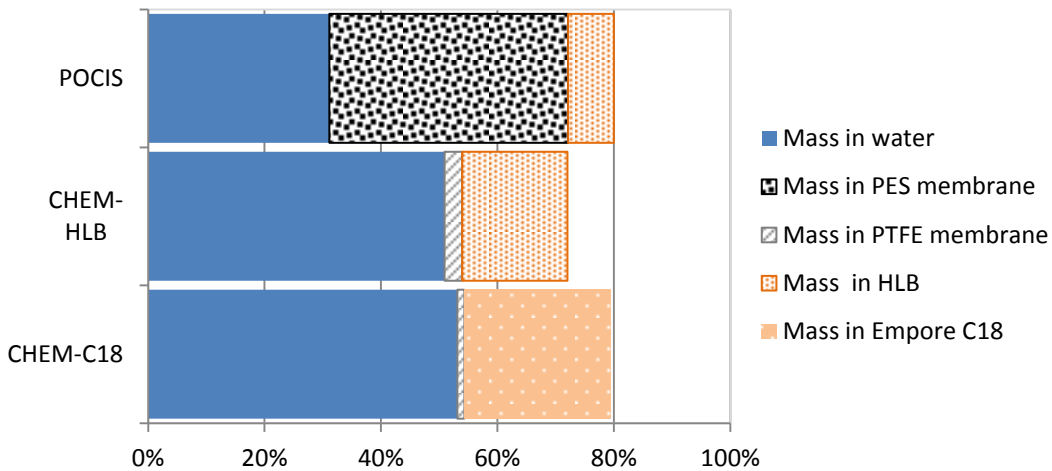


Figure 7-6. Mass distribution of NAs in components of the POCIS and Chemcatcher uptake experiments after 4 d

As a result of a high NAs uptake in the C18 disk the concentration of NAs in water decreased close to half of the initial value. For this reason, the uptake rate could not be estimated using the initial NAs concentration in solution. A more accurate way is taking into account the change in concentration by solving for the uptake rate, R_s

$$M = R_s C_{wo} \left[\exp\left(\frac{-R_s}{V}\right) \right] t \quad (7-2)$$

Where M is the mass adsorbed on the sorbent material, C_{wo} is the initial concentration of NAs in solution, V is the volume of solution and t is the exposure time. The uptake rates for commercial NAs estimated using this equation were $0.33 \text{ L/d} \pm 0.03 \text{ L/d}$ and $0.19 \text{ L/d} \pm 0.01 \text{ L/d}$ when using C18 and HLB respectively. A high uptake rate is usually desirable for concentrating higher volumes of water than those obtained from grab samples. The uptake rate was almost double using C18 in comparison with HLB. A disadvantage of using HLB resin in the Chemcatcher housing was that 17% of the resin mass was lost. Additionally, using Empore disks has the advantage that they are easier to extract and assemble.

7.4. Conclusions

The feasibility of using POCIS or Chemcatcher to sample NAs was tested using Fluka NAs. POCIS presented limitations to be used as a passive sampler for NAs due to a high partitioning onto the PES membrane and low diffusion to the HLB resin. Commercial NAs had high affinity to many polymers used in standard extraction and quantification methods; great care must be taken to understand these potential interferences and avoid or account for these interferences when quantifying NA concentrations. In terms of optimum membrane material a PTFE membrane provides protection to the receiving phase without interfering in the NAs' adsorption process. The Chemcatcher was assessed using two different sorbents, HLB and C18 disk, in both cases using PTFE membrane. The uptake rate was higher using C18 than HLB resin. The C18 disk had a high recovery of commercial NAs using sonication bath and methanol. Additionally, its adsorptive capacity showed to be appropriate for monitoring campaigns of up to one month when tested on commercial NAs. The Chemcatcher sampler with PTFE membrane and C18 disk showed potential to monitor NAs in the LAR. This sampler was further evaluated in Chapter 8.

7.5. References

3M Purification Inc. "Empore Extraction Disks: Instructions for Use [online]." http://solutions.3m.com/wps/portal/3M/en_US/Empore/extraction/center/technical-library/disk-instructions/ (accessed January 2013).

Allan, I. J., Booij, K., Paschke, A., Vrana, B., Mills, G. A., and Greenwood, R. (2009). "Field performance of seven passive sampling devices for monitoring of hydrophobic substances." *Environmental Science and Technology*, 43(14), 5383-5390.

Alvarez, D. A., Petty, J. D., Huckins, J. N., Jones-Lepp, T. L., Getting, D. T., Goddard, J. P., and Manahan, S. E. (2004). "Development of a passive, in situ, integrative sampler for hydrophilic organic contaminants in aquatic environments." *Environmental Toxicology and Chemistry*, 23(7), 1640-1648.

Alvarez, D. A., Stackelberg, P. E., Petty, J. D., Huckins, J. N., Furlong, E. T., Zaugg, S. D., and Meyer, M. T. (2005). "Comparison of a novel passive sampler to standard water-column sampling for organic contaminants associated with wastewater effluents entering a New Jersey stream." *Chemosphere*, 61(5), 610-622.

American Petroleum Institute. (2003). "Reclaimed Substances: Naphthenic Acid." *Rep. No. 201-14906B*, American Petroleum Institute, Washington D.C. <http://www.epa.gov/hpv/pubs/summaries/resbscat/c14906rs.pdf> (accessed January 2013).

El-Shenawy, N., Greenwood, R., Abdel-Nabi, I., and Nabil, Z. (2009). "Comparing the Passive sampler and biomonitoring of organic pollutants in water: a laboratory study." *Ocean Science Journal*, 44(2), 69.

EPCOR. (2012). "Water Quality Monthly Summary." <http://www.epcor.com/water/reports-edmonton/Documents/wq-edmonton-july-2012.pdf> (August 2012, 2012).

Fedkin, M. V., Zhou, X. Y., Hofmann, M. A., Chalkova, E., Weston, J. A., Allcock, H. R., and Lvov, S. N. (2002). "Evaluation of methanol crossover in proton-conducting polyphosphazene membranes." *Mater Letter*, 52(3), 192-196.

Kingston, J. K., Greenwood, R., Mills, G. A., Morrison, G., and Persson, L. (2000). "Development of a novel passive sampling system for the time-averaged measurement of a range of organic pollutants in aquatic environments." *Journal of Environmental Monitoring*, 2 487.

Kuster, M., De, I. C., Eljarrat, E., López, d. A., and Barceló, D. (2010). "Evaluation of two aquatic passive sampling configurations for their suitability in the analysis of estrogens in water." *Talanta*, 83(2), 493-499.

Schramm, L. L. (2000). *Surfactants: Fundamentals and Applications in the Petroleum Industry*. Cambridge University Press, Cambridge, UK.

Shiow-Fern, N., Rouse, J., Sanderson, D., and Eccleston, G. (2010). "A comparative study of transmembrane diffusion and permeation of ibuprofen across synthetic membranes using Franz diffusion cells." *Pharmaceutics*, 2 209.

Sjöblom, J., Havre, T. E., and Vindstad, J. E. (2003). "Oil/Water-Partitioning and Interfacial Behavior of Naphthenic Acids." *Journal of Dispersion Science & Technology*, 24(6), 789-801.

Vermeirssen, E. L. M., Bramaz, N., Hollender, J., Singer, H., and Escher, B. I. (2009). "Passive sampling combined with ecotoxicological and chemical analysis of pharmaceuticals and biocides – evaluation of three Chemcatcher™ configurations." *Water Research*, 43(4), 903-914.

Yaws, C. L. (1999). *Chemical Properties Handbook: Physical, Thermodynamics, Environmental Transport, Safety & Health Related Properties for Organic & Inorganic Chemical*. McGraw-Hill, USA.

Chapter 8. Evaluation of uptake rates for commercial naphthenic acids using chemcatcher passive sampler

8.1. Introduction

The uptake rate for passive samplers depends on factors related to its configuration (ratio of exposure area to mass of sorbent), environmental factors (temperature, turbulence, biofouling), and the compound to be sampled (diffusivity, hydrophobicity). It is important to assess the effect of environmental factors in the uptake rate and make the appropriate corrections to the concentration obtained in monitoring campaigns. Additionally, it is necessary to know when the sampler will be within the integrative regime in the application of passive samplers. It is usually desired to work during the initial integrative sampling stage retrieving the sampler before it reaches equilibrium. In this stage, it is assumed that the desorption is negligible and the device acts as an infinite sink of contaminants. Therefore, the amount of analyte accumulated is linearly proportional to the deployment time and TWA concentration in water.

In the previous Chapter, the feasibility of using the polar organic chemical integrative sampler (POCIS) or Chemcatcher was assessed. In this Chapter, the performance of the Chemcatcher sampler was evaluated in lab experiments using commercial naphthenic acids (NAs). The objectives of this section are to evaluate the Chemcatcher uptake rate for NAs sampling, assess their performance and give some recommendations regarding the standard operating procedure (SOP) for its analysis in the lab. The performance experiments aimed to answer important questions such as (i) How long can these samplers be deployed with a linear uptake, (ii) Which environmental factors affect the most the uptake, (iii) How significant is the lag time response, (iv) How well does the sampler integrate changes in the NA concentration of the water.

8.2. Materials and methods

Chemcatcher PTFE housings were acquired from the School of Biological Sciences, University of Portsmouth. The Empore™ C18 disk 47 mm was from 3M (St. Paul, MN). The Zefluor™ (PTFE) membrane was from Pall (Port Washington, NY). The solvent methanol HPLC grade was purchased from Fisher Scientific (Edmonton, AB). Commercial naphthenic acids (Fluka) were obtained from Sigma-Aldrich (Oakville, ON). The commercial NAs stock solution was prepared in methanol with a nominal concentration of 1000 mg/L (w/v) using an analytical balance accurate to 0.1 mg. The Fluka stock solution was kept in a glass vial with Teflon® cap at 4 °C when not used.

Deionized water (DIW) and Edmonton tap water (TW) were used. The TW had an average pH of 7.7, hardness 163 mg CaCO₃/L, TDS 214 mg/L and TOC 2.2 mg/L (monthly water quality report, EPCOR 2012).

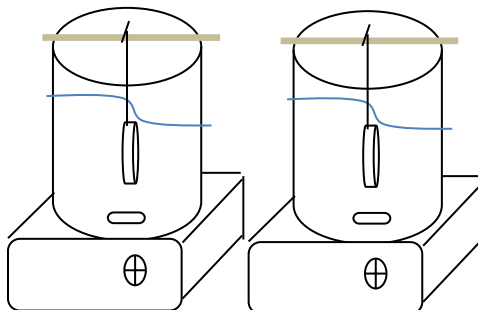


Figure 8-1. Microcosms experiment

Fluorescence spectroscopy was used for the NAs quantification in all the experiments. The fluorescence intensity was obtained using a Varian fluorescence spectrophotometer model Cary Eclipse from Agilent Technologies (Mississauga, ON) in a quartz cuvette (10 mm x 10 mm) with a PTFE stopper. The instrument settings and the calibration curves for organic solvents and water were reported in Chapter 6. The calibration curve for aqueous solution was obtained from the 280 nm excitation wavelength and the 340 nm emission wavelength (See *Appendix N*). All the experiments were performed in replicate, and the results averaged unless stated differently.

8.2.1. Environmental factors influencing adsorption of NAs

The environmental factors experiments were performed using the microcosms with renewal method (Alvarez et al. 2005). In this method, each assembled sampler was suspended in a glass beaker containing NAs solution using a plastic fishing line. The beaker was covered with aluminum foil to avoid loss through evaporation. The sampler was immersed in 2 L of NAs solution at an initial concentration of 1 mg/L in DIW. The solution was renewed in the same beaker every 24 h \pm 1 h. Before renewal, 20 mL of the solution was collected for NAs determination using fluorescence. The Chemcatcher was assembled according to Kingston, *et al.* (2000) by placing the adsorbent material and PTFE membrane in the supporting case made of PTFE. The extractions of NA from the disk and membrane were performed separately by using sonication. Disk or membranes were rinsed with 2 x 20 mL methanol in a 40-mL glass vial with Teflon cap, and the rinsate adjusted to 50 mL in a volumetric flask.

The effects of temperature, pH, hardness and turbulence were assessed using a fractional factorial design with four factors and two levels (2^{4-1}). The low and high levels were selected to represent extreme conditions in the Athabasca River and tributaries (see *Appendix L*). The order of each one of the eight combinations (Table 8- 1) was randomly assigned, and two replicates were run for each one. A laboratory refrigerator (Coldmatic General, DEI 615) was used to keep the temperature at 4 °C; otherwise, the experiments were run at room temperature (20 °C). The pH was adjusted using 1 M sodium hydroxide, and the hardness using a stock solution of calcium chloride dihydrate, which represented 150,000 mg/L CaCO₃.

Table 8- 1. Factorial design for assessing the effect of temperature, pH, hardness and turbulence in the uptake rate

Factor Comb.	T (°C)	pH	HARD (mg CaCO ₃ /L)	TURB (RPM)
I	20	7	300	60
II	4	9	300	60
III	20	9	75	60
IV	4	9	75	300
V	4	7	75	60
VI	20	9	300	300
VII	4	7	300	300
VIII	20	7	75	300

8.2.2. Integrative experiment and lag time

The linear uptake was assessed using a flow-through system adapted from de la Cal et al. (2008) to maintain a constant concentration during the 30-day exposure experiment without daily intervention. The setup consisted in a 20-L glass container (17 L effective volume) covered with aluminum foil and with a lateral opening to let water be wasted (Figure 8-2). The system used two peristaltic pumps, one for a 100 mg/L Fluka NAs stock solution in methanol and the second for tap water. After getting the first estimates of the uptake rate, pump flows were adjusted in order to maintain a NAs concentration ~ 1 mg/L. The water flow was measured at the beginning and end of the experiment as 12 mL/min for tap water and 0.12 mL/min for the NAs stock solution. The residence time of the solution in the tank was 22.5 h. The system used two magnetic stirrers at a medium speed (4 from 1 – 7 scale) to mix the solution and simulate river turbulence. The temperature was monitored daily with a thermometer placed in the water tank. A 20 mL sample was obtained daily to measure the concentration of NAs in water.

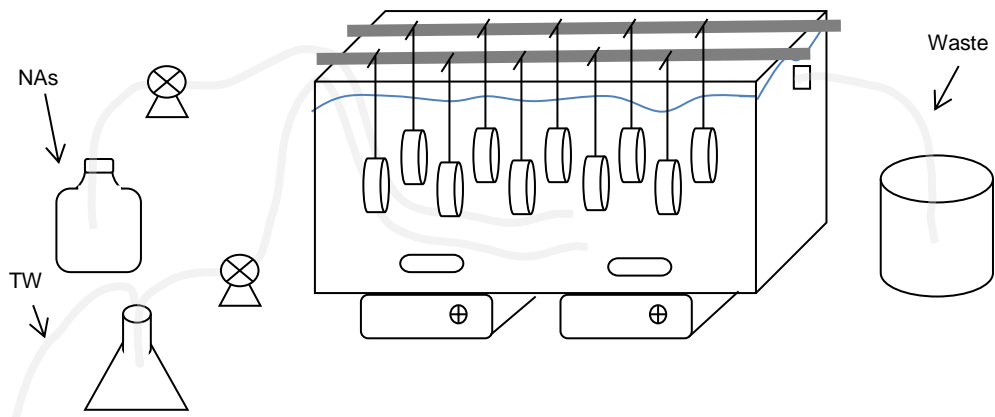


Figure 8-2. Flow-through set up for integrative time experiment

The experiment started after reaching steady-state conditions, and ten C18 Chemcatcher samplers were suspended in the tank in a prearranged random order using fishing line. These samplers were retrieved in pairs at day 5, 10, 15, 23 and 30. After retrieval, the disks and membranes were extracted with methanol as explained in the previous section and the NAs concentration in methanol was measured using fluorescence. The mass of NAs adsorbed over the water concentration was plotted against time and the linearity was assessed. Additionally, the integrative ratio (IR) was obtained comparing the mass adsorbed after 5 d (M_5) and 10 d (M_{10}) of treatment. The IR gives an indication of whether there is a lag time in the initial phase of the sampling campaign.

$$IR = \frac{M_{10}}{2 \times M_5} \quad (8-1)$$

8.2.3. Changes of NAs concentration in solution

Microcosms with renewal experiments were also run in replicate to know how well the Chemcatcher integrates changes in concentration of NAs in water. The sampler response to concentration spikes was assessed by comparing the TWA concentration calculated using the mass extracted with the known average concentration of NAs. The sampler was exposed to a base commercial NAs concentration of 1 mg/L for four days. On the fifth day, the concentration was increased ~10 fold for 2 d, and then returned to background concentration for four more days as shown in Figure 8-5.

Similarly, to measure the offloading of NAs, the TWA concentration was estimated using the mass adsorbed in the sampler. In this case, the sampler was exposed to a base

concentration of 1 mg/L for four days, and on the fifth day the sampler was exposed to DIW for two days. After that, samplers were immersed for 4 more days in 1 mg/L solution of commercial NAs in DIW. A correction was performed to take into account the NAs concentration decrease in the solution following first-order kinetics during the 24 h period before renewal. The daily average concentration was calculated using the following equation:

$$\bar{C}_w = C_{wo} \frac{V}{R_s} \left[1 - \exp\left(\frac{-R_s}{V}\right) \right] \quad (8-2)$$

Where R_s is the uptake rate, V is volume, and C_w is the concentration of analyte in water average over one day and initial.

8.2.4. Storage conditions

Four Chemcatcher-C18 samplers were exposed to 1 mg/L of Fluka NAs in TW in the flow-through system for four days. After retrieval, the control sampler was extracted immediately with methanol, while the remaining samplers were wrapped in aluminum foil and stored for one week under different temperatures, 20 °C, 4 °C, and -20 °C. The difference in the mass of sorbed NAs extracted for the different storage temperatures was analyzed. In addition, the change in concentration of a 100 mg/L NAs solution in methanol was analyzed when it was stored in a glass vial with Teflon cap for one month at the same temperatures used for the samplers. For these experiments, no replicates were run.

8.2.5. Matrix effects on the uptake rate using river water

The matrix effects were assessed using river water collected from the North Saskatchewan River (RW) in Edmonton. This water was stored at 4 °C when not used, and was analyzed for pH (8.41), conductivity (297 μ S/cm), hardness (151 mg CaCO₃/L), TSS (74.78 mg/L), DOC (3.99 mg/L), and DIC (27.94 mg/L). The uptake rate was obtained using this water in a 4-day microcosm experiment at 1 mg/L commercial NAs concentration. The experiment followed the same procedure described in Section 7.3.5 for the Chemcatcher sampler. The uptake rate was compared with the results obtained in DIW. The NAs partitioning to TSS from the RW (6.6 mg) was assessed following the method previously described for membranes and sorbents, Section 7.3.4. The TSS were removed by centrifugation at 3750 rpm after being shaken in a 40 mL solution of 2 mg/L NAs for 24 h. The partitioning coefficient was also measured by further removing small particles with a 0.20 μ m filter.

8.3. Results and discussion

8.3.1. Environmental effects on commercial NAs passive sampling

The environmental effects experiments showed that the main effects are due to temperature, turbulence and the interaction of these two factors (Figure 8- 3). According to these results, the uptake rate would be reduced by four fold in winter in comparison to summer due to the change in water temperature from 4 °C to 20 °C (Figure 8-3a). The temperature in the Athabasca River and tributaries was queried in the RAMP website (www.ramp-alberta.org) on 04 May 2013 and the minimum temperature from 1997 to 2009 was 0 °C and maximum of 25 °C. It has been reported that an increase in temperature increases the sampling rate and Arrhenius plots showed correlations greater than 60% (Kingston, et al., 2000). A theoretical maximum two-fold increase in the D_w over a 20 °C temperature range correlates to a 50% change in the uptake rate.

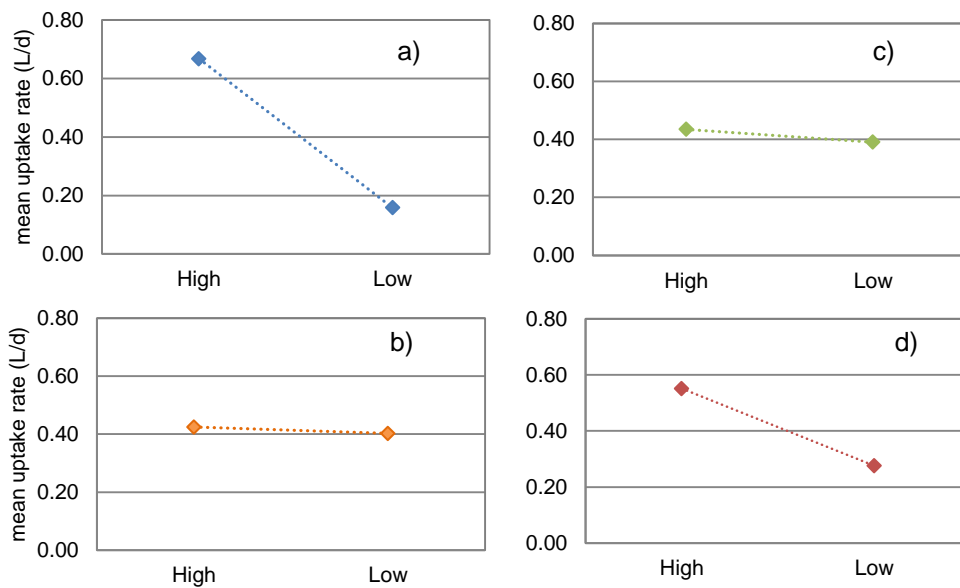


Figure 8-3. Uptake rate of Fluka NAs onto C18 disk at high and low a) temperature, b) hardness, c) pH, and d) turbulence (lines are used to guide the eye, see levels in Table 2.4-1)

Stirring velocity of 300 rpm used for these experiments increased the uptake two fold in comparison to 60 rpm (Figure 8-3d). The uptake rate changes depending on whether the mass transfer is under boundary layer control or membrane control. The maximum uptake rate can be obtained for samplers in which the limiting barrier is the aqueous boundary layer (Kot-Wasik et al. 2007). For chemicals under membrane control, the

sampling rate remains nearly constant regardless of the surrounding flow-turbulence conditions. NAs uptake in the Chemcatcher were under aqueous boundary layer control as indicated by a two-fold increase in sampling rates with stirring.

The water pH (7 and 9) and hardness (75 mg CaCO₃/L and 300 mg CaCO₃/L) had a minimum effect in comparison with the turbulence and temperature (Figure 8-3). The average uptake rate at room temperature and low turbulence at all pH and hardness conditions was 0.42 L/d ± 0.03 L/d. The interaction of turbulence and temperature has a significant effect on the uptake rate. The Athabasca River and tributaries have low temperature and flow during winter, while they have high temperature and turbulence in the summer. This would require adjusting the uptake rate to the observed temperature and turbulence. Protective cages can decrease the turbulence effect. Likewise, performance reference compounds (PRC) can be used to correct the uptake rate due to turbulence. The use of PRCs has been tested in C18 disks for in situ calibration of the uptake for hydrophobic micropollutants including polyaromatic hydrocarbons and organochlorine pesticides using offload kinetics (Vrana et al. 2006).

8.3.2. Integrative sampling time

The average NAs concentration in the glass tank was 0.35 ± 0.14 mg/L during the 30-day exposure time with pH 8.11 ± 0.07 and temperature 22 ± 1 °C. The turbulence in this system may not be equivalent to the turbulence used in the microcosms with renewal experiments, since a 17-L rectangular tank was stirred using two un-rated magnetic stirrers at a medium speed. The water concentration of NAs was lower than the value estimated using the uptake rate from the preliminary experiments, in part due to a higher uptake rate, and partitioning onto the tubing and silicon from the tank. However, this concentration is still representative of the TWA concentration in the Athabasca River close to the oil sands. The average NAs concentration in the Athabasca River and its tributaries from 2009 to 2010 using GC-MS-ion trap was 0.18 mg/L (www.ramp-alberta.org, Aug 22nd, 2011).

Figure 8-4 shows that the samplers did not reach equilibrium regime, and they may be used in monthly sampling campaigns as integrative samplers. The slope of the linear fit represents an uptake rate of 0.41 L/d, which is similar to uptake rates obtained from pH and hardness tests at room temperature. The uptake rate calculated using the microcosms with renewal set up was 0.42 L/d at the lower end of turbulence and 0.67 L/d at the higher end. The uptake rate obtained using the continuous system was very close to the one obtained at 60 rpm in the batch system.

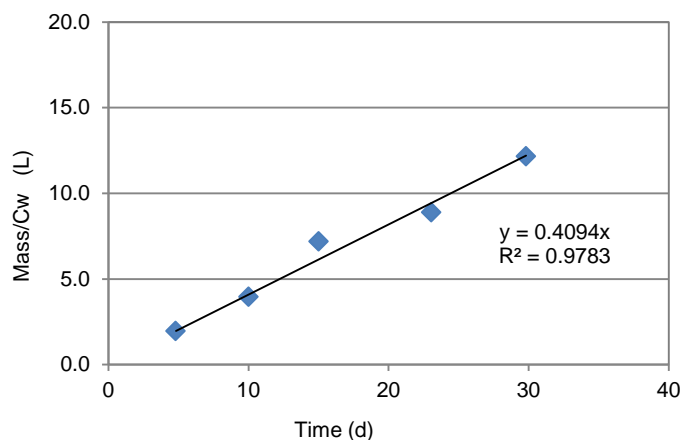


Figure 8-4. Integrative behavior for commercial NAs uptake in Chemcatcher

The integrative ratio obtained from the sampler retrieved at day 5 and day 10 was calculated using equation 8-1. This ratio was 0.96, which means that the mass obtained in 10 days would be slightly lower than the obtained in two consecutive 5-day experiments. As a result, there was not a lag time observed, but the opposite, the sampler gets a head start of about 9 h. However, this is about 1% of a 30-day sampling campaign and very likely not significant. An integrative ratio < 1 could be due to the sampler reaching equilibrium or saturation and slowing down the uptake. However, from the integrative experiment the sampler is still far from reaching equilibrium regime after ten days. The second option is that at the beginning of the exposure time the sampler is having a higher uptake as it is getting conditioned with the aquatic environment. The average IR for all the consecutive pairs of samplers retrieved (M_5 - M_{10} , M_{10} - M_{15} , M_{15} - M_{23} , and M_{23} - M_{30}) was 1.01. This was calculated by changing the coefficient in equation 8-1, for the ratio between the days at which the samplers were retrieved (i.e. 15 d / 10 d). This integrative ratio close to 1, and the high R^2 observed in Figure 8-4 supports the linear uptake of commercial NAs by the Chemcatcher sampler.

8.3.3. Chemcatcher response to fluctuations in concentration of NAs

The changes in concentration of commercial NAs in solution followed the pattern presented in Figure 8-5. For these experiments, the TWA concentration calculated using the daily water concentration, and the concentration estimated from the sampler extraction were compared. The daily initial concentration was known, and the daily average concentration was corrected using equation 8-2 to take into account sorption of NAs in the 24 h. The TWA concentration was estimated using the mass extracted after the 10-day experiment and the uptake rate of 0.40 L/day. This uptake rate was obtained

under similar conditions in the environmental effects experiment at pH 7, room temperature and stirring rate of 60 rpm.

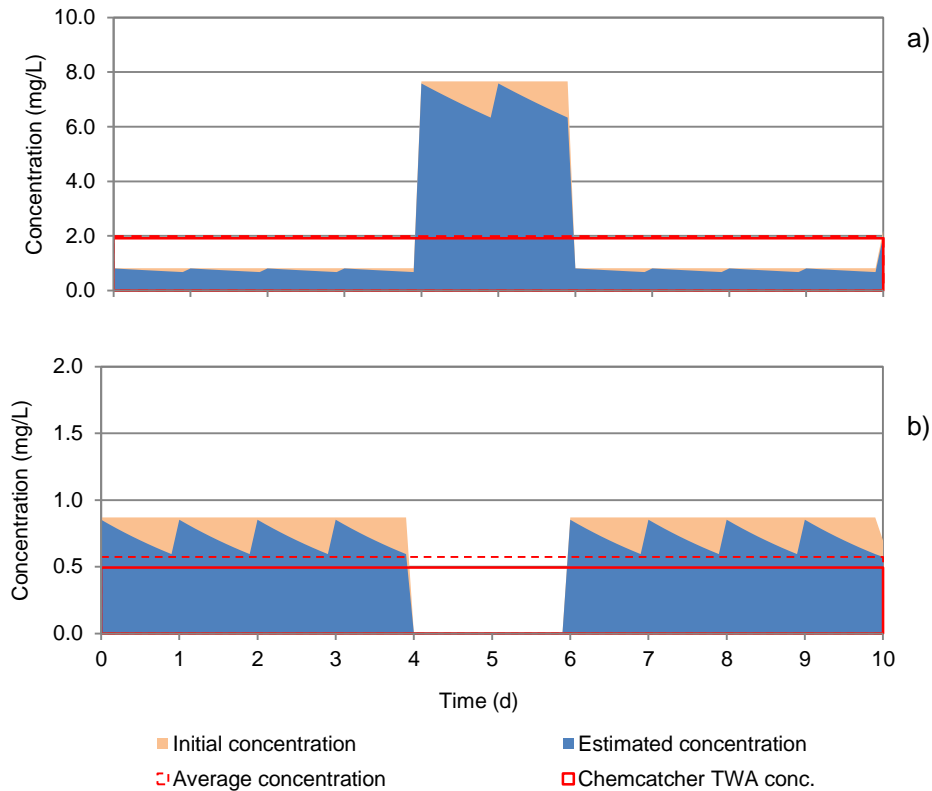


Figure 8-5. Chemcatcher performance estimating the TWA concentration (a) spike, or (b) decrease in concentration of Fluka NAs; both in the midst of sampling period

The TWA concentration in water estimated from the mass of NAs adsorbed onto the C18 sampler for the offloading experiment was 0.49 mg/L. However, the calculated average water concentration was 0.57 mg/L (0.72 mg/L for eight days and 0 mg/L for two days). This represents an underestimation of 14%, which may be due to offloading from the sampler in the two days without NAs in solution. Similarly, the concentration of NAs in water estimated from the C18 sampler for the spiking experiment (Figure 8-5a) was 1.92 mg/L, while the calculated concentration using the daily average concentration was 1.98 mg/L. The concentration was very close with only 3% underestimation. This result suggests that the sampler had a fast response to substantial increase and subsequent decrease in concentration and can integrate it to the TWA concentration. Nevertheless, it cannot tell how high the individual spikes were, and if they could have an effect on acute toxicity and potential fish kill.

In general, the C18 sampler performed well to changes of concentration in the middle of the sampling period. In a study using POCIS to assess its performance to changes in

concentration of 3 herbicides (K_{ow} 1.98, 2.87 and 3.21) the differences in TWA were from 11% to 49% (Mazzella et al. 2008). Further analysis should be performed for spikes at the beginning and end of the 30-day exposure time. A slightly higher uptake rate was observed in the first 5 days of the integrative experiment performed in this study. For this reason, an overestimation in the TWA concentration may be expected if the spike occurs in the first days of the experiment when the sampler is being conditioned. Although the sampler was integrative for the 30-day exposure experiment, under different conditions such as higher temperature or turbulence the sampler could be closer to equilibrium, and the uptake rate could decrease at the end of this period. As a result, a spike in the last days of the 30-day exposure could underestimate the TWA concentration. The offloading could also be more significant at the end of the 30-day exposure when the concentration gradient between the sampler and the background concentration in the aqueous environment is higher.

8.3.4. Storage conditions

The mass of Fluka NAs extracted from the Chemcatcher–C18 sampler, and determined by fluorescence did not change significantly after storing the sampler for one week at 4 °C or -20 °C (< 5%) (Figure 8-6). However, the mass extracted from the sampler stored at room temperature decreased 24%. Even though the sampler was wrapped in aluminium foil, there could be some evaporation and biodegradation of the NAs at room temperature. For this reason, it is recommended to store the sampler at low temperatures.

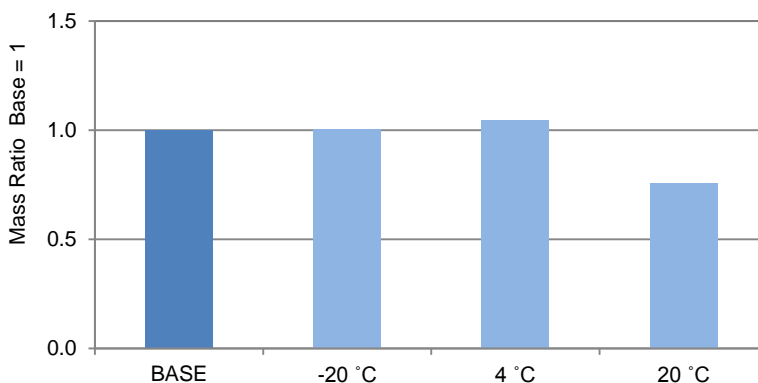


Figure 8-6. Change in the mass of adsorbed NAs after storing Chemcatcher sampler at different temperature

The commercial naphthenic acids were stable when they are in methanol and stored in glass vials with Teflon caps. The decrease in concentration was < 7% after one month, even when stored at room temperature with and without light exposure (See *Appendix M*). Longer storage at lower temperature warrants further investigation.

8.3.5. Matrix effect of river water

The uptake rate for commercial (Fluka) NAs onto C18 disk was only 0.24 L/d when using RW in the microcosm experiments. There were important matrix effects, with a decrease in the uptake rate of 27% of that obtained with DIW at the same temperature and turbulence. Biofilm formation could add an extra transfer barrier to the sampler when using RW; however, the experiment lasted only 4 days and there was not a visible biofilm layer. Another factor to consider is that some NAs could partition to colloids and small particles. This would decrease the true dissolved concentration. In addition, NAs biodegradation could occur at higher rates than before; however, the mass balance performed was similar as before with DIW (80%).

The NAs partitioning to the TSS after centrifugation was $\log K_p = 4.10$. The partitioning coefficient increased to $\log K_p = 4.5$ by removing small particles with a 0.20 μm filter. This value is similar to the one obtained with PES membrane and could explain the lower uptake rate using river water. The dissolved organic matter (DOM) could also reduce the uptake rate due to the formation of complexes that are too large to cross the membrane, for molecular interactions that increase polarity and for competitive adsorption with other organic compounds. Gourlay *et al.* (2005) reported a reduced accumulation of hydrophobic organic contaminants into SPMDs due to DOM from the aquatic environment.

The effect of other major ions (chloride, magnesium, potassium, sodium, sulphate, sulphide) also has to be considered as a potential factor changing the uptake rate in this experiment. The ionic strength can affect the NAs solubility, adsorption coefficients, and as a result the uptake rate. By obtaining the relative standard deviation (RSD, standard deviation/mean) for all the major ions in the Athabasca River and tributaries (RAMP, 2013), chloride, sodium, sulphate and sulphide highly fluctuate with RSDs > 50%. Headley *et al.* (2011) demonstrated the salting-out effects on the characterization of NAs using electrospray ionization with general enhancement of Z = -4 species and reduction of Z = -8, -10, -12, -14 species relative to others monocarboxylic acids (i.e. decrease in solubility of polycyclic NAs). The concentration of chloride ions has shown to affect the distribution of NAs in environmental samples, and it has been suggested that salts should be monitored concurrently with NAs (Headley *et al.* 2012). Metals can also contribute to

the matrix effects. At high pH the NAs moieties become reactive towards metal cations forming metal naphthenates which precipitate in water (Brandal. 2005).

8.4. Conclusions

Chemcatcher with C18 sorbent and PTFE membrane had high uptake rate and did not reach equilibrium during the 30-day experiment when tested on commercial (Fluka) NAs, giving initial confidence that it could be used in monthly sampling campaigns. Additionally, the sampler did not have a significant uptake lag time in the first five days of uptake ($IR = 0.96$). The sampler performed well to changes in NAs concentrations with an underestimation of the time weighted-average concentration < 15%. However, it cannot say the size and the length of potential spikes in NAs concentrations that could be acutely toxic. The temperature and turbulence had a high effect on the uptake rate (4-fold and 2-fold respectively). That could be potentially addressed using PRCs for uptake rate corrections in sampling campaigns. The mass of NAs extracted from the C18 disk did not change significantly after one week when it was stored at 4 °C or -20 °C. Storage of passive samplers at higher temperature should be avoided, while storage of commercial NAs in methanol resulted in minor concentration changes. Further research is required to understand better the physical behavior of NAs and their uptake rates using river water, due to salts, metals and partitioning to colloids and the sampling of the truly dissolved phase.

8.5. References

Alvarez, D. A., Stackelberg, P. E., Petty, J. D., Huckins, J. N., Furlong, E. T., Zaugg, S. D., and Meyer, M. T. (2005). "Comparison of a novel passive sampler to standard water-column sampling for organic contaminants associated with wastewater effluents entering a New Jersey stream." *Chemosphere*, 61(5), 610-622.

Brandal, O. (2005). "Interfacial (o/w) properties of naphthenic acids and metal naphthenates, naphthenic acid characterization and metal naphthenate inhibition". Norwegian University of Science and Technology, Norway.

de la Cal, A., Kuster, M., de Alda, M. L., Eljarrat, E., and Barceló, D. (2008). "Evaluation of the aquatic passive sampler Chemcatcher for the monitoring of highly hydrophobic compounds in water." *Talanta*, 76(2), 327-332.

EPCOR. (2012). "Water Quality Monthly Summary." <http://www.epcor.com/water/reports-edmonton/Documents/wq-edmonton-july-2012.pdf> (August 2012, 2012).

Gourlay, C., Miege, C., Noir, A., Ravelet, C., Garric, J., and Mouchel, J. M. (2005). "How accurately do semi-permeable membrane devices measure the bioavailability of polycyclic aromatic hydrocarbons to *Daphnia magna*?" *Chemosphere*, 61(11), 1734-1739.

Headley, J. V., Barrow, M. P., Peru, K.M., Derrik, P. J. (2011) "Salting-out effects on the characterization of naphthenic acids from Athabasca oil sands using electrospray ionization." *Journal of Environmental Science and Health, Part A: Toxic/Hazardous Substances and Environmental Engineering*, 46:8, 844-854.

Headley, J. V., Peru, K.M., Fahlman, B., McMartin, D. W., Mapolelo, M. M., Rodgers, R. P., Lobodin, V. V., Marshall, A. G. (2012) " Comparison of the levels of chloride ions to the characterization of oil sands polar organics in natural waters by use of Fourier transform ion cyclotron resonance mass spectrometry." *Energy and Fuels*, 26, 2585 – 2590.

Kot-Wasik, A., Zabiegała, B., Urbanowicz, M., Dominiak, E., Wasik, A., and Namieśnik, J. (2007). "Advances in passive sampling in environmental studies." *Analalytica Chimica Acta*, 602(2), 141-163.

Mazzella, N., Debenest, T., and Delmas, F. (2008). "Comparison between the polar organic chemical integrative sampler and the solid-phase extraction for estimating herbicide time-weighted average concentrations during a microcosm experiment." *Chemosphere*, 73(4), 545-550.

RAMP. (2013). "Query water quality data [online]." <http://www.ramp-alberta.org/data/Water/water.aspx> (accessed November 2013).

Vrana, B., Mills, G. A., Dominiak, E., and Greenwood, R. (2006). "Calibration of the Chemcatcher passive sampler for the monitoring of priority organic pollutants in water." *Environmental Pollution*, 142(2), 333-343.

Chapter 9. Evaluation of uptake rates for OSPW-NAs using Chemcatcher passive sampler

9.1. Introduction

Naphthenic acids (NAs) are a complex mixture of carboxylic acids with more than 3000 chemically different elemental compositions identified. These compounds range from 15 to 55 carbons with cyclic (1 - 6 rings) and aromatic (1 - 3 ring) structures, which may contain two to four oxygen molecules and sulfur (Qian et al. 2001). Classical NAs have been described using the formula $C_nH_{2n+Z}O_2$, where n indicates the carbon number, and Z indicates the number of hydrogen lost for each saturated ring structure in the molecule (Schramm 2000).

In the previous Chapter, the performance of the Chemcatcher sampler was evaluated using commercial NAs. Commercial NAs have a different mixture of compounds than environmental samples. The results from the LC-MS/MS analysis, performed as part of this research, confirmed that the commercial NAs and the oil sands process-affected water (OSPW) acid extract had different n and Z distribution (*Appendix P*. Raw data for NAs analysis using LC-MS/MS from Axys Analytical). The OSPW extract had more alicyclic compounds ($Z \geq -4$) while Fluka's NAs were mainly acyclic ($Z = 0$). Additionally, Fluka NAs had a high content of compounds with 19 carbons, while the OSPW-NAs had mainly < 17 carbons. Since the NAs are a mixture of compounds, it is complicated to obtain a close enough standard for research purposes. For this reason, the uptake rates were evaluated for an OSPW acid extract which is more representative of environmental NAs.

9.2. Materials and methods

Fresh OSPW was obtained from a bitumen producer in Northern Alberta's oil sands mining region. The OSPW-NAs stock solution was obtained following the liquid-liquid extraction method outlined by Jivraj *et al.* (1995) as explained in Chapter 6. The concentration of NAs in this solution was 1045 mg/L as measured by LC-MS/MS.

Uptake rates of natural NAs onto C18 disk and HLB resin were tested using the OSPW acid extract. The uptake rate experiments were performed for four days using the microcosms with renewal method described in Section 8.2.1. The 2 L NAs solution used TW for HLB resin, whereas DIW (pH 7) and RW were used for C18. The NAs were quantified using fluorescence spectroscopy using the settings presented in Chapter 6.

Additionally, the sorbent extracts in methanol were sent to a commercial lab (Axys Analytical Services Ltd., Sydney, BC) for NAs quantification using liquid chromatography-mass spectroscopy (LC-MS/MS) with a Waters (Milford, MA, USA) 2690 HPLC coupled to a Micromass Quattro Ultima MS/MS. The NAs concentration from the mass spectroscopy technique was analyzed using 3D graphs, with one axis showing the number of carbons (n) and in another axis the number of rings (Z) from the classical description of NAs, $C_nH_{2n+Z}O_2$. All the experiments were performed in replicate, and the results averaged unless stated differently.

9.3. Results and discussion

9.3.1. Chemcatcher uptake rates using OSPW extract

The average decrease in the concentration of OSPW-NAs in reagent water before renewal (24 h) was only 11%. The mass balance using the recovery in the PTFE membrane, C18 disk and the remaining mass in solution before renewal was 92%. The uptake rate using C18 was 0.05 L/d (in DIW pH 7). This value was almost one order of magnitude higher when Fluka NAs were used instead of OSPW extract (0.40 L/d vs, 0.05 L/d). The uptake rate was even lower using HLB resin instead of C18 (0.03 L/d). The uptake rate of OSPW-NAs for the C18 configuration decreased to 0.03 L/d when river water was used. The decrease in the uptake rate close to half using HLB resin instead of C18, and using RW instead of DIW was also observed for commercial NAs (Chapter 8).

9.3.2. Selective adsorption of OSPW-NAs compounds

The C18 and HLB extracts had different n and Z distributions from the original OSPW stock solution distribution (Figure 9-1). Most of the compounds adsorbed were either $Z = 0$ or $Z \leq -10$, and at the right side of the graph with carbon numbers 15 and ≥ 18 . The results showed that the sampler did not adsorb significantly many of the compounds in the OSPW-NAs solution. However, many of the adsorbed compounds were representative of the commercial solution.

The differences between the OSPW stock solution and the Chemcatcher sorbent extract were also observed in the fluorescence signal, suggesting that not all the fluorophores were adsorbed. The fluorescence EEM contour plots (Figure 9-2) showed a noticeable change in the intensity fingerprint between the OSPW-NAs stock solution and the NAs adsorbed onto the Chemcatcher. The stock solution fluoresced at higher emission and excitation wavelengths. The peak at the 280 nm excitation curve changed from an emission wavelength close to 340 nm in the stock solution to 310 nm for the HLB extract

and 320 nm for the C18 extract. However, it did not change when using Fluka NAs for the uptake experiments.

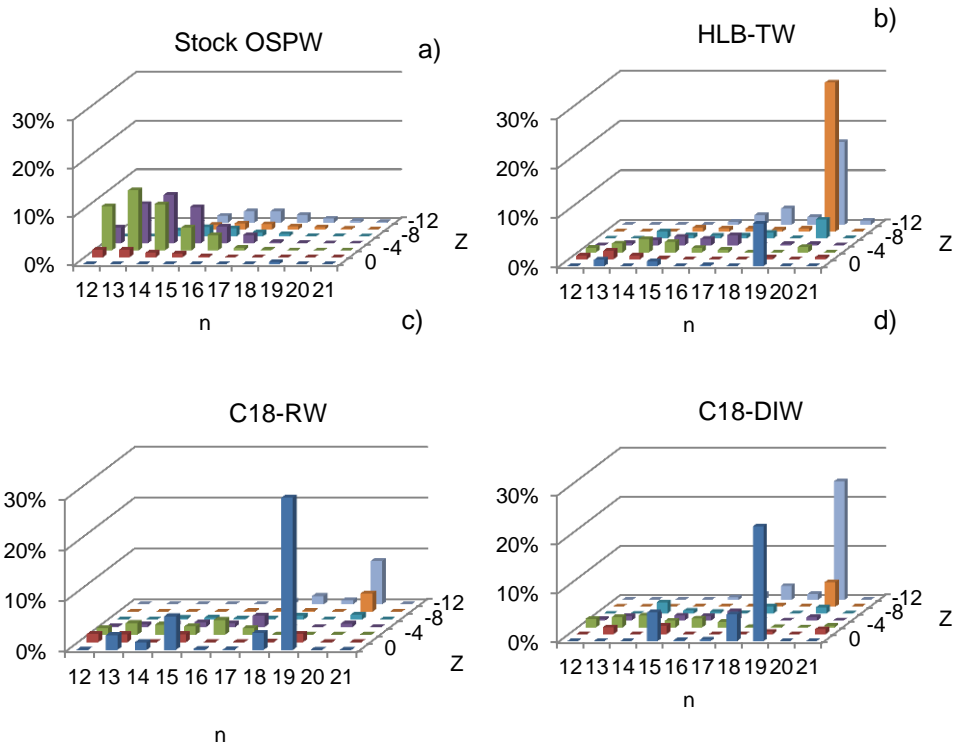


Figure 9-1. LC-MS/MS profile of a) OSPW NAs stock solution, and OSPW NAs adsorbed onto b) HLB resin TW, c) C18 disk RW, and d) C18 disk DIW, after uptake experiments

The selectivity of the sampler was supported by the synchronous signal ($\Delta\lambda = 10$ nm) as the peak observed in the OSPW-NAs solution at 340 nm (see Chapter 6) was not present in the sample extract.

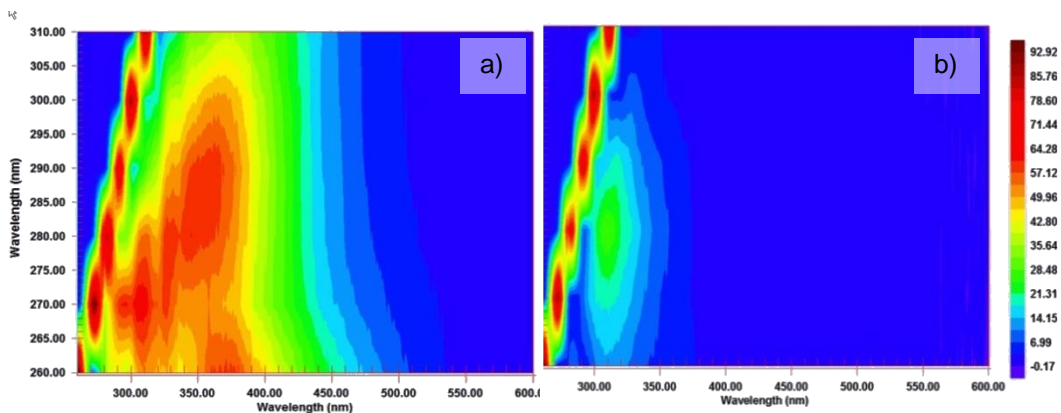


Figure 9-2. EEM contour plots for a) OSPW acid extract stock solution diluted to 11 mg/L b) extract from C18 disk after uptake experiment in DIW, 6 mg/L

9.3.3. Different uptake rates obtained analyzing the extracts by fluorescence or LC-MS/MS

Even though the concentration of NAs in solution derived using LC-MS/MS and fluorescence at the beginning of the experiment were very close, the concentration of the C18 extracts measured using LC-MS/MS was about 10 times lower than the one obtained using fluorescence spectroscopy. This may be the result of a selective adsorption of compounds that fluoresce at different wavelength and intensity than the originally used in the calibration curve changing the response factor. As a result of the difference in NAs concentration from the extracts, the uptake rate estimated was lower using mass spectroscopy analysis by the same ratio. The uptake rates derived by measuring the extract concentration with LC-MS/MS were 0.002 L/d C18-RW, 0.003 L/d HLB-TW, and 0.003 L/d C18-DIW.

9.3.4. Uptake rate of individual compounds using LC-MS/MS

Individual uptake rates were calculated for the 60 compounds identified in the LC-MS/MS analysis. About 84% of the OSPW-NAs compounds had an uptake rate ≤ 0.003 L/d, and only 1% had an uptake rate ≥ 0.05 L/d. In contrast, only 25% of the Fluka NAs compounds were ≤ 0.003 L/d and about 50% ≥ 0.05 L/d. For this reason, the uptake rate for the OSPW and Fluka NAs were also an order of magnitude different using the same analytical method to measure the NAs (OSPW < Fluka). The average uptake rate estimated from the LC-MS/MS analysis for Fluka NAs was 0.14 L/d. This is about three times lower than the one previously obtained using fluorescence spectroscopy.

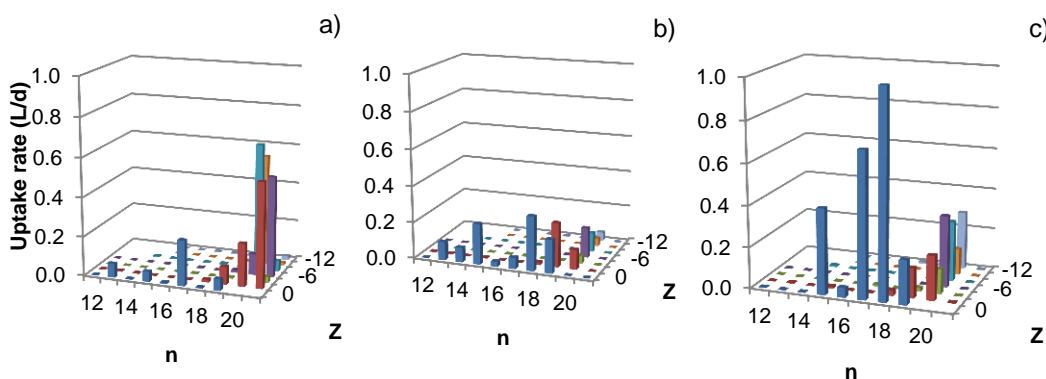


Figure 9- 3. Uptake rate for different n and Z numbers in Chemcatcher experiments, a) HLB resin in tap water, b) C18 disk in river water, and c) C18 disk in deionized water

9.3.5. Uptake rate for n and Z groups

The uptake rate of OSPW-NAs was higher for compounds with $Z = 0$ and for compounds with 20 carbons (Figure 9- 3). The values were as high as 1.03 L/d using C18 and DIW for $C_{18}H_{36}O_2$, and 0.64 L/d using HLB and tap water for $C_{20}H_{32}O_2$. In Figure 9-4, it is observed that the average uptake obtained from the three samplers increased with the carbon number, except for $n = 21$. This agrees with other studies where the most hydrophobic compounds typically have the higher uptake rate values (Stuer-Lauridsen 2005). Regarding the number of rings (Figure 9-4b), the uptake rate using C18 sampler was higher for $Z = 0$, without another clear trend.

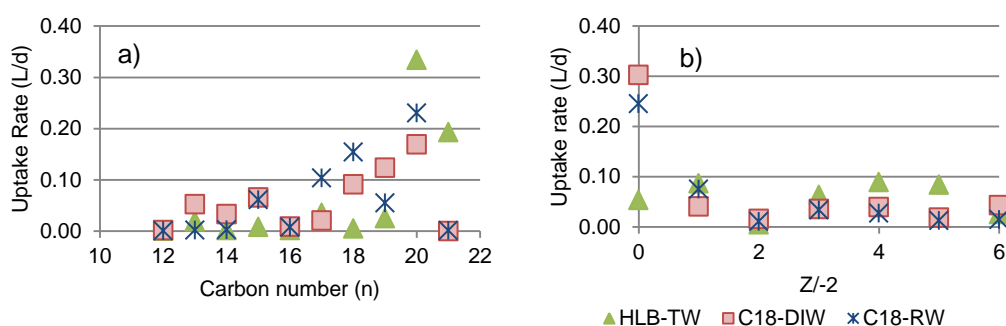


Figure 9-4. Correlation of average uptake rate of OSPW NAs on different Chemcatcher configurations vs. NAs structure a) carbon, and b) Z numbers

9.4. Conclusions

The Z and n distributions were significantly different for the commercial NAs and OSPW-NAs stock solutions. The uptake rates for the different compounds in the NAs mixture changed by orders of magnitude as measured using LC-MS/MS. The uptake rate was higher for alicyclic compounds with more carbons for the Chemcatcher using C18. Because these compounds were more abundant in the commercial NAs mixture, the overall uptake rate obtained for Fluka NAs was higher than the one obtained for OSPW-NAs. For this reason, it could be challenging to have a general uptake rate for NAs, and uptake rates may be required for each compound or group of compounds depending to the n and Z distribution. Alternatively, NAs indicators or target compounds could be selected in the future. Further work using known sources of OSPW will help us evaluate if the source is a factor in NA uptake from the oil sands.

9.5. References

Jivraj, M. N., MacKinnon, M., and Fung, B. (1995). *Naphthenic acids extraction and quantitative analyses with FT-IR spectroscopy*. Syncrude Canada Ltd, Edmonton, Canada.

Qian, K., Robbins, W. K., Hughey, C. A., Cooper, H. J., Rodgers, R. P., and Marshall, A. G. (2001). "Resolution and Identification of Elemental Compositions for More than 3000 Crude Acids in Heavy Petroleum by Negative-Ion Microelectrospray High-Field Fourier Transform Ion Cyclotron Resonance Mass Spectrometry." *Energy Fuels*, 15(6), 1505-1511.

Schramm, L. L. (2000). *Surfactants: Fundamentals and Applications in the Petroleum Industry*. Cambridge University Press, Cambridge, UK.

Stuer-Lauridsen, F. (2005). "Review of passive accumulation devices for monitoring organic micropollutants in the aquatic environment." *Environmental Pollution*, 136(3), 503-524.

Chapter 10. General Conclusions and Recommendations for Future Research

This thesis explored modeling, analytical and sampling techniques that can be applied for water quality management in the Athabasca River. The dissolved oxygen (DO) model developed for the Upper Athabasca River (UAR) can be used as a management tool with updated sediment oxygen demand (SOD) values to forecast the DO in low flow years and evaluate mitigation measures. The main conclusions for Part 1 of the Thesis are:

- (1) The model developed for the UAR using CE-QUAL-W2 reproduced the water temperature for the seven years simulated. The ice cover was adequately predicted for all seven winters, and the simulation of nutrients, and phytoplankton primary productivity were satisfactory. The water surface elevation was well reproduced in the open water period; however, it was underpredicted in the ice-cover period due to the lack of ice roughness in the model's code.
- (2) The DO concentration was very sensitive to changes in the SOD rate used. The DO calibration was improved by implementing an annual SOD based on the biochemical oxygen demand (BOD) load.
- (3) The model was used to estimate the capacity of the river to assimilate BOD loads in order to maintain a DO concentration of 7 mg/L, which represents the chronic provincial guideline plus a buffer of 0.5 mg/L. Based on the model relationships between the key parameters DO, flow and BOD, the results revealed a maximum assimilative BOD load lower than the maximum permitted load. In addition, the model predicted the minimum assimilative flow at average BOD load. Climate change scenarios could increase the frequency of the predicted minimum flow.
- (4) A three-level warning system is proposed to manage the BOD load proactively at different river discharges. Other mitigation options were explored such as upgrading the wastewater treatment of the major BOD point source and oxygen injection into the effluents.
- (5) The calibrated model can be used as a management tool to guide engineering control measures and predict DO in low flow years.
- (6) This thesis documents the model development methodology, including assumptions, data preparation steps and techniques used to deal with limited and irregular data. This information would be useful for scientists dealing with similar model developments for other rivers.

The potential toxicity of naphthenic acids (NAs) coming from oil sands development is a major concern for the Lower Athabasca River (LAR). Quantification of NAs in water has been traditionally performed after extraction with organic solvents followed by analytical methods that are complex and costly for continuous monitoring purposes. This study examined the application of fluorescence in organic solvents as an effective alternative. This analytic method is compatible with the extraction of passive samplers. These samplers are desired to improve our ability to quantify mass loading of NAs in this difficult and costly northern environment, and they were further explored in this research. The main conclusions of Part 2 of the thesis are:

- 1) Polar organic solvents can improve the performance of fluorescence spectroscopy to quantify NAs in comparison with other commonly used solvents including water. Methanol was selected for method optimization having a strong linearity and a low relative standard deviation for concentrations lower than 250 mg/L. The method sensitivity was improved using a methanol-deionized water mixture (50:50) as a solvent.
- (1) The synchronous fluorescence of NAs in methanol with a reduced offset value of $\Delta\lambda = 10$ nm demonstrated potential for fingerprinting. The relative abundance of the peaks changed between the oil sands process affected water extract and commercial NAs.
- 2) In the uptake rate experiments performed for the polar organic chemical integrative sampler (POCIS), high partitioning of target NAs to the polyether sulfone (PES) membrane was observed in combination with low diffusion to the resin. For this reason, this sampler (widely used for polar compounds) is not adequate for NAs sampling.
- 3) Alternative membranes were evaluated and the PTFE (Teflon ®) membrane performed better with lower partitioning and higher mass transfer to the intended sorbent. The Chemcatcher with PTFE membrane and C18 disk can potentially be used for NAs sampling, which provides the foundation for a novel sampling method in the LAR.
- (2) The performance of the Chemcatcher sampler was evaluated using commercial NAs. The uptake rate is highly affected by the water temperature and turbulence, which may need to be addressed with performance reference compounds (PRCs). The sampler was integrative for 30 days, and a reduced lag time made the sampler perform well to changes in NAs concentration in a spike and offloading experiment.
- (3) When the Chemcatcher was evaluated using oil sands process-affected water (OSPW) NAs the uptake rate was one order of magnitude lower than that

obtained using commercial NAs. This appears to be due to the selective adsorption of acyclic ($Z = 0$) compounds with a high number of carbons (n), which are more abundant in the commercial NAs. Uptake rates may be required for each compound or group of compounds in the NA mixture depending on the n and Z distribution. Due to the great number of compounds in the NAs mixture, target compounds may need to be identified before further optimization of the sampler.

- (4) The uptake rate of commercial NAs was lower using river water than tap water, likely due to partitioning to colloids. However, further experiments are required to better characterize the uptake rate for these conditions.

Recommendations for future research:

The Upper Athabasca River DO model could be enhanced by:

- (1) The developer of CE-QUAL-W2 is currently working on a 3D version of this model. The current model could be migrated to the new version when available. By including the lateral discretization, the model may account for the open leads downstream of the pulp mills.
- (2) It is recommended to include ice friction in the model's code to improve the prediction of the pollutant's travel time in winter. The code may also be improved by including the snow-water-equivalent to estimate the albedo and better predict the ice-break up.
- (3) The water quality in some tributaries is very scarce. The model would improve the calibration by including more recent and representative information, especially for Berland, La Biche and Pembina Rivers. The interpolation of monthly tributary water quality information to daily interval can be assessed using the river flow and regression models such as LOADEST. A watershed model like SWAT or HPSF can also be used to improve the loading from tributaries.
- (4) Based on the model results it is recommended to use updated SOD values instead of fixed values in time. More work may be required to derive the SOD from other variables such as river's velocity, nutrients, BOD and autochthonous organic matter.
- (5) The bathymetry used was more than 40 years old. Additionally, there were long reaches without any cross-section. If possible, it would be recommended to include updated information.

The main recommendations for future research in the quantification and monitoring of NAs are:

- (1) In general, fluorescence spectroscopy shows to be a quick method for NAs determination having the same limitations than other analytic techniques due to the lack of an appropriate standard which response factor is characteristic of environmental samples. An option that could be explored is to find a “NAs indicator” or a target compound that could be used to monitor and regulate NAs contamination, in a similar way that *E. Coli* is used for coliform bacteria.
- (2) It is imperative to continue with the characterization of the NAs fractions that contribute the most to its toxicity and target those compounds for further monitoring.
- (3) It is recommended to identify the specific compounds that are responsible for the fluorophores observed in the fluorescence signal. The synchronous signal can be further explored for fingerprinting of the different NAs sources.
- (4) Even though Chemcatcher (PTFE and C18 disk) showed promising results with commercial NAs, the uptake rate changed drastically using OSPW-NAs. The application of these samplers would require the use of uptake rates for the different compounds or groups of compounds (n and Z) in the NAs mixture. It is recommended that target compounds are determined for further optimization of the Chemcatcher.
- (5) The used of PRCs to adjust the NAs concentration to the field temperature, turbulence, and sampler biofilm needs to be further evaluated.

Appendices

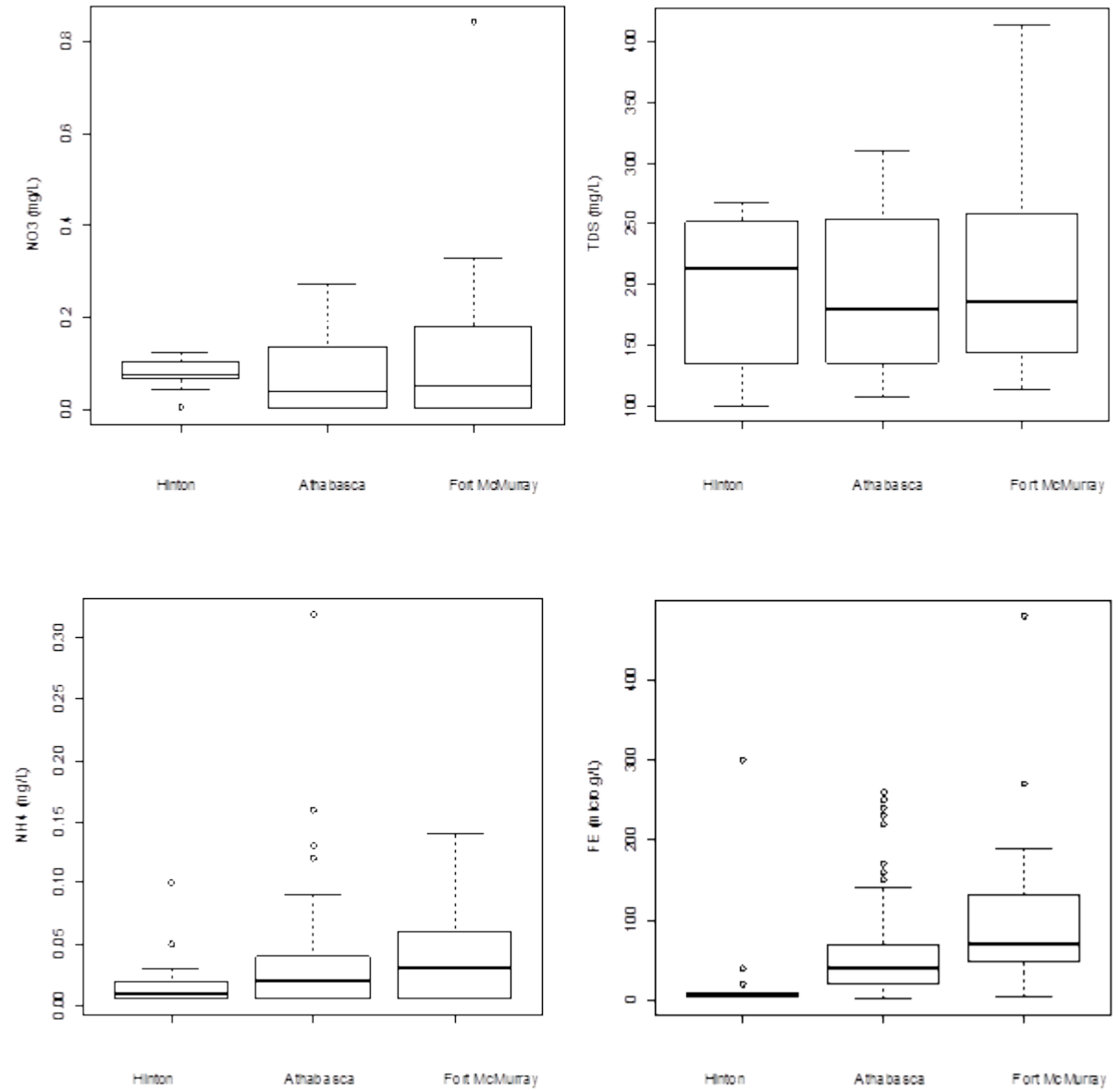
Appendix A. Difference between previous model set up and this model

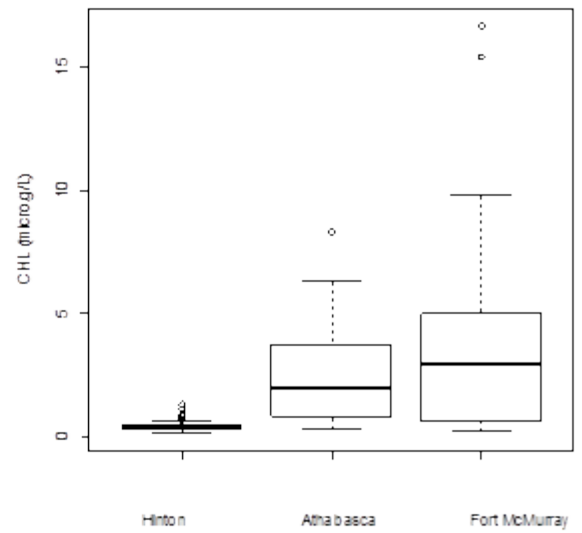
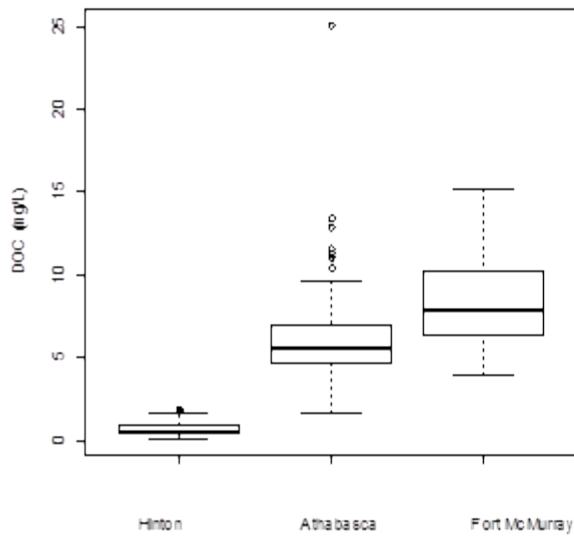
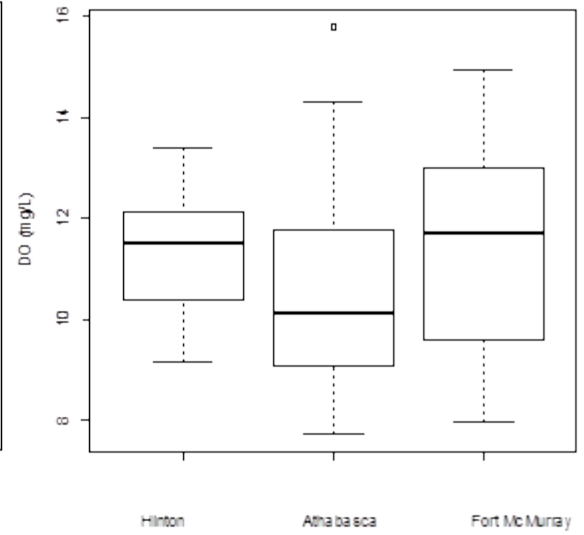
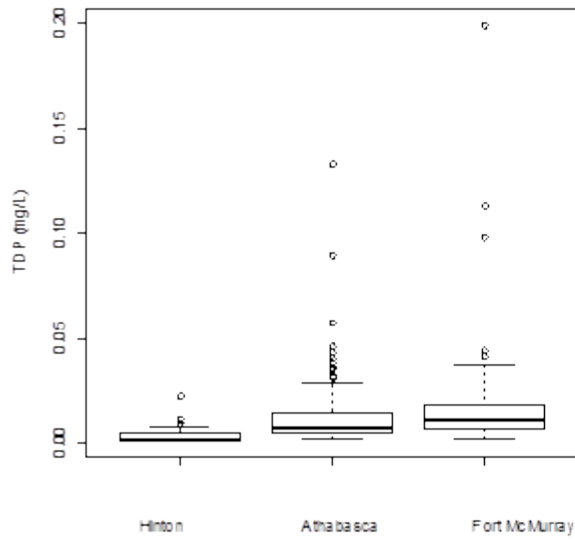
Table A- 1. Differences between the previous model setup and this model

Characteristic	Yu, 2006	This study
CE-QUAL-W2 version	3.2	3.6
Months simulated	October to April	Year round
Years	2000-2003	2000-2006
River reach	Athabasca – Grand Rapids	Hinton- Grand Rapids
River reach length	260 km	813 km
Segments	102 (3.2 ± 1.4 km)	229 (3.2 ± 0.88 km)
Slopes	4	5
Tributaries	4	10
Trib. Flow estimation	Coefficient with AR at Athabasca	Coefficient with contiguous tributary
Trib. Water quality	8 constituents	15 constituents
Parameters calibrated	DO, NH4, NO3, ALG	DO, NH4, NO3, ALG, PO4
Met. Stations	1	4
Point sources	2	6
Simulation's run time	2h	24h
Computational grid	All segments same max. depth	Max. depth changed accordingly to survey
SOD value used	0.30 at 8°C	0.20 – 1.30 at 20 °

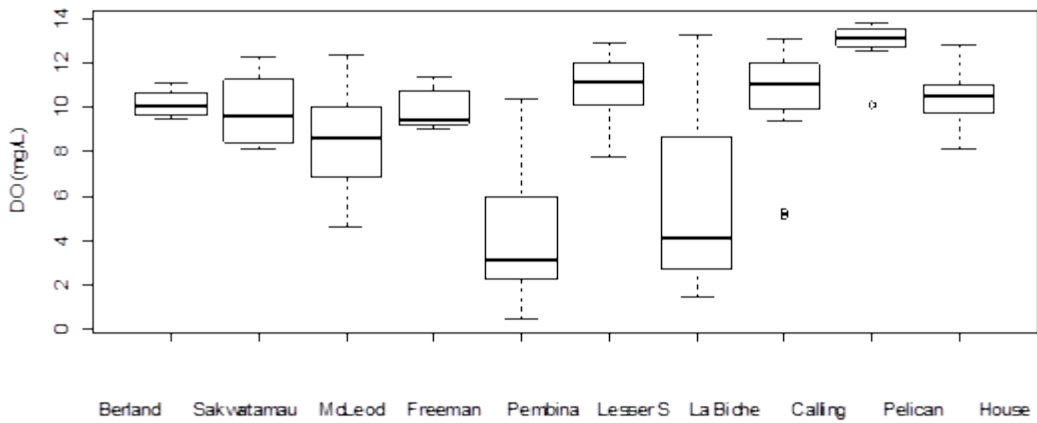
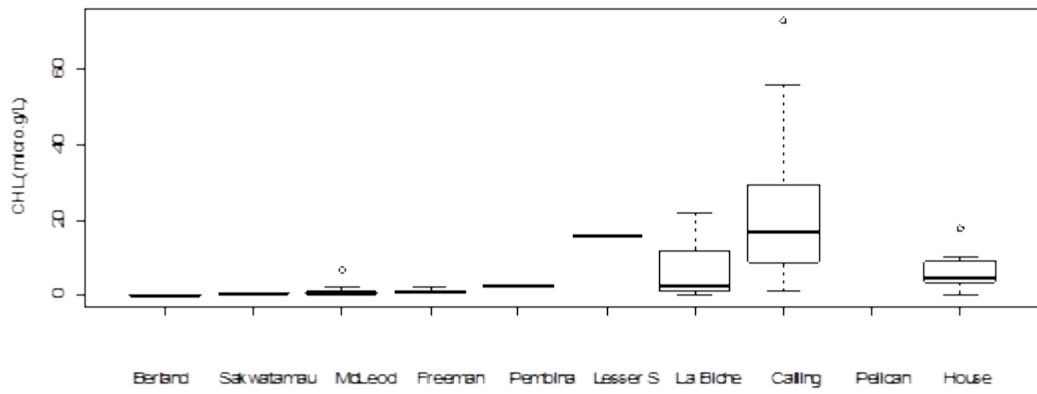
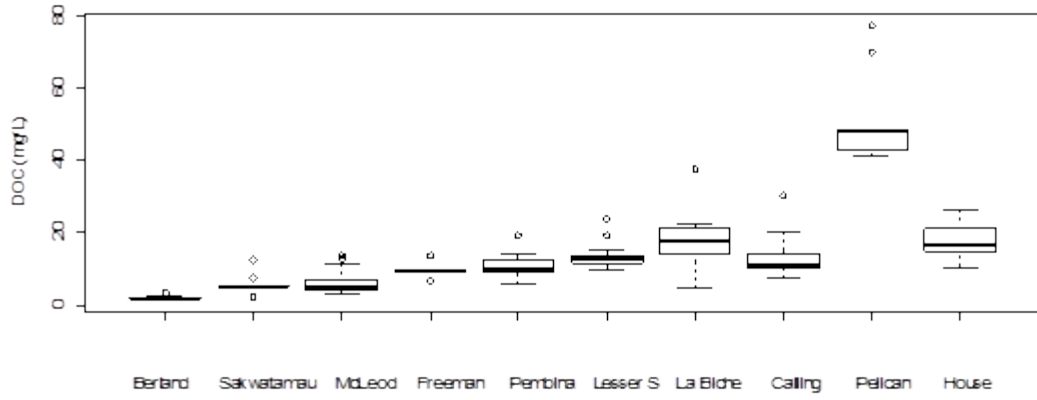
Appendix B. Box plots for in-stream, tributaries and pulp mills constituent concentration

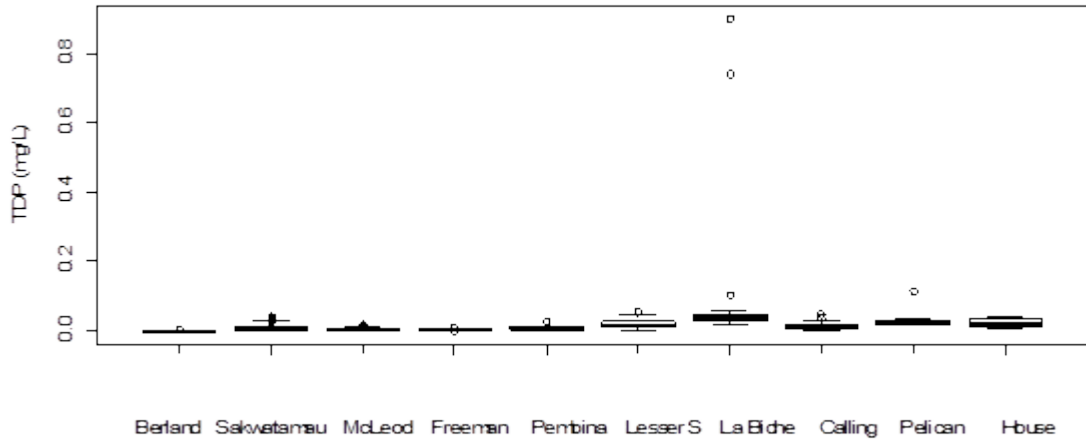
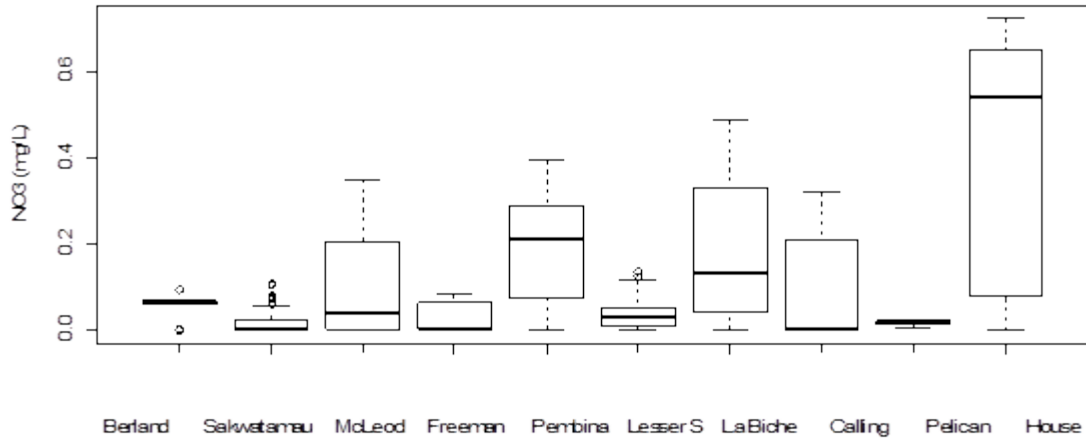
In-stream data



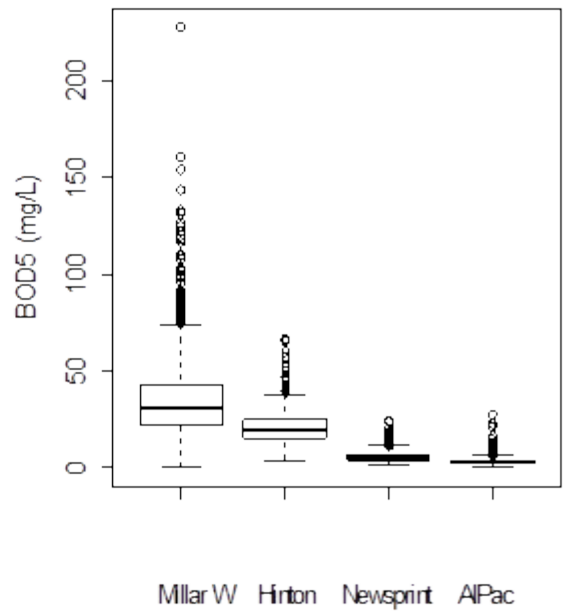
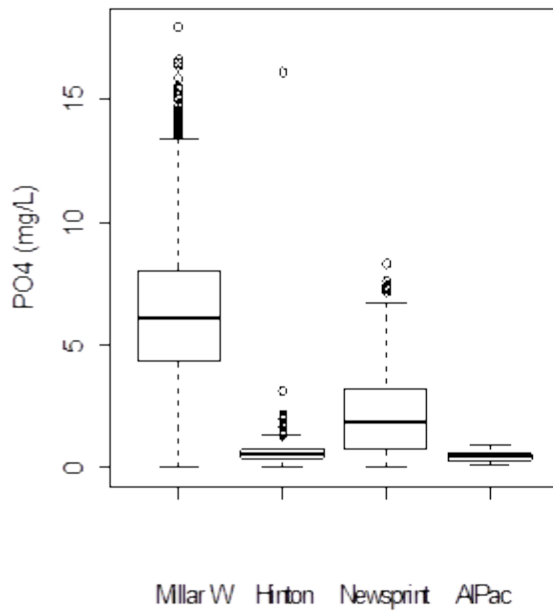
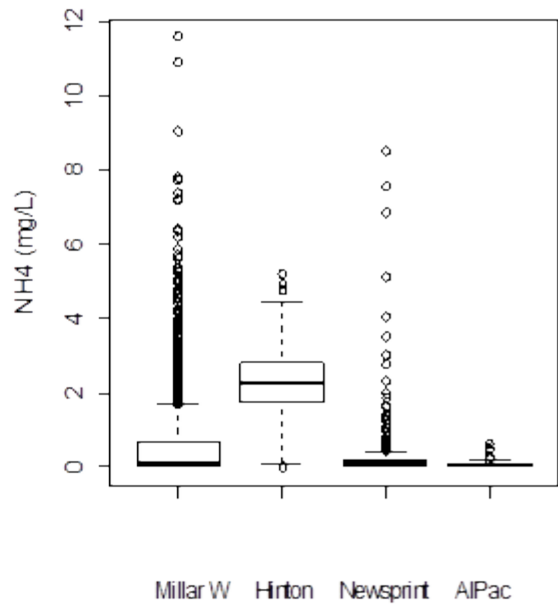
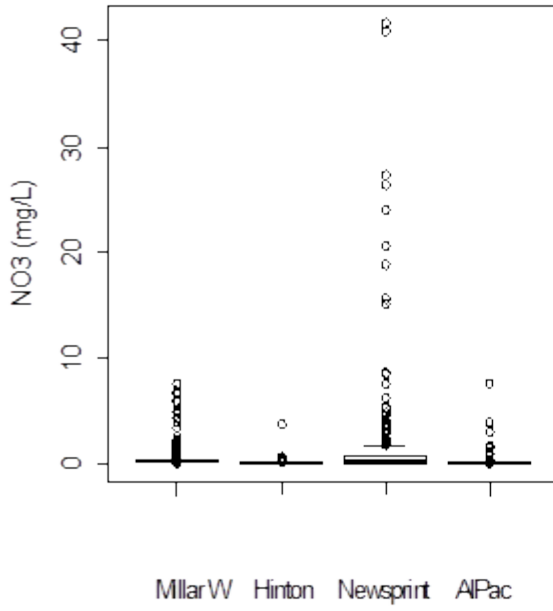


Tributaries





Pulp mills



Appendix C. Water quality available for tributaries

The water quality available for the tributaries was very limited. Most of the information was more than ten years old, and the average number of samples for the different parameters was only 20. The tributaries with less information available were Berland, Freeman, Pembina, Pelican and House River. From these tributaries, the impact of this lack of information can be higher in the case of Berland and Pembina River which flow represents the 24% and 15% respectively from the total flow accounted from tributaries. Additionally, most of the tributaries had samples in February and March, but few of them were sampled in November and December.

Table B- 1. Parameters and number of water quality samples available for tributaries from historic data

Tributaries	TDS	OM	PO4	NH4	NO3	SI	FE	ALG	DO	ALK	TIC	Period
Berland River	6	9	9	9	9	9	9	1	8	7	7	1984-1996
Sakwatamau River	11	10	52	72	71	13	7	2	9	12	12	1990-1997 & 2006
McLeod River	35	96	94	71	75	41	45	40	59	44	44	1988-2005 & 2006
Freeman River	3	5	5	5	5	4	4	2	5	3	3	1988-1996 & 2006
Pembina River	7	8	8	7	8	8	10	1	8	8	8	1988-1996 & 2006
Lesser Slave River	15	46	45	39	38	42	47	0	43	42	42	1984-2005 & 2006
La Biche River	15	18	19	19	19	17	15	15	16	16	16	1984-1996 & 2006
Calling River	18	28	28	29	29	27	16	19	27	28	28	1984-1996 & 2006
Pelican River	6	9	4	8	9	8	8	0	14	8	8	1989-1996
House River	12	14	13	8	14	6	8	7	16	13	13	1984-1996

In order to have more data all the tributaries monthly concentration was integrated and the averages were obtained. Based on this information the TDS, NH4, NO3, DSI, TIC and ALK are higher in the low flow months, January through March. These may be due to the lower dilution that can be achieved. On the other hand, the ISS is higher during the months with a high flow (April and July), and it can be explained from the turbulence that the river has in these months. From the monthly average, the DO also shows the expected behavior with low values in the under-ice period (January-March).

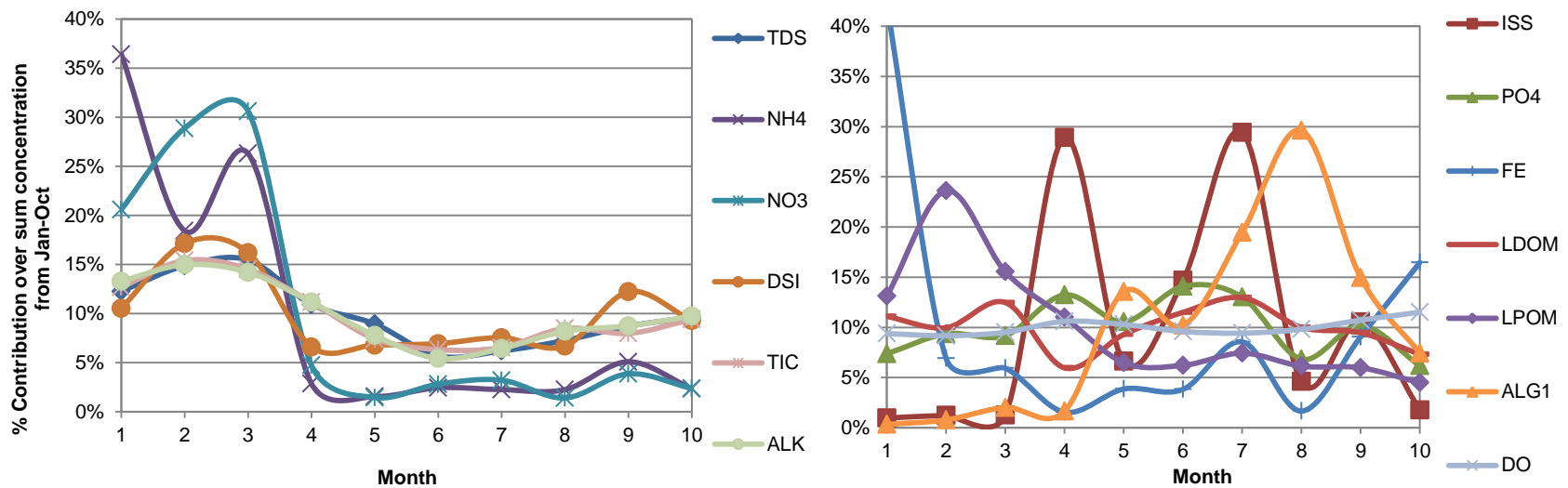


Figure B- 1. Seasonal trend of constituents average monthly concentration for the tributaries

Table B- 2. Overall tributaries' monthly average concentration for state variables (mg/L) (Not available = "-")

Month	TDS	ISS	PO4	NH4	NO3	DSI	FE	LDOM	RDOM	LPOM	RPOM	ALG	DO	TIC	ALK
1	231.2	5.3	0.008	0.284	0.140	5.985	7.354	12.49	12.49	0.474	1.107	0.013	9.25	50.26	183.2
2	279.9	6.7	0.010	0.144	0.196	9.741	1.205	11.23	11.23	0.854	1.992	0.031	9.04	60.95	206.3
3	291.1	6.9	0.010	0.205	0.208	9.216	1.035	14.05	14.05	0.562	1.312	0.081	9.38	57.47	195.7
4	206.0	158.2	0.014	0.022	0.032	3.760	0.271	6.72	6.72	0.398	0.930	0.067	10.45	44.20	154.0
5	168.5	36.3	0.011	0.012	0.010	3.863	0.673	10.46	10.46	0.234	0.547	0.547	10.14	29.40	106.9
6	107.5	80.3	0.015	0.019	0.019	3.945	0.667	12.95	12.95	0.225	0.524	0.411	9.46	25.06	74.9
7	116.7	161.0	0.014	0.018	0.022	4.290	1.492	14.60	14.60	0.269	0.627	0.785	9.29	25.92	88.8
8	136.8	25.2	0.007	0.018	0.010	3.804	0.290	11.27	11.27	0.222	0.518	1.195	9.67	33.61	113.0
9	164.4	57.6	0.011	0.040	0.026	6.949	1.580	10.66	10.66	0.216	0.504	0.603	10.57	31.60	120.5
10	180.8	9.7	0.006	0.018	0.016	5.290	2.871	8.23	8.23	0.162	0.378	0.300	11.35	37.20	134.1
11	-	0.1	0.001	0.003	0.002	5.600	0.420	2.04	2.04	0.078	0.182	-	-	-	-
12	-	-	-	-	-	-	0.242	-	-	-	-	-	8.00	-	-
Aver.	200.0	41.36	0.010	0.088	0.079	6.398	1.308	11.31	11.31	0.392	0.914	0.457	9.785	41.95	144.7

The concentration of each tributary was also compared with the overall average concentration. This is a measure of the level of contamination of each river and its impact in the calibration. Pelican, Freeman and Pembina River were not taken into account, because they have very few samples. Berland and Sakwatamau River appear to have lower concentrations, while La Biche and Hose River are higher.

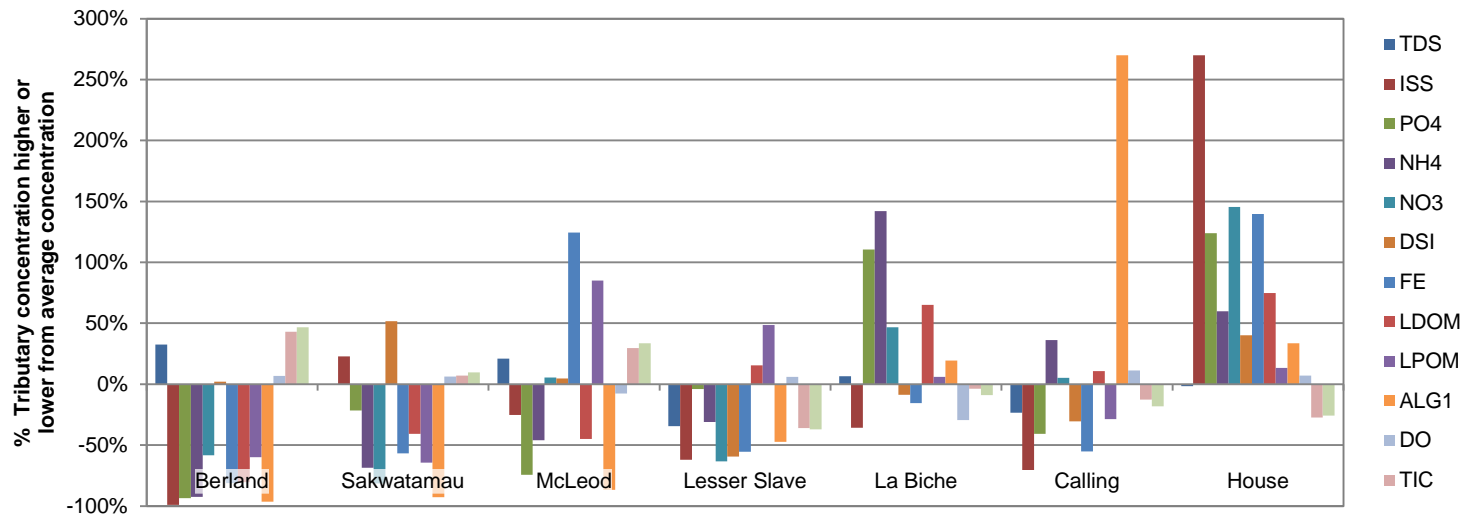


Figure B- 2. Tributary relative concentration in comparison to the overall average for each constituent

Table B- 3. Tributaries' average concentration from January through October (mg/L)

River	TDS	ISS	PO4	NH4	NO3	DSI	FE	LDOM	RDOM	LPOM	RPOM	ALG	DO	TIC	ALK
Berland	263.7	0.5	0.001	0.004	0.037	6.43	0.258	1.89	1.89	0.073	0.169	0.013	10.38	62.12	216.3
Sakwatamau	198.1	60.5	0.009	0.017	0.016	9.56	0.595	5.68	5.68	0.065	0.151	0.027	10.33	46.52	161.9
McLeod	240.8	36.8	0.003	0.028	0.093	6.60	3.094	5.28	5.28	0.336	0.783	0.049	8.98	56.32	197.1
Freeman	223.8	3.2	0.003	0.069	0.028	11.18	0.378	8.15	8.15	0.100	0.233	0.040	10.07	47.25	171.4
Pembina	251.1	12.6	0.004	0.085	0.085	6.54	0.318	7.41	7.41	0.294	0.686	0.193	7.81	53.44	201.3
Lesser Slave	130.2	18.7	0.010	0.036	0.032	2.55	0.615	11.09	11.09	0.269	0.629	0.193	10.32	27.74	92.9
La Biche	212.2	31.6	0.023	0.128	0.129	5.74	1.165	15.85	15.85	0.192	0.449	0.438	6.86	41.83	134.3
Calling	152.2	14.5	0.006	0.072	0.092	4.37	0.616	10.63	10.63	0.129	0.301	1.356	10.83	38.00	120.6
Pelican	258.3	5.1	0.010	0.767	0.016	8.62	2.747	40.88	40.88	3.987	9.304	NA	13.01	28.40	106.0
House	195.8	182.3	0.024	0.084	0.215	8.83	3.303	16.80	16.80	0.206	0.480	0.490	10.41	31.57	109.5

Table B- 4. Tributaries average bi-weekly water temperature (°C) (Not available = "-")

From	to	JDAY	Berland	Sakwatamau	McLeod	Freeman	Pembina	Lesser S	La Biche	Calling	Pelican	House	Average
1	15	8	-	-	-0.2	-	-0.1	0.0	-	-	-	-	-0.11
16	30	23	-	-	-	-	0.0	-0.2	0.2	0.1	0.0	-	0.03
31	45	38	0.0	0.0	-	0.3	-0.3	-0.1	-	-	-	-0.5	-0.09
46	60	53	0.0	-	-0.1	0.0	-0.1	-0.1	0.1	0.0	-0.3	-0.3	-0.08
61	75	68	-	-	-	-	0.0	-0.1	-0.1	0.0	-0.1	0.0	-0.04
76	90	83	-	-	-	-	-	0.0	-	-	-	-	-0.04
91	105	98	-	0.2	0.1	-	-	-0.2	-	-	-	-	0.03
106	120	113	-	1.3	-	-	-	-	-	-	-	-	1.33
121	135	128	-	6.5	-	-	-	9.6	-	-	-	-	8.07
136	150	143	-	-	10.4	-	-	10.0	-	-	-	-	10.21
151	165	158	-	14.4	-	-	15.7	14.1	15.5	13.0	-	13.5	14.35
166	180	173	-	12.4	-	-	-	-	-	15.8	-	-	14.08
181	195	188	-	15.0	-	-	-	-	-	19.4	-	-	17.20
196	210	203	-	-	18.3	-	-	18.1	-	-	-	-	18.21
211	225	218	-	19.3	-	-	18.6	19.8	18.3	17.2	-	-	18.64
226	240	233	-	-	19.6	-	-	16.3	-	-	-	-	17.97
241	255	248	-	15.5	12.6	-	-	-	-	-	-	-	14.07
256	270	263	7.6	7.5	-	9.6	8.2	11.6	9.4	12.1	-	-	9.42
271	285	278	-	-	10.4	9.7	7.2	7.9	6.9	6.4	-	-	8.09
286	300	293	-	0.0	5.6	-	-	3.5	-	5.3	-	-	3.60
331	345	338	-	-	-	-	-	0.1	-	-	-	-	0.13
346	360	353	-	-	-	-	-	0.1	-	-	-	-	0.06

Appendix D. Dissolved oxygen at Grand Rapids, air temperature at Athabasca and pulp mills load 2000-2006

Dissolved oxygen

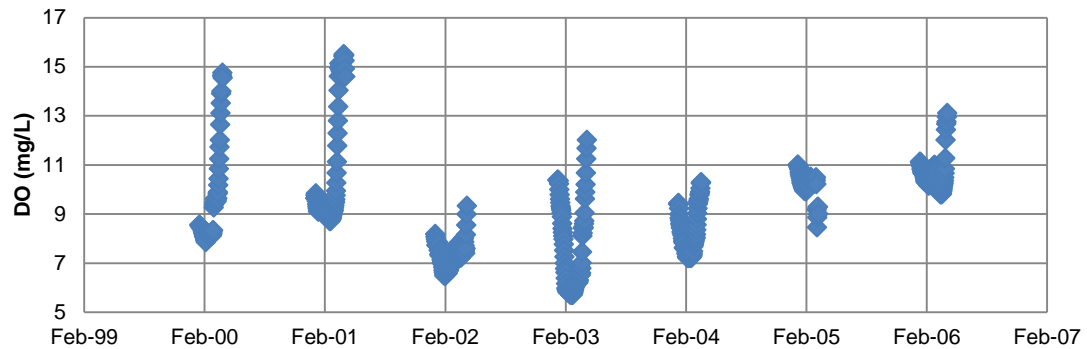


Figure D- 1. Dissolved oxygen at Grand Rapids

Table D- 1. Average DO concentration for winter months at Grand Rapids (mg/L)

Year	January	February	March	Grand Total
2000	8.48	8.14	10.09	9.19
2001	9.38	9.16	11.63	10.16
2002	7.56	6.74	7.41	7.22
2003	9.49	6.29	6.31	7.02
2004	8.63	7.39	8.83	8.19
2005	10.49	10.16	9.81	10.18
2006	10.81	10.35	10.24	10.39
Grand Total	9.24	8.32	9.16	8.86

Air temperature

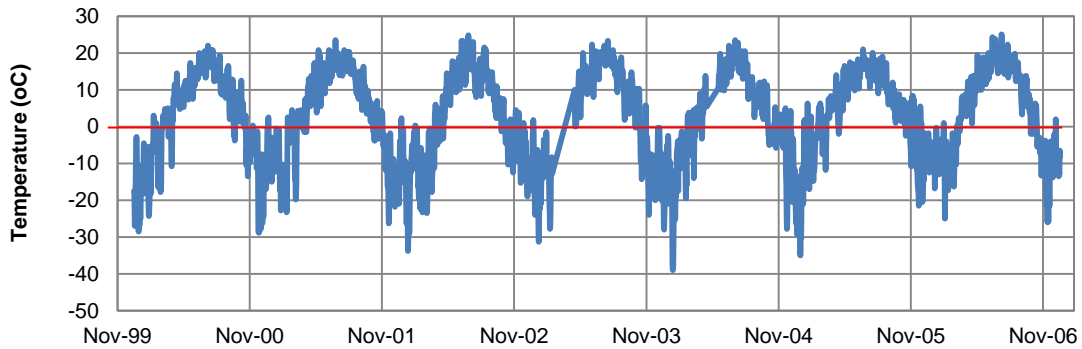


Figure D- 2. Daily average temperature at Athabasca Station

Table D- 2. Monthly average air temperature at Athabasca station (°C)

Year	Nov	Dec	Jan	Feb	Mar	Apr	Grand Total
2000	-	-	-16.33	-10.44	-3.51	3.55	-6.70
2001	-5.02	-16.77	-6.82	-13.88	-2.47	4.19	-6.75
2002	-2.31	-15.08	-14.94	-8.00	-13.11	-2.70	-9.45
2003	-2.69	-9.34	-14.36	-11.68	-6.92	4.30	-6.78
2004	-8.87	-12.06	-18.00	-9.07	-3.63	4.15	-7.96
2005	-0.75	-11.42	-16.17	-6.90	-1.16	5.99	-5.12
2006	-0.79	-8.45	-8.34	-9.48	-5.53	7.44	-4.18
Grand Total	-3.40	-12.19	-13.56	-9.92	-5.19	3.85	-6.71

Pulp mills load

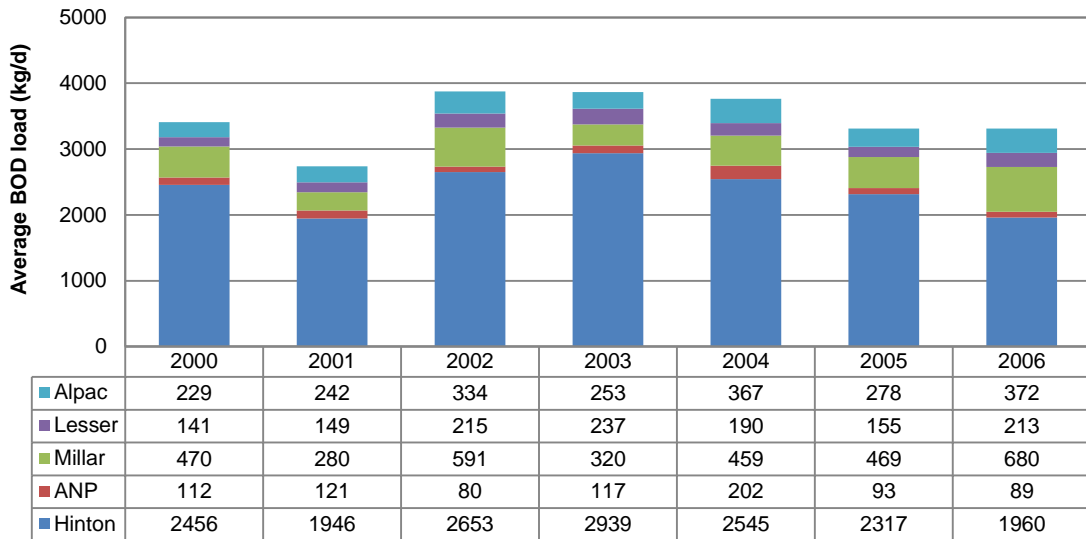


Figure D- 3. Pulp mills average BOD load from December to March

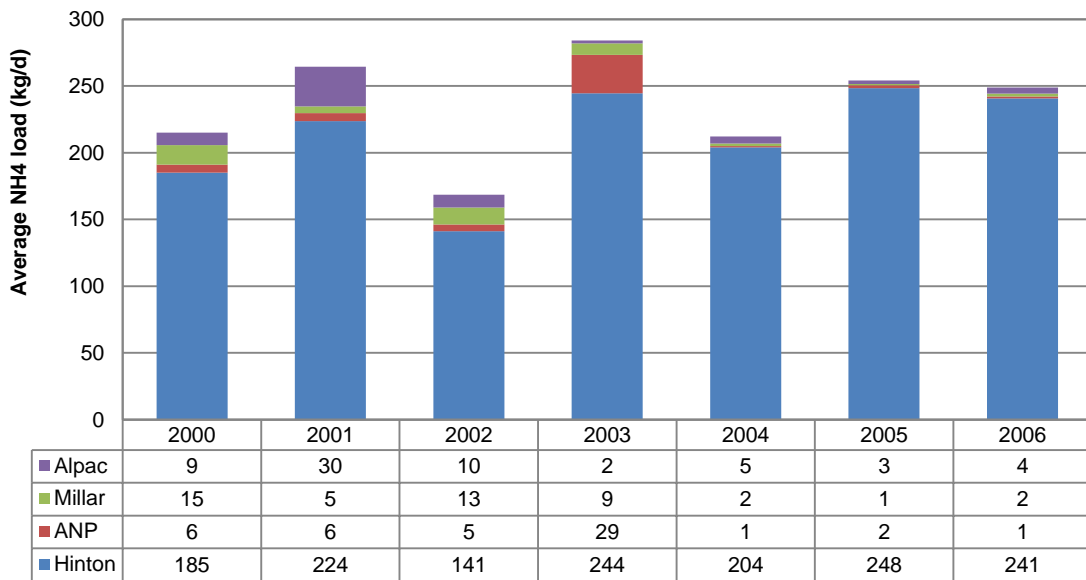


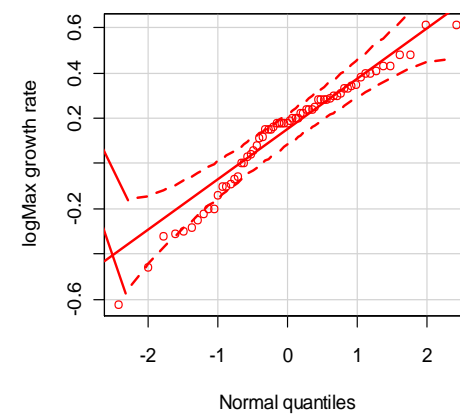
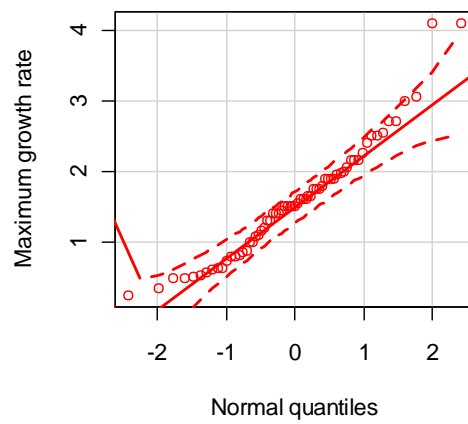
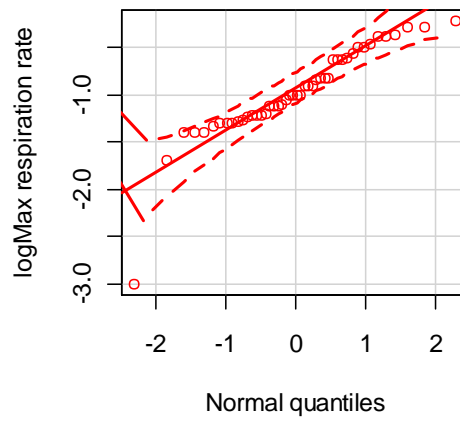
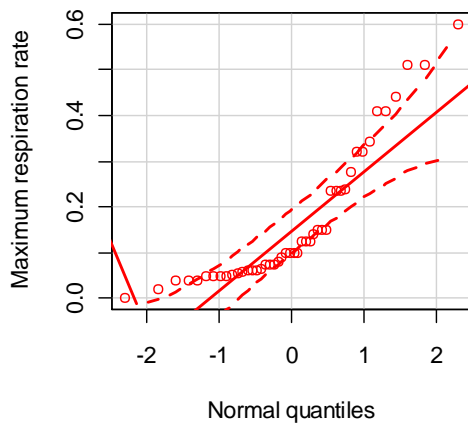
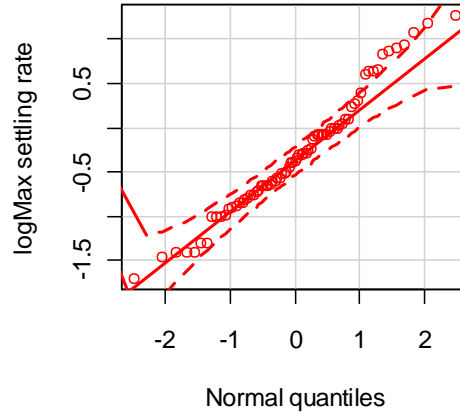
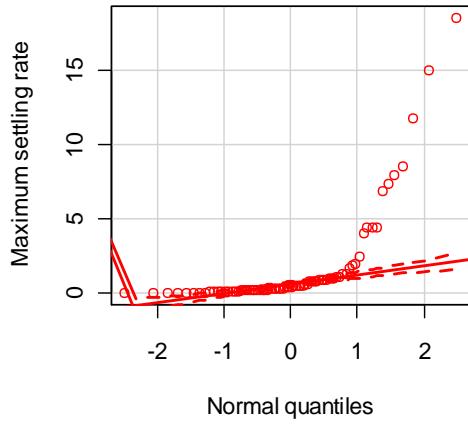
Figure D- 4. Pulp mills average ammonia load from December to March

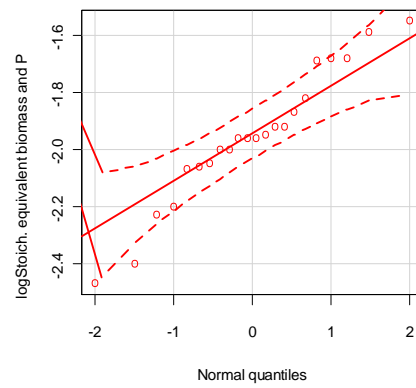
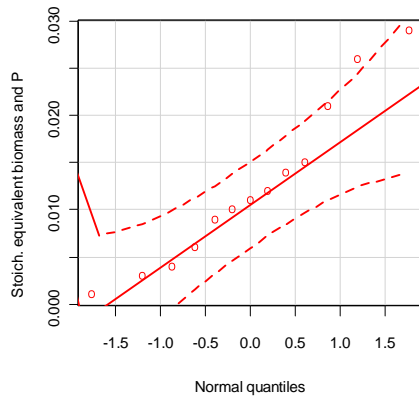
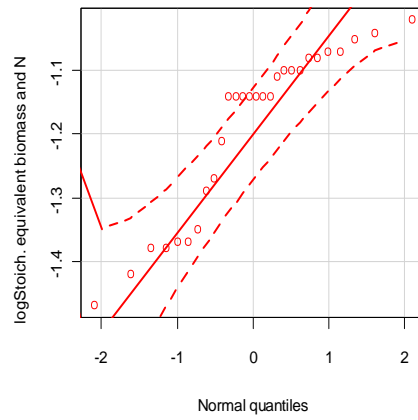
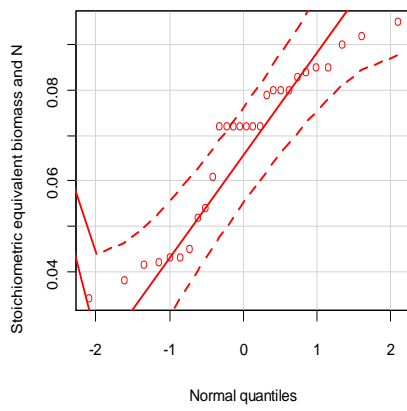
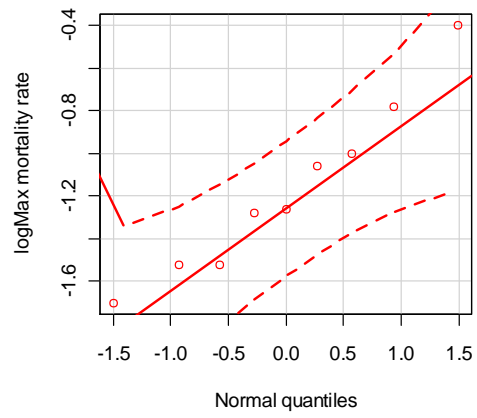
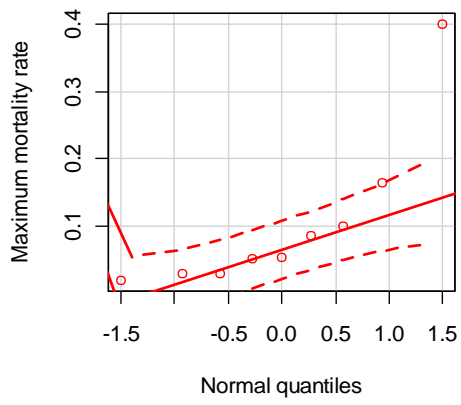
Appendix E. Normality check for LHS analysis

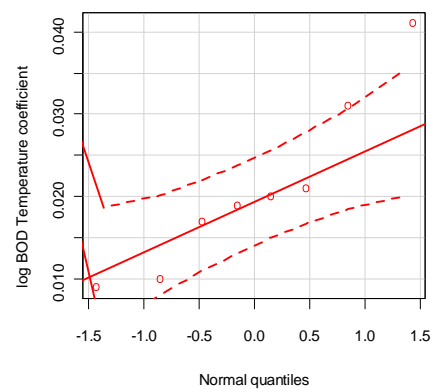
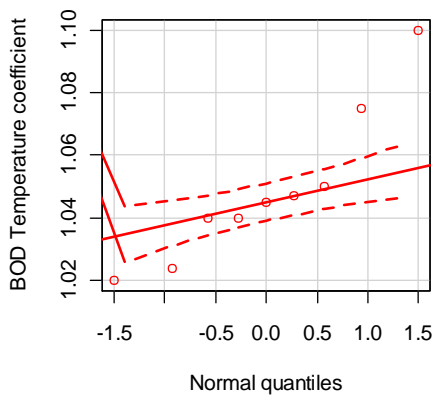
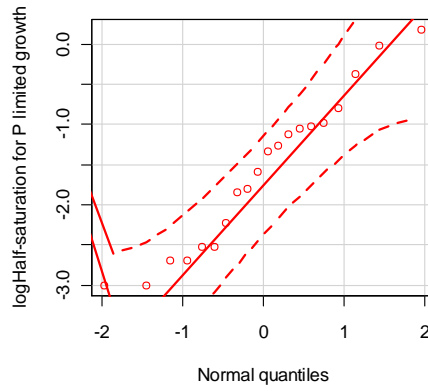
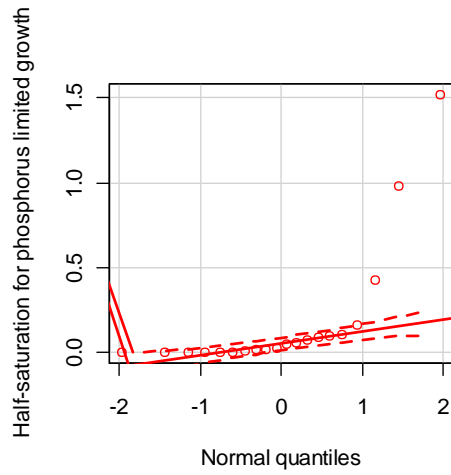
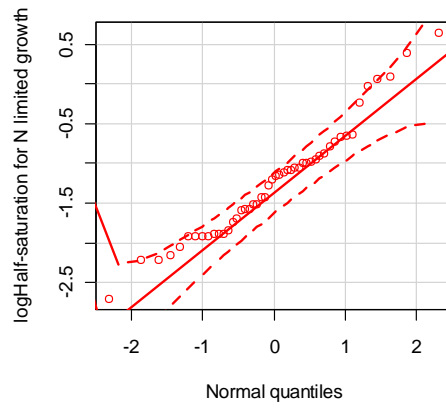
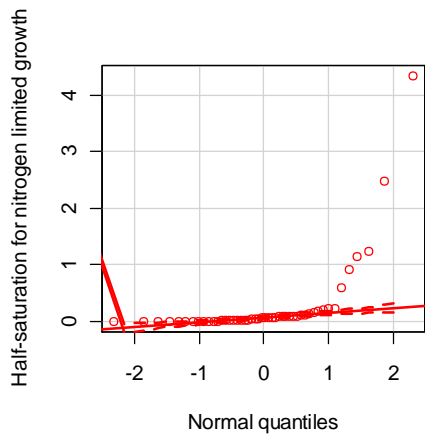
Table E- 1. Constants used in the LHS analysis and their values selected after calibration

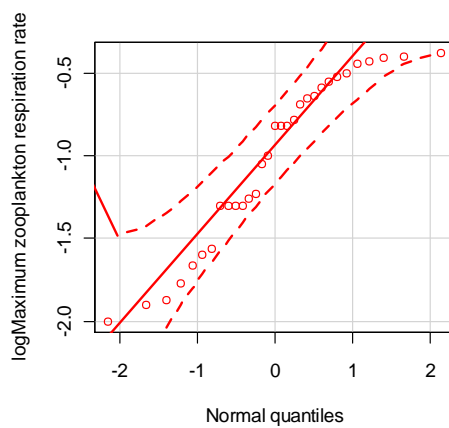
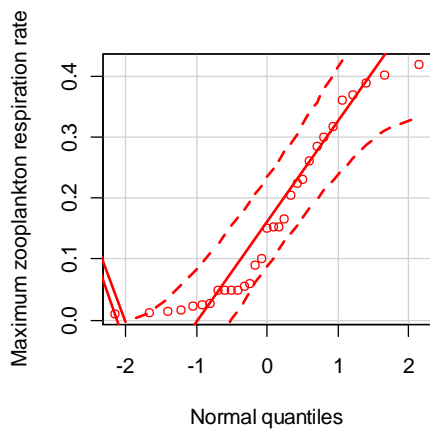
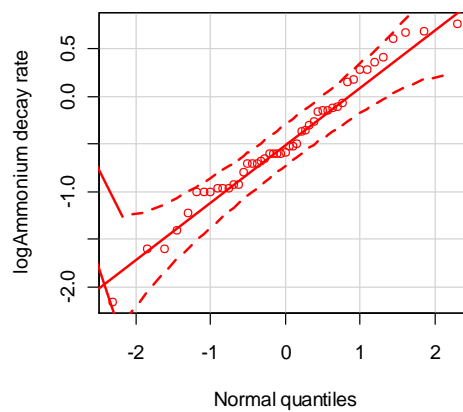
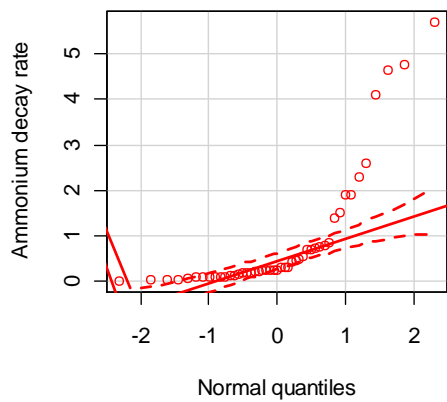
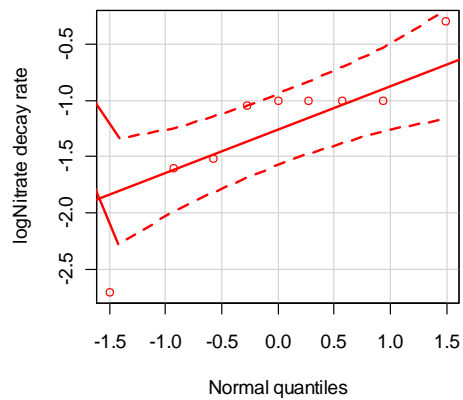
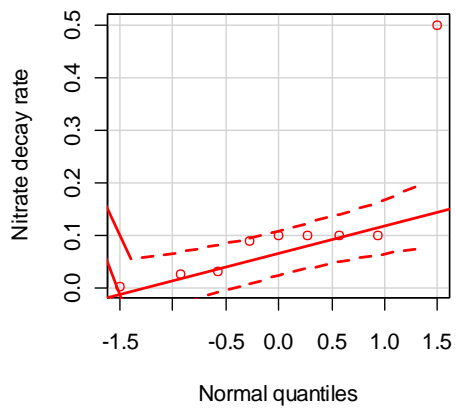
Constant or kinetic coefficient		Count	Average	Min.	Max.	StdDev	Distribution	Used
Maximum algal growth rate, d-1	AG	65	1.580	0.240	4.100	0.82	Normal	2.0
Maximum algal respiration rate, d-1	AR	46	0.165	0.001	0.600	0.15	Logarithmic	0.04
Maximum algal excretion rate, d-1	AE	8	0.030	0.014	0.044	0.01	Normal	0.04
Maximum algal mortality rate, d-1	AM	9	0.104	0.020	0.400	0.12	Logarithmic	0.10
Maximum algal settling rate, d-1	AS	75	1.687	0.020	18.600	3.38	Logarithmic	0.10
Algal half-saturation for P limited growth, g m ³ -1	AHSP	20	0.182	0.001	1.520	0.39	Logarithmic	0.004
Algal half-saturation for N limited growth, g m ³ -1	AHSN	48	0.281	0.002	4.340	0.74	Logarithmic	0.014
Light saturation intensity, W m-2	ASAT	9	51.333	10.00	135.0	40.28	Normal	75.0
Stoichiometric equivalent algal biomass and P	AP	29	0.011	0.000	0.029	0.01	Normal	0.01
Stoichiometric equivalent algal biomass and N	AN	28	0.067	0.034	0.095	0.02	Normal	0.08
Stoichiometric equivalent algal biomass and C	AC	29	0.441	0.265	0.600	0.07	Normal	0.45
Labil DOM decay rate d-1	LDOMD K	9	0.297	0.100	0.640	0.17	Normal	0.10
Labil POM decay rate d-1	LPOMD K	9	0.018	0.003	0.059	0.02	Logarithmic	0.08
POM settling rate	POMS	10	2.673	0.030	9.000	3.40	Normal	0.10
5-day decay rate at 20°C, d-1	KBOD	45	0.468	0.008	3.000	0.62	Logarithmic	0.10
Temperature coefficient	TBOD	9	1.049	1.020	1.100	0.02	Logarithmic	1.02
Ammonium decay rate, d-1	NH4DK	47	0.887	0.007	5.700	1.36	Logarithmic	1.2
Nitrate decay rate, d-1	NO3DK	9	0.116	0.002	0.500	0.15	Logarithmic	0.07
Sediment oxygen demand, g/m ² /d	SOD	25	0.426	0.094	1.330	0.28	Logarithmic	0.2-1.3

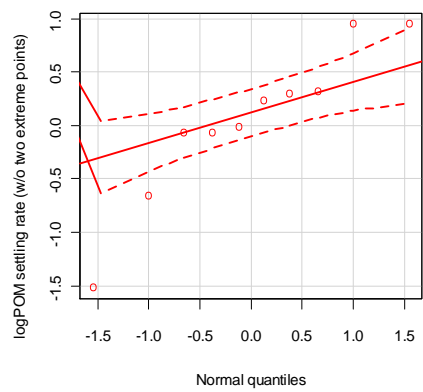
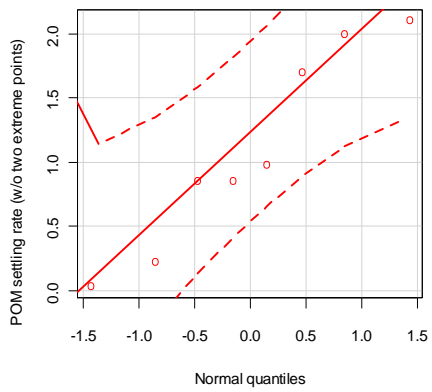
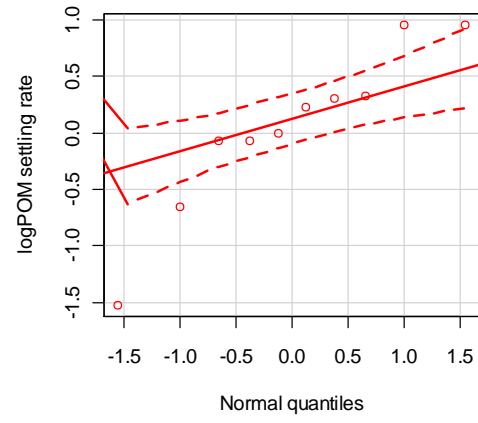
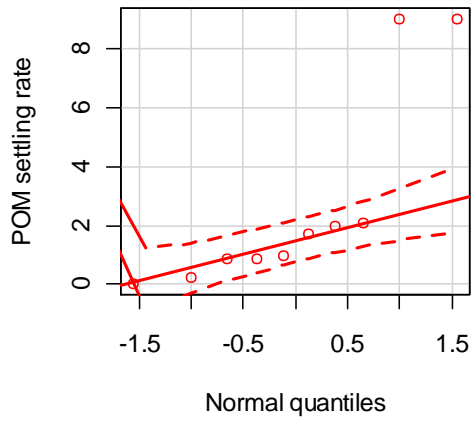
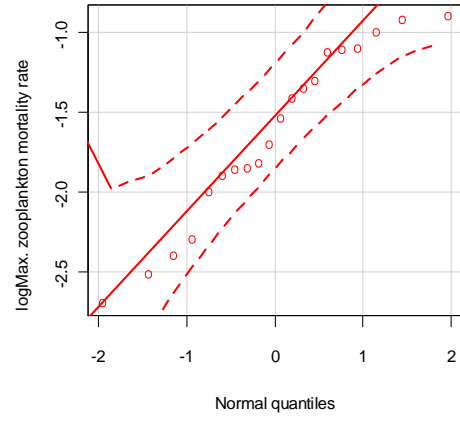
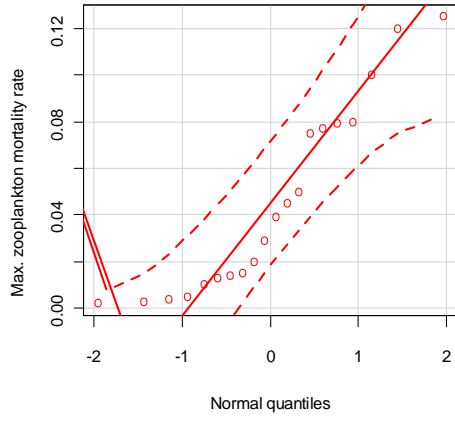
Normality check

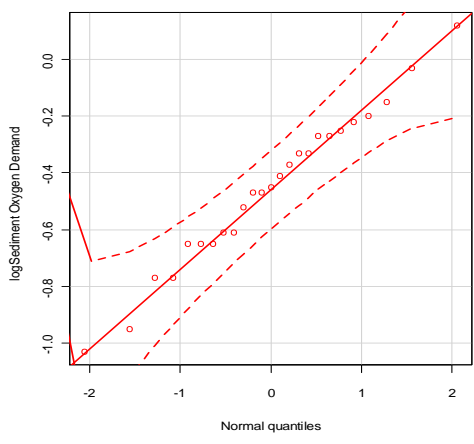
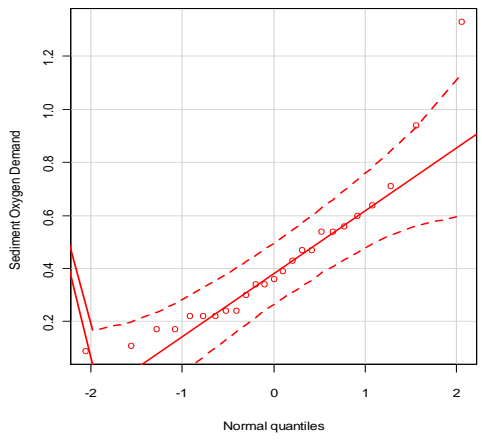
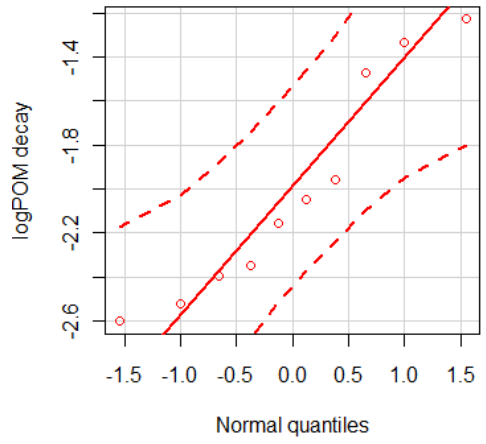
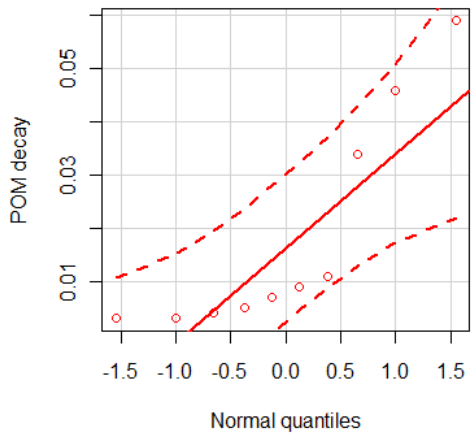
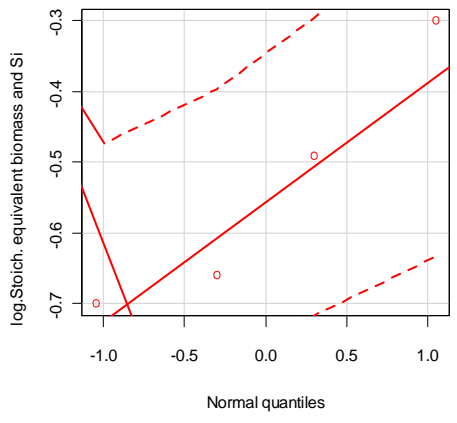
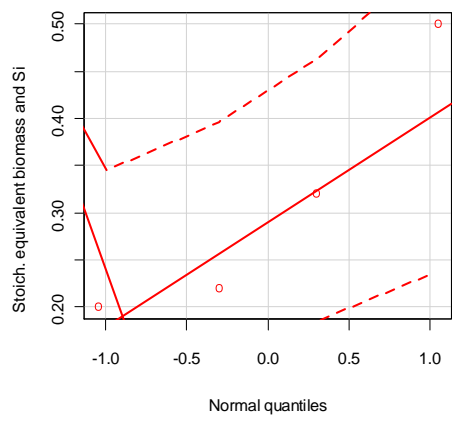


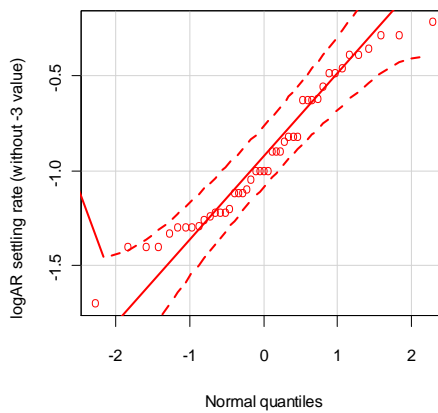
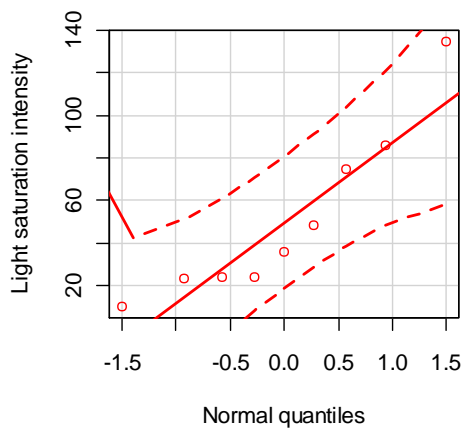
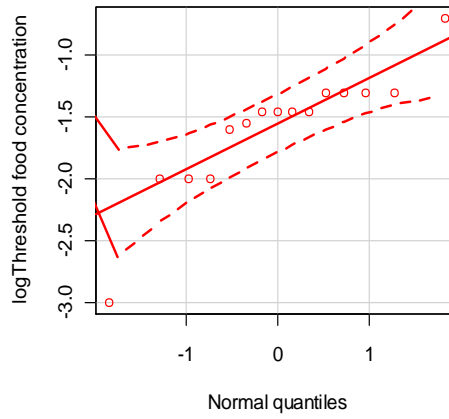
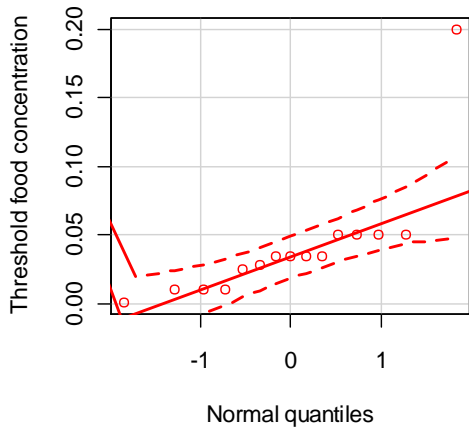
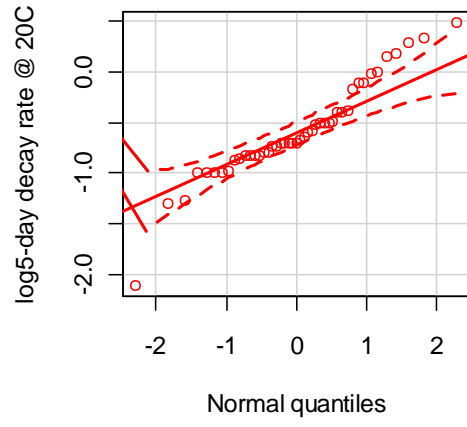
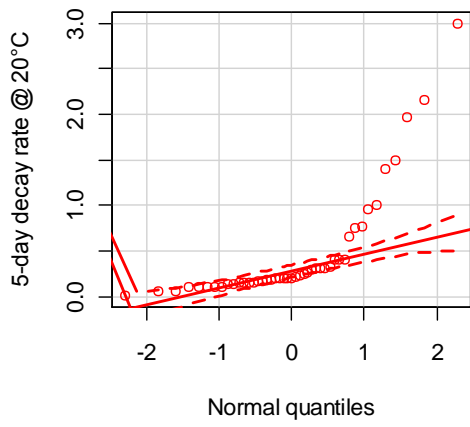


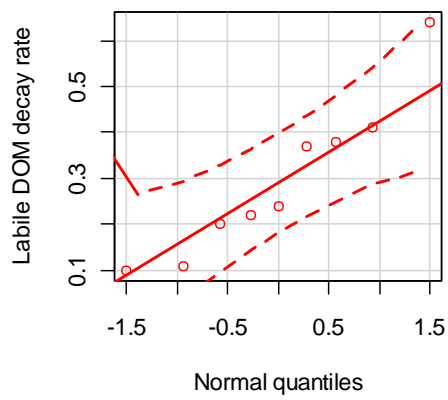
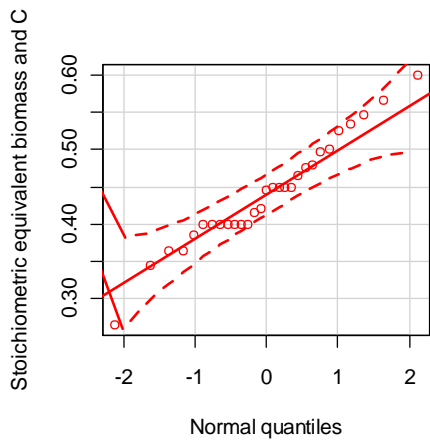
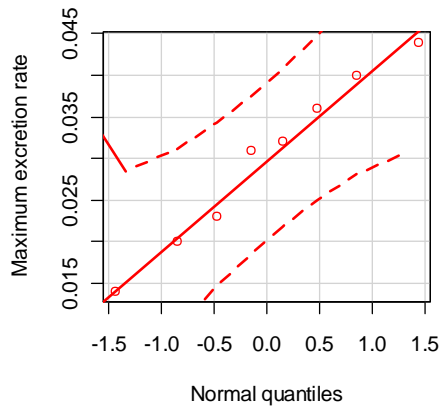












Appendix F. Preliminary run from Town of Athabasca to Grand Rapids

A preliminary run was made from Athabasca to Grand Rapids to compare the results with the previous modeling effort (Yu, 2006). By comparing the DO calibration graphs for 2001, 2002 and 2003 it was observed an improvement in the DO calculation. However, the MAE cannot be directly compared because the number of observed data reported by Yu is different to the total observed values, and is hard to know which values were considered in the calculation. The MAE for DO at Grand Rapids simulation starts at Athabasca Town was 0.86 mg/L, 0.32 mg/L and 0.62 mg/L for the winters 2000-2001, 2001-2002 and 2002-2003 respectively.

The DO is well replicated in five of the seven years simulated. However, 2005 and 2006 were two winters with high DO concentration and the model under estimate this concentration. It is likely that there was some error in measuring the DO on March 15th, 2006, which affected the results (the concentration observed in the town of Athabasca was lower (9.39 mg/L) than the concentration that day in Grand Rapids (10.07 mg/L)). A model configured for this river section (about 200 km) only includes ALPAC, and does not reflect the cumulative impacts of different scenarios in the watershed. Therefore, the model domain needs to be extended from Hinton to Grand Rapids.

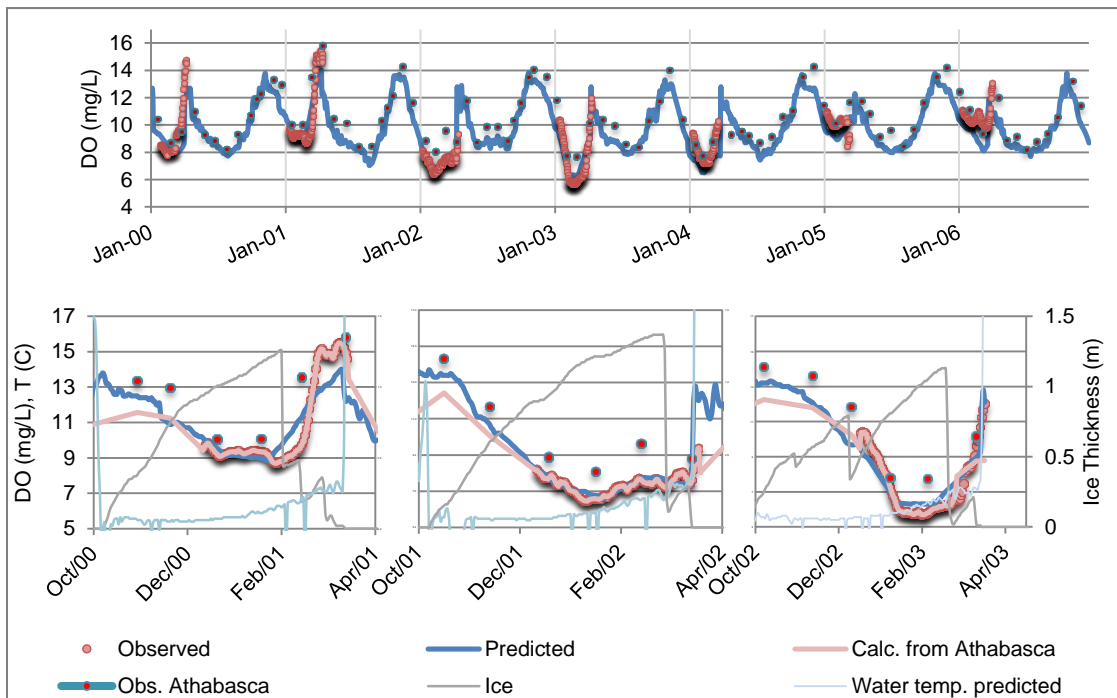


Figure F- 1. DO simulation at Grand Rapids starting the model domain at Town of Athabasca

Appendix G. Error measures used

Root Mean Square Error

$$RMSE = \sqrt{\frac{1}{N} \sum_{n=1}^N (P_n - O_n)^2}$$

Fractional Root Mean Square Error

$$FRMSE = \frac{RMSE}{\sqrt{\frac{1}{N} \sum_{n=1}^N O_n^2}}$$

Mean Absolute Error

$$MAE = \frac{1}{N} \sum |P_n - O_n|$$

Relative Mean Absolute Error

$$RMAE = \frac{MAE}{\bar{O}}$$

Mean Error

$$ME = \bar{P} - \bar{O}$$

Relative Mean Error

$$RME = \frac{\bar{P} - \bar{O}}{\bar{O}}$$

Appendix H. Extended results for calibration and validation

Hydrodynamics

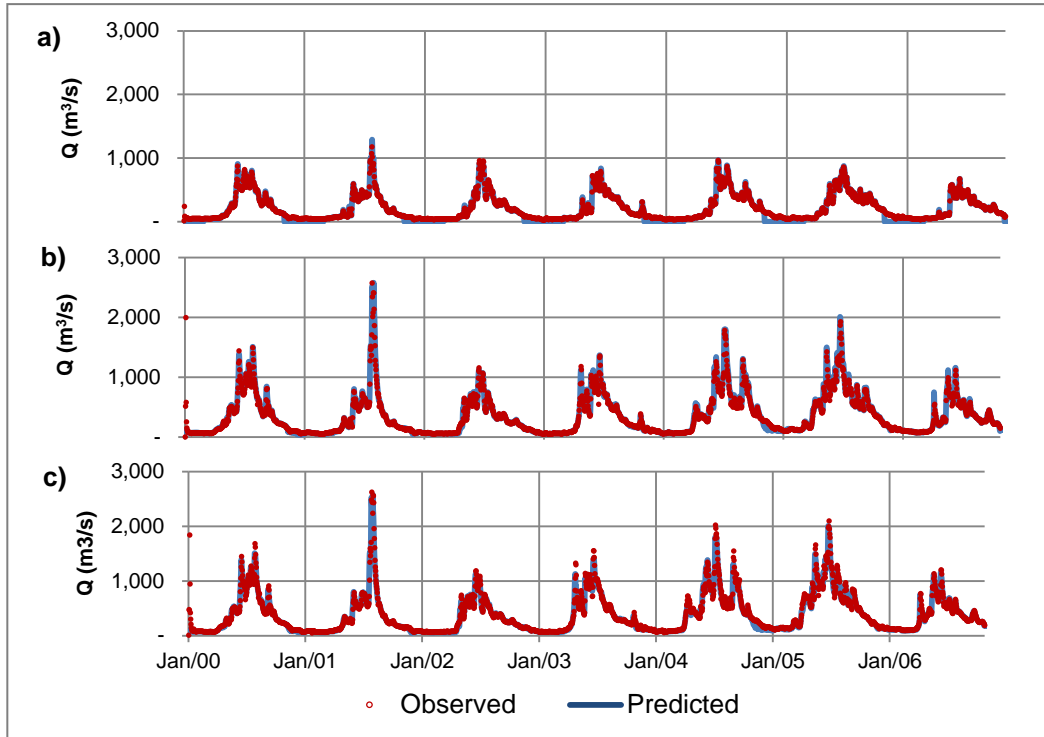


Figure H- 1. Flow calibration and validation for a) Windfall, b) Athabasca, c) Grand Rapids station estimated from watershed ratio using Athabasca and Fort MacMurry stations

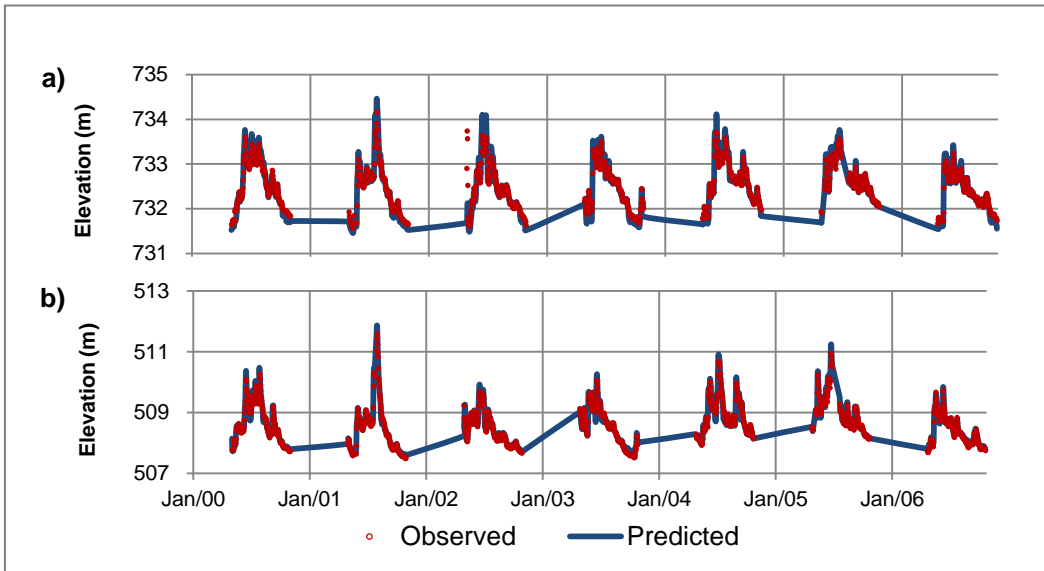


Figure H- 2. Elevation calibration and validation for a) Windfall and b) Athabasca station

Water Temperature

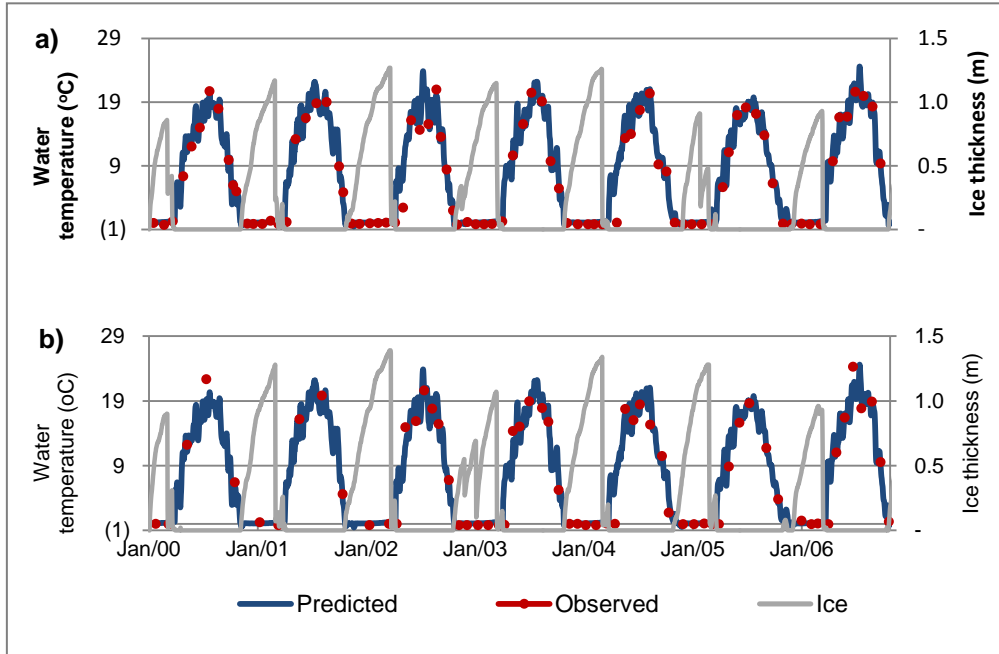


Figure H- 3. Temperature calibration and validation for a) Athabasca, b) Grand Rapids station

Table H- 1. Error measures for elevation calibration

Station	RMSE	MAE (m)	ME	FRMSE	RMAE (%)	RME
Windfall	0.11	0.09	0.02	<0.01	0.01	<0.01
Athabasca	0.24	0.21	0.15	0.05	0.04	0.03
Average	0.18	0.15	0.08	0.02	0.03	0.02

Table H- 2. Error measures for water temperature calibration

Station	RMSE	MAE (°C)	ME	FRMSE	RMAE (%)	RME
Athabasca	1.15	0.78	0.64	10.10	9.55	7.86
Grand Rapids	2.93	1.67	1.39	25.71	20.68	17.27
Average	2.04	1.23	1.02	17.91	15.12	12.57

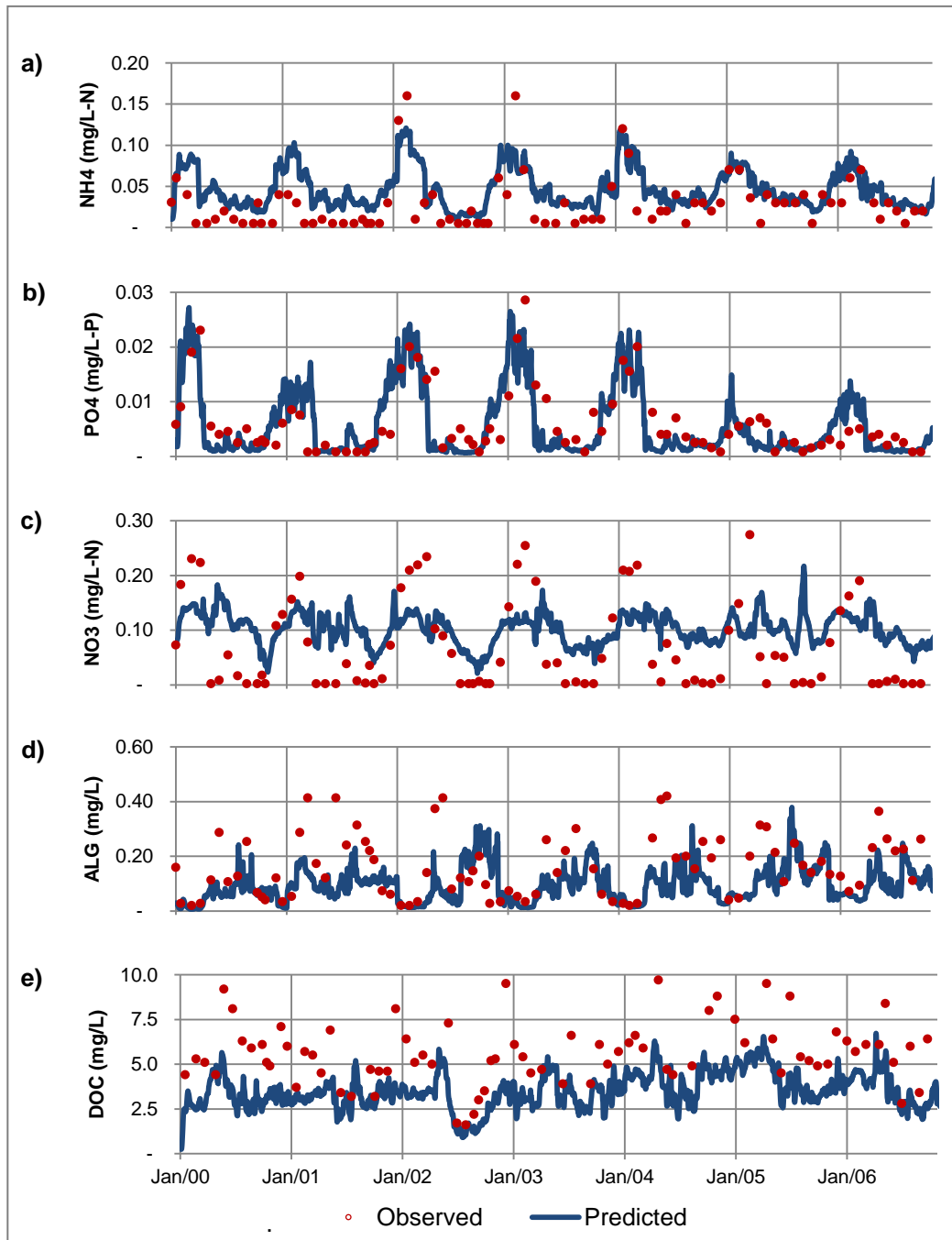


Figure H- 4. Water quality calibration and validation for Athabasca station a) ammonia, b) phosphates, c) nitrates-nitrites, d) algae, e) dissolved organic carbon

Table H- 3. Error measures for water quality calibration at Athabasca

Parameter	RMSE	MAE (mg/L)	ME	FRMSE	RMAE (%)	RME
DO	1.59	1.16	-0.57	14.72	10.88	-5.4
ALG	0.13	0.08	-0.07	68.78	57.69	-52.2
NO3	0.053	0.043	0.009	44.41	53.70	11.7
NH4	0.032	0.016	-0.007	70.03	61.47	-26.79
PO4	0.006	0.004	-0.001	61.29	62.83	-8.1

Table H- 4. Error measures for water quality validation at Athabasca

Parameter	RMSE	MAE (mg/L)	ME	FRMSE	RMAE (%)	RME
DO	1.42	1.10	-0.76	13.33	10.46	-7.2
ALG	0.14	0.10	-0.19	62.34	54.64	-47.2
NO3	0.058	0.049	0.029	63.35	87.27	52.0
NH4	0.026	0.018	-0.014	59.00	55.86	-43.8
PO4	0.004	0.003	-0.002	66.19	69.86	-4.3

Table H- 5. Error measures for water quality calibration at Grand Rapids

Parameter	RMSE	MAE (mg/L)	ME	FRMSE	RMAE (%)	RME
DO	1.74	1.37	0.52	19.31	14.94	5.7
ALG	0.149	0.104	-0.091	67.51	58.45	-51.2
NO3	0.047	0.037	0.011	36.27	39.17	11.5
NH4	0.020	0.015	-0.024	59.41	61.42	10.9
PO4	0.006	0.005	0.001	68.11	63.75	-14.3

Table H- 6. Error measures for water quality validation at Grand Rapids

Parameter	RMSE	MAE (mg/L)	ME	FRMSE	RMAE (%)	RME
DO	1.83	1.59	-1.28	18.73	16.37	-13.2
ALG	0.168	0.129	-0.118	59.63	53.31	-48.7
NO3	0.059	0.049	0.029	59.87	75.36	44.6
NH4	0.025	0.018	-0.012	52.91	44.99	-30.8
PO4	0.007	0.005	-0.002	73.37	70.35	-24.6

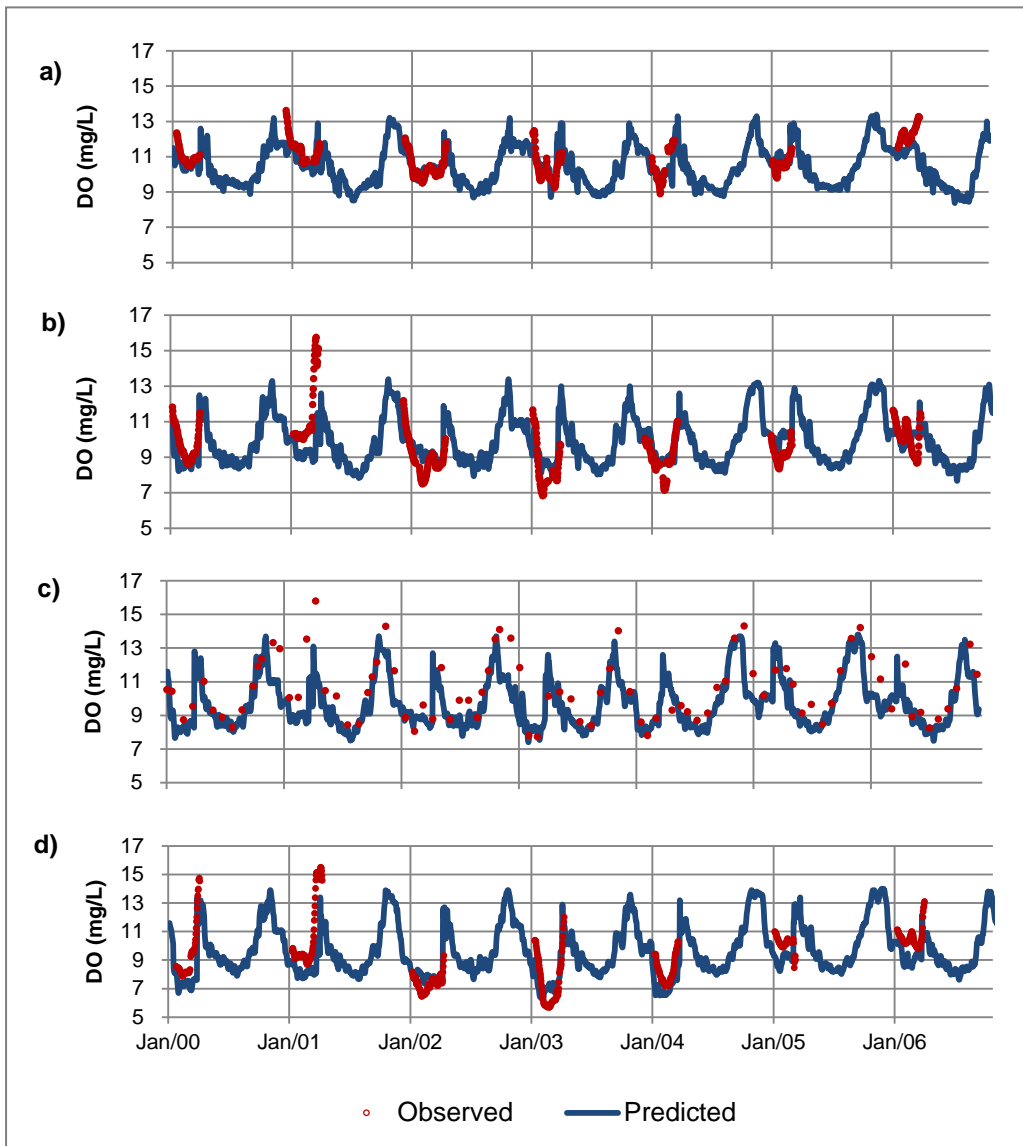


Figure H- 5. DO calibration and validation for a) Windfall, b) Smith, c) Athabasca, d) Grand Rapids

Table H- 7. Error measures for DO at different stations

Station	RMSE	MAE (mg/L)	ME	FRMSE	RMAE (%)	RME
Windfall	0.72	0.54	-0.18	6.63	5.00	-1.63
Smith	1.28	0.95	-0.01	13.33	9.94	-0.09
Athabasca	1.50	1.07	-0.80	13.94	10.13	-7.52
Grand Rapids	1.66	1.32	-0.77	17.87	14.49	-8.50

Appendix I. Extended results for model application

Pulp mills' maximum government permit BOD load

Table I- 1. Base scenarios and maximum permitted BOD load (January-February)
AV (average values), CF (critical flow), MAXL (permitted BOD loads)

Scenario	DO (mg/L)			Description
	Average	Min	Av. Difference	
AV	8.07	7.85	-	Average values used for input files (2000- 2006)
CF	7.43	7.21	-	0.70Q of influent, and main tributaries
MAXL	5.90	5.57	1.53	CF and maximum BOD load

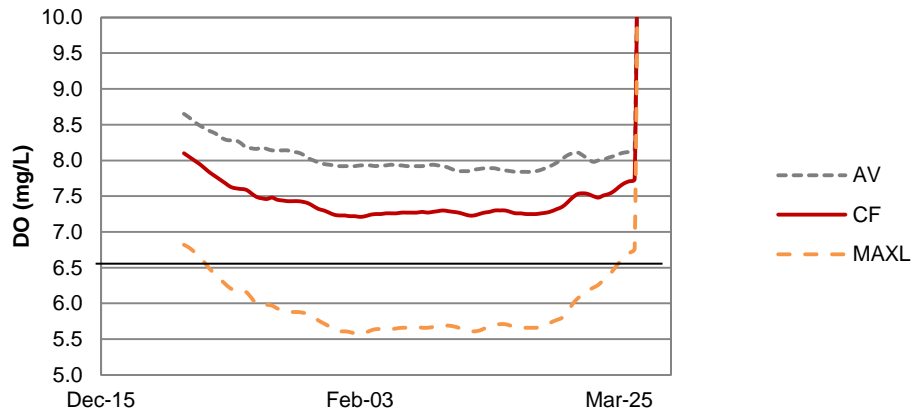


Figure I- 1. Scenarios with average conditions (AV), critical flow (CF), and pulp mills' maximum BOD permitted load under CF

Comparison of different parameters at low flow

Table I- 2. Scenarios with change of one variable CF (critical flow), TB (tributaries load increase), 1BOD (effluents BOD increase 1σ), DO (DO decrease), SOD (SOD increase)

Scenario	DO (mg/L)			Description
	Average	Min	Av. Difference	
CF	7.43	7.21	-	0.70Q of influent, and main tributaries (Berland, McLeod, Pembina, Lesser Slave)
TB	7.48	7.26	-0.05	1.43 times the concentration of nutrients and organic matter in all tributaries
1BOD	7.13	6.89	0.29	Pulp mills' BOD concentration 1 standard deviation higher
DO	7.02	6.70	0.41	DO concentration in the influent and main tributaries 1 standard deviation lower
SOD	6.90	6.65	0.53	SOD in all branches 1.43 times higher

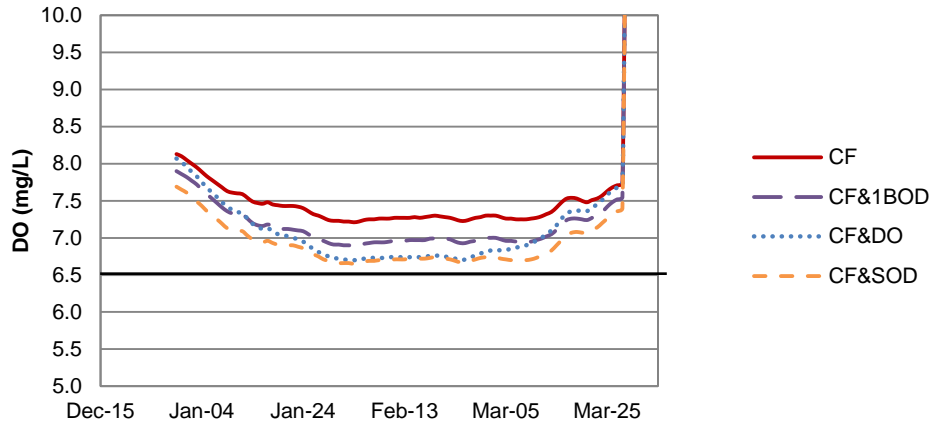


Figure I- 2. Worst case scenario at critical flow changing one variable: BOD increase 1σ (CF&1BOD), DO decrease 1σ (CF&DO), SOD increase 43% (CF&SOD)

Scenarios using critical flow and combining more than one variable

Table I- 3. Scenarios using critical flow and BOD increase 1σ and DO decrease 1σ (1BOD&DO), BOD increase 1σ and SOD increase 43% (1BOD&SOD), BOD increase 1σ , or SOD increase 43% and DO decrease 1σ (1BOD&SOD&DO)

Scenario	Average	DO min (mg/L)	Av. difference
CF	7.43	7.21	-
1BOD&DO	6.71	6.35	0.72
1BOD&SOD	6.60	6.33	0.83
1BOD&SOD&DO	6.23	5.84	1.20

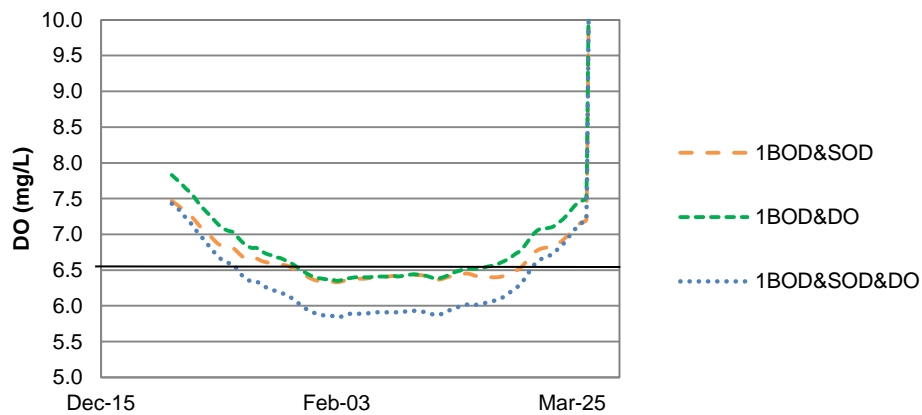


Figure I- 3. BOD increase 1σ and DO decrease 1σ (1BOD&DO), BOD increase 1σ and SOD increase 43% (1BOD&SOD), BOD increase 1σ , SOD increase 43% and DO decrease 1σ (1BOD&SOD&DO)

Climate change

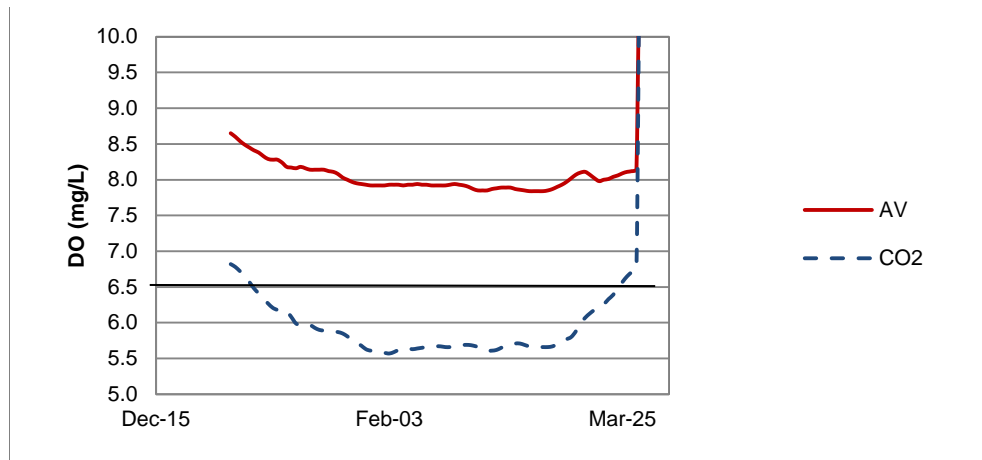


Figure I- 4. Climate change scenario (CO₂), Average conditions (AV)

Engineering controls

Table I- 4. Engineering controls applied under worst case scenario 1BOD&SOD&DO (January-February) Wastewater treatment upgrading (HPM), DO injection (15,000 lb/d O₂), all pulp mills shut down (0BOD)

Scenario	DO (mg/L)			Description
	Average	Min	Av. difference	
HPM	6.60	6.30	-0.42	Using ALPAC's BOD concentration for Hinton Pulp Mill's effluent
15,000 lb/d O ₂	6.76	6.44	-0.55	Oxygen injection in the pulp mills' effluents
0BOD	7.17	6.87	-0.94	All pulp mills shut down

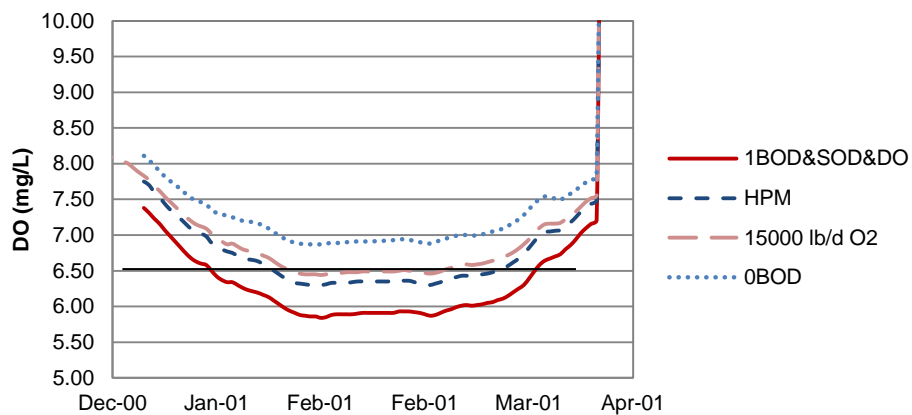


Figure I- 5. Engineering controls. Wastewater treatment upgrading (HPM), DO injection (15,000 lb/d O₂), all pulp mills shut down (0BOD)

Appendix J. Alberta Environment NAs synoptic survey using POCIS

Alberta Environment performed a NAs synoptic survey (2009-2011) using POCIS in the Athabasca River and tributaries. The quantification method used was LC-MS/MS. After disassembly the POCIS and scraping the resin, the inner surface of the membrane was rinsed with methanol (no fixed volume). This rinse and additional methanol were used for the resin elution. Because they were not expecting high adsorption of NAs onto the membrane, the membrane rinsing might not have recovered all the mass. In previous experiments, the recovery by random rinsing of the membrane inner surface was $35\% \pm 7\%$.

Using this% recovery and the uptake rate obtained from the lab experiments the concentration in the surface water was estimated. The average concentration obtained with POCIS was compared with grab samples analyzed in 2009-2010 by GC-MS-ion trap (RAMP, 2012). In general, the grab samples showed higher concentration. However, the samples might not have been taken exactly during the same period. Passive samplers accumulate the freely dissolved fractions, and other field applications have found a higher concentration from grab samples due to the colloidal fraction co-analyzed (Aguilar-Martinez, et al., 2011).

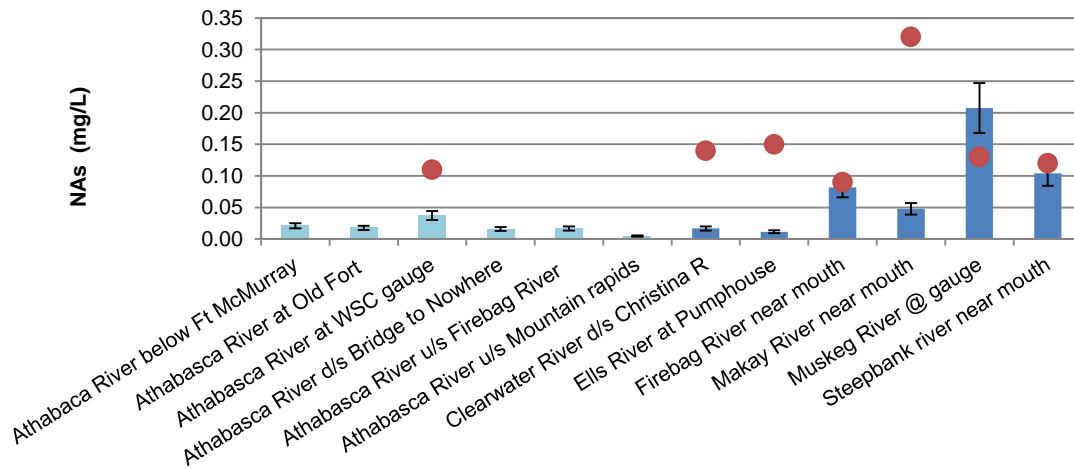


Figure J- 1. NAs concentration in the Athabasca River (light blue) and tributaries (dark blue) estimated from synoptic survey. Error bars reflect uncertainty in mass recovery from membrane random rinsing. Red dots show average concentration (2009-2010) from RAMP grab samples quantified by GC-MS-ion trap

The NAs mass measured from the POCIS had a higher relative contribution from compounds with 13-16 carbons and with two and three rings (Figure J- 2). Similar distribution has been observed in oil sands tailings water (Clemente & Fedorak, 2005). However, in tailing ponds the contribution of acyclic compounds is usually higher than the observed in these samples. This could be explained by the higher biodegradability of these compounds.

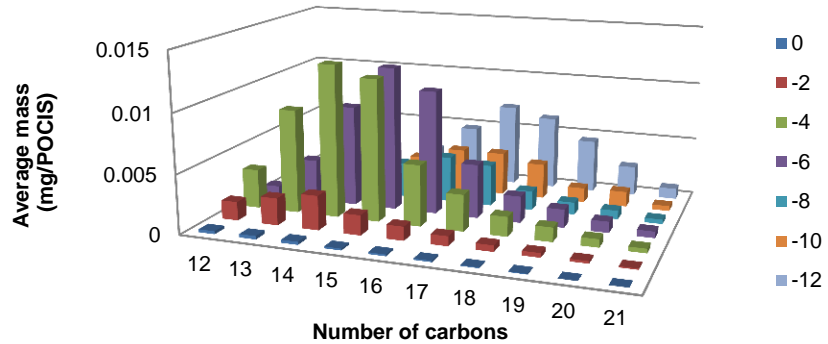


Figure J- 2. Average NAs mass per POCIS for different carbon numbers and Z numbers

Appendix K. Lab Pictures



Figure K- 1. Varian fluorescence spectrophotometer

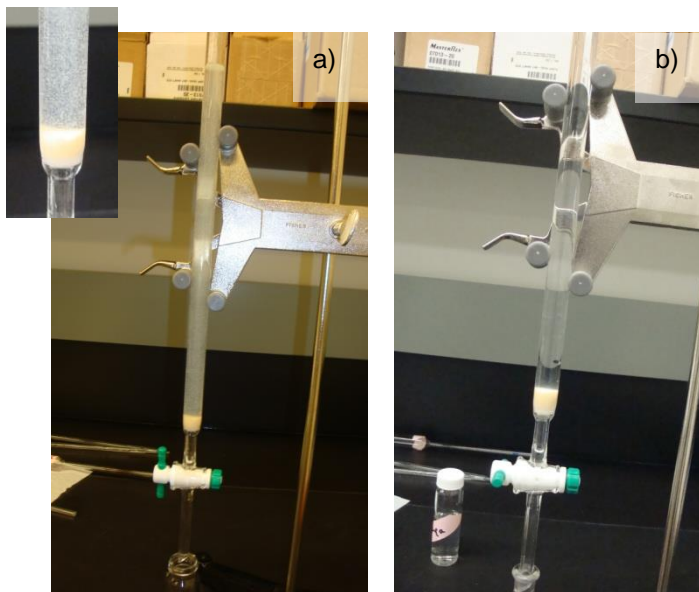


Figure K- 2. Recovery experiment a) spike with NAs solution in water b) extraction with methanol

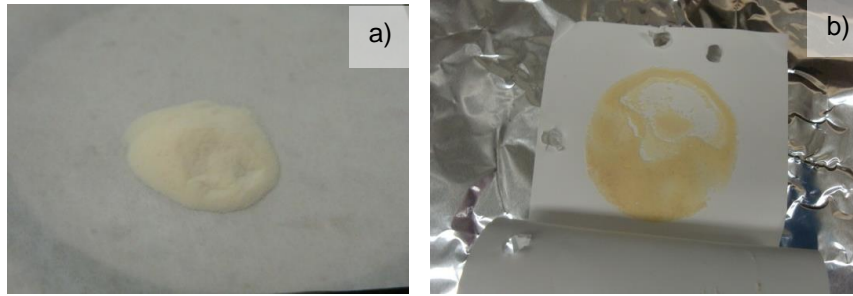


Figure K- 3. HLB Oasis resin a) before experiment b) after drying

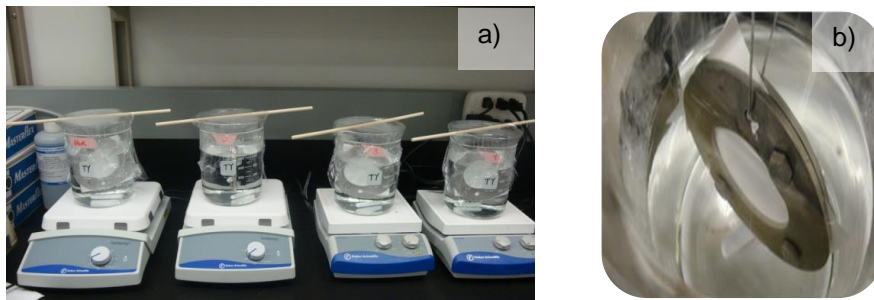


Figure K- 4. Preliminary POCIS uptake experiment a) set up, b) POCIS

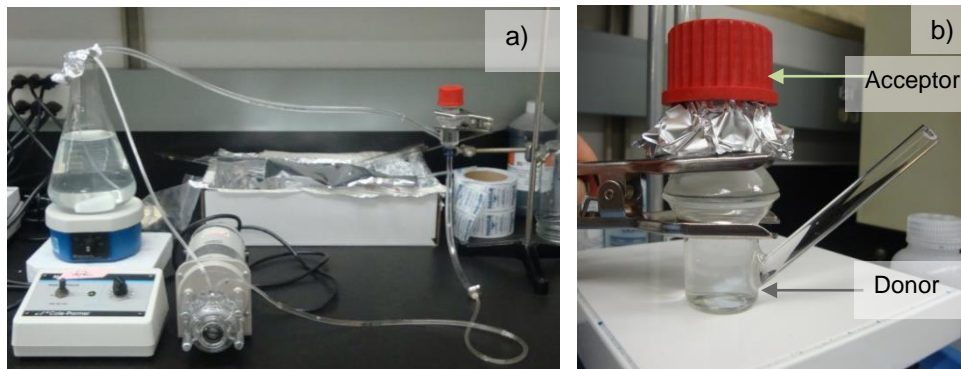


Figure K- 5. Diffusion experiment setup a) for continuous flow b) batch Franz cell



Figure K- 6. Flow-through system for integrative experiment

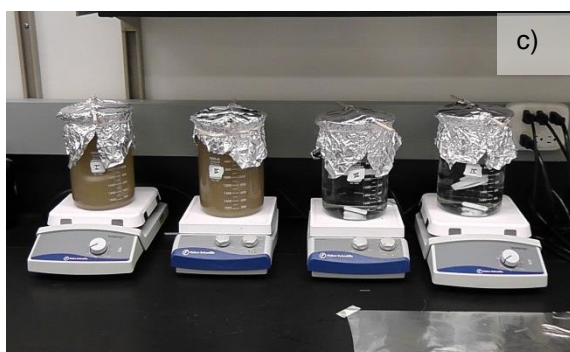


Figure K- 7. Chemcatcher uptake experiments a) environmental effects at room temperature, b) environmental effects at 4 °C, c) Matrix effects with river water and OSPW extract

Appendix L. Lower Athabasca River and tributaries pH and hardness

The pH and Hardness are based on the information found in the RAMP website for Athabasca River and tributaries and presented in Tables and Figures L-1 and L-2.

Table L- 1. pH in the lower Athabasca River and tributaries from 1997 to 2009

	Average	Max	Min	StdDev
Athabasca River	8.12	8.40	7.70	0.15
Ells River	8.09	8.60	7.70	0.19
Firebag River	7.97	8.40	7.20	0.27
Mackay River	8.06	8.60	7.45	0.24
Muskeg River	8.00	8.40	7.00	0.42
Steepbank River	8.10	8.50	7.60	0.22
Tar River	8.17	8.50	7.80	0.15
Grand Total	8.08	8.60	7.00	0.23

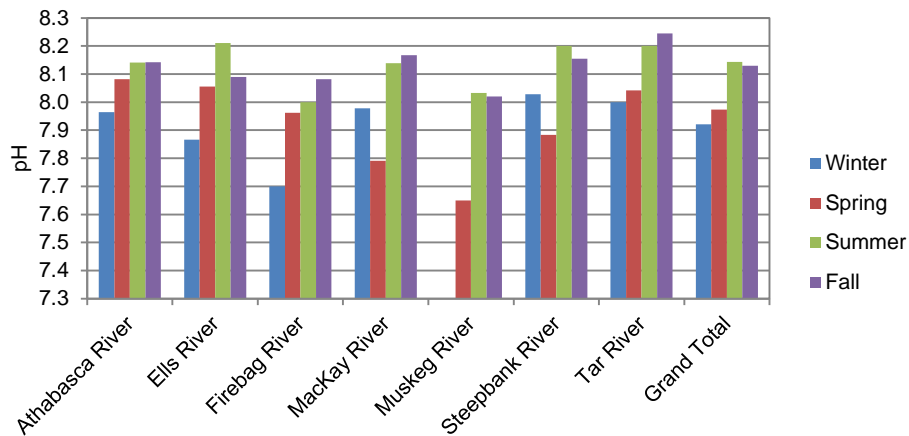


Figure L- 1. Average seasonal behaviour of pH in the Lower Athabasca River and tributaries

Table L- 2. Hardness (mg/L CaCO₃) in the Lower Athabasca River and tributaries from 1997 to 2009

	Average	Max	Min	StdDev
Athabasca River	113.68	185.00	68.00	24.49
Ells River	92.27	143.00	65.00	16.74
Firebag River	99.06	144.00	58.00	21.46
Mackay River	129.83	398.00	42.80	83.72
Muskeg River	179.00	343.00	101.00	55.28
Steepbank River	129.45	329.00	49.00	72.34
Tar River	152.63	321.00	68.90	56.90
Grand Total	123.84	398.00	42.80	54.45

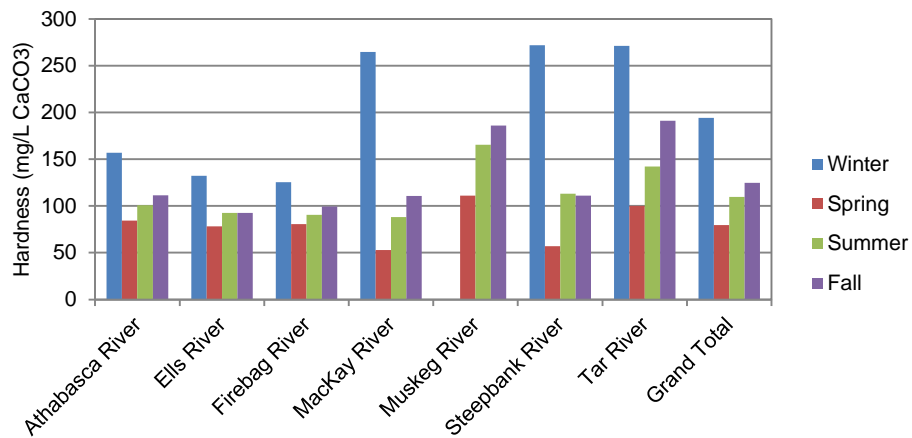


Figure L- 2. Average seasonal behaviour of hardness in the Lower Athabasca River and tributaries

Appendix M. Preliminary experiments: degradation, evaporation and partitioning of NAs

Evaporation of commercial NAs

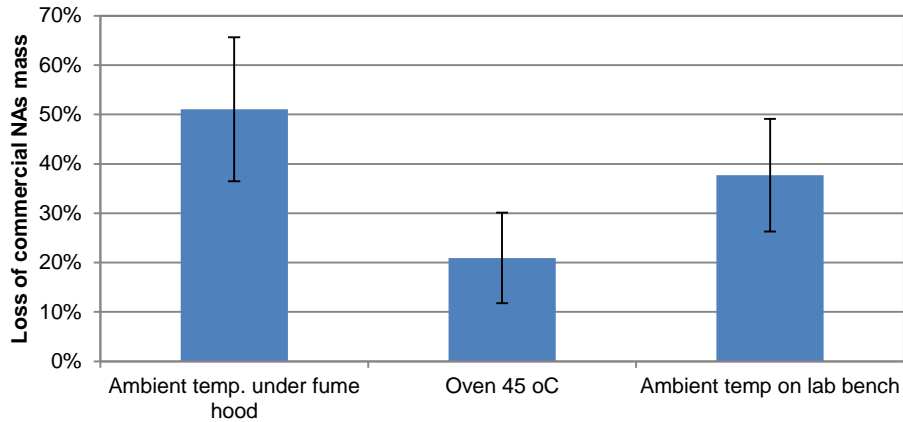


Figure M- 1. Loss in concentration in one month period under different conditions

MasterFlex tubing

Three sample tubes from the MasterFlex Tubing Test Kit (7 cm) were submerged in 15 mL of a 200 mg/L NAs solution in methanol for about 48 h. None of them changed the color of the solution. No change in appearance of the tubes was observed.

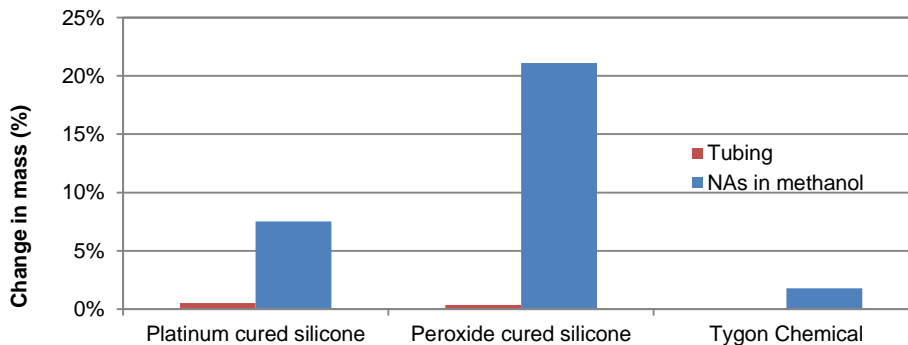


Figure M- 2. Change in mass of tubing and NAs in solution

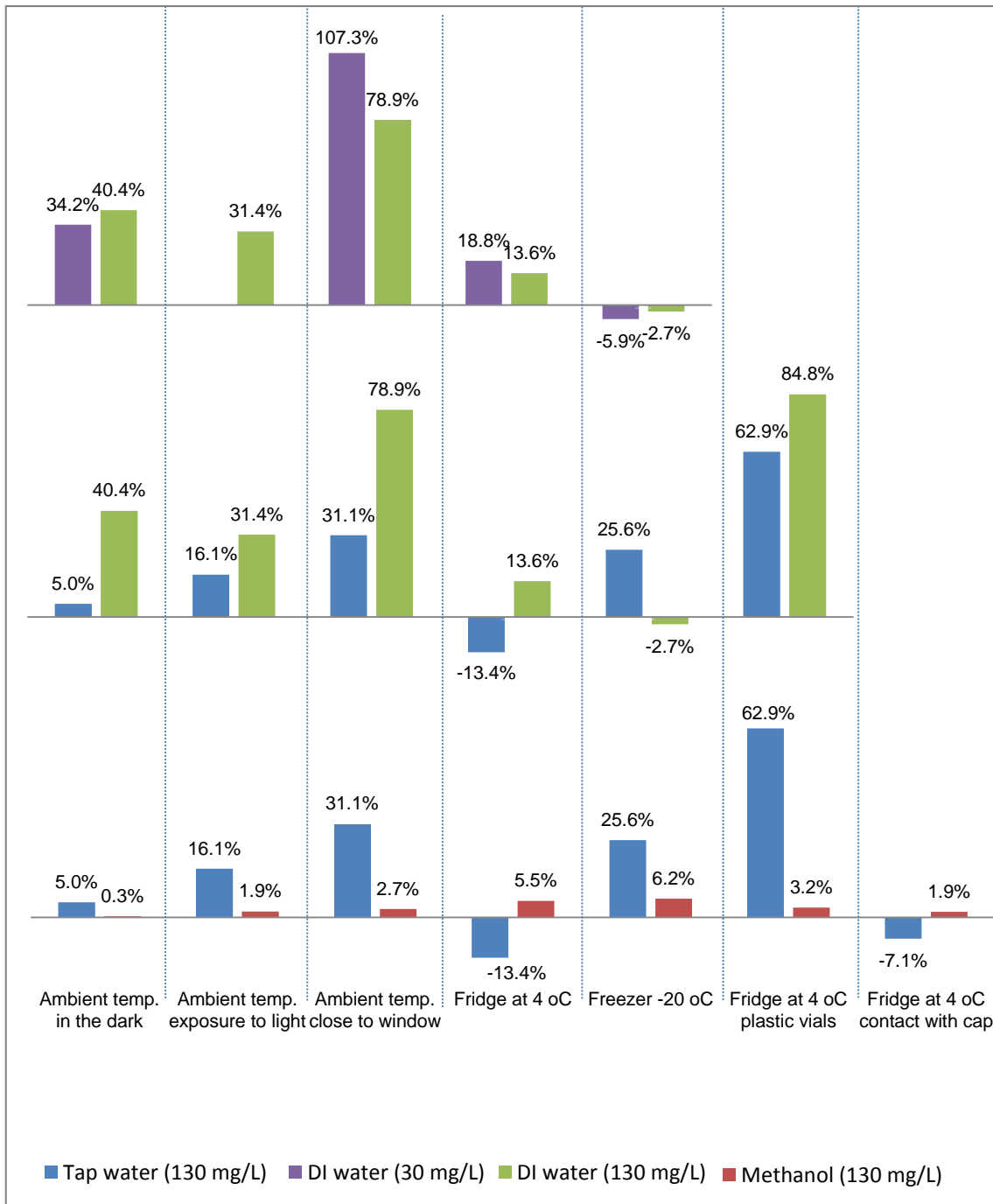


Figure M- 3. Change on NAs concentration after 30 days of storage under different conditions

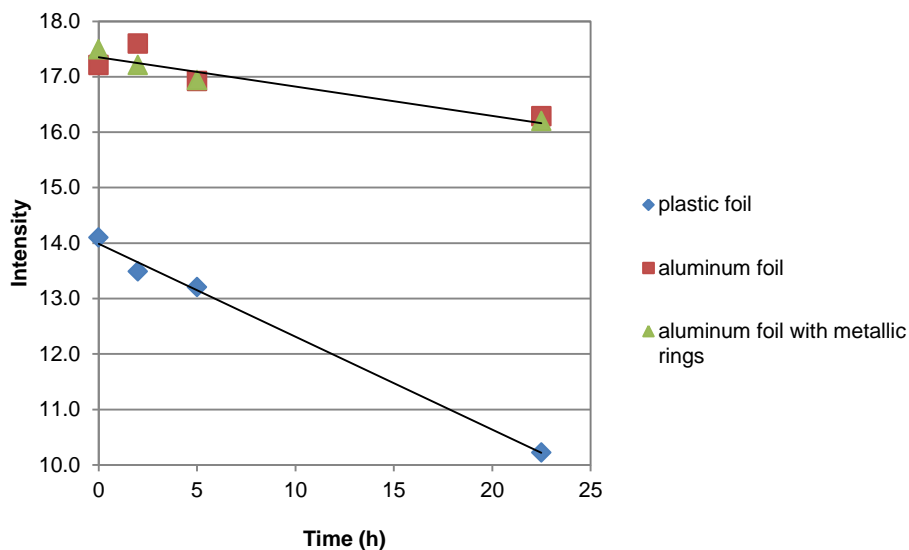


Figure M- 4. Change in fluorescence intensity using aluminum foil or plastic foil to cover the microcosms without sampler

Table M- 1. Partitioning experiment

Sorbent type	Int. 340	Av. Int	Mass sorbent (g)	Cw NAs (mg/L)	Mw NAs (mg)	Mass NAs in sorbent (mg)	g NAs/g Water	g NAs/ g Sorb	Log Kp
BLK-24h	21.80			3.93	0.16				
BLK-24h	20.00			3.59	0.14				
PTFE-I-24h	15.95		0.0223	2.84	0.11	0.04	2.84E-06	0.002	2.84
PTFE-II-24h	15.25	15.60	0.0243	2.71	0.11	0.05	2.71E-06	0.002	2.87
C18-I-24h	2.77		0.0451	0.39	0.02	0.14	3.90E-07	0.003	3.91
C18-II-24h	2.69	2.73	0.0428	0.38	0.02	0.14	3.76E-07	0.003	3.95
CELL-I-24h	5.61		0.0053	0.92	0.04	0.12	9.19E-07	0.023	4.39
CELL-II-24h	6.36	5.99	0.0052	1.06	0.04	0.11	1.06E-06	0.022	4.32
LDPE-I-24h	8.21		0.0052	1.40	0.06	0.10	1.40E-06	0.019	4.14
LDPE-II-24h	9.09	8.65	0.0042	1.57	0.06	0.09	1.57E-06	0.022	4.16
NYL-I-24h	12.67		0.0065	2.23	0.09	0.05	2.23E-06	0.008	3.58
NYL-II-24h	12.52	12.59	0.0068	2.20	0.09	0.06	2.20E-06	0.008	3.57
HLB-I-24h	1.44		0.0099	0.14	0.01	0.14	1.43E-07	0.014	4.99
HLB-II-24h	2.02	1.73	0.0101	0.25	0.01	0.13	2.51E-07	0.013	4.72
PES-I-24h	4.36		0.0062	0.69	0.03	0.12	6.87E-07	0.019	4.44
PES-II-24h	3.67	4.02	0.0061	0.56	0.02	0.12	5.59E-07	0.020	4.55
PES-III-48h	2.72		0.0059	0.38	0.02	0.13	3.82E-07	0.022	4.76
PES-IV-48h	3.24	2.98	0.0059	0.48	0.02	0.12	4.79E-07	0.021	4.64

Appendix N. Calibration curves for low concentration of NAs in water

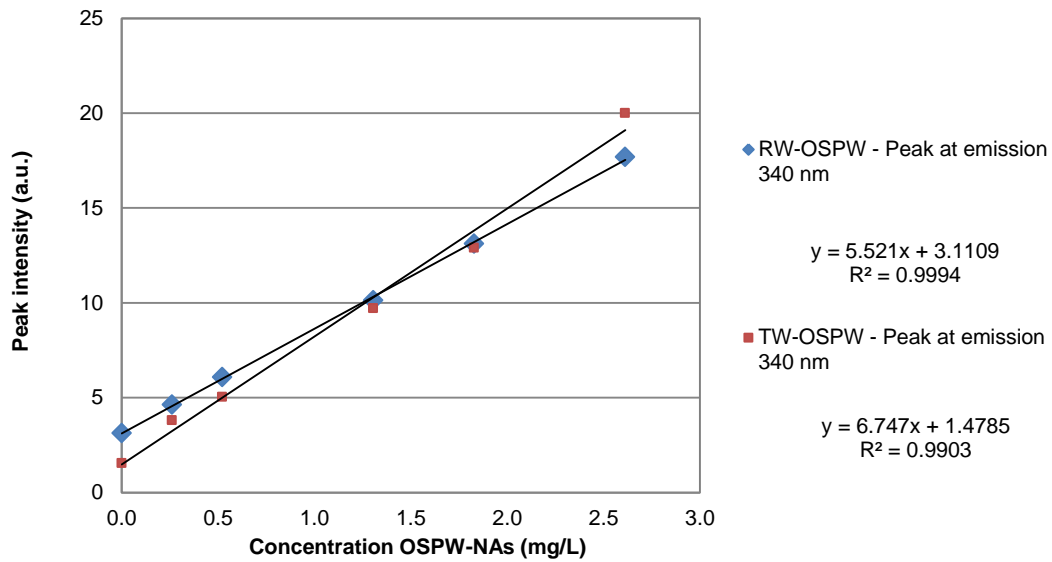


Figure N- 1. Calibration curve for OSPW-NAs in river water (RW) and tap water (TW)

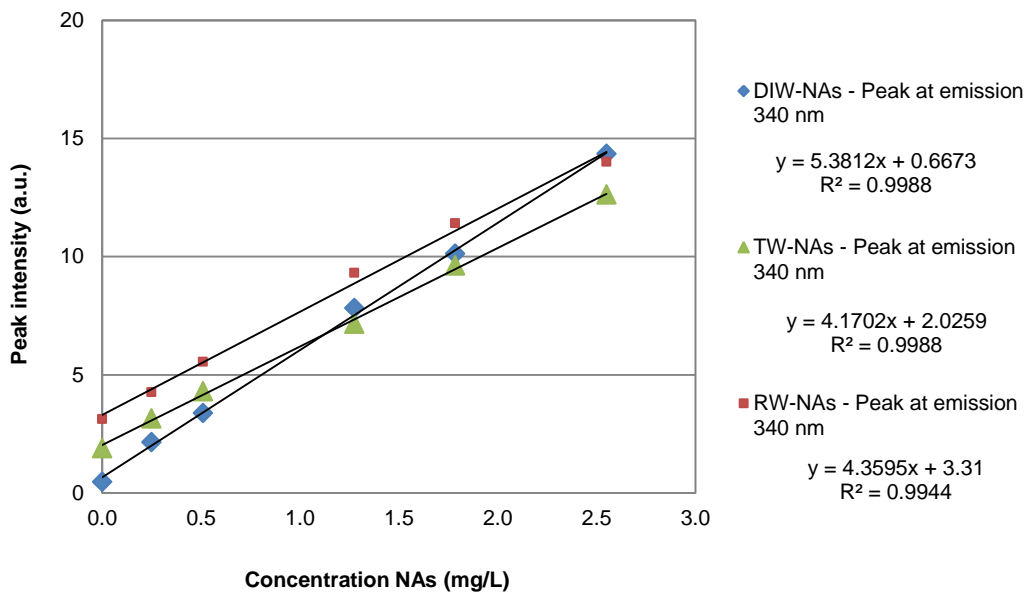


Figure N- 2. Calibration curve for commercial NAs in deionized water (DIW) river water (RW) and tap water (TW)

Appendix O. Example of uptake rate calculation

EFFECTS

Date	2-07-12	9-07-12		Ex	T	pH	hard	turb
Conc.	1 mg/L	Days	4	I	20	7	300	60
Volume	2 L	No	1					

Water

DI Water	at 340 nm		
Slope	5.3812	Blank	0.6673

Extraction

Methanol	For intensity < 350 nm		
Slope	3.349	Blank	6.94

Co-1		Peak	at 340	Conc.
D1	1	7.33	5.58	0.91
D3	3	7.24	5.06	0.82
Aver.		7.28	5.32	0.86

	Peak	Conc.	Volume	Mass	R
PTFE	15.43	2.54	0.05	0.13	
C18-I	85.36	23.41	0.05	1.17	0.34
C18-I	73.27	19.80	0.05	0.99	0.32
Average				1.08	0.33

Cw-1		Peak	at 340	Conc.
D1	1	6.02	3.39	0.51
D2	2	6.65	3.78	0.58
D3	3	6.40	3.54	0.53
D4	4	6.26	3.70	0.56
Aver.		6.33	3.60	0.55
Change in water				37%

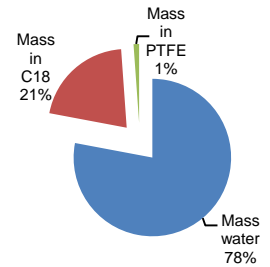
Rs using solver

$$M = (Rs \cdot Cwo \cdot \exp(-RS/V \cdot t))$$

Rs	0.40
	0.00

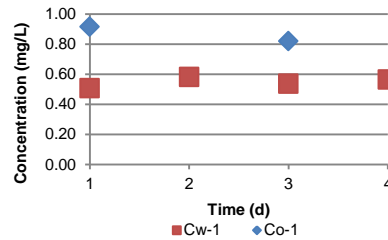
Mass balance

Mass in Mass recovered	6.92	6.24
Mass water	5.60	5.42
Mass in C18	4.36	4.37
Mass in PTFE	1.17	0.99
Recovery	0.06	0.06
	81%	87%



Co-2		Peak	at 340	Conc.
D1	1	6.55	4.63	0.74
D3	3	6.96	5.10	0.82
Aver.		6.75	4.86	0.78

Cw-2		Peak	at 340	Conc.
D1	1	5.90	3.48	0.52
D2	2	6.22	3.70	0.56
D3	3	6.40	3.54	0.53
D4	4	6.26	3.70	0.56
Aver.		6.19	3.60	0.55
Change in water				30%



Appendix P. Raw data for NAs analysis using LC-MS/MS from Axy's Analytical

BATCH	1	2	2	1	1	1	1	2	2
CLIENT ID	1-Stock OSPW	2-Stock NAs Aldrich	3-HLB-TW	4-C18-RW	5-C18-DIW	Lab Blank	Spiked Matrix	Lab Blank	Spiked Matrix
AXYS ID	L18288-1	L18288-2	L18288-3	L18288-4	L18288-5	WG40839-101	WG40839-102	WG41359-101	WG41359-102
WORKGROUP	WG40839	WG41359	WG41359	WG40839	WG40839	WG40839	WG40839	WG41359	WG41359
Sample Size	0.00162 L	0.000350 L	0.00158 L	0.00162 L	0.00161 L	0.00200 L		0.00200 L	
UNITS	ug/L	ug/L	ug/L	ug/L	ug/L	ug/L	% Recov	ug/L	% Recov
Compound									
C12H18O2	2710	1130	< 0.158	0.535	1.12	0.681	87.5	0.199	74
C12H20O2	7590	18900	2.32	4.43	6.18	3.49	82.6	1.03	76
C12H22O2	1330	31900	1.97	5.49	< 0.157	8.04	77.1	1.17	72.8
C12H24O2	47	8020	< 0.158	< 0.156	< 0.157	< 0.127	79.5	< 0.125	78
C13H20O2	6780	4170	1.19	1.86	3.07	0.803	79.9	< 0.125	74.5
C13H22O2	10300	27700	4.64	7.8	7.63	4.19	78.8	1.1	71.2
C13H24O2	1290	26700	4.36	5.3	5.08	7.58	77.6	1.07	70.3
C13H26O2	47.6	51800	3.34	9.68	< 0.157	26.2	66.3	1.52	62.4
C14H20O2	1090	1250	3.74	0.953	8.25	2.29	81.5	0.357	77.3
C14H22O2	8350	8820	2.88	2.49	4.29	1.9	77.2	0.339	68.2
C14H24O2	7930	30200	7.04	6.64	8.56	7.6	79	1.45	69.3
C14H26O2	768	19000	2.03	< 0.156	< 0.157	6.04	69.6	0.687	62.1
C14H28O2	31.6	41900	< 0.158	5.13	< 0.157	< 0.127	60.9	< 0.125	57.6
C15H18O2	1220	172	< 0.158	< 0.156	< 0.157	0.779	74.1	< 0.125	68.5
C15H20O2	800	986	2.12	< 0.156	< 0.157	< 0.127	81.4	< 0.125	76.4
C15H22O2	1630	1980	1.92	1.16	2.13	3.72	80.6	0.197	71.5
C15H24O2	6260	12700	4.57	3.17	3.54	5.59	83.1	0.529	70.1
C15H26O2	3900	29500	5.58	5.49	4.98	7.01	79.9	1.09	68.8
C15H28O2	648	36000	< 0.704	5.3	6.09	7.61	169	< 0.125	119

Continued

BATCH	1	2	2	1	1	1	1	2	2
CLIENT ID	1-Stock OSPW	2-Stock NAs Aldrich	3-HLB-TW	4-C18-RW	5-C18-DIW	Lab Blank	Spiked Matrix	Lab Blank	Spiked Matrix
AXYS ID	L18288-1	L18288-2	L18288-3	L18288-4	L18288-5	WG40839-101	WG40839-102	WG41359-101	WG41359-102
WORKGROUP	WG40839	WG41359	WG41359	WG40839	WG40839	WG40839	WG40839	WG41359	WG41359
Sample Size	0.00162 L	0.000350 L	0.00158 L	0.00162 L	0.00161 L	0.00200 L		0.00200 L	
UNITS	ug/L	ug/L	ug/L	ug/L	ug/L	ug/L	% Recov	ug/L	% Recov
Compound									
C16H32O2	11.1	16100	< 0.158	< 1.22	< 1.06	< 0.621	121	< 0.163	90.3
C17H22O2	1950	574	5.08	2.34	4.12	4.45	89.5	0.564	88.5
C17H24O2	944	1070	1.58	0.561	< 0.157	0.817	89.3	0.181	76.5
C17H26O2	701	1840	1.56	0.638	0.558	1.81	90.3	0.231	77.5
C17H28O2	1450	13300	5.34	7.58	6.63	5.53	196	2.18	140
C17H30O2	460	24900	1.48	4.48	4.15	3.03	184	0.564	130
C17H32O2	34.7	14300	< 0.158	< 0.158	< 0.157	< 0.127	147	< 0.125	114
C17H34O2	1.56	5240	< 0.724	< 0.386	< 2.20	< 0.776	119	< 0.206	97.7
C18H24O2	1370	517	8.52	5.57	10.2	10.5	123	1.41	126
C18H26O2	583	807	1.22	0.672	0.877	1.21	89.2	< 0.125	78.3
C18H28O2	462	2310	3.04	2.42	5.39	3.48	229	0.962	153
C18H30O2	264	6900	< 0.158	< 0.156	< 0.157	1.02	114	< 0.125	92.5
C18H32O2	65.8	8700	< 0.158	< 0.214	< 0.409	< 0.127	148	0.545	100
C18H34O2	5.92	6200	< 0.158	< 0.356	< 0.320	< 0.127	113	3.43	95.4
C18H36O2	18.8	22000	< 0.158	11.2	19.3	< 0.244	74.2	< 0.125	74.7
C19H26O2	734	293	4.12	2.65	4.24	8.86	128	0.613	140
C19H28O2	428	1160	1.58	< 0.156	< 0.157	1.86	208	< 0.125	147
C19H30O2	100	1290	< 0.158	< 0.156	< 0.157	< 0.127	189	< 0.125	137
C19H32O2	49.3	2970	0.65	< 0.156	< 0.157	0.992	154	0.169	124
C19H34O2	13.9	3440	< 0.158	< 0.172	< 0.486	< 0.133	127	< 0.125	109
C19H36O2	11.7	15200	1.05	5.67	< 3.40	< 0.791	92.8	< 0.125	93.5
C19H38O2	387	230000	22.3	142	83.1	< 7.60	82.6	< 0.607	89.4
C20H28O2	305	506	43.2	28.7	85.8	45.2	256	1.6	1290

Continued

BATCH	1	2	2	1	1	1	1	2	2
CLIENT ID	1-Stock OSPW	2-Stock NAs Aldrich	3-HLB-TW	4-C18-RW	5-C18-DIW	Lab Blank	Spiked Matrix	Lab Blank	Spiked Matrix
AXYS ID	L18288-1	L18288-2	L18288-3	L18288-4	L18288-5	WG40839-101	WG40839-102	WG41359-101	WG41359-102
WORKGROUP	WG40839	WG41359	WG41359	WG40839	WG40839	WG40839	WG40839	WG41359	WG41359
Sample Size	0.00162 L	0.000350 L	0.00158 L	0.00162 L	0.00161 L	0.00200 L		0.00200 L	
UNITS	ug/L	ug/L	ug/L	ug/L	ug/L	ug/L	% Recov	ug/L	% Recov
Compound									
C20H30O2	141	774	79.2	12.3	17.9	14.1	214	5.53	174
C21H36O2	< 0.311	450	< 0.158	< 0.156	< 0.157	< 0.127	102	< 0.125	102
C21H38O2	2.6	749	< 0.158	< 0.156	1.25	< 0.127	85.2	< 0.125	91.4
C21H40O2	2.07	674	1.1	< 0.156	3.73	< 0.127	75.3	0.133	78.1

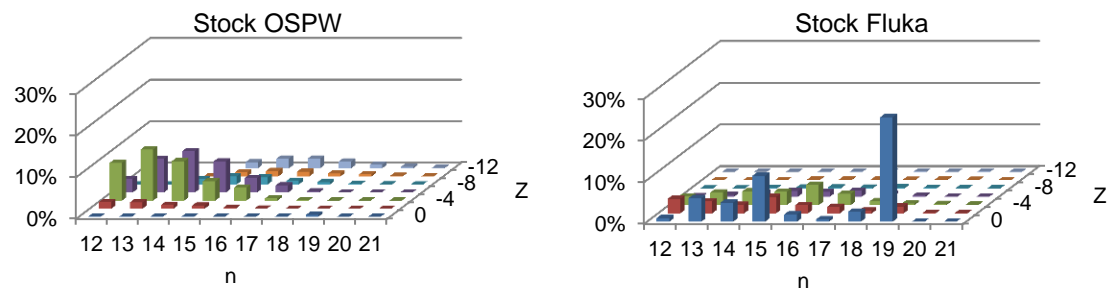


Figure P- 1. Carbon number and Z distribution for commercial (Fluka) and OSPW acid extract stock solutions

Appendix R. Mass balance for POCIS experiment using different exposure periods

The mass adsorbed in the membrane at the end of the experiment was much higher than the mass adsorbed to the resin even at longer exposure periods.

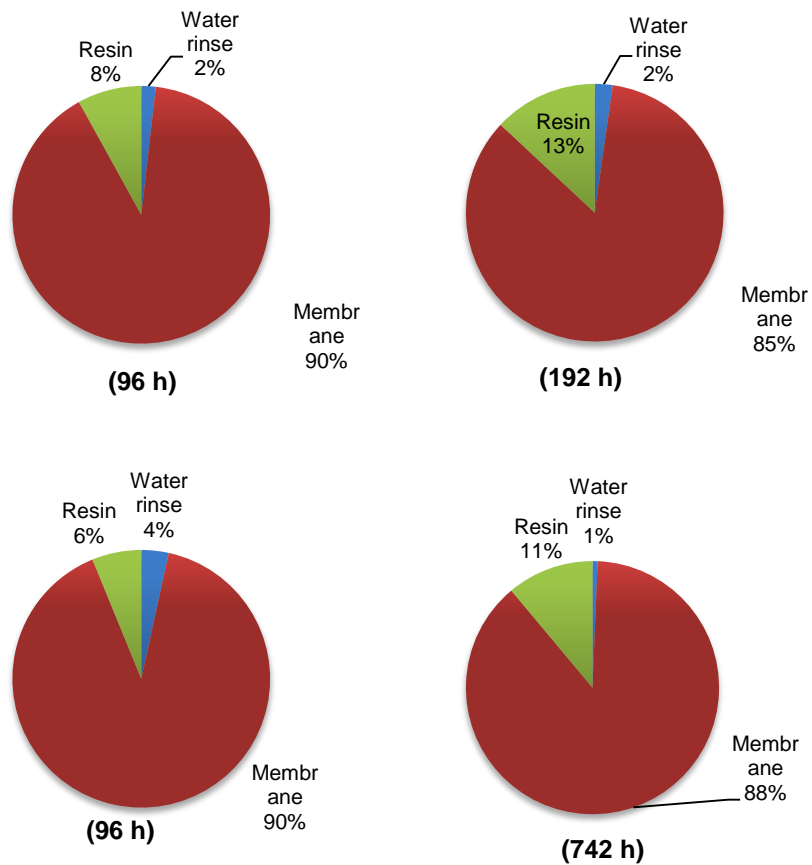


Figure R- 1. NAs mass distribution after extraction